

AD A136 414

DEVELOPMENT OF FATIGUE AND CRACK PROPAGATION DESIGN AND  
ANALYSIS METHODOLOGY (U) GENERAL DYNAMICS FORT WORTH TX  
FORT WORTH DIV Y H KIM ET AL. MAR 83

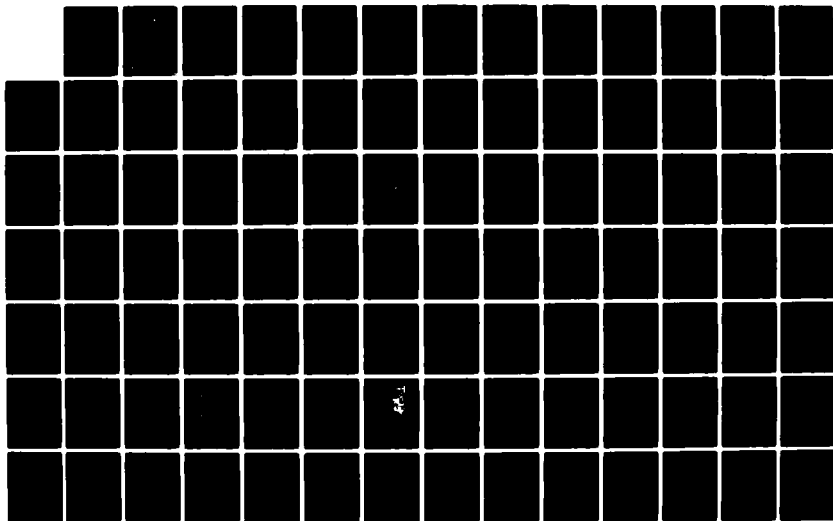
1/3

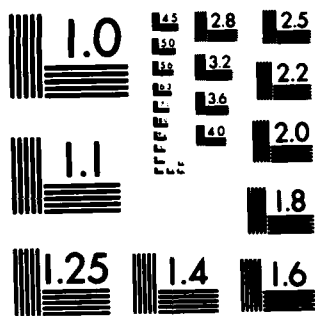
UNCLASSIFIED

NADC-83126-60-VOL-1 N62269-81-C-0268

F/G 20/11

NL





MICROCOPY RESOLUTION TEST CHART  
NATIONAL BUREAU OF STANDARDS-1963-A



**DEVELOPMENT OF FATIGUE AND CRACK PROPAGATION  
DESIGN AND ANALYSIS METHODOLOGY IN A CORROSIVE  
ENVIRONMENT FOR TYPICAL MECHANICALLY-FASTENED JOINTS  
VOLUME I - PHASE I DOCUMENTATION**

A136414

Y. H. Kim  
S. M. Speaker  
D. E. Gordon  
S. D. Manning  
STRUCTURES AND DESIGN DEPARTMENT  
GENERAL DYNAMICS FORT WORTH DIVISION  
P.O. Box 748  
Fort Worth, Texas 76101  
and  
R. P. Wei  
LEHIGH UNIVERSITY  
Bethlehem, PA 18015

**MARCH 1983**

DEC 28 1983

A

Final Report for Period May 1983 - September 1982

*Approved for Public Release; Distribution Unlimited*

DTIC FILE COPY

Prepared For  
Department of the Navy  
NAVAL AIR DEVELOPMENT CENTER  
Warminster, PA 18974

83 12 28 011

Unclassified

SECURITY CLASSIFICATION OF THIS PAGE (When Data Entered)

REPORT DOCUMENTATION PAGE		READ INSTRUCTIONS BEFORE COMPLETING FORM
1. REPORT NUMBER NADC-83126-60 Vol. I	2. GOVT ACCESSION NO. A1-A136 484	3. RECIPIENT'S CATALOG NUMBER
4. TITLE (and Subtitle) Development of Fatigue and Crack Propagation Design and Analysis Methodology in a Corrosive Environment for Typical Mechanically Fastened Joints Vol. I- Phase I Documentation		5. TYPE OF REPORT & PERIOD COVERED Final Report May 1981 - September 82
7. AUTHOR(S) Y. H. Kim, R. P. Wei, D. E. Gordon, S. M. Speaker, S. D. Manning		6. PERFORMING ORG. REPORT NUMBER
9. PERFORMING ORGANIZATION NAME AND ADDRESS General Dynamics Fort Worth Division P. O. Box 748, Fort Worth, TX 76101		8. CONTRACT OR GRANT NUMBER(s) N62269-81-C-0268
11. CONTROLLING OFFICE NAME AND ADDRESS Naval Air Development Center (NADC) Warminster, PA 18974		10. PROGRAM ELEMENT, PROJECT, TASK AREA & WORK UNIT NUMBERS 62241N WF41400, ZA-61A
14. MONITORING AGENCY NAME & ADDRESS (if different from Controlling Office)		12. REPORT DATE March 1983
		13. NUMBER OF PAGES 218
		15. SECURITY CLASS. (of this report) Unclassified
		15a. DECLASSIFICATION/DOWNGRADING SCHEDULE
16. DISTRIBUTION STATEMENT (of this Report)  Approved for public release; distribution unlimited.  :		
17. DISTRIBUTION STATEMENT (of the abstract entered in Block 20, if different from Report)		
18. SUPPLEMENTARY NOTES The subcontractor/consultant for this report was R. P. Wei, Lehigh University, Bethlehem, PA 18015		
19. KEY WORDS (Continue on reverse side if necessary and identify by block number) Corrosion fatigue, crack initiation, crack propagation, corrosive environments		
20. ABSTRACT (Continue on reverse side if necessary and identify by block number) A corrosion fatigue methodology has been developed for predicting the crack initiation and crack propagation behavior of mechanically-fastened joints. An experimental test program was also conducted using 7075-T7651 aluminum alloy and 8-annealed Ti-6Al-4V alloy to evaluate the effects of environment, test frequency, R-ratio, holding-time, and stress level on corrosion fatigue behavior. (Continued)		

Unclassified

SECURITY CLASSIFICATION OF THIS PAGE(When Data Entered)

## 20. Abstract (Continued)

Based on this investigation, it was concluded that:

1. The reaction between aqueous environments and the 7075-T7651 aluminum alloy appears to be limited. Hence, a special crack propagation model for corrosion fatigue is not required for design.

2. A better understanding of the corrosion fatigue behavior of  $\beta$ -annealed Ti-6Al-4V alloy is needed before a reliable predictive methodology can be developed for mechanically-fastened joints.

3. The corrosion fatigue predictive methodology developed looks promising for constant amplitude applications. Now, the predictive methodology needs to be further developed to account for spectrum loading and variance in the input data base. ←

Accession No.	
NTIS Class.	
DTIC No.	
Classification	
Justification	
Excluded	
Excluded	
Available	
Dist	
A-1	

Unclassified

SECURITY CLASSIFICATION OF THIS PAGE(When Data Entered)

FOREWORD

This program is conducted by General Dynamics Fort Worth Division (GD/FWD), with Lehigh University (Prof. R. P. Wei) as subcontractor/consultant. This report was prepared under Contract No. N62269-81-C-0268. The program is sponsored by the Naval Air Development Center, Warminster, PA, with Dr. E. Lee and Mr. P. Kozel as the project engineers. M. S. Rosenfeld of NADC initiated the program. Dr. S. D. Manning and Dr. Y. H. Kim of General Dynamics' Material Research Laboratory are the Program Manager and Principal Investigator, respectively.

The following GD/FWD personnel supported the Phase I effort as follows: S. M. Speaker (corrosion fatigue state-of-the-art assessment, fatigue crack propagation tests, model evaluation) and D. E. Gordon (material/specimen procurement, stress controlled crack initiation tests and eddy current measurements basic property tests, data evaluation). Metallurgy Laboratory personnel, W. T. Kaarlela, W. S. Margolis, R. O. Nay and F. C. Nordquist, provided testing support. P. Thomas typed the reports.

Phase I is documented in two volumes as follows:

Vol. I - Phase I Documentation

**Vol. II- Corrosion Fatigue State-of-the-Art Assessment**

This report (Vol. I) documents the corrosion fatigue methodology development, the experimental tests performed and the preliminary evaluation of the methodology.

## TABLE OF CONTENTS

<u>Section</u>	<u>Page</u>
I INTRODUCTION	1
1.1 Program Objectives	1
1.2 Scope	2
1.3 Organization	3
II CORROSION FATIGUE METHODOLOGY DEVELOPMENT	5
2.1 Introduction	5
2.2 Crack Initiation Models	5
2.2.1 Stress-Initiation Life Model	6
2.2.2 Strain-Initiation Life Model	9
2.3 Mechanistic Crack Propagation Models	14
2.3.1 Controlling Processes and Models	15
2.3.2 Quantification of the Mechanistic Propagation Models	16
2.3.3 Model Summaries	19
2.3.4 Implications of the Models	22
2.4 Corrosion Fatigue Predictive Methodology	25
III PHASE I EXPERIMENTAL TEST PROGRAM	29
3.1 Introduction	29
3.2 Test Plan	30
3.2.1 Test Matrix	30
3.2.2 Materials	30
3.2.3 Specimen Designs	38
3.2.4 Test Environment	45
3.2.5 Environmental Chambers	47

## TABLE OF CONTENTS (Continued)

<u>Section</u>	<u>Page</u>
3.3 Experimental Procedures	50
3.3.1 Data Acquisition	51
3.3.2 Basic Material Properties Test Procedures	65
3.3.3 Fatigue Crack Initiation Test Procedures	68
3.3.4 Fatigue Crack Propagation Test Procedures	70
IV PHASE I TEST RESULTS	75
4.1 Introduction	75
4.2 Basic Materials Properties	75
4.3 Fatigue Crack Initiation Results	82
4.3.1 7075-T7651 Aluminum Alloy	82
4.3.2 $\beta$ -Annealed Ti-6Al-4V Alloy	92
4.4 Fatigue Crack Propagation Results and Evaluations	97
4.4.1 7075-T7651 Aluminum Alloy	99
4.4.2 $\beta$ -Annealed Ti-6Al-4V Alloy	114
V EVALUATION OF CORROSION FATIGUE MODELS	135
5.1 Introduction	135
5.2 Evaluation of Stress-Initiation Life Model	135
5.2.1 Evaluation of Model Parameters and Fit	135
5.2.2 Conclusions	155
5.3 Evaluation of Crack Propagation Models	157

## TABLE OF CONTENTS (Continued)

<u>Section</u>	<u>Page</u>
VI CONCLUSIONS AND RECOMMENDATIONS	161
6.1 Conclusions	161
6.2 Recommendations	163
VII PHASE II TEST PLAN	165
7.1 Introduction	165
7.2 Test Objectives and Philosophy	165
7.3 Test Variables	167
7.4 Test Plan	167
7.5 Specimen Preconditioning	167
APPENDIX A - Fatigue Crack Propagation Results for 7075-T7651 Aluminum Alloy	179
APPENDIX B - Fatigue Crack Propagation Results for $\beta$ -Annealed Ti-6Al-4V Alloy	195
REFERENCES	215

NADC-83126-60 Vol. I

THIS PAGE INTENTIONALLY LEFT BLANK

## LIST OF ILLUSTRATIONS

<u>Figure</u>		<u>Page</u>
1	Schematic Representation of Stress-Initiation Life Model	10
2	Schematic Representation of Strain-Initiation Life Model	13
3	Elements of the Corrosion Fatigue Methodology	27
4	Pole Figures for the Rolling Plane of $\beta$ -Annealed Ti-6Al-4V Alloy Plate: (a) (0002) Pole, and (b) 1010 Pole	37
5	Tensile Specimen Geometry	40
6	Compact Tension Type Specimen Geometry (7075-T7651 Aluminum Alloy)	41
7	Compact Tension Type Specimen Geometry $\beta$ -Annealed Ti-6Al-4V Alloy	42
8	Cyclic Stress-Strain Specimen Geometry	43
9	Fatigue Crack Initiation Specimen Geometry	44
10	Schematic Drawings of Environmental Chamber for Compact Tension Specimens	48
11	Environmental Chamber Geometry for the Stress-Controlled Crack Initiation Tests	49
12	Automated Eddy Current Inspection System	52
13	Effect of Surface Roughness in Fastener Holes on the Eddy Current Signal	54
14	Eddy Current Scans Showing Onset of Cracking in Fatigue Cycled Coupon	56
15	Eddy Current Scans Showing Onset of Cracking in Fatigue Cycled Coupon $\beta$ -Annealed Ti-6Al-4V Alloy	57
16	Relationship Between Eddy-Current Signal Amplitude and Fatigue Crack Depth for 7075-T7651 Aluminum Alloy	58

## LIST OF ILLUSTRATIONS (Continued)

<u>Figure</u>		<u>Page</u>
17	Relationship Between Eddy-Current Signal Amplitude and Fatigue Crack Depth for $\beta$ -Annealed Ti-6Al-4V Alloy	59
18	Calibration Curve of Crack Length Versus Normalized Compliance for $\beta$ -Annealed Ti-6Al-4V Alloy	62
19	Calibration Curve of Crack Length Versus Electrical Potential for $\beta$ -Annealed Ti-6Al-4V Alloy	63
20	A Stable Set of Hysteresis Loops for 7075-T7651 Aluminum Alloy	80
21	Monotonic and Cyclic Stress-Strain Curves for 7075-T7651 Aluminum Alloy	81
22	A Stable Set of Hysteresis Loops for $\beta$ -Annealed Ti-6Al-4V Alloy	83
23	Monotonic and Cyclic Stress-Strain Curves for $\beta$ -Annealed Ti-6Al-4V Alloy	84
24	Comparison of $\Delta\sigma$ Versus $N_i$ Curves (Dry Air & 3.5% NaCl) for 7075-T7651 Aluminum Alloy ( $a_0=0.010''$ )	87
25	Effect of Frequency on $N_i/N_f$ Ratio for 7075-T7651 Aluminum Alloy ( $a_0=0.010''$ )	90
26	Comparison of $\Delta\sigma$ Versus $N_i$ Curves (Dry Air & 3.5% NaCl) for $\beta$ -Annealed Ti-6Al-4V Alloy ( $a_0=0.010''$ )	94
27	Effect of Frequency on $N_i/N_f$ Ratio for $\beta$ -Annealed Ti-6Al-4V ( $a_0=0.010''$ )	98
28	Effect of Environment on Crack Growth Rates for 7075-T7651 Aluminum Alloy at Room Temperature ( $R=0.05$ , $f=6$ Hz)	100
29	Comparison of Crack Growth Rates for 7075-T7651 Aluminum Alloy in Both Dry Air and 3.5% NaCl Solution at Room Temperature ( $R=0.05$ )	101
30	Comparison of Crack Growth Rates for 7075-T7651 Aluminum Alloy in Both Dry Air and 3.5% NaCl Solution at Room Temperature ( $R=0.3$ )	102

## LIST OF ILLUSTRATIONS (Continued)

<u>Figure</u>		<u>Page</u>
31	Effect of R Ratio on Crack Growth Rates for 7075-T7651 Aluminum Alloy in Dry Air at Room Temperature (R = 0.05, 0.3)	104
32	Effect of R Ratio on Crack Growth Rates for 7075-T7651 Aluminum Alloy Exposed to 3.5% NaCl Solution at Room Temperature (f = 6 Hz; R = 0.05, 0.2, 0.3, and 0.4)	105
33	Effect of Frequency on Crack Growth Rates for 7075-T7651 Aluminum Alloy in Dry Air at Room Temperature (R = 0.05, f = 0.1 Hz, 1 Hz and 6 Hz)	107
34	Effect of Frequency on Crack Growth Rates for 7075-T7651 Aluminum Alloy in Dry Air at Room Temperature (R = 0.3, f = 0.1 Hz, 1 Hz and 6 Hz)	108
35	Effect of Frequency on Crack Growth Rates for 7075-T7651 Aluminum Alloy Exposed to 3.5% NaCl Solution at Room Temperature (R = 0.05; f = 1 Hz, 0.3 Hz, and 6 Hz)	109
36	Effect of Frequency on Crack Growth Rates for 7075-T7651 Aluminum Alloy Exposed to 3.5% NaCl Solution at Room Temperature (R = 0.03; f = 0.1 Hz, 0.3 Hz, 1 Hz, 3 Hz and 6 Hz)	110
37	Effect of Frequency on Fatigue Crack Growth in 7075-T7651 Aluminum Alloy Tested in a 3.5% NaCl Solution at Room Temperature	111
38	Effect of Holding Time on the Kinetics of Fatigue Crack Growth in 7075-T7651 Aluminum Alloy Exposed to 3.5% NaCl Solution at Room Temperature (R = 0.05)	113
39	Crack Propagation Rate vs. $\Delta K$ for $\beta$ -Annealed Ti-6Al-4V Alloy in Distilled Water, in ASTM Artificial Sea Water, and in 3.5% NaCl + H <sub>2</sub> SO <sub>4</sub> (pH = 3.5)	115
40	Kinetics of Fatigue Crack Growth in $\beta$ -Annealed Ti-6Al-4V Alloy in Vacuum (@ <10 <sup>-5</sup> Pa) at Room Temperature (f = 5 Hz, R = 0.05).	116
41	Crack Propagation Rate vs. $\Delta K$ for $\beta$ -Annealed Ti-6Al-4V Alloy in a 3.5% NaCl Solution at Room Temperature (f = 10 Hz, R = 0.05, 0.2 and 0.4).	118

## LIST OF ILLUSTRATIONS (Continued)

<u>Figure</u>		<u>Page</u>
42	Kinetics of Fatigue Crack Growth in $\beta$ -Annealed Ti-6Al-4V Alloy Exposed to 3.5% NaCl Solution at Room Temperature ( $f = 0.3$ Hz, $R = 0.05$ )	119
43	Kinetics of Fatigue Crack Growth in $\beta$ -Annealed Ti - 6Al - 4V Alloy Exposed to 3.5% NaCl Solution at Room Temperature ( $f = 3$ Hz, $R = 0.05$ )	120
44	Kinetics of Fatigue Crack Growth in $\beta$ -Annealed Ti - 6Al - 4V Alloy Exposed to 3.5% NaCl Solution at Room Temperature ( $f = 0.3$ Hz, $R = 0.3$ )	121
45	Kinetics of Fatigue Crack Growth in $\beta$ -Annealed Ti - 6Al - 4V Alloy Exposed to 3.5% NaCl Solution at Room Temperature ( $f = 3$ Hz, $R = 0.3$ )	122
46	Kinetics of Fatigue Crack Growth in $\beta$ -Annealed Ti - 6Al - 4V Alloy Exposed to 3.5% NaCl Solution at Room Temperature ( $f = 10$ Hz, $R = 0.3$ )	123
47	Effect of Frequency on Fatigue Crack Growth in $\beta$ -Annealed Ti-6Al-4V Alloy Tested in 3.5% NaCl Solution at Room Temperature	124
48	Representative SEM microfractographs of $\beta$ -Annealed Ti-6Al-4V Alloy Tested in Fatigue in 3.5% NaCl Solution at Room Temperature ( $R = 0.05$ ): (a) $f = 10$ Hz, (b) $f = 0.3$ Hz, and (c) $f = 0.03$ Hz. Magnification: 80X. (Plate No. 13-001, 91-103, 13-069)	126
49	SEM Microfractographs of Region B in Figure 48b, Showing Crack Growth Across $\alpha$ -platelets and $\alpha/\beta$ Interfaces: (a) 200X, and (b) 800X. (Plate No. 13-103, 13-104)	127
50	SEM Microfractographs from Mating Surfaces of Region A in Figure 48a Showing Fine Fatigue Striations: (a) Ductile Appearing Striations, and (b) Brittle Appearing Striations on Mating Surface. Magnification: 1000X. (Plate No. 13-024, 13-025)	129
51	Effect of Holding Time on the Kinetics of Fatigue Crack Growth in $\beta$ -Annealed Ti-6Al-4V Alloy Exposed to 3.5% NaCl Solution at Room Temperature ( $R = 0.05$ )	131

## LIST OF ILLUSTRATIONS (Continued)

<u>Figure</u>		<u>Page</u>
52	Effect of Holding Time on the Kinetics of Fatigue Crack Growth in $\beta$ -Annealed Ti-6Al-4V Alloy Exposed to 3.5% NaCl Solution at Room Temperature ( $R = 0.05$ )	132
53	Comparison of $\Delta\sigma$ Versus $N_i$ Curves (Dry Air + 3.5% NaCl) for 7075-T7651 Aluminum Alloy ( $a_0 = 0.010''$ )	144
54	Comparison of $\Delta\sigma$ Versus $N_i$ (Dry Air + 3.5% NaCl) for $\beta$ -Annealed Ti-6Al-4V Alloy ( $a_0 = 0.010''$ )	145
55	95% Confidence Interval for $\Delta\sigma$ Versus $N_i$ for 7075-T7651 Aluminum Alloy in Dry Air ( $f = 6 \text{ Hz}$ ; $a_0 = 0.010''$ )	149
56	95% Confidence Interval for $\Delta\sigma$ Versus $N_i$ for 7075-T7651 Aluminum Alloy in 3.5% NaCl Solution ( $a_0 = 0.010''$ )	150
57	95% Confidence Interval for $\Delta\sigma$ Versus $N_i$ for $\beta$ -Annealed Ti-6Al-4V Alloy in Dry Air ( $f = 6 \text{ Hz}$ ; $a_0 = 0.010''$ )	151
58	95% Confidence Interval for $\Delta\sigma$ Versus $N_i$ for $\beta$ -Annealed Ti - 6Al - 4V Alloy in 3.5% NaCl Solution ( $a_0 = 0.010''$ )	152
59	Strain-Controlled Specimen	173
60	Compact Tension Specimen for $\beta$ -Annealed Ti-6Al-4V Alloy	174
61	Dog-Bone Specimen	175
62	Setup for Bolt Load Transfer Tests	176

NADC-83126-60 Vol. I

THIS PAGE INTENTIONALLY LEFT BLANK

## LIST OF TABLES

<u>Table</u>		<u>Page</u>
1	Phase I Test Plan for Basic Properties	31
2	Phase I Test Plan for Fatigue Crack Initiation Tests (Stress-Controlled)	32
3	Phase I Test Plan for Evaluating the Effects of Environment, R Ratio, Frequency and Holding Time on Fatigue Crack Propagation	33
4	Phase I Test Plan for Evaluating the Effects of Environment on Fatigue Crack Propagation	34
5	Chemical Composition of $\beta$ -Annealed Ti-6Al-4V Alloy GD Specification FMS-1109D	39
6	Chemical Composition of ASTM Artificial Sea Water (ASTM-D1141)	46
7	Tensile Properties for 7075-T7651 Aluminum Alloy and $\beta$ -Annealed Ti-6Al-4V Alloy	76
8	Fracture Toughness Properties for 7075-T7651 Aluminum and $\beta$ -Annealed Ti-6Al-4V Alloy	76
9	Stress Corrosion Properties for 7075-T7651 Aluminum Alloy	78
10	$K_{ISCC}$ of $\beta$ -Annealed Ti-6Al-4V Alloy	79
11	Normalized Number of Cycles to Crack Initiation ( $a_0 = 0.010''$ ) and Failure for 7075-T7651 Aluminum Alloy in Dry Air and in a 3.5% NaCl Solution	85
12	Small-Sample Test Evaluations for Differences in Mean $N_i$ for Different Frequencies (7075-T7651; 3.5% NaCl)	89
13	Normalized Number of Cycles to Crack Initiation ( $a_0 = 0.010''$ ) and Failure for $\beta$ -Annealed Ti-6Al-4V Alloy in Dry Air and a 3.5% NaCl Solution	93
14	Small-Sample Test Evaluations for Differences in Mean $N_i$ for Different Frequencies $\beta$ -Annealed Ti-6Al-4V Alloy	96

## LIST OF TABLES (Continued)

<u>Table</u>		<u>Page</u>
15	Summary of Stress-Initiation Life Model Parameters for Aluminum and Titanium	141
16	Summary of Crack Initiation Results ( $a_0 = 0.010''$ ) Stress-Initiation Life Model Parameters and Statistics (7075-T7651 Aluminum Alloy)	142
17	Summary of Crack Initiation Results ( $a_0 = 0.010''$ ) Stress-Initiation Life Model Parameters and Statistics ( $\beta$ -Annealed Ti-6Al-4V Alloy)	143
18	Test Variables	168
19	Summary of Test Specimens for Phase II	169
20	Phase II Tests for Task 5	170
21	Phase II Verification Tests for Task 6	171
22	Titanium Crack Growth Tests for Phase II	172

LIST OF SYMBOLS

- a = Radius of elliptical hole in the major axis
- $a_0$  = Crack initiation crack size
- A = Empirical constant determined from plot of  $\log N_i$  versus  $\Delta\sigma_{eff}^2 - \Delta\sigma_{th}^2$
- b = Radius of elliptical hole in the minor axis or fatigue-strength exponent
- B = Fatigue-strength exponent or  $\Delta\sigma_{th}^2$
- C = Fatigue-ductility exponent or  $N_i \Delta\sigma^2$
- CF = Corrosion fatigue
- D = Diffusivity of Hydrogen
- $\left(\frac{da}{dN}\right)_e$  = Rate of fatigue crack growth in an aggressive environment
- $\left(\frac{da}{dN}\right)_{cf}$  = Cycle-dependent corrosion fatigue crack growth rate
- $\left(\frac{da}{dN}\right)_{cf} = \left[ \left(\frac{da}{dN}\right)_{cf,s}^* - \left(\frac{da}{dN}\right)_r \right] \phi$
- $\left(\frac{da}{dN}\right)_{cf,s}^*$  = Cycle-dependent rate of "pure" corrosion fatigue crack growth
- $\left(\frac{da}{dN}\right)_{cf,s}$  = Saturation fatigue crack growth rate for the transport and surface reaction controlled case
- $\left(\frac{da}{dN}\right)_r$  = Rate of fatigue crack growth in an inert environment
- $\left(\frac{da}{dN}\right)_{scc}$  = Contribution of sustained-load crack growth (i.e., by stress corrosion cracking) at K levels above  $K_{Iscc}$

LIST OF SYMBOLS (Continued)

$E$	=	Elastic modulus or error
$E_d$	=	Activation energy for hydrogen diffusion
$f$	=	Cyclic load frequency
$G_B$	=	Binding energy of hydrogen atoms to a dislocation
$k$	=	Boltzmann's constant
$k_c$	=	Reaction rate constant
$K_I$	=	Stress intensity factor
$K_{Ic}$	=	Critical stress intensity factor for static loading and plane strain conditions or plane-strain fracture toughness
$K_{Iscc}$	=	Plane strain stress intensity threshold below which subcritical cracks will not propagate under static loading
$K_Q$	=	Tentative value of plane strain fracture toughness
$K_t$	=	Elastic stress concentration factor
LCF	=	Low cycle fatigue
$M$	=	Molecular weight of the gas
$n'$	=	Cyclic work hardening exponent
$N_f$	=	Number of cycles to failure
$N_i$	=	Number of cycles to fatigue crack initiation
$N_o$	=	Density of surface sites
$p$	=	Pressure at the crack tip
$p_o$	=	Pressure of gas in surrounding environment

## LIST OF SYMBOLS (Continued)

- $R$  = Stress ratio or gas constant  
 $t$  = Time  
 $T$  = Absolute temperature  
 $U_{CRIT}$  = Critical energy for fatigue crack initiation  
 $\bar{X}$  = Mean  
 $Z$  = No. of standard deviations from the mean  
 $\alpha, \beta$  = Empirical constant for surface roughness and gas flow, respectively  
 $\sigma'_f$  = Fatigue-strength coefficient  
 $\sigma_{ys}$  = Yield strength of the material  
 $\sigma'_o$  = Cyclic yield stress  
 $\sigma(\bar{X})$  = Standard deviation for  $\bar{X}$   
 $\Delta\sigma$  = Stress range  
 $\Delta\sigma_{eff}$  = Effective stress range =  $\sigma_{max} - \sigma_{min}$   
                   where load sequence or load interaction does not occur  
 $\Delta\sigma_{th}$  = Threshold stress for crack initiation corresponding to the fatigue limit  
 $\Delta\sigma_{rms}$  = Root mean squared  $\Delta\sigma = \sqrt{\frac{\sum_{i=1}^k \Delta\sigma_i^2}{n}}$   
 $\Delta\epsilon_{rms}$  = Root mean squared  $\Delta\epsilon = \sqrt{\frac{\sum_{i=1}^k \Delta\epsilon_i^2}{n}}$

LIST OF SYMBOLS (Continued)

$\epsilon'_f$	=	Fatigue-ductility coefficient
$\Delta\epsilon$	=	Total strain range
$\Delta\epsilon_e$	=	Elastic strain range
$\Delta\epsilon_p$	=	Plastic strain range
$\Delta K$	=	Range of stress intensity factor
$\phi$	=	Areal fraction for corrosion fatigue
$\nu$	=	Poisson's ratio

## SUMMARY

A mechanistic-based corrosion fatigue (CF) methodology has been developed for predicting the crack initiation and crack propagation behavior of mechanically-fastened joints. In Phase I, the CF methodology was evaluated using constant amplitude test results.

An experimental corrosion fatigue test program was conducted using 7075-T7651 aluminum alloy and  $\beta$ -annealed Ti-6Al-4V alloy in order to: (1) develop a better understanding of the effects of environment, test frequency, R-ratio, holding-time and stress level on corrosion fatigue behavior, (2) provide experimental data needed to evaluate the CF methodology developed, and (3) provide a basis for developing the Phase II test plan.

Based on the Phase I effort it was concluded that:

1. The fatigue crack growth rate for 7075-T7651 aluminum alloy appears to be independent of the test frequency and holding-time in the aqueous environments. This implies that the reaction between the aqueous environment and 7075-T7651 aluminum alloy is limited and

suggests that a special crack propagation model for corrosion fatigue is not required for this alloy for design.

2. The corrosion fatigue behavior of  $\beta$ -annealed Ti-6Al-4V alloy is a complex function of the environment, test frequency, and R-ratio. A better understanding of the basic mechanisms is needed before a reliable predictive corrosion fatigue methodology can be developed for mechanically-fastened joints.

3. The corrosion fatigue predictive methodology looks promising for constant amplitude applications. In Phase II, the methodology should be further developed to account for spectrum loading and variance in the input data base.

## SECTION I

### INTRODUCTION

#### 1.1 PROGRAM OBJECTIVES

The objectives of this program are to:

1. Develop and verify an analytical methodology for predicting the crack initiation and crack propagation behavior of mechanically-fastened joints in a corrosive environment.
2. Develop corrosion fatigue test/data acquisition methods and guidelines for acquiring statistically-valid data needed to implement the analytical methodology.
3. Study the effects of various factors influencing the corrosion fatigue behavior (initiation and propagation) of mechanically-fastened joints.

This program is referred to as the "Corrosion Fatigue" program or CF program in this report.

## 1.2 SCOPE

The CF program, initiated on 1 June 1981, is divided into two phases and tasks as follows:

### Phase I - Methodology Assessment/Development and Test Plan

- o Task 1 - Methodology and Data State-of-the-Art Assessment
- o Task 2 - Methodology Development
- o Task 3 - Test Plan Development

### Phase II - Data Acquisition and Methodology Evaluation

- o Task 4 - Experimental Methodology Development and Evaluation
- o Task 5 - Acquisition of Data for Prediction of Environmentally-Assisted Crack Growth in Aircraft Joints
- o Task 6 - Prediction Methodology Evaluation and Verification

This report (Vol. I) documents Task 2 and 3. Task 1 is documented in Volume II.

## 1.3 ORGANIZATION

The report also includes six other sections as follows:

- o Section II - Corrosion Fatigue Methodology  
Development
- o Section III - Phase I Experimental Test Program
- o Section IV - Phase I Test Results
- o Section V - Evaluation of Corrosion Fatigue  
Models
- o Section VI - Conclusions and Recommendations
- o Section VII - Phase II Test Plan

This is followed by Appendices A and B and a list of references.

NADC-83126-60 Vol. I

THIS PAGE INTENTIONALLY LEFT BLANK

## SECTION II

### CORROSION FATIGUE METHODOLOGY DEVELOPMENT

#### 2.1 INTRODUCTION

The corrosion fatigue (CF) methodology developed in Phase I is described and discussed in this section. First, two crack initiation models and two crack propagation models are discussed for possible corrosion fatigue applications. Then, analytical procedures are described for predicting crack initiation and crack propagation under spectrum loading and a corrosive environment.

#### 2.2 CRACK INITIATION MODELS

Mechanistic and fundamental phenomena for corrosion fatigue crack initiation are discussed in the state-of-the-art assessment report (Vol. II). These phenomena are discussed both in general terms and in quantitative, analytical terms in this section. The corrosion fatigue crack initiation process is complicated. We believe that crack initiation is due to the mechanical force from cyclic loads which causes a to-and-fro motion of dislocations along slip planes. This leads to the formation of slip steps. In an aqueous environment a localized electrochemical potential is created. This results in a preferential corrosive attack

at these slip steps which accelerates the process of corrosion fatigue crack nucleation.

Two mechanistic models are proposed for analytically quantifying fatigue crack initiation life in a corrosive environment: (1) stress-initiation life model and (2) strain-initiation life model. These models are described and discussed in this section. Applications of these models to spectrum loading using the "RMS Method" or the "Palmgren-Miner Linear-Cumulative-Damage Rule," are discussed in Volume II.

#### 2.2.1 Stress-Initiation Life Model

This model is based on a critical local plastic strain accumulation criterion. For blunt notches including fastener holes, Kim, Fine, and Mura [1,2] derived an expression for the number of cycles to fatigue crack initiation for constant amplitude loading. In their derivation, elastic-plastic micro-mechanics at the tip of a smooth-ended notch or fastener hole [3,4] was extended to the cyclic loading case in order to predict the number of cycles to crack initiation. The number of cycles to initiation was expressed as a function of effective stress amplitude,  $\Delta\sigma_{eff}$ , notch geometry (circular for fastener

holes) and some measurable material properties such as cyclic work hardening rate, Young's modulus and cyclic yield stress. The following two assumptions were made on the basis of mechanistic and phenomenological understandings:

1. With stress cycling, displacements are locally accumulated at singularities encountered on the surface near a stress concentration (in particular, extrusions-intrusions along slip bands, constituent particles, inclusions and grain boundaries).

2. Fatigue crack initiation occurs when the accumulated displacement at these singularities reaches a critical value.

Based on these assumptions, the stress-initiation life model is formulated as a "critical dissipated energy criterion" for crack initiation. The final expression is shown in Eq. 1 for an elliptical hole.

$$N_1 = \frac{\pi EU_{crit} (1+n')}{8(1-\nu)} \left(\frac{b}{a}\right) \left[ \Delta\sigma_{eff}^2 - \Delta\sigma_{th}^2 \right]^{-1} \quad (1)$$

where  $N_1$  = number of cycles to fatigue crack initiation

$E$  = Young's modulus

$U_{crit}$  = critical energy for initiation, which may be determined experimentally

$n'$  = cyclic work hardening exponent

$\nu$  = Poisson's ratio

$a$  = Semi-major axis of elliptical hole

$b$  = Semi-minor axis of elliptical hole

$\Delta\sigma_{eff}$  = effective stress range

$\Delta\sigma_{th}$  = threshold value of  $\Delta\sigma$  for crack initiation corresponding to the fatigue limit

The model is simplified for the case of a fastener hole where  $a = b$ , by treating the term  $\frac{\pi U_{crit}}{8(1-\nu)}$  as an empirical constant  $A$ .

$$N_1 = A \left[ E \cdot (1+n') \right] \left[ \Delta\sigma_{eff}^2 - \Delta\sigma_{th}^2 \right]^{-1} \quad (2)$$

The empirical constants  $A$  and  $\Delta\sigma_{th}$  can be readily determined from plots of  $\log N_i$  vs.  $\log(\Delta\sigma_{eff}^2 - \Delta\sigma_{th}^2)$ . For constant amplitude cyclic loading, where load sequence or load interaction does not occur,  $\Delta\sigma_{eff}$  is simply  $\sigma_{max} - \sigma_{min}$ . For spectrum loading,  $\Delta\sigma_{eff}$  can be replaced by  $\Delta\sigma_{rms}$  as explained in Section 3.3.3 of Volume II.

Since  $A$  and  $\Delta\sigma_{th}$  are determined experimentally, Eq. 2 is semi-empirical. Fig. 1 conceptually illustrates the relationships between plots of  $\log N_i$  vs.  $\log(\Delta\sigma_{eff}^2 - \Delta\sigma_{th}^2)$  and those of  $N_i$  vs.  $\Delta\sigma_{eff}$ . This representation demonstrates how well Eq. 2 predicts a well-known S-N type of fatigue crack initiation. The value of  $A$  in Eq. 2 is expected to be lower in a corrosive environment due to load-electrochemical interaction. The fatigue crack initiation life decreases as  $A$  decreases. Thus,  $A$  and  $\Delta\sigma_{th}$  should serve as useful indices of the severity of the environment (Ref. Subsection 5.2).

### 2.2.2 Strain-Initiation Life Model

This method is referred to as the "Coffin-Manson Type Low Cycle Fatigue (LCF) Approach." Coffin and Manson [5,6] established that plastic strain-life data could be linearized with log-log coordinates. Using data for several

(1) STRESS-INITIATION LIFE MODEL (CRITICAL LOCAL PLASTIC STRAIN ACCUMULATION CRIT.)

$$N_1 = A [E \cdot (1 + n')] [\Delta \sigma_{eff}^2 - \Delta \sigma_{th}^2]^{-1}$$

(Ref. 4)

A = EMP. CONST.

E = YOUNG'S MODULUS

n' = CYCLIC WORK HARDENING EXP.

$\Delta \sigma_{eff} = \sigma_{max} - \sigma_{min}$

$\Delta \sigma_{th}$  = THRESHOLD VALUE (EXPERIMENTAL VALUE)

$N_1$  = CYCLES TO INITIATION

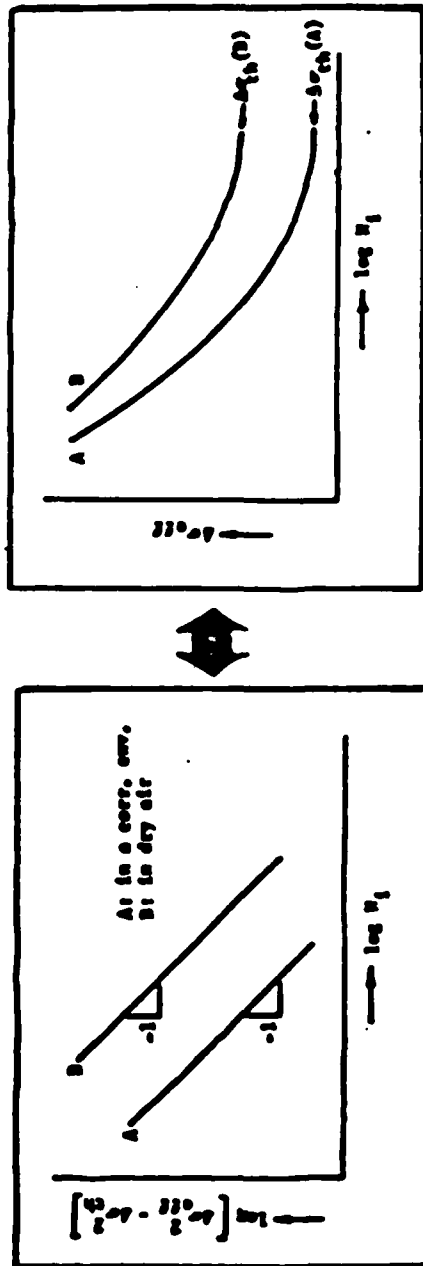


Fig. 1 Schematic Representation of Stress-Initiation Life Model

metals and alloys, plastic strain and cycles to failure were related by the power-law equation, Eq. 3.

$$\frac{\Delta \epsilon_p}{2} = \epsilon_f' (2N_f)^c \quad (3)$$

where  $\Delta \epsilon_p$  = plastic-strain range

$N_f$  = Number of cycles to failure

$c$  = fatigue-ductility exponent ( $c < 0$ )

$\epsilon_f'$  = fatigue-ductility coefficient

Eq. 3 has also been verified by other investigators [7-10] for various alloys, including 7075-T7651 aluminum alloy and  $\beta$ -annealed Ti-6Al-4V alloy.

Recently, investigators [11,12] have verified the Coffin-Manson strain life approach using strain-initiation life data [13,14]. Eq. 3 can be modified by substituting  $N_i$  for  $N_f$ , if cyclic parameters are determined from the plots of  $\Delta \epsilon_p$  vs.  $N_i$  instead of  $\Delta \epsilon_p$  vs.  $N_f$  plots. Thus,

$$\frac{\Delta \epsilon_p}{2} = \epsilon_f' (2N_i)^c \quad (4)$$

where  $2N_i$  is the reversals to fatigue crack initiation.

Fig. 2 schematically shows how cyclic strain-life parameters can be determined from the plots of log of strain amplitude vs. log of cycles to fatigue crack initiation (modified Coffin-Manson plots). The total applied cyclic strain amplitude is the sum of two components, elastic strain and plastic strain. From Fig. 2, elastic and plastic strain may be expressed by Eq. 6 and Eq. 7, respectively.

$$\text{Total strain range; } \Delta\epsilon = \Delta\epsilon_e + \Delta\epsilon_p \quad (5)$$

$$\text{Elastic strain; } \frac{\Delta\epsilon_e}{2} = \frac{\sigma_f'}{E} (2N_1)^b \quad (6)$$

$$\text{Plastic strain; } \frac{\Delta\epsilon_p}{2} = \epsilon_f' (2N_1)^c \quad (7)$$

where  $\sigma_f'$  = fatigue-strength coefficient

$\epsilon_f'$  = fatigue-ductility coefficient

$b$  = fatigue-strength exponent ( $b < 0$ )

$c$  = fatigue-ductility exponent ( $c < 0$ )

The parameters above can be determined using a Coffin-Manson type plot illustrated in Fig. 2. Total strain can be expressed by these cyclic parameters and  $N_1$ , cycles to initiation as shown in Eq. 8.

$$\frac{\Delta\epsilon}{2} = \frac{\sigma_f'}{E} (2N_1)^b + \epsilon_f' (2N_1)^c \quad (8)$$

(2) STRAIN-INITIATION LIFE MODEL (MODIFIED COFFIN-MANSON TYPE LCF APP.)

$$\frac{\Delta \epsilon}{2} = \underbrace{\frac{\sigma_f'}{E} (2 N_i)^b}_{\text{ELASTIC}} + \underbrace{\epsilon_f' (2 N_i)^c}_{\text{PLASTIC}}$$

$\Delta \epsilon$  = TOTAL STRAIN (STRAIN-CONTROLLED)

$\sigma_f'$  = FATIGUE-STRENGTH COEFF.

$\epsilon_f'$  = FATIGUE-DUCTILITY COEFF.

$b$  = FATIGUE-STRENGTH EXP.

$c$  = FATIGUE-DUCTILITY EXP.

$N_i$  = CYCLES TO INITIATION

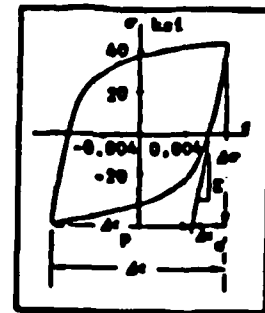
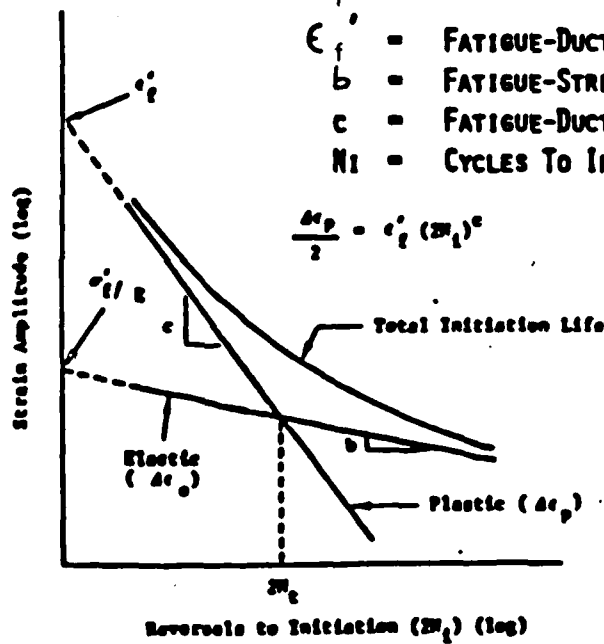


Fig. 2 Schematic Representation of Strain-Initiation Life Model

The cyclic parameters,  $\sigma_f'$  and  $\epsilon_f'$ , should vary depending on the environment. In general, higher values are expected for the cyclic parameters in a chemically deleterious environment than in dry air because of embrittlement. This reduces the number of cycles to crack initiation in a corrosive environment,  $N_i$ , at a given strain level.

For strain-controlled tests, or for tests where the total strain is known, initiation life can be estimated by Eq. 8, once all other parameters in Eq. 8 are determined in a given environment. This method is considered a powerful tool, because the corrosion fatigue cyclic parameters, based on Eq. 8, provide a means for predicting corrosion fatigue initiation life which is a major portion (approximately 50%-90%) of the overall corrosion fatigue life of fastened joints. Strain-controlled tests will be performed in Phase II to evaluate the Coffin-Manson approach for crack initiation. Stress concentration at a fastener hole will be used to relate the data from smooth specimens to the results for specimens with fastener holes.

### 2.3 MECHANISTIC CRACK PROPAGATION MODELS

There are two key questions with respect to mechanistic propagation models. The first question is -- What is a "realistic" corrosion fatigue crack propagation model where significant parameters are taken into account? Such

parameters include the loading, load ratio (R), frequency, holding time (i.e., time for sustained load and environmental exposure), rest time (i.e., time for no-load and exposure to environment), and "severeness" of the environment. The second question is -- How can the mechanistic models be quantified to predict corrosion fatigue crack growth behavior?

### 2.3.1 Controlling Processes and Models

To address the first question, it is essential to recognize two facts. Firstly, the precise mechanism for corrosion fatigue crack growth (hydrogen embrittlement versus active path dissolution) is not fully understood. Secondly, corrosion fatigue crack growth results from a sequence of processes, with the fracture process as the final step in this sequence. The crack growth rate is determined by the slowest process in this sequence. If each of the preceding processes is fast relative to the cracking process, then the precise mechanism for corrosion fatigue is not important in modeling the cracking response. The hydrogen embrittlement mechanism, however, is now favored by most workers for corrosion fatigue of aluminum and titanium alloys and high-strength steels.

The processes involved in corrosion fatigue (also in stress corrosion cracking) include transport of the deleterious species or environment to the crack tip region, reactions of the environment with the fresh crack surfaces at the crack tip (or dissolution), hydrogen entry and diffusion to the fracture zone, and the local process of fracture. Based on the concept of a rate determining process, models for transport-controlled and surface-reaction-controlled fatigue crack growth have been proposed by Weir et al. [15] and Wei and Simmons [16]. A model for diffusion-controlled crack growth has been proposed by Kim [17]. To be useful, the models must be linked to the actual corrosion fatigue crack growth rate. These models include the effect of holding time, but do not address the possible contributions of rest time (e.g., blunting of the crack by localized corrosion).

### 2.3.2 Quantification of the Mechanistic Propagation Models

The mechanistic model has been linked to the corrosion fatigue crack growth rate using the superposition model suggested by Wei et al. [18,19]. In the original formulation, the environmentally-assisted fatigue crack growth rate,  $(da/dN)_e$ , is the sum of three components.

$$\left. \begin{aligned} (da/dN)_e &= (da/dN)_r + (da/dN)_{cf} + (da/dN)_{scc} \\ &= (da/dN)_r + (da/dN)_{cf} + \int_0^T |da/dt(K)| dt \end{aligned} \right\} \quad (9)$$

$(da/dN)_r$ , the rate of fatigue crack growth in an inert environment, represents the contribution of "purely mechanical" fatigue. This component is essentially independent of frequency, holding time and waveform at temperatures where creep is not important. This component is a function of only stress (or stress intensity  $K$ ) level and load ratio (the ratio of minimum and maximum load in one loading cycle). However, internal hydrogen in alloys such as titanium alloys can contribute to crack growth in the absence of influence from an external environment. In such cases, an additional influence of frequency is expected. The influence of internally dissolved hydrogen may be explicitly considered as a part of this term, or as a part of the cycle-dependent corrosion fatigue crack growth rate  $(da/dN)_{cf}$ .

$(da/dN)_{cf}$  represents the cycle-dependent contribution, requiring the synergistic interaction of fatigue and environment. Thus, this term is a function of  $\Delta K$ , environment, frequency and perhaps waveform, but is not expected to depend on load ratio  $R$  [19]. This term is expected to contribute a major portion of crack growth rate enhancement to aluminum and titanium alloys in deleterious environments. The mechanistic propagation model has been quantified by relating  $(da/dN)_{cf}$  to the rate determining

processes described previously, and is described in the following section.

The third term in Eq. 9,  $(da/dN)_{scc}$ , represents the contribution of sustained-load crack growth (e.g., stress corrosion cracking) at  $K$  levels above the stress corrosion cracking threshold ( $K_{Iscc}$  or  $K_{scc}$ ). This contribution is a function of stress or stress intensity level, load ratio, waveform (including holding time), and environment. Mechanistic consideration of  $(da/dN)_{scc}$  follows directly from that for sustained-load crack growth. This consideration has been described by Wei [20], and is not included here.

Recent review of the superposition model [21] suggests that an alternate formulation might be more appropriate. In the proposed formulation, "pure" fatigue and "corrosion" fatigue are considered as parallel processes, each with a characteristic rate  $(da/dN)_r$  and  $(da/dN)_{cf,s}^*$ . The sustained-load contribution results from a consecutive (or subsequent) process, and contributes a rate  $(da/dN)_{scc}$  to the overall process. If  $\phi$  is the areal fraction for corrosion fatigue, then the measured crack growth rate, is given by the following expression.

$$\left. \begin{aligned} (da/dN)_e &= (da/dN)_r (1 - \phi) + (da/dN)_{cf,s}^* \phi + (da/dN)_{scc} \\ &= (da/dN)_r + [(da/dN)_{cf,s}^* - (da/dN)_r] \phi \\ &\quad + (da/dN)_{scc} \end{aligned} \right\} (10)$$

The form of Eq. 10 is identical to the original model, and all of the fundamental arguments remain unchanged. The term  $[(da/dN)_{cf,s}^* - (da/dN)_r]\phi$  is identified with the cycle-dependent corrosion fatigue,  $(da/dN)_{cf}'$  term in the original formulation. This new formulation is fundamentally more attractive because the rate  $(da/dN)_{cf,s}^*$  can be more readily associated with the various microstructural elements and their interactions with the environment (or hydrogen). To keep the notations simple, the mechanistic models will be discussed in terms of the original formulation of the superposition model.

### 2.3.3 Model Summaries

For gaseous environments, the specific models for  $(da/dN)_{cf}'$  or  $[(da/dN)_{cf,s}^* - (da/dN)_r]\phi$ , are as follows [15-17]:

#### Transport Control:

$$(p_o/2f)_s = \left[ 436 \frac{\beta^*}{\alpha} f(R) \frac{\sigma_{ys}^2}{N_o k T E^2} \left( \frac{T}{M} \right)^{1/2} \right]^{-1} \quad (11a)$$

$$\frac{(da/dN)_{cf}}{(da/dN)_{s,s}} = 436 \frac{\beta^*}{\alpha} f(R) \frac{\sigma_{ys}^2}{N_o k T E^2} \left( \frac{T}{M} \right)^{1/2} \frac{p_o}{2f} \quad (11b)$$

$$\frac{(da/dN)_{cf}}{(da/dN)_{cf,s}} = \frac{(p_o/2f)}{(p_o/2f)_s} \quad (11c)$$

$$f(R) = \frac{1}{4} \left[ \left( \frac{1+R}{1-R} \right)^2 + \frac{1}{2} \right] \quad (11d)$$

Surface Reaction Control:

$$\frac{(da/dN)_{cf}}{(da/dN)_{cf,s}} = 1 - \exp(-k_c p_0 / 2f) \quad (12a)$$

$$\frac{(da/dN)_{cf}}{(da/dN)_{cf,s}} = 1 - \exp(-k_c p_0 / 2f) \quad (12b)$$

Diffusion Control:

$$\left(\frac{da}{dN}\right)_{cf} = A \exp(-G_B/RT) \sqrt{\frac{pd}{2f}} (\Delta K/\sigma'_0)^2 \quad (13)$$

In the transport and surface reaction controlled models, subscript s denotes the values at saturation, which is defined as the maximum in environmental effect and corresponds to the attainment of complete reactions with the active crack surfaces during each loading cycle. The terms in the equations are as follows:  $f$  = cyclic load frequency;  $k_c$  = reaction rate constant;  $M$  = molecular weight of the gas;  $N_0$  = density of surface sites;  $p_0$  = pressure of gas in the surrounding environment;  $k$  = Boltzmann's constant; and  $T$  = absolute temperature.  $E$  and  $\sigma_{ys}$  are the elastic modulus and yield strength of the material, respectively. The parameter  $\beta^*/a$  is a ratio of empirical constants for surface roughness and flow, and appears to be a constant (equal to approximately 3.8). For the diffusion controlled model,  $A$  = proportionality constant;  $G_B$  = binding energy of hydrogen atoms to a dislocation;  $R$  = gas constant;  $p$  = pressure at

the crack tip;  $D$  = diffusivity of hydrogen;  $t$  = time available for reaction; and  $\sigma_c'$  = cyclic yield stress. For consistency,  $t$  is again taken to be equal to  $1/2f$ . Additionally, the diffusion controlled growth model must recognize the potential contribution of dissolved hydrogen (particularly in the case of titanium alloys). The precise form of the expression  $(da/dN)_{cf}$  depends on the "laws" governing the flow of hydrogen to the crack tip caused by the interaction of hydrogen with the stress (strain) field and the outward flow produced by the resulting concentration gradient.

These mechanistic models have been developed for the case of pure (single component) gases. For the case of multi-component gases (such as air), the competing effects of other components (either beneficial or deleterious) must be accounted for [17]. Extension of these models to corrosion fatigue crack growth in aqueous environments can be made; at least conceptually. Liquid transport and transport of specific species, and electrochemical (or metal-liquid) reactions must now be considered. For the purpose of this program, the key variables of concern are frequency, holding time, and  $\Delta K$  (or load ratio). The dependence of crack growth rates on these variables can be readily extracted from consideration of models for gaseous environments. Rest time, on the other hand, is not considered in these models and must be addressed separately to determine its significance.

#### 2.3.4 Implications of the Models

For design applications, it is necessary to assess the validity and to define the range of applicability of each of the models. A considerable amount of experimental support has been developed at Lehigh University for the transport controlled model. Some support for the other two models is available, but must be supplemented by additional data from this and other programs. The range of applicability of the models is governed by the transfer of control from one rate controlling process to another. The environmental conditions (viz., pressure and temperature) that dictate this transfer of control may be determined, in principle, by equating  $(da/dN)_{cf}$  for each case and then calculating the pressure-temperature relationship for the transfer. In practice, the conditions for transfer can be predicted only if the parameters in the models are known with sufficient accuracy and detail. Specific comments can be made, however, about the aluminum and titanium alloys and the environments of interest to this program.

Measurements of the kinetics of reactions of water vapor with aluminum and titanium alloys have been made at Lehigh University under other programs. These measurements

indicate that these reactions are extremely rapid (corresponding to an initial sticking coefficient of nearly one). As such, surface reaction cannot be the rate controlling process for these alloy-environment systems. For gases, therefore, fatigue crack growth conforms to transport control at  $(p_o/2f)$  below  $(p_o/2f)_s$  defined previously. Typically,  $(p_o/2f)_s$  is of the order of 10 Pa-s. At  $(p_o/2f)$  greater than  $(p_o/2f)_s$  and in aqueous environments, one would expect transfer of control to one of the subsequent processes; namely, hydrogen diffusion.

For the case of corrosion fatigue of aluminum and titanium alloys in aqueous environments, the models to be considered are in essence the transport-controlled model (at saturation) and the diffusion-controlled model. Evaluation of the models is to be made principally through the dependence of  $(da/dN)_{cf}$  on frequency and holding time. The transport controlled model predicts an independence of frequency and holding time, and the diffusion-controlled model yields an inverse square-root dependence on frequency or on holding time. These models were derived considering the rate controlled processes, and do not allow for other restrictions. The diffusion-controlled model was derived with the implicit assumption that the supply of hydrogen would be ample. However, because the extent of reactions of

water vapor with aluminum and titanium alloys is limited, this assumption is violated. The controlling process for crack growth in water vapor thereby becomes unclear when  $(p_0/2f)$  exceeds  $(p_0/2f)_s$ . It is not clear whether the assumption of continuous supply of hydrogen is valid for the case of aqueous environments, or whether liquid-phase transport might be rate controlling. In any case, the pressure term in the model must be replaced, perhaps by hydrogen fugacity at the input surface, and additional experimental and modeling efforts are needed to resolve these critical issues.

Although the effect of  $\Delta K$  is included explicitly only for the diffusion controlled model, the dependence of  $(da/dN)_{cf}$  on  $(\Delta K)^2$  is implied for the other two models. If the amount of hydrogen produced per cycle is proportional to the available fresh surface area, the hydrogen will probably be concentrated in a zone near the crack tip. As a result, the "saturation" growth rate,  $(da/dN)_{cf,s}$ , for the transport and surface reaction controlled case, is expected to be a function of  $(\Delta K)^2$  and independent of the load ratio (R). This aspect needs to be verified.

## 2.4 CORROSION FATIGUE PREDICTIVE METHODOLOGY

Elements of the corrosion fatigue predictive methodology for mechanically-fastened joints are conceptually described in Fig. 3. The basic approach for the predictive methodology is described and discussed in this section. Further details are also given in Volume II.

In Phase I, the approach for the corrosion fatigue predictive methodology was developed and selected elements were also evaluated. For example, the stress-initiation life model for fatigue crack initiation and the superposition model for crack propagation were evaluated in Phase I. However, further details of the methodology will be developed, evaluated, and verified in Phase II.

Fatigue crack initiation and crack propagation are treated separately. The total fatigue life, or time-to-failure (TTF), is the sum of the initiation life and the propagation life. The predictive methodology will include a statistical approach which accounts for the effects of the variance in the experimental data base on the analytical prediction for time-to-crack initiation (TTCI) and the time-to-failure. Details of the statistical approach will be developed and evaluated in Phase II.

Both the stress-initiation life model [1,2] and the strain-initiation life model [5,6] will be considered for predicting the TTCI. The TTCI will be determined for a selected crack size in a fastener hole (e.g.,  $a_0 = 0.010"$  using the baseline data developed in Phase I and Phase II. Details for predicting the TTCI for fastener holes (load and unloaded) for a corrosive environment and spectrum loading will be worked out in Phase II of the program.

The fatigue crack propagation from  $a_0$  to  $a_{cr}$  will be determined using a deterministic crack growth approach (see Fig. 3). It is assumed that existing state-of-the-art tools (e.g., cycle counting schemes, retardation model, analytical crack growth computer program, etc.) can be used to make crack growth predictions for a mechanically-fastened joint subjected to a corrosive environment and spectrum loading.

The CF analysis tools for predicting the TTCI and the TTF for a mechanically-fastened joint will be incorporated into a predictive methodology in Phase II.

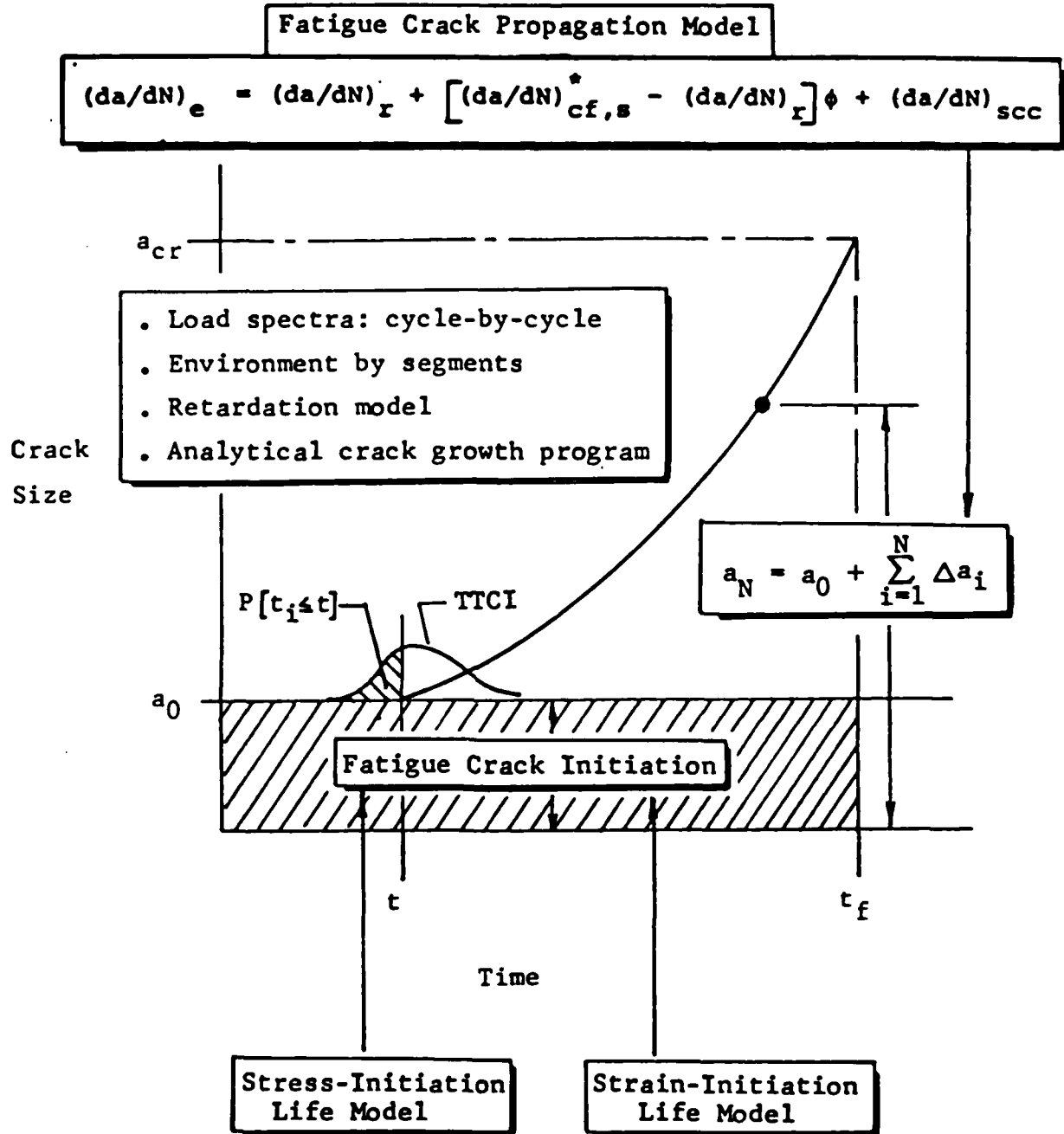


Fig. 3 Elements of the Corrosion Fatigue Methodology

NADC-83126-60 Vol. I

THIS PAGE INTENTIONALLY LEFT BLANK

### SECTION III

#### PHASE I EXPERIMENTAL TEST PROGRAM

##### 3.1 INTRODUCTION

An experimental test program was conducted in Phase I. The basic objectives of this initial test program were:

1. Provide experimental data needed to evaluate and verify the corrosion fatigue models for crack initiation (stress-initiation life) and for crack propagation (Ref. Subsection 2.3).

2. Identify the most significant variables affecting corrosion fatigue crack initiation and crack propagation and investigate the effects of selected variables on the overall fatigue life.

3. Develop an appropriate experimental data base to further the understanding of the corrosion fatigue mechanisms and to provide a basis for developing the Phase II test plan.

The Phase I experimental test program is described in this section. Details of the test plan and the experimental

procedures used are described and discussed. Experimental results are documented in Section IV.

### 3.2 TEST PLAN

Essential details of the test plan are described in this section.

#### 3.2.1 Test Matrix

The Phase I test matrix is described in Tables 1-4. Basic material property tests are described in Table 1. Fatigue crack initiation tests and fatigue crack propagation tests performed are noted in Tables 2 and 3, respectively. Finally, in Table 4 the tests for investigating the effects of different environments on crack propagation are shown.

#### 3.2.2 Materials

Two materials were used for the Phase I testing: 7075-T7651 aluminum alloy and  $\beta$ -annealed Ti-6Al-4V alloy. The justifications for using these materials and material descriptions are discussed below.

Table 1 Phase I Test Plan for Basic Properties

Test		Specimen Type	No. Specimen	Subtotal
TS		A	○ ●	2
$K_c$		B	○ ● ○ ●	4
$K_{scc}$		B	○ ● ○ ●	4
Cyclic $\sigma$ vs. $\epsilon$	S.W. D.A.	C	○ ●	2
	S.W.	C	○ ●	2
				14

## Notation

- : 7075-T7651 Aluminum Alloy  
 ● :  $\beta$ -annealed Ti-6Al-4V Alloy

## Specimen Types

- A : Round Tensile Specimen (Fig. 5)  
 B : Compact Tension Specimen  
     (7075-T7651; Fig. 6)  
     (Ti-6Al-4V ( $\beta$ ); Fig. 7)  
 C : Dogbone Specimen (Fig. 8)

Table 2 Phase I Test Plan for Fatigue Crack Initiation Tests  
(Stress-Controlled)

$\Delta\sigma$ (ksi)	Test Conditions			Subtotal
	Dry Air	3.5% NaCl Solution		
	6Hz	1Hz	6Hz	
25	o	---	o	32
22.5	o	---	o	
20	ooo	ooo	oooo	
18	o	---	o	
17	ooo	---	---	
16.5	---	ooo	ooo	
16.2	o	---	---	
16	o	---	o	
15	---	---	o	
14	o	---	o	
13.6	---	---	o	
70	•	---	•	30
60	•	---	---	
55	•	---	•	
50	•••	•••	•••	
45	•	---	•	
40	•	---	•	
35	•	•••	••••	
32.5	•	---	•	
30	---	---	•	
27.5	---	---	•	
Notation: o 7075-T7651 Aluminum Alloy				62

Notation: o 7075-T7651 Aluminum Alloy  
• 8-Annealed Ti-6Al-4V Alloy

Dogbone Specimen (Fig. 9)

**Table 3 Phase I Test Plan for Evaluating the Effects of Environment, R Ratio, Frequency and Holding Time on Fatigue Crack Propagation**

Envir. →		Dry Air or Vac.		3.5% NaCl				Subtotal
R Ratio →		0.05	0.3	0.05	0.2	0.3	0.4	
Freq. (Hz) (sine wave)	0.1	o	o	o ●	---	o ●	---	34
	0.3	---	---	o ●	---	o ●	---	
	1.0	o ●	o ●	o ●	---	o ●	---	
	3.0	---	---	o ●	---	o ●	---	
	5.0	●	---	---	---	---	---	
	6.0	o	o	o	o	o	o	
	10.0	---	●	●	●	●	●	
Hold T. (Trapez.)	$\tau_1$	---	---	o ●	---	---	---	6
	$\tau_2$	---	---	o ●	---	---	---	
	$\tau_3$	---	---	o ●	---	---	---	
								40

Notation: o 7075-T7651 Aluminum Alloy (Compact Ten. Spec.; Fig. 6)  
 o  $\beta$ -Annealed Ti-6Al-4V Alloy (CTS; Fig. 7)

Table 4 Phase I Test Plan for Evaluating the Effects of Environment on Fatigue Crack Propagation

Frequency (HZ)	R Ratio	Environment			Subtotal
		ASTM Art. S.W.	3.5% NaCl+H <sub>2</sub> SO <sub>4</sub>	Distilled H <sub>2</sub> O	
3	0.05	●	●	●	3
6	0.05	○	○	○	3
					6

Notation: ○ 7075-T7651 Aluminum Alloy (Compact Tension Spec.; Fig. 6)  
 ● 8-Annealed Ti-6Al-4V Alloy (CTS; Fig. 7)

3.2.2.1 7075-T7651 Aluminum Alloy

Aluminum-base alloys are commonly used in today's high performance Naval aircraft. Beginning in the mid-1960's, the use of 7XXX alloys in the higher strength (-T6) temper was drastically reduced because of their susceptibility to exfoliation and stress corrosion cracking. There are no 7075, 7178 or 7079 alloys in the -T6 condition on the S3-A Viking or the F-14A Tomcat. Usage of 7075-T6 alloy on the Navy's F-18A Hornet is restricted to sheet gages less than 0.081-inch (2.06 mm), where quenching is sufficiently rapid to preclude microstructures susceptible to exfoliation or stress corrosion. There is heavy reliance on exfoliation-resistant 7075-T7651 for sheet and light gage plate in each of these aircraft. For this reason, 7075-T7651 was selected for the coordinated AGARD program on corrosion fatigue [22], and it was selected to be the baseline material in this program.

The material was supplied as 0.50-inch (12.7 mm) plate, and sufficient quantities were purchased to cover both Phase I and Phase II testing. Because of an availability problem with the -T7651 temper, plates of -T651 temper were purchased and re-heat treated by the vendor to the T7651 condition. Exfoliation corrosion tests were then performed by the vendor to ensure that the material met

specifications. Basic material properties are presented in Subsection 4.2.

3.2.2.2  $\beta$ -Annealed Ti-6Al-4V Alloy

$\beta$ -annealed Ti-6Al-4V alloy is used extensively as engine components, highly-loaded critical parts on helicopters, F-14 primary structure, and in limited applications on the F-18. The corrosion fatigue behavior of titanium alloys has been observed to be vastly different from aluminum alloys, and because of its optimum resistance to fatigue crack growth,  $\beta$ -annealed Ti-6Al-4V alloy was selected for study in this program.

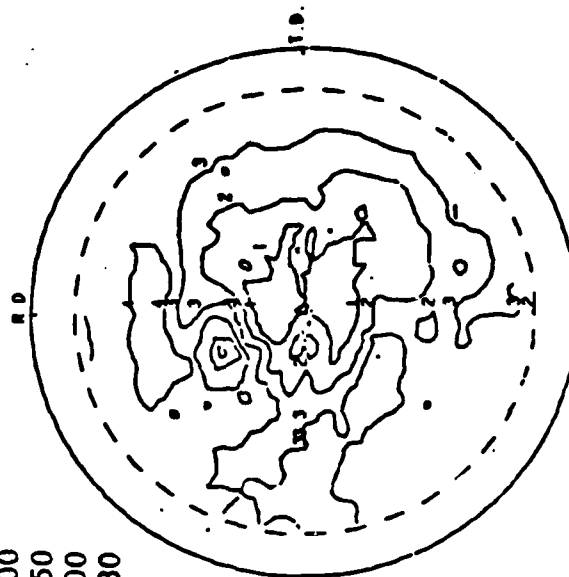
A 0.875-inch (22.23mm) thick plate of titanium was used in this study. Sufficient material remains from this plate for use in Phase II testing.

The texture of the 0.875-inch thick plate was determined by X-ray analyses. (0002) and (1010) pole figures for the rolling plane of the plates are shown in Fig. 4. It is seen that the rolling texture is complex. The primary texture, however, has been identified as (1013) [2023]. In other words, most of the grains are oriented with the (1013)

P04 Ti-6Al-4V Alloy ( $10\bar{1}0$ )

Contour Values

- 1 2.00
- 2 2.50
- 3 3.00
- 4 3.50
- 5 4.00
- 6 4.30



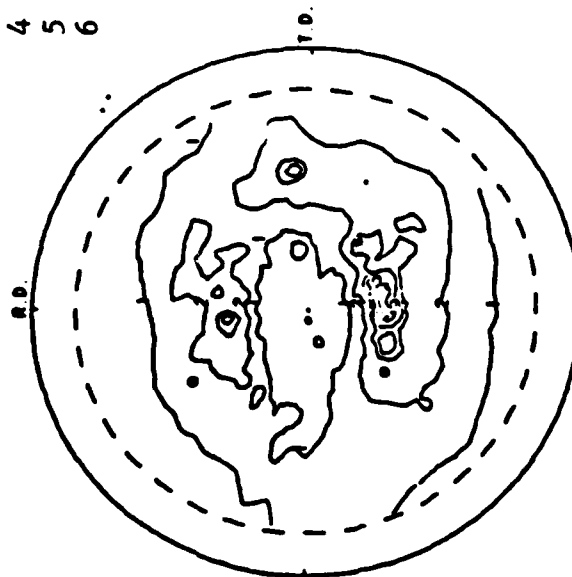
Total No. of Lines Drawn = 1380

(b)

B04 Ti-6Al-4V Alloy (0002)

Contour Values

- 1 3.00
- 2 5.00
- 3 6.00
- 4 10.00
- 5 13.00
- 6 15.00
- 7 16.00
- 8 20.00



Total No. of Lines Drawn = 1287

(a)

Fig. 4 Pole figures for the rolling plane of  $\beta$ -Annealed Ti-6Al-4V alloy plate: (a) (0002) pole, and (b) ( $10\bar{1}0$ ) pole.

planes parallel to the rolling plane and with the [2023] and [1210] directions along the rolling and transverse directions, respectively. The chemical composition of the material, according to GD specification FMS-1109D is shown in Table 5. Basic material properties are presented in Section 4.2.

### 3.2.3 Specimen Designs

Four basic specimen types were used for Phase I testing: a round tensile specimen, a compact tension specimen with two different H/W, a square cross-sectional dogbone specimen and a rectangular cross-sectional dogbone specimen with a fastener hole. The tensile tests for both materials were conducted using the round tensile specimen shown in Fig. 5.  $K_{IC}$ ,  $K_{ISCC}$  and fatigue crack propagation testing was performed using compact tension specimens (Figs. 6 and 7). The specimen used for 7075-T7651 testing is shown in Fig. 6, (H/W) = 0.486; and the specimen used for Ti-6Al-4V testing is shown in Fig. 7, (H/W) = 0.6. Round robin tests have been previously performed using specimens with H/W = 0.486 [e.g., 23]. Both H/W ratios used (i.e., 0.486 and 0.6) are allowed under ASTM standard E647. However, E647 adopts H/W = 0.6 to conform with E399. Low cycle fatigue tests for both materials were performed using the dogbone specimen design shown in Fig. 8, and the fatigue crack initiation tests were performed using the design shown in Fig. 9.

Table 5 Chemical Composition of  $\beta$ -Annealed Ti-6Al-4V Alloy  
According to GD Spec. FMS-1109D

Element	Composition (Weight percent)
Titanium	Remainder
Aluminum	5.5 - 6.3
Vanadium	3.5 - 4.5
Iron	0.25 max.
Carbon	0.08 max.
Hydrogen	0.0175 max.
Oxygen	0.060 - 0.130
Nitrogen	0.03 max.
Other Impurities	0.40 max.

(SPECIMEN A)

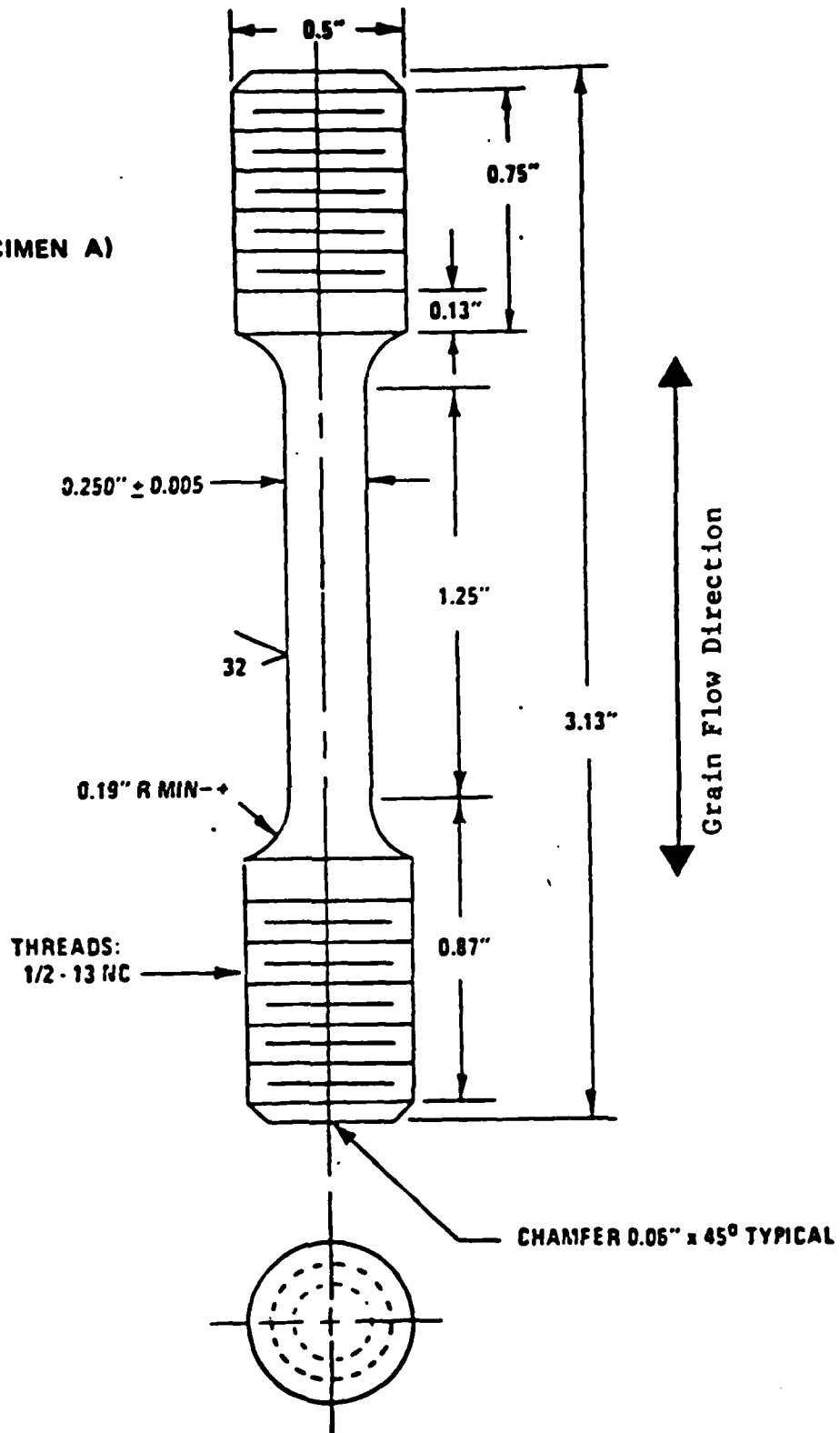
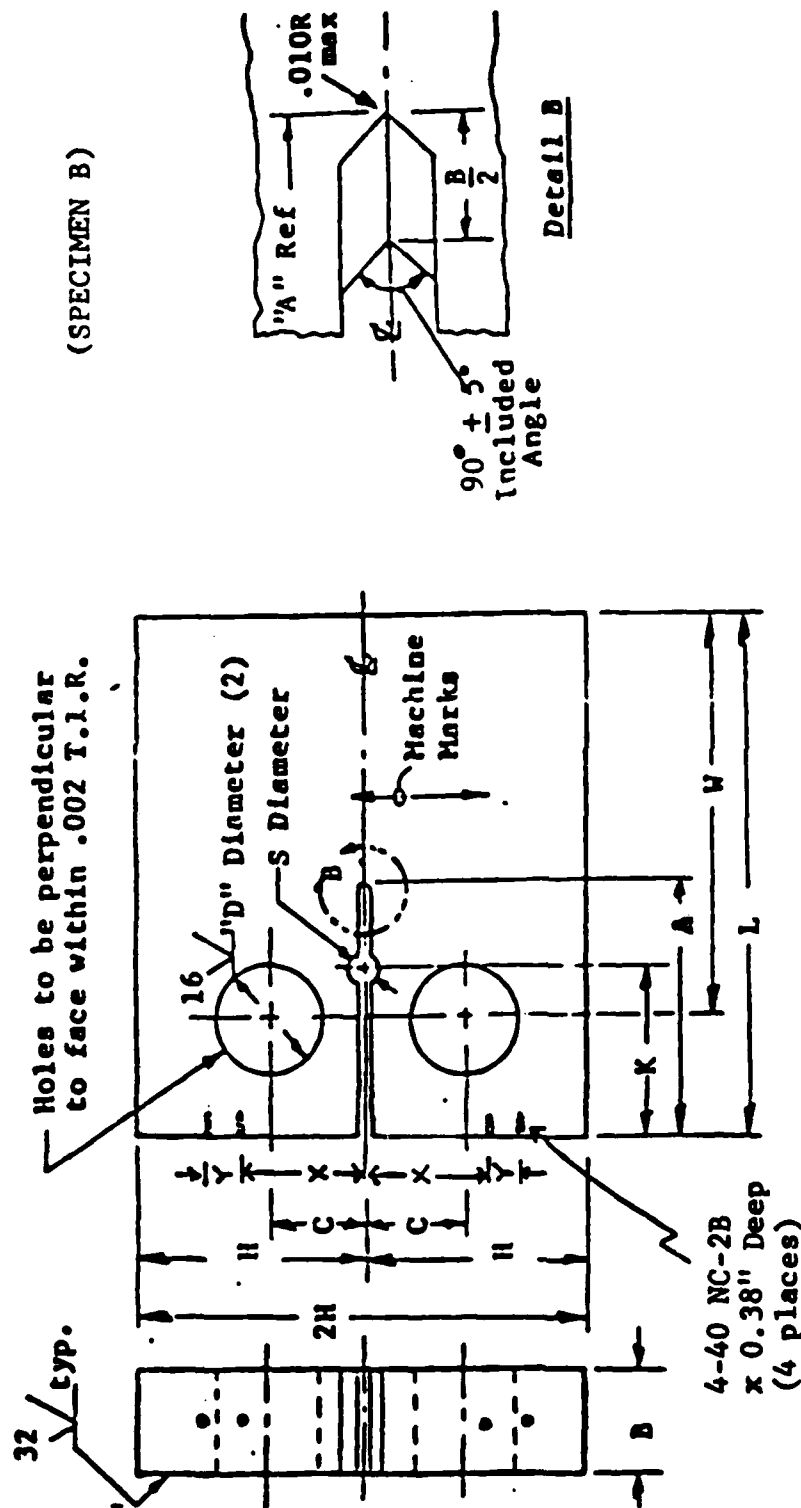


Fig. 5 Tensile Specimen Geometry

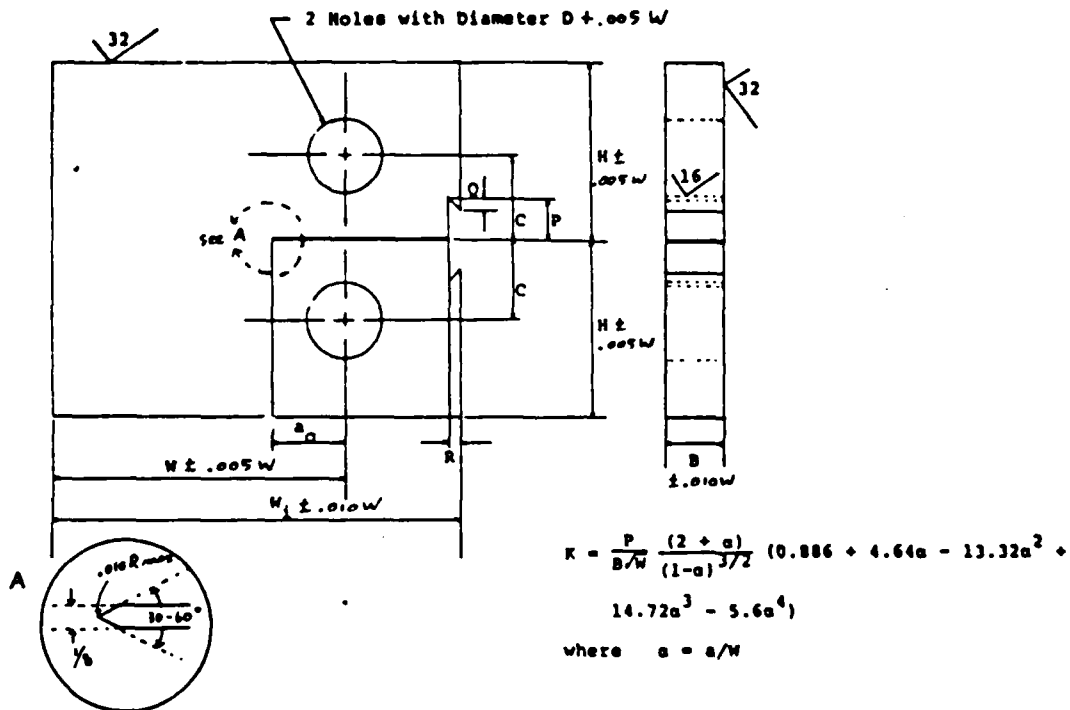


GD/FWD's Compact Tension Crack Growth Specimen FTJ 10940-463 (Unit in inch)

B	W	L	2H	C	A	T	D	K	S	X	Y
+ .010	+ .002	+ .005	+ .010	+ .005	+ .010	max	-.010 + .005	+ .010	+ .010	+ .005	+ .010
.45	2.50	3.20	2.48	.550	1.35	.100	.500	1.02	1.88	.825	.25

Fig. 6 Compact Tension Type Specimen Geometry (7075-T7651 Aluminum Alloy)

(SPECIMEN B)



	B	$a_0$	W	H	$W_1$	C	D	P	Q	R
cm	1.26	1.59	6.35	3.81	8.90	1.78	1.59	0.889	0.254	0.254
in.	0.497	0.625	2.50	1.50	3.50	0.70	0.625	0.35	0.1	0.1

Fig. 7 Compact Tension Type Specimen Geometry  
(8-Annealed Ti-6Al-4V Alloy)

(SPECIMEN C)

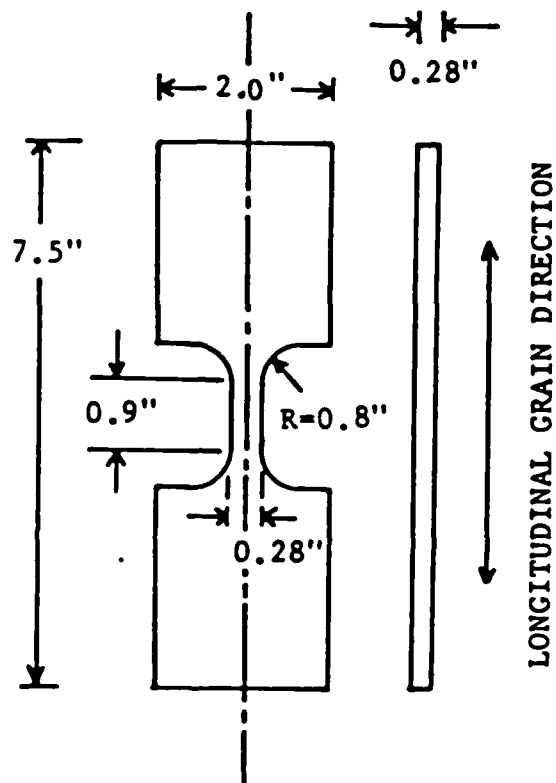


Fig. 8 Cyclic Stress-Strain Specimen Geometry

(SPECIMEN D)

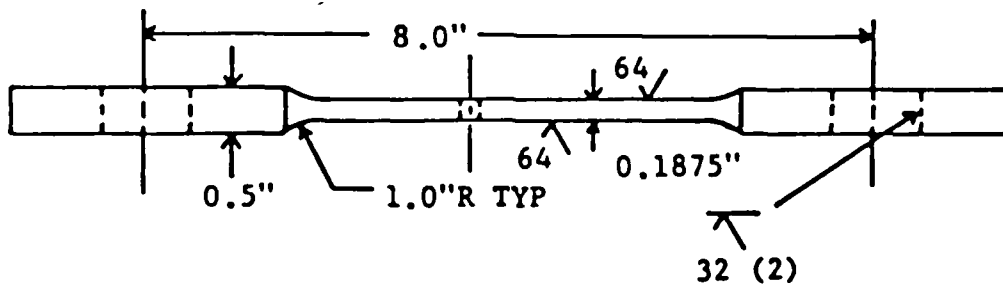
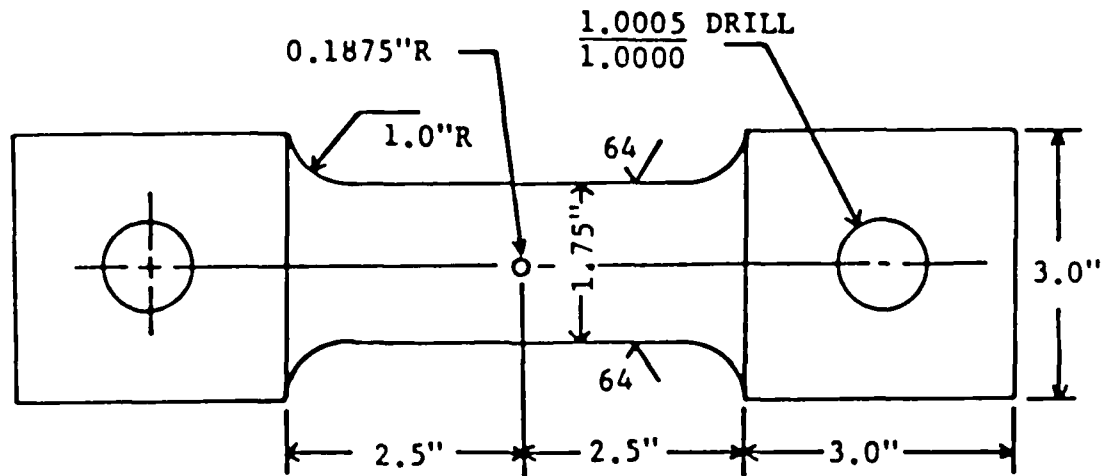


Fig. 9 Fatigue Crack Initiation Specimen Geometry

#### 3.2.4 Test Environment

The baseline aggressive environment for Phase I testing was 3.5% NaCl solution at room temperature because of its reproducibility and convenience. The test solution was prepared by dissolving reagent grade NaCl in triply-distilled water. The average solution pH was about 6.5 over the duration of each test. Reference fatigue data were obtained either in a vacuum or in dry air for comparison with the corrosion fatigue data. Tests in vacuum were made inside a commercial ultrahigh vacuum chamber that had been modified to provide mechanical force feed-throughs at pressures below 10  $\mu$ Pa. Tests were also performed to determine any effect of alternate environments. The environments selected were: ASTM artificial seawater, 3.5% NaCl solution + H<sub>2</sub>SO<sub>4</sub>, and distilled water. The chemical composition of ASTM artificial seawater is given in Table 6. For the 3.5% NaCl + H<sub>2</sub>SO<sub>4</sub> environment, H<sub>2</sub>SO<sub>4</sub> was added to obtain a solution of pH = 3.5.

All Phase I testing was performed in a constant immersion environment with periodic changing of the solution to maintain fresh solution at all times.

Table 6 Chemical Composition of ASTM  
Artificial Sea Water (ASTM-D1141)<sup>\*†</sup>

Compound	Concentration, g/liter
NaCl	24.53
MgCl <sub>2</sub>	5.20
Na <sub>2</sub> SO <sub>4</sub>	4.09
CaCl <sub>2</sub>	1.16
KCl	0.695
NaHCO <sub>3</sub>	0.201
KBr	0.101
H <sub>3</sub> BO <sub>3</sub>	0.027
SrCl <sub>2</sub>	0.025
NaF	0.003
Ba (NO <sub>3</sub> ) <sub>2</sub>	0.0000994
Mn (NO <sub>3</sub> ) <sub>2</sub>	0.0000340
Cu (NO <sub>3</sub> ) <sub>2</sub>	0.0000308
Zn (NO <sub>3</sub> ) <sub>2</sub>	0.0000096
Pb (NO <sub>3</sub> ) <sub>2</sub>	0.0000066
AgNO <sub>3</sub>	0.00000049

\* Chlorinity of this sea water is 19.38

† The pH after adjustment with 0.1N NaOH solution is 8.2

### 3.2.5 Environmental Chambers

The environmental chamber design shown in Fig. 10 was used for testing the compact tension specimens. The chamber is made of Plexiglas with two aluminum outside pieces for fastening it to the specimen. An "O"-ring provides a water-tight seal between the chamber and the specimen surface. The two chamber halves are clamped together using three bolts which thread into one of the aluminum support pieces. The problem with this type of environment chamber is that as the crack grows, the opening displacement of the specimen notch gets larger. This requires some type of flexible seal at the notch. After trying several methods, it was found that a layer of Dow Corning 3145 RTV silicone rubber sealant/adhesive performed the best. This material was put around the notch of the specimen and the front end of the environmental chamber. Directly from the tube, this material is formable and extremely tacky. However, after leaving it to set overnight at room temperature, it cures to a smooth, rubber sealant with excellent adhesive properties. It is very flexible and resistant to all the environments tested in this program.

Details of the environmental chamber used for the stress-controlled fatigue crack initiation tests are shown in Fig. 11. Chambers were fastened to the specimen using

Plexiglass chamber

Aluminum support bracket

Groove for "O" ring

See-through window

[Actual size]

Chamber mounted on specimen

Fig. 10 Schematic Drawings of Environmental Chamber for Compact Tension Specimens

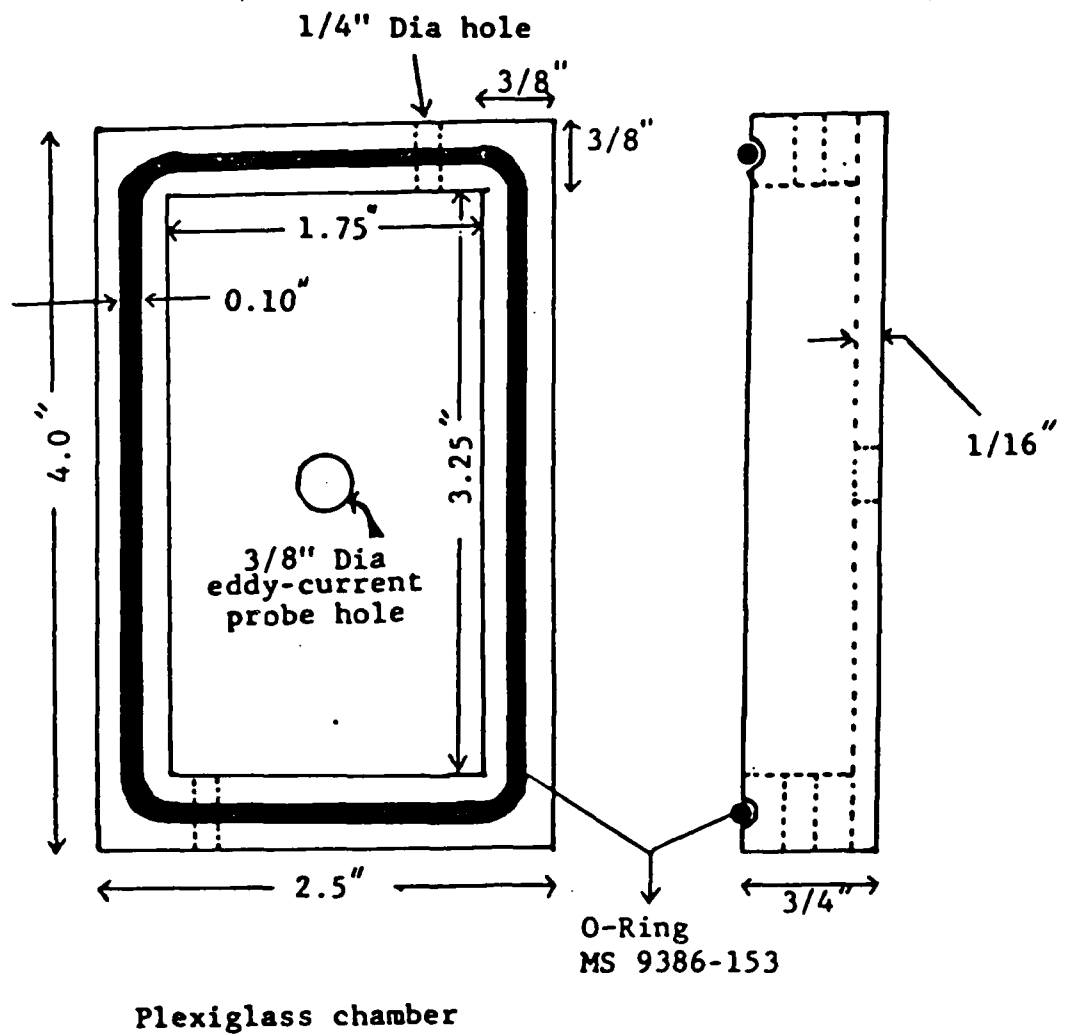


Fig. 11 Environmental Chamber Geometry for the Stress-Controlled Crack Initiation Tests

C-clamps. The hole in the chamber allows access for eddy current detection probes during testing to monitor fatigue crack initiation.

For all Phase I testing, the specimen was constantly immersed in the environment. The environment was then periodically removed and replaced with fresh solution. Environmental chambers were also used for dry air testing by placing desiccant crystals in the chamber.

### 3.3 EXPERIMENTAL PROCEDURES

The experimental procedures (i.e., test set, equipment used, data acquisition methods, etc.) are described and discussed in this section. Phase I tests were conducted at the GD/FWD and at Lehigh University. Every effort was made to ensure the test results would be consistent for the two laboratories.

Most of the crack propagation tests for the aluminum alloy were conducted by GD/FWD. Lehigh University conducted the crack propagation tests for the titanium alloy and the hold time tests (Table 3) for both aluminum and titanium alloys.

### 3.3.1 Data Acquisition

Several methods of data acquisition were used for the Phase I test program. However, all initiation data were obtained using an eddy current technique, and most propagation test data were obtained using either an automated compliance technique or an electrical potential technique.

#### 3.3.1.1 Eddy Current Technique

The eddy current technique was used to detect cracks in open fastener holes. The automated eddy current inspection system used is shown in Fig. 12. This unit includes an Automation Industries Model EM-3300 eddy current unit, a variable drive/speed miniscanner head, a bandpass filter plus amplifier, and a dual channel recorder. Special high-sensitivity probes developed by the Reluxtrol Company (CREG Model 102 Probes) were used to obtain the highest resolution possible in detecting crack initiation.

The minimum crack size that can be detected in a fastener hole using this system depends on the quality of the hole being inspected. Factors affecting hole quality which can also influence the eddy current signal are surface

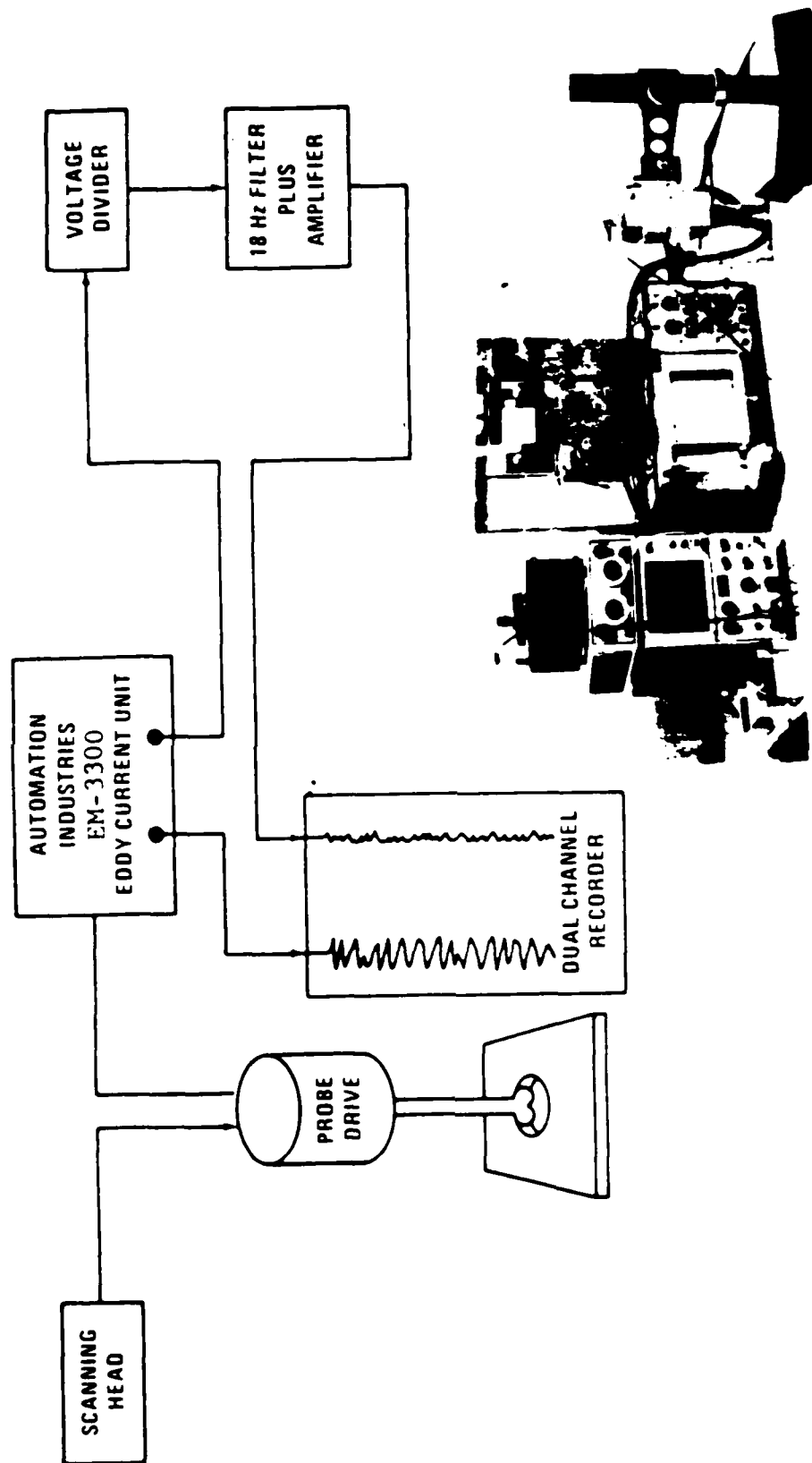


Fig. 12 Automated Eddy Current Inspection System

roughness, hole out-of-roundness, scratches, gouges, smears, etc. An example of how surface can affect the signal is shown in Fig. 13. A considerably lower background signal is obtained in a hole having 20-25 $\mu$ -inch r.m.s. surface finish. A small fatigue crack would be much more difficult to detect in the hole with the rougher finish.

In general, the 7XXX aluminum fastener holes drilled by conventional drilling technique used by General Dynamics production line, crack depths as small as 0.002-inch (0.0005 mm) are detectable with the high-sensitivity probes in conjunction with the EM-3300 eddy current unit.

Shown in Fig. 14 is an example of eddy current scans of fastener holes in stress-controlled aluminum coupons. Fatigue cycling was stopped at various intervals and an eddy current hole inspection was made. In automatic scanning, the eddy current probe is first positioned coaxially with the fastener hole, the inspection drive speed is selected, and the probe is driven through the fastener hole. The eddy current probe rotates as it is being driven. Translation speed of the probe is approximately 0.025-inch per revolution as the probe follows a helical motion through the hole. The large deflection at the left portion of the scans (Fig. 14) is due to the probe entering the hole while the

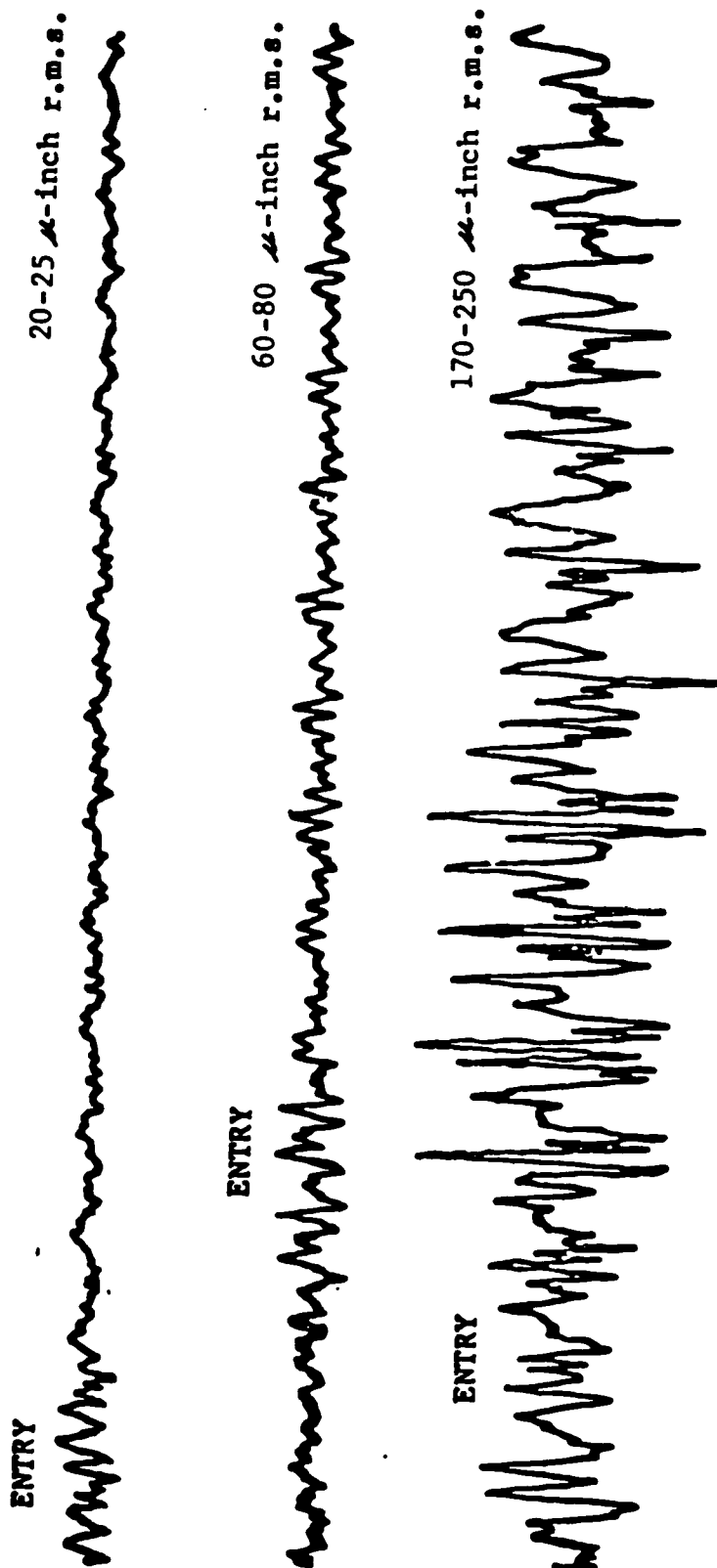
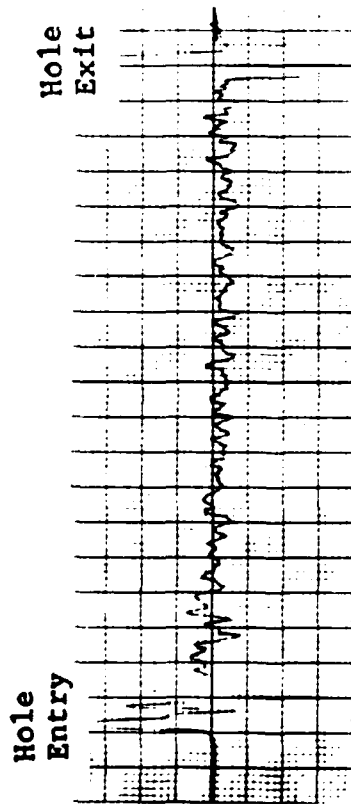


Fig. 13 Effect of Surface Roughness in Fastener Holes on the Eddy Current Signal

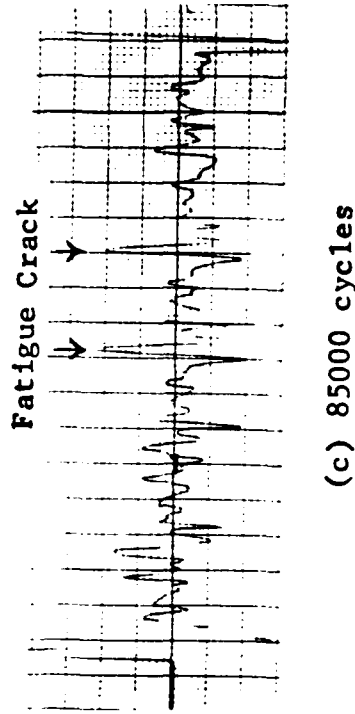
large deflections at the right is due to the probe leaving the hole. The number of deflections observed for a single fatigue crack depends on the diameter of the eddy current coil and length of the fatigue crack in the hole. For instance, in Fig. 14, the same fatigue crack produced two deflections. Typical eddy current scans showing onset of cracking in  $\beta$ -Annealed Ti-6Al-4V alloy are shown in Fig. 15.

The amplitude of the eddy current signal is proportional to the depth of the fatigue crack for crack depths less than approximately 0.020-inch. For crack depths greater than 0.020-inch, the eddy current signal starts to saturate for the operating frequency used. This frequency produces a fairly shallow skin depth in aluminum alloys increasing the sensitivity to small cracks at the surface.

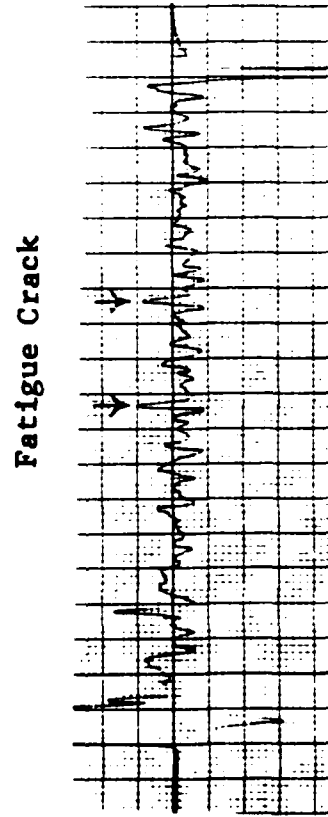
The eddy current signals can be converted to crack depths. For example typical correlation plots for eddy current signal and crack depth are shown in Figs. 16 and 17 for aluminum and titanium (6Al-4V) alloys, respectively. The eddy current signals are not as sensitive to small fatigue cracks in  $\beta$ -annealed Ti-6Al-4V alloy as in 7075-T7651 aluminum alloy. A crack depth of approximately 0.070-in. is required before the eddy current signal saturates.



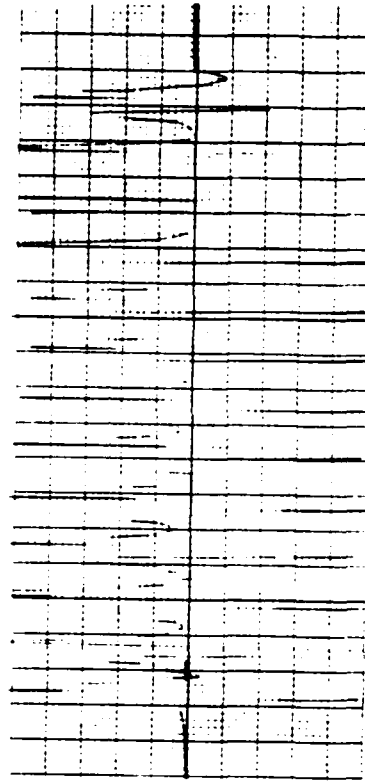
(a) 75000 cycles



(c) 85000 cycles

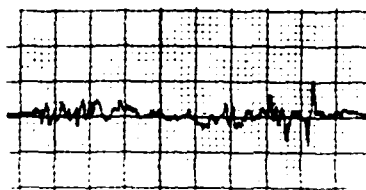


(b) 80000 cycles



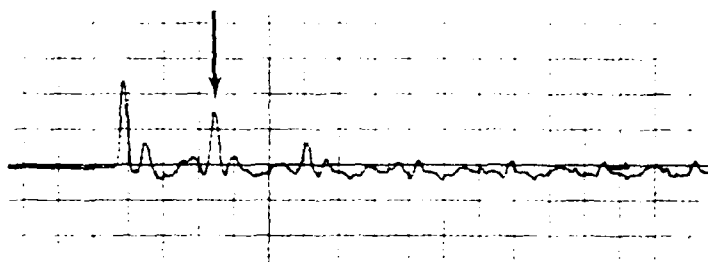
(d) 90000 cycles

Fig. 14 Eddy Current Scans Showing Onset of Cracking in Fatigue Cycled Coupon

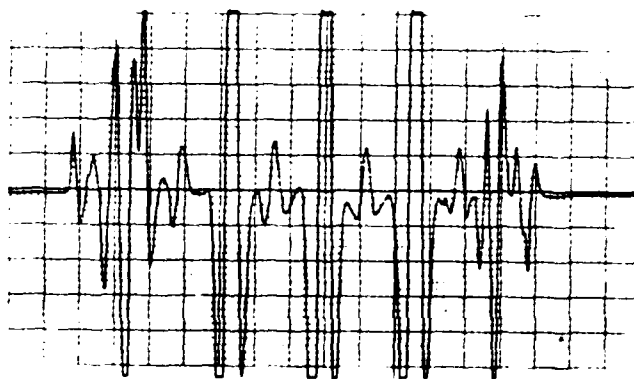


(a) 20000 cycles

Fatigue Crack



(b) 30000 cycles



(c) 40000 cycles

Fig. 15 Eddy Current Scans Showing Onset of Cracking in Fatigue Cycled Coupon ( $\beta$ -Annealed Ti-6Al-4V Alloy)

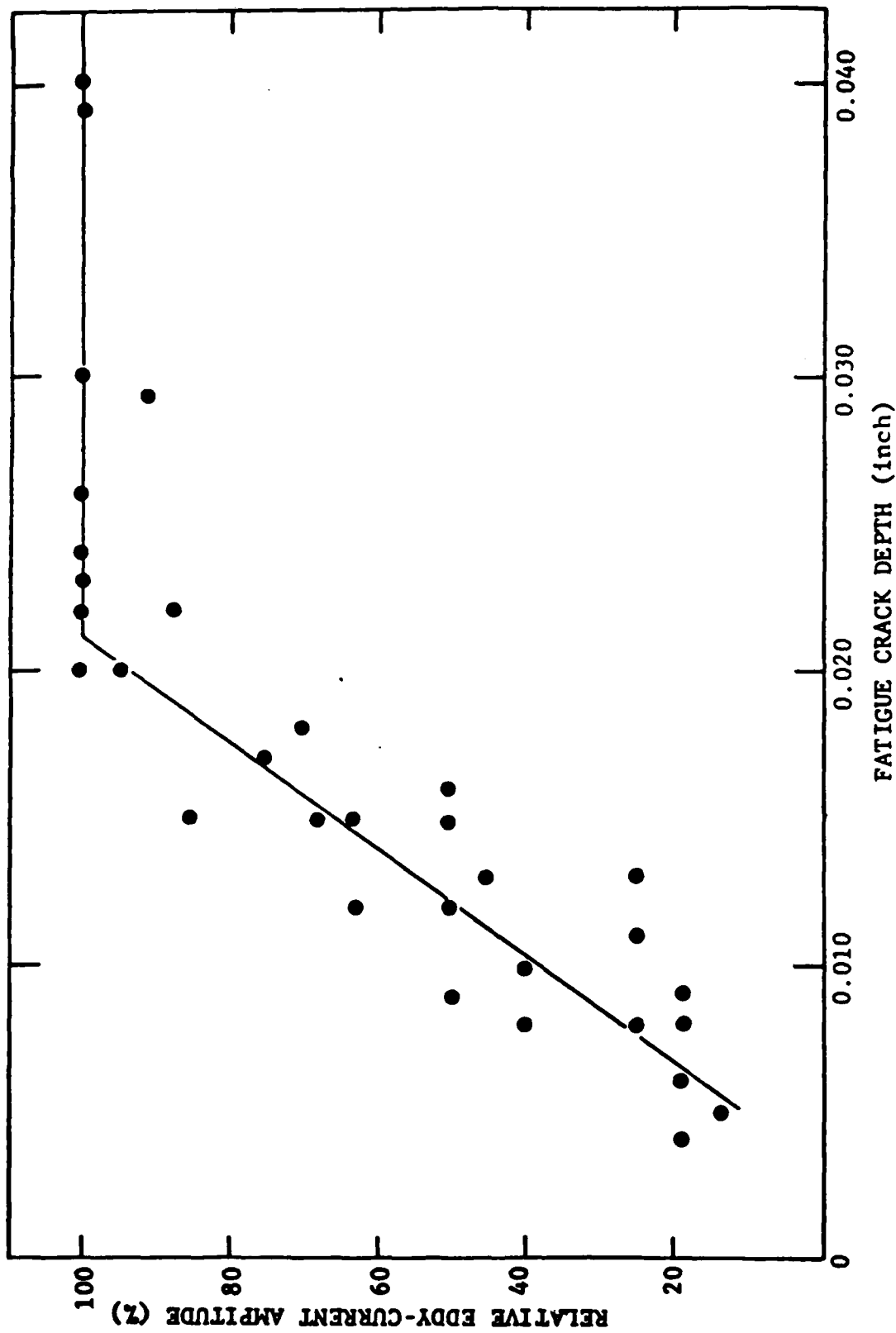


Fig. 16 Relationship Between Eddy-Current Signal Amplitude and Fatigue Crack Depth for 7075-T7651 Aluminum Alloy

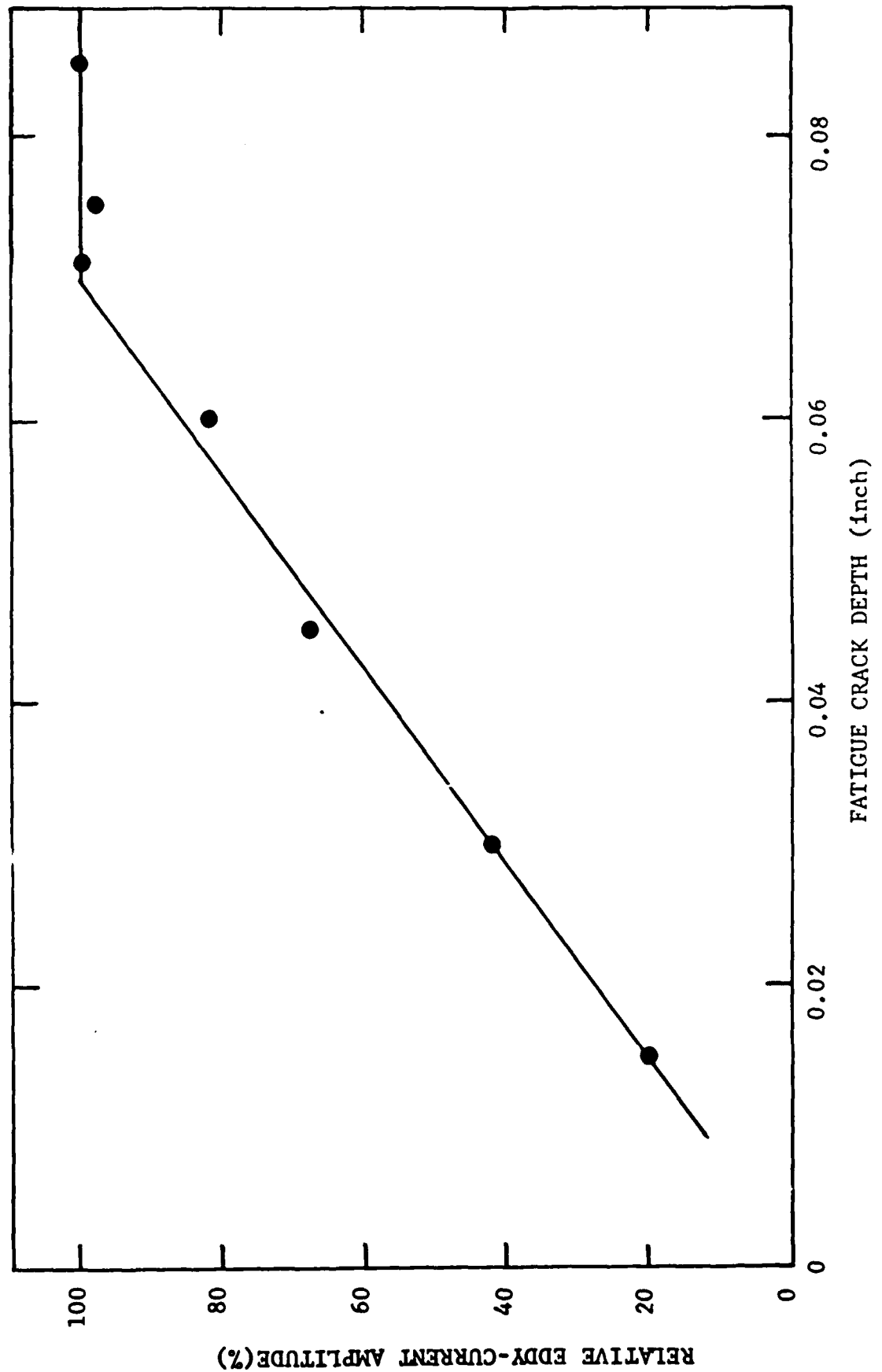


Fig. 17 Relationship Between Eddy-Current Signal Amplitude and Fatigue Crack Depth for  $\beta$ -Annealed Ti-6Al-4V Alloy

3.3.1.2 Compliance and Electrical Potential Techniques

Early in the fatigue crack propagation testing, a low power microscope and finely divided scale were used to monitor crack growth in the specimen. Although this technique is simple to use and requires no computerization, it is costly and time consuming. This method was also used to check other data acquisition techniques used.

Crack length was measured during the tests by using either a crack-mouth-opening-displacement (CMOD) gage or clip gage or an a.c. electrical potential system. For the specimen geometry and clip gage location, calibration had to be established experimentally. Reference marks were scribed onto the polished surfaces of calibration specimens along the expected path of crack growth, and the crack was extended by fatigue in air. As the fatigue crack reached each of the fiduciary marks, fatigue cycling was interrupted. The electrical potential and the slope of CMOD versus load (or V/P) were recorded, and a replica of each of the specimen surfaces was made. Note that the potential was measured automatically at the maximum load points during fatigue and represented the average of 20 successive readings. The slope V/P was obtained by linear regression analysis of CMOD vs. load data over 3 cycles. The load

range was chosen to minimize the influence of crack closure. After fracture of the specimen, the actual crack front was observed and corrections were applied to the crack length measurements made from the replicas to account for the effect of crack front curvature. The average crack lengths thus obtained were used to obtain the experimental calibration equations. Calibration data for the titanium alloy are shown in Figs. 18 and 19.

Compliance Method [24]

$$a = 63.5 (0.9979 - 4.355 U) \quad (14)$$

(in mm)

$$U = \frac{1}{\left(\frac{BEV}{P}\right)^{1/2} + 1}$$

a = crack length

W = specimen width = 2.5-inch (63.5 mm)

B = specimen thickness

P = applied load

E = elastic modulus

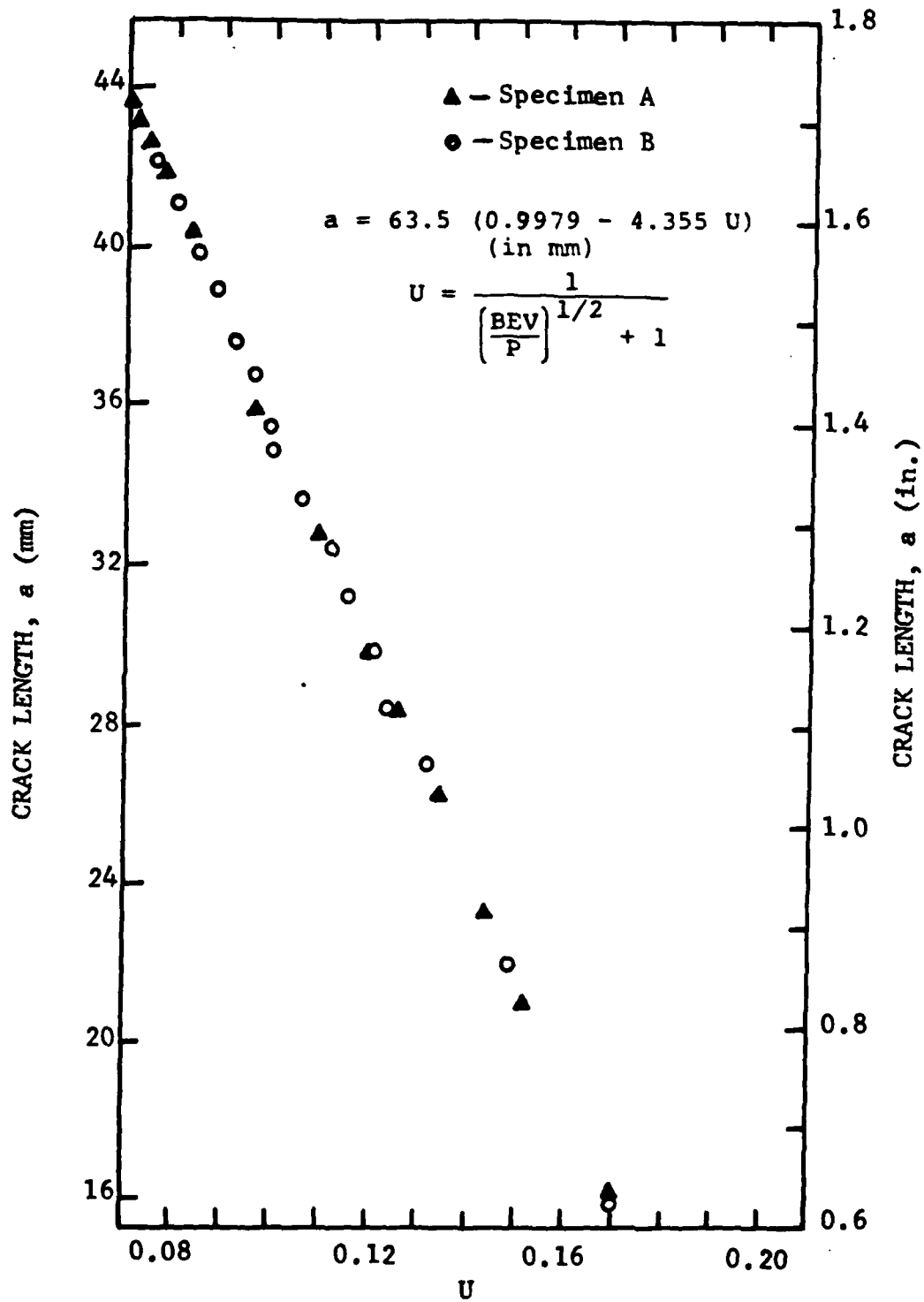


Fig. 18 Calibration Curve of Crack Length Versus Normalized Compliance for  $\beta$ -Annealed Ti-6Al-4V Alloy

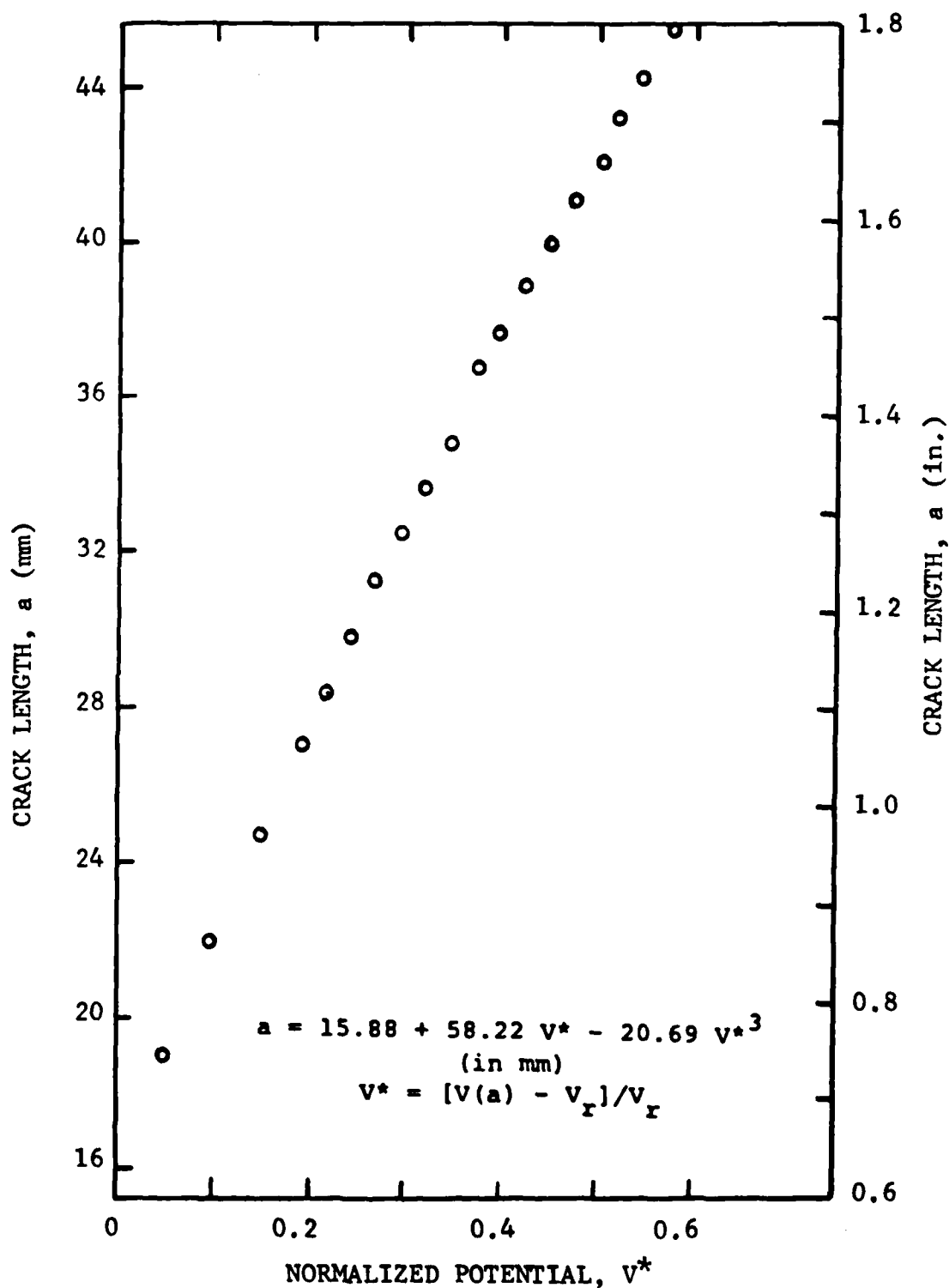


Fig. 19 Calibration Curve of Crack Length Versus Electrical Potential for  $\beta$ -Annealed Ti-6Al-4V Alloy

V = crack mouth opening displacement (CMOD)

ac. Potential Method [25]

$$a = 15.88 + 58.22 V^* - 20.69 V^{*3} \text{ (in mm)} \quad (15)$$

where  $V^* = [V(a) - V_R]/V_R = \text{normalized potential}$

$V(a)$  = potential corresponding to crack length a

$V_R$  = reference potential corresponding to the  
initial notch

The a.c. potential method was used for testing in vacuum, and the displacement or compliance method was used for all of the other tests. Accuracy of crack length measurement with the a.c. system was estimated to be better than 1 pct, for crack lengths from about 20 to 48 mm (0.8 to 1.85 in.). The resolution was better than 0.01 mm (0.004 in.) based on 20 nV resolution in electrical potential.

3.3.1.3 Fractography

A scanning electron microscope was used to characterize the morphology of fracture surfaces. Entire broken halves

of the specimens were placed inside the microscope for examination. For selected specimens, both broken halves were placed inside the microscope, and mating areas of the fracture surfaces were examined. Specimen tilt was about an axis parallel to the direction of crack growth. Fractographs are presented and briefly discussed in Section IV.

### 3.3.2 Basic Material Properties Test Procedures

Tensile tests were performed on a closed-loop MTS machine at moderate strain rates. Yield strengths, ultimate tensile strengths, percent elongation, and reduction of area were measured using a single coupon for each material (i.e., 7075-T7651 aluminum alloy and  $\beta$ -annealed Ti-6Al-4V alloy). Tensile test results are presented in Subsection 4.2.

Fracture toughness static testing was conducted on an AMTEK servo-hydraulic test machine of 60000 lbs. capacity. A 12000 lbs load indicating range was used. A strain gaged, compliance gage of NASA design was used to measure crack opening displacement(COD). The  $P_Q$  load was measured using the 5% secant offset method. The load-compliance curves showed considerable plasticity and the  $K_{Ic}$  results were invalid because of insufficient specimen thickness. Fatigue

crack lengths were measured on a Scherr Tumico measuring microscope at 1/4, 1/2, 3/4 thicknesses and averaged.

Sustained load-long time static testing on the stress corrosion specimens was conducted on a Riehle creep machine of 12000 lb. capacity. A modified creep extensometer was attached to the milled notch knife edges and COD was continuously monitored on a strip chart. Plexiglass containers, suitably sealed with "O" rings and "duct-seal" confined the 3.5% NaCl solution to the crack front.

In the case of the titanium samples, the  $K_{Isc}$  threshold was determined by step loading the specimen. Approximately every 48 hours the  $K_Q$  was increased by adding more dead weight to the machine's loading mechanism. The COD curve was monitored and if no crack growth could be observed, then the load was increased. This was continued until failure resulted.

In the case of the aluminum, incubation time for stress corrosion crack growth had to be considered and tests were conducted for 1000 hours duration after the final stress intensity level was established. The practice followed was to load the aluminum  $K_{Isc}$  specimens to a given  $K_Q$  ; if no crack growth was measured on the compliance recorder in 100

hours, the load was increased and the procedure repeated. Load increments were stopped when the  $K_{IC}$  of the material was approached. Neither of the aluminum specimens failed under corrosion conditions so they were statically tested and a  $K_Q$  value was obtained in addition to the  $K_{Isc}$  result. Fatigue crack length and final corrosion crack length were measured optically as with the titanium specimen.  $K_{IC}$  and  $K_Q$  were calculated using ASTM 399-78 formulas corrected for  $(H/W)=0.49$ .

Cyclic stress-strain fatigue specimens were machined with the loading axis parallel to the rolling direction. They were polished parallel to the gage length with 6 $\mu$ m diamond polishing compound. The total strain-controlled fatigue tests were performed in lab air of 30-40% relative humidity and in 3.5% NaCl at room temperature on a closed loop electrohydraulic MTS machine (50 kip capacity) controlled by fully reversed ( $R = \sigma_{min} / \sigma_{max} = -1$ ) triangular strain amplitude waves. Cyclic stress-strain curves were determined by the "incremental step test method", in which total strain amplitude is increased in steps and decreased in steps, until a stable set of hysteresis loops is obtained.

For tests in laboratory air, a saturated, stable hysteresis-loop set was obtained after the 6th decreasing block for 7075-T7651 aluminum alloy and after the 7th decreasing block for  $\beta$ -annealed Ti-6Al-4V alloy. The outermost tip of each stable hysteresis loop in compression was converted from load-voltage/strain-voltage to stress / strain and plotted. Cyclic stress-strain curves were also determined in 3.5% NaCl solution. Results are presented in Subsection 4.2.

### 3.3.3 Fatigue Crack Initiation Test Procedures

Stress-controlled fatigue crack initiation tests were performed on 7075-T7651 aluminum alloy and  $\beta$ -annealed Ti-6Al-4V alloy specimens in dry air and in 3.5% NaCl solution. A dogbone type of specimen with an open center-hole was used (Ref. Fig. 9). The stress concentration factor ( $K_t$ ) due to the hole in the specimen was approximately 2.6 (based on net section stress).

All tests were performed on servo-controlled, hydraulically-actuated load frames. A special hardware interface was used to monitor each load frame and to assure proper load control.

All specimens were tested in the as-machined condition without any prior preconditioning (e.g., presoaking in 3.5% NaCl and pretesting). Fatigue tests were conducted using a sinusoidal wave form and an R ratio of 0.05. Two different loading frequencies were used (i.e., 1 Hz and 6 Hz).

Specimens were mounted in the load frames and the two environmental chamber halves (Ref. Fig. 11) were clamped to the specimen. The open hole in each chamber half was plugged with a hard-rubber plug.

The environmental chamber was filled with 3.5% NaCl solution and the solution was periodically drained and refilled with a fresh solution. For the dry air tests, the test setup was the same except desiccant was used in the chamber instead of 3.5% NaCl solution.

Stress-controlled tests were performed for selected  $\Delta\sigma$  values and environments (dry air and 3.5% NaCl solution). The number of cycles to initiate a 0.010" crack in the open hole was determined using the eddy current technique described in Subsection 3.3.1.1.

Eddy current inspections were periodically made as follows. The 3.5% NaCl solution was first drained to a

level below the open hole. then the rubber plugs were removed to permit an eddy current inspection of the hole in the specimen. Following an inspection, the rubber plugs were replaced in the chambers and the chambers were refilled with 3.5% NaCl solution.

The number and frequency of the eddy current inspections varied -- depending on the  $\Delta\sigma$  level used. For example, eddy current inspections were made approximately every 25000 cycles for the low  $\Delta\sigma$  tests and more frequently for the higher  $\Delta\sigma$  tests.

After the number of cycles to crack initiation ( $a_i = 0.010"$ ) had been determined, the tests were continued until the specimens failed. Test results are presented in Section 4.2.

#### 3.3.4 Fatigue Crack Propagation Test Procedures

Compact tension (CT) specimens (Figs. 6 and 7) were used in the crack growth studies. Specimen dimensions and test procedures generally conform to ASTM Method of Test E647 [26]. The specimens were oriented in the LT orientation, with the crack plane perpendicular to the longitudinal

direction and crack growth along the transverse direction of the plate. An initial notch (or crack starter) approximately 0.625-inch (15.9 mm) in length was introduced into each specimen by either a thin wafer saw or electrodischarge machining (EDM). Some specimens were polished using emery cloth and then aluminum oxide powder to remove machining marks. Then finely-divided plastic scales were mounted on both sides. This was to facilitate reading crack lengths with a low-power travelling microscope. Each specimen was precracked in fatigue through a decreasing sequence of loads that terminated at the desired load level (or initial  $K$ ) for the actual experiment. The precracking procedure provided a fatigue crack of about 0.17-inch (4.4mm) in length from the starter notch, corresponding to a crack length of about 0.80-inch (20.3 mm) at the start of each experiment. This precracking procedure ensured that the subsequent fatigue crack growth would be through material that had not been altered by the notch preparation procedure, and would be unaffected by the starter notch geometry. Titanium specimens were precracked while exposed to the test environment, whereas the aluminum specimens were precracked in laboratory air. However, data was not taken until after the crack had fatigued approximately 0.020-inches (0.50 mm) in the environment.

The stress intensity factors,  $K$ , for the specimens are given by Eqs. 16 and 17.

Aluminum (Fig. 6)

$$K = \frac{P\sqrt{a}}{BW} [30.96 - 195.8\alpha + 730.8\alpha^2 - 1186.3\alpha^3 + 754.6\alpha^5] \quad (16)$$

Titanium (Fig. 7)

$$K = \frac{P}{B\sqrt{W}} \frac{(2 + \alpha)}{(1 - \alpha)^{3/2}} \left( 0.886 + 4.64\alpha - 13.32\alpha^2 + 14.72\alpha^3 - 5.6\alpha^4 \right) \quad (17)$$

where:

$\alpha = a/W$

$B =$  thickness

$W =$  specimen width (2.50-inch)

$P =$  applied load

$a =$  crack length.

The fatigue crack growth experiments were carried out in an automated closed-loop hydraulic testing machine operated in load control at the predetermined stress ratio,  $R$ . Four different test procedures were employed. In procedure A, tests were carried out under constant amplitude loading at a prescribed frequency and load ratio. Occasional shifts in

frequency were made to examine the influence of slow cycling frequencies. The other three procedures involved testing at constant  $\Delta K$ , using an automated load shedding routine. In procedure B,  $\Delta K$  was maintained constant for crack growth of approximately 0.10-inch (2.5 mm) at a predetermined frequency. Then  $\Delta K$  was increased and the procedure repeated. In procedure C,  $\Delta K$  was maintained constant, while cycling frequency was changed to cover a range of frequencies on a single test specimen. In procedure C, the level of  $\Delta K$  was changed so that the influence of holding time can be examined at several  $\Delta K$  levels on a single specimen.

Load or  $\Delta K$  control was estimated to be greater than  $\pm 1$  pct. Test frequency ranged from 0.03 Hz to 10 Hz,  $\Delta K$  from 4.5 to 30 ksi  $\sqrt{\text{in.}}$  (4.9 to 33 MPa $\sqrt{\text{m}}$ ) for the aluminum and from 9.1 to 41 ksi  $\sqrt{\text{in.}}$  (10 to 45 MPa $\sqrt{\text{m}}$ ) for the titanium, and R ratio from 0.05 to 0.4.

For examining the effect of holding time, a triangular waveform at 1 Hz was used as reference (zero holding time) and was modified by holding at maximum load for prescribed time intervals (with no holding time at the minimum load in the cycle). In other words, the waveform consisted of an up-ramp of 0.5 s, holding a maximum load, and a down-ramp of

AD-A136 414

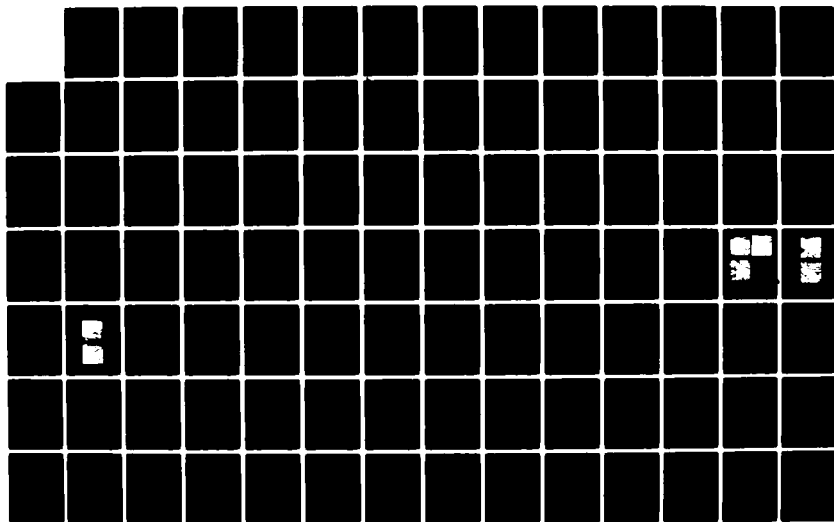
DEVELOPMENT OF FATIGUE AND CRACK PROPAGATION DESIGN AND  
ANALYSIS METHODOL..(U) GENERAL DYNAMICS FORT WORTH TX  
FORT WORTH DIV Y H KIM ET AL. MAR 83  
NADC-83126-60-VOL-1 N62269-81-C-0268

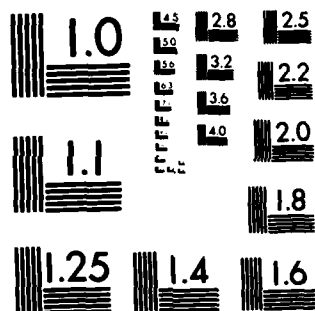
23

UNCLASSIFIED

F/G 20/11

NL





MICROCOPY RESOLUTION TEST CHART  
NATIONAL BUREAU OF STANDARDS-1963-A

0.5 s. Holding times of 0, 1 and 2.33 s were selected which provided an equivalent frequency of 1, 0.5 and 0.3 Hz, respectively. These holding times (or frequencies) bracket the frequency at which the maximum environmental effect was observed in the titanium alloy.

The sustained-load (or stress corrosion) crack growth tests were carried out using titanium specimens and a step-loading technique. The applied load was increased in a stepwise fashion. It was held constant for 30 min. to 2 h after each incremental increase in load to establish the absence of detectable crack growth, and was increased by the next increment. If continuous crack growth was detected, the load was then maintained constant. Otherwise, the load was increased until a K level of about  $71.4 \text{ ksi}\sqrt{\text{in.}}$  ( $65 \text{ MPa}\sqrt{\text{m}}$ ) was reached, and the test was then terminated.

## SECTION IV

### PHASE I TEST RESULTS

#### 4.1 INTRODUCTION

Test results from the Phase I effort are presented and discussed in this section. Results are tabulated and plotted in various forms. Crack initiation and crack propagation test results are presented and discussed. However, the stress-initiation life model and the crack propagation models are evaluated in detail in Section V.

#### 4.2 BASIC MATERIAL PROPERTIES

Tensile test results for 7075-T7651 aluminum alloy and for  $\beta$ -annealed Ti-6Al-4V alloy are shown in Table 7. The values for 7075-T7651 aluminum alloy are considered typical. Tensile properties for the titanium alloy conform to FMS-1109D specification minimums.

Fracture toughness values for 7075-T7651 aluminum alloy and  $\beta$ -annealed Ti-6Al-4V alloy are shown in Table 8. For both materials, the specimens were not thick enough for a plane strain condition. Average  $K_{IC}$  values of  $33.2 \text{ ksi}\sqrt{\text{in.}}$

**Table 7 Tensile Properties for 7075-T7651 Aluminum Alloy and  $\beta$ -Annealed Ti-6Al-4V Alloy**

MATERIAL	TYS (ksi)	TUS (ksi)	% ELONG. in 1"	% RA
7075-T7651 Aluminum Alloy	66.3	76.7	12	31.6
$\beta$ -Annealed Ti-6Al-4V Alloy	127.0	136.0	10	17.7

**Table 8 Fracture Toughness Properties for 7075-T7651 Aluminum Alloy and  $\beta$ -Annealed Ti-6Al-4V Alloy**

MATERIAL	ORIENTATION	SPEC. NO.	B IN.	W IN.	A IN.	P <sub>Q</sub> LBS	P <sub>MAX</sub> LBS	K <sub>IC</sub> KSI- $\sqrt{\text{in}}$
Ti-6Al-4V TYS = 127 KSI R/W = 0.6	L-T	TKC1	.498	2.503	1.460	8400	9640	136.6 (1) (2)
	L-T	TKC2	.496	2.488	1.452	8460	9350	138.7 (1)
		AVG						137.7
7075-T7651 TYS = 66.3 KSI R/W = 0.486	L-T	AKC1	.450	2.550	1.268	2250	3260	34.4 (1) (2)
	L-T	AKC2	.449	2.549	1.253	2270	3155	32.0 (1) (2)
		AVG						33.2

Invalid K<sub>IC</sub> because:

- (1) Insufficient thickness to meet  $B \geq 2.5 (K_{IC}/TYS)^2$
- (2)  $P_{MAX}/P_Q \geq 1.1$

and 137.7 ksi  $\sqrt{\text{in.}}$ , based on two specimens for each material, were obtained for the 7075-T7651 aluminum alloy and for the  $\beta$  - annealed Ti - 6Al - 4V alloy, respectively. The average  $K_{Ic}$  value for the titanium alloy, based on plane stress conditions, is considerably higher than the value expected under plane strain conditions.

Stress corrosion properties for the 7075-T7651 aluminum alloy and for the  $\beta$  - annealed Ti - 6Al - 4V alloy are shown in Tables 9 and 10, respectively. Results are based on two test specimens for each material.  $K_Q$  for one aluminum coupon was higher than normal. This was probably due to crack front blunting. The titanium alloy results for two specimens were fairly consistent. For example,  $K_{Isc}$  values ranged from  $\sim 70$  ksi  $\sqrt{\text{in.}}$  to 85 ksi  $\sqrt{\text{in.}}$ .

Figure 20 shows a stabilized set of hysteresis loops for 7075-T7651. The outermost tip of each loop in compression was converted to stress-strain and plotted in Fig. 21. Comparison of the monotonic and cyclic stress strain curves indicate neither cyclic softening nor cyclic hardening. The stress-strain curves have also been determined in 3.5% NaCl solution. These results are identical to those obtained in laboratory air. This was expected because the testing time for this low cycle fatigue test was too short to transfer

Table 9 Stress Corrosion Properties for 7075-T7651 Aluminum Alloy

SPECIMEN NO.	WIDTH W, INCH	THICKNESS B, INCH	CRACK LENGTH A, INCH	LOAD LBS.	$K_Q$ KSI $\sqrt{\text{in}}$	TIME IN HOURS
AKS1	2.549	0.449	1.2637	2100	29.89	Initial
			1.275	2100	30.29	1017 NF
			RESIDUAL STRENGTH			
AKS2	2.550	0.449	1.275	2650	38.22*	Static Test
			1.2732	3000	43.16	Initial
			1.3958	3000	50.27	1007NF
			RESIDUAL STRENGTH			
			1.3958	3180	53.28**	Static Test

Compact Tension Specimen in 3.5% NaCl Solution

H/W = .486

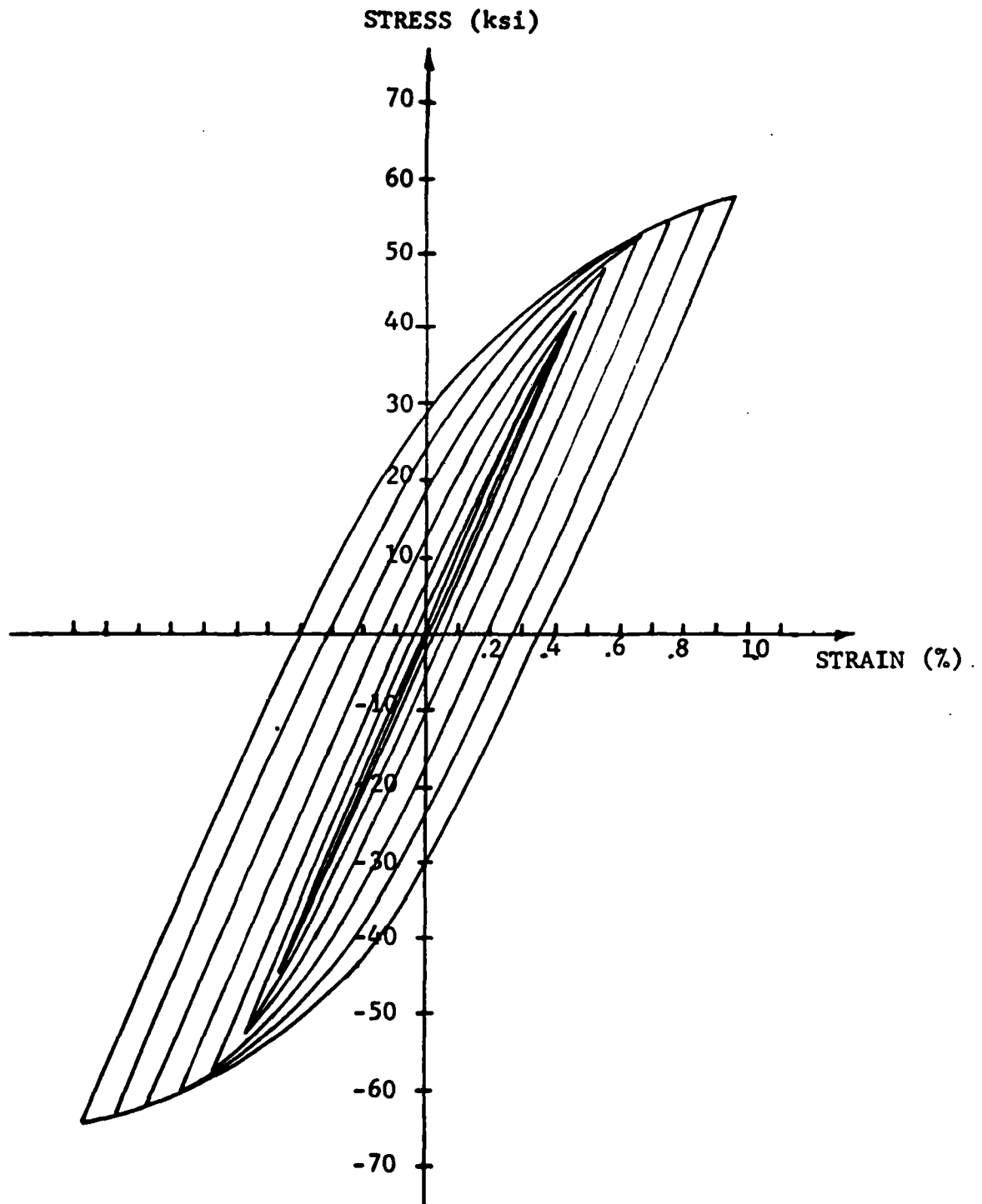
\*  $K_Q$  because  $P_{\max}/P_Q > 1.1$ \* Probable crack front blunting making  $K_Q$  higher than normal

Table 10  $K_{Isc}$  of  $\beta$ -Annealed Ti-6Al-4V Alloy

SPECIMEN NO.	WIDTH W, INCH	THICKNESS B, INCH	CRACK LENGTH A, INCH	LOAD LBS	$K_Q$ KSI $\sqrt{IN}$	TIME TO FAIL, HOURS
TKS1*	2.501	0.498	1.153	3000	32.8	68.7 NF
				3700	40.4	47.9
				4200	45.8	48.2
				4800	52.4	71.8
				5300	57.9	47.8
				5800	63.4	47.6
				6400	69.9	120.1
				7400	80.8	0.16
TKS2**	2.502	0.497	1.167	4800	53.4	50.4 NF
				5200	57.8	65.2
				5600	62.3	48.3
				6000	66.7	48.1
				6400	71.1	71.4
				6800	75.6	47.8
				7200	80.0	53.1
				7600	84.5	3.5

Sustained Load in 3.5% NaCl Solution

\* $K_{Isc} \approx 70$  to  $81 \text{ ksi}\sqrt{\text{in.}}$ \*\* $K_{Isc} \approx 80$  to  $85 \text{ ksi}\sqrt{\text{in.}}$



**Fig. 20** A Stable Set of Hysteresis Loops for 7075-T7651 Aluminum Alloy

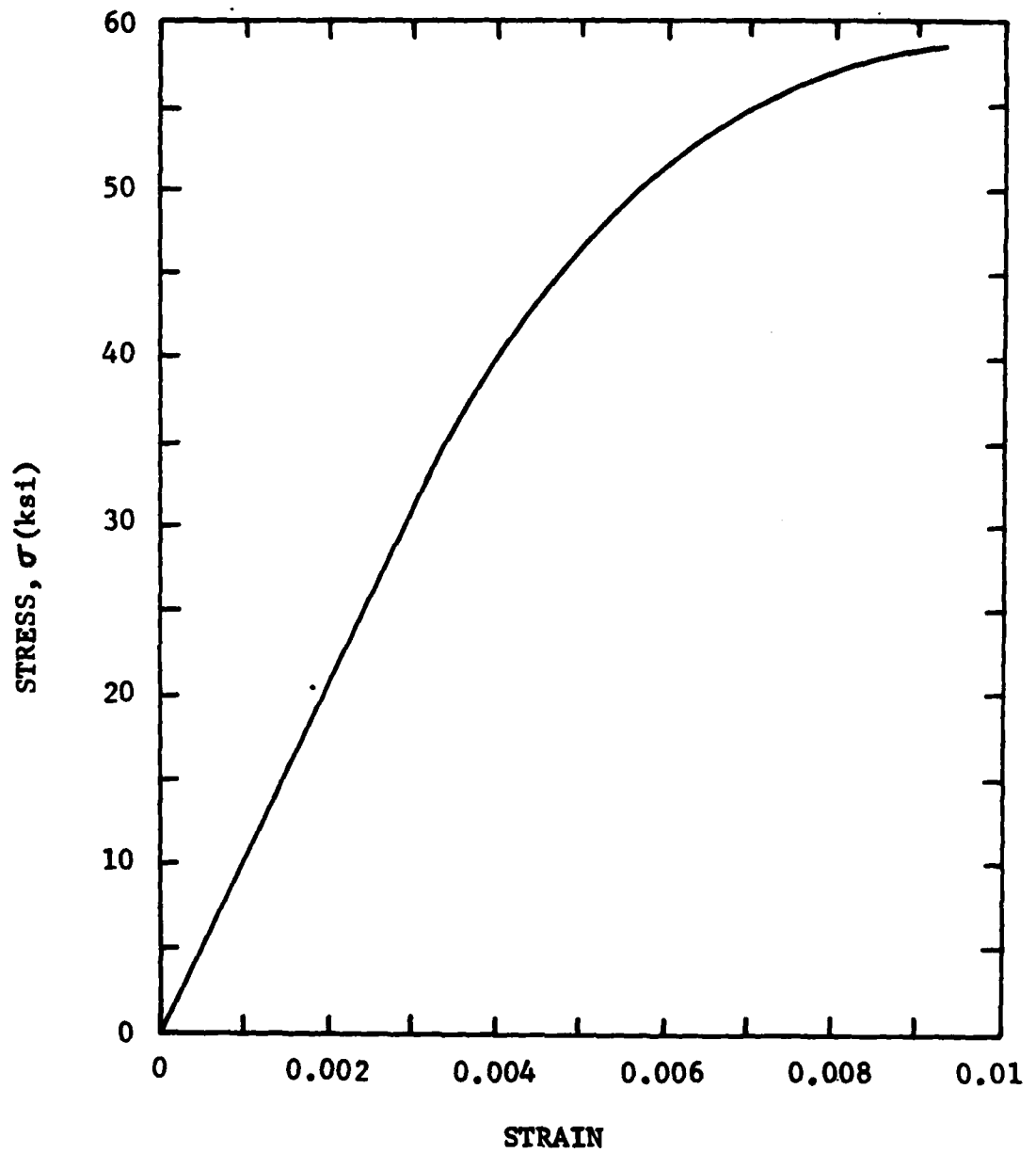


Fig. 21 Cyclic Stress-Strain Curve For 7075-T7651 Aluminum Alloy

enough hydrogen atoms to appreciably change the bulk properties.

Figure 22 shows a stabilized set of hysteresis loops for  $\beta$ -annealed Ti-6Al-4V alloy. A comparison of the cyclic and monotonic stress-strain curves is shown in Fig. 23. This comparison clearly shows slight cyclic softening at a total strain greater than 0.7%. Like the aluminum alloy, results in 3.5% NaCl solution were identical to those in laboratory air.

#### 4.3 FATIGUE CRACK INITIATION RESULTS

Fatigue crack initiation test results for the applicable aluminum and titanium alloys are presented and discussed in this section. The results are presented in various forms for comparison and evaluation.

##### 4.3.1 7075-T7651 Aluminum Alloy

Experimental results for the 7075-T7651 aluminum alloy are summarized in Table 11 for dry air and 3.5% NaCl environments. Results are presented for the number of cycles to crack initiation ( $a_c = 0.010"$ ) and for the number of cycles to failure. The results given in Table 11 are

$\beta$  - Annealed Ti-6Al-4V Alloy

Specimen No. TSS-1

7th Decreasing Block

(Saturated)

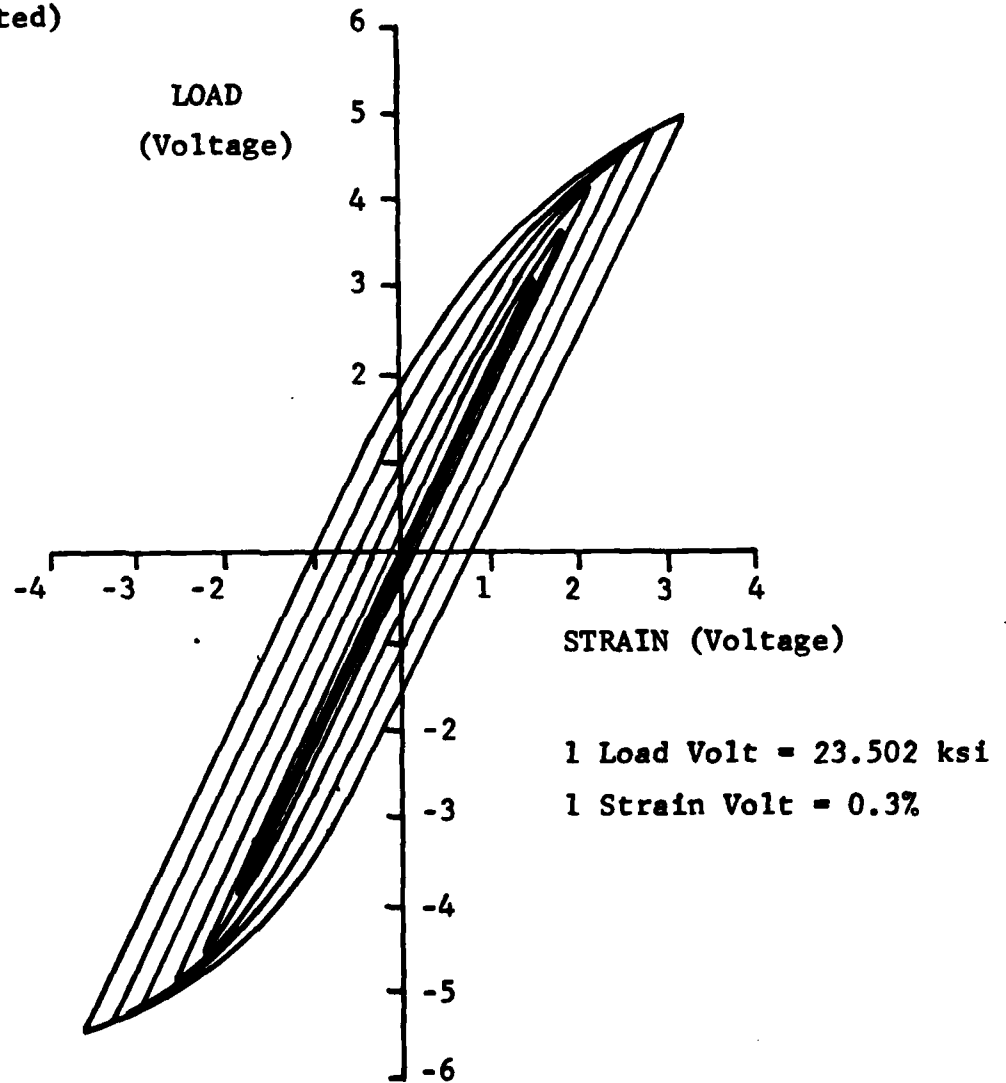


Fig. 22 A Stable Set of Hysteresis Loops for  $\beta$ - Annealed Ti-6Al-4V Alloy

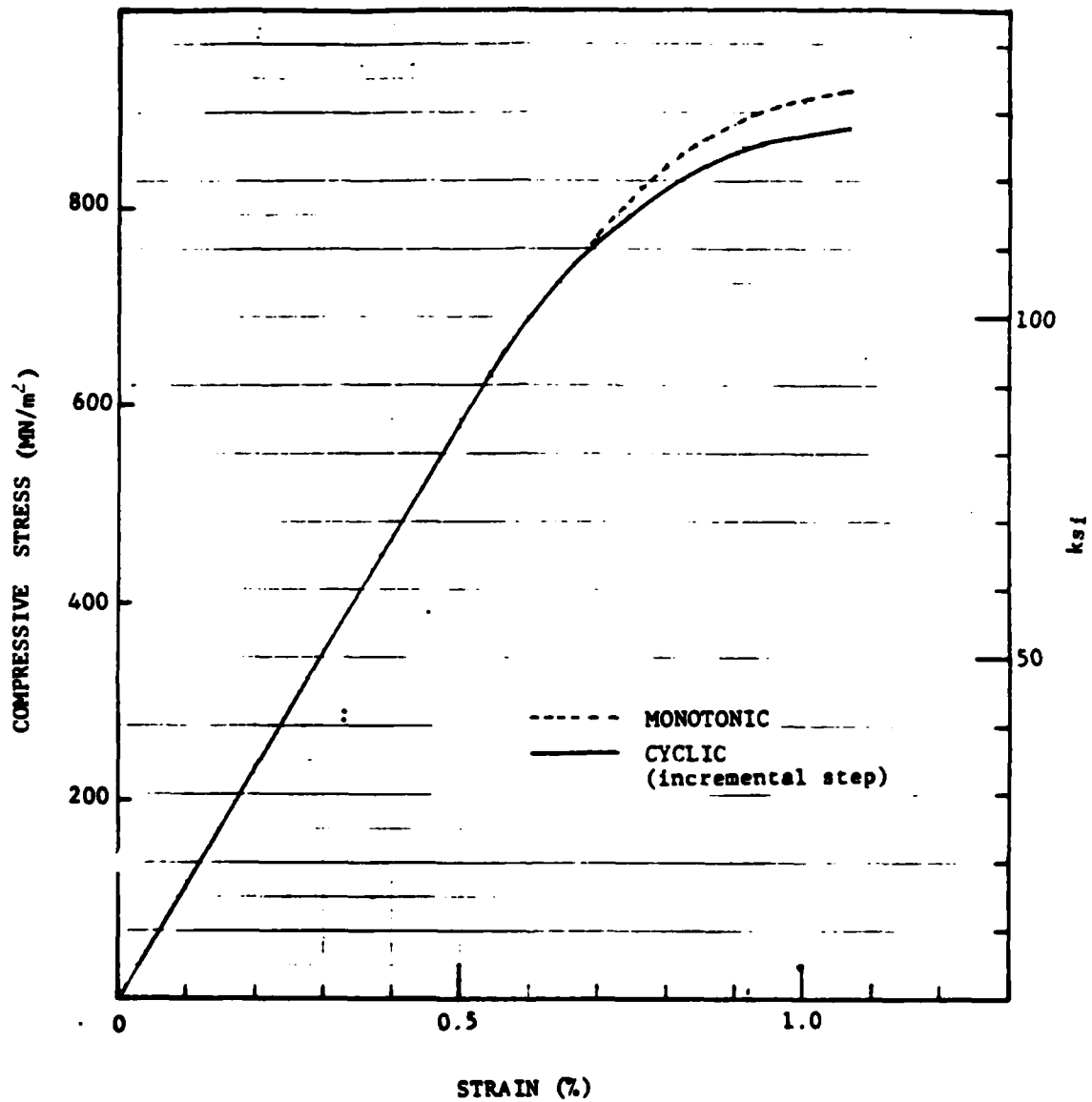
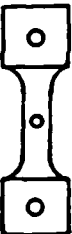
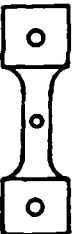


Figure 23 Monotonic and Cyclic Stress-Strain Curves for 8-Annealed Ti-6Al-4V Alloy

Table 11 Normalized Number of Cycles to Crack Initiation ( $a_0 = 0.010''$ ) and Failure for 7075-T7651 Aluminum Alloy in Dry Air and in 3.5% NaCl Solution

ENVIRONMENT	SPECIMEN		FREQUENCY (HZ)	$\Delta\sigma$ (KSI)	NO. OF CYCLES TO INITIATION ( $a_0 = 0.010''$ ) $N_i$	NO. OF CYCLES TO FAILURE $N_f$
	TYPE	NO.				
DRY AIR		AI04	6	14	>1,085,000 ①	>1,085,000 ②
		AI03	6	16	>1,240,000 ①	>1,240,000 ②
		AI09	6	16.2	830,000	912,128
		AI08	6	17	105,000	139,176
		AI16	6	17	102,000	>102,000 ②
		AI17	6	17	103,000	>103,000 ②
		AI01	6	18	120,000	163,808
		AI05	6	20	57,000	72,741
		AI14	6	20	46,000	62,157
		AI15	6	20	46,500	61,128
		AI07	6	22.5	42,000	56,874
		AI02	6	25	25,000	30,742
3.5% NaCl		AI29	6	13.6	----- ③	288,190
		AI23	6	14	308,000	343,936
		AI26	6	15	260,000	300,000
		AI22	6	16	103,000	128,269
		AI31	6	16.5	85,000	100,778
		AI32	6	16.5	83,500	93,623
		AI33	6	16.5	74,500	89,441
		AI37	1	16.5	57,000	63,852
		AI38	1	16.5	62,000	70,349
		AI39	1	16.5	95,000	106,554
		AI21	6	18	37,000	44,495
		AI11	6	20	17,500	27,379
		AI12	6	20	23,500	34,376
		AI13	6	20	16,500	23,673
		AI24	6	20	23,000	30,378
		AI34	1	20	21,300	25,508
		AI35	1	20	22,000	29,743
		AI36	1	20	19,000	22,500
		AI25	6	22.5	18,000	24,450
		AI27	6	25	13,500	15,000

**NOTES:**

1. Test stopped before initiating an 0.010" crack.
2. Not tested to failure.
3. Crack size >0.010" before first eddy current reading.

further evaluated and discussed in the following subsection and in Section V.

#### 4.3.1.1 Effect of Environment

Crack initiation results for dry air and 3.5% NaCl from Table II are plotted in Fig. 24 for selected stress ranges. For the stress ranges studied, the crack initiation resistance in 3.5% NaCl is substantially less than in a dry air environment. The crack initiation results in 3.5% NaCl for 7075-T7651 aluminum alloy qualitatively agree with previous findings reported in the literature [27,28].

For 7075-T7651 aluminum alloy, microcracks are known to initiate caused by further development of persistent slip bands (and thus, slip steps) due to the to-and-fro motion of dislocations along slip planes from the cyclic mechanical force. Therefore, in a corrosive environment, the preferential electrochemical attack on the predominant slip planes, with distorted metal acting as anode and undistorted metal acting as cathode, accelerates the process of crack nucleation.

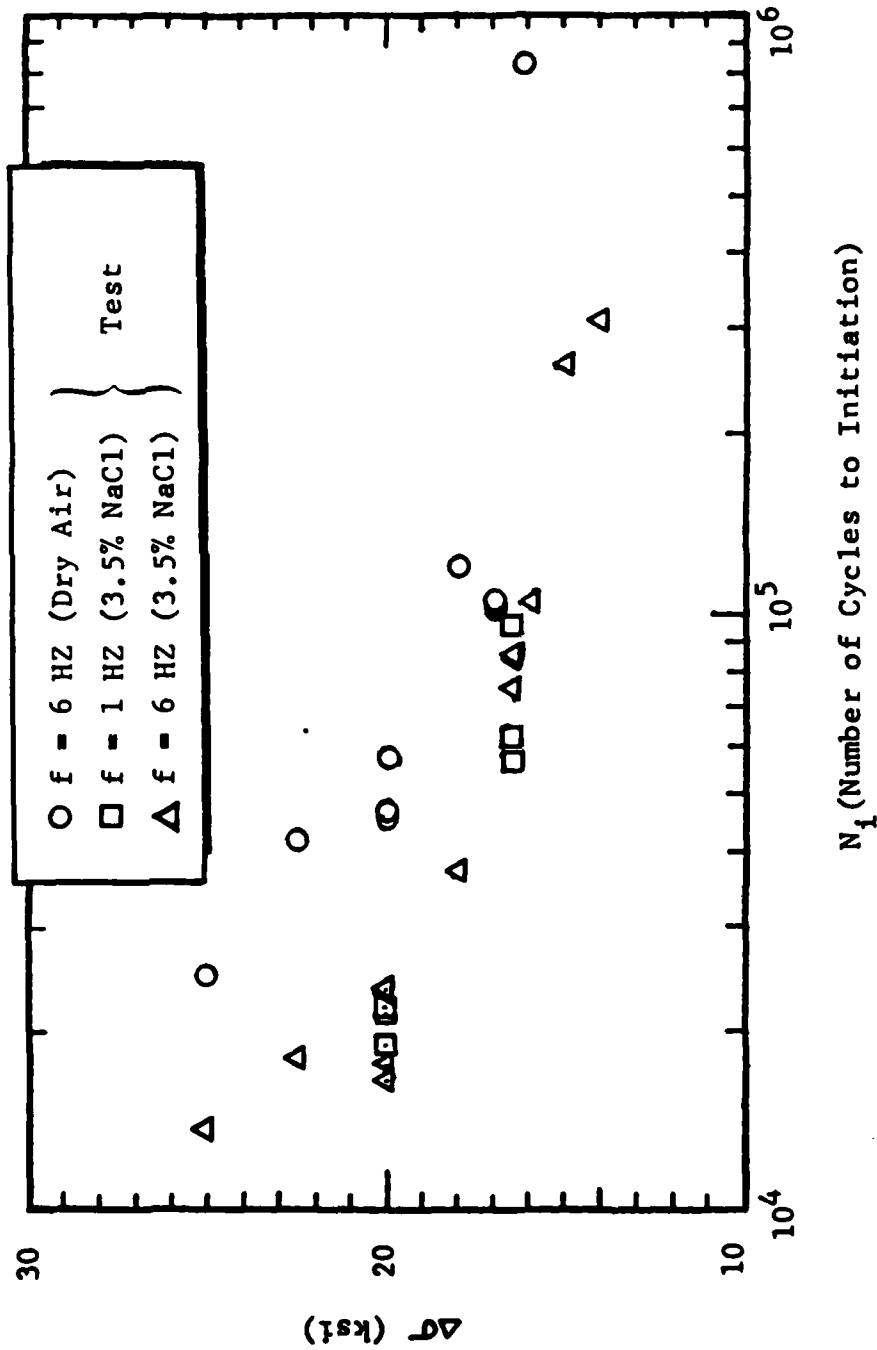


Fig. 24 Comparison of  $\Delta\sigma$  Versus  $N_i$  Curves (Dry Air & 3.5% NaCl) for 7075-T7651 Aluminum Alloy ( $a_0 = 0.010''$ )

#### 4.3.1.2 Effect of Frequency

Is there a significant difference in the mean  $N_i$  values for two different loading frequencies (i.e.,  $f = 1$  Hz and 6 Hz) at  $\alpha = 0.05$  significance level? A standard small-sample test [e.g., 29] is made to address this question.

Two tests for differences in the mean  $N_i$  value are shown in Table 12 for  $\Delta\sigma = 16.5$  ksi and 20 ksi and a 3.5% NaCl environment.  $N_i$  results were obtained from Table 11. The  $N_i$  mean ( $\bar{X}$ ) and standard deviation ( $S(x)$ ) for applicable frequencies are indicated.

In both cases considered, the test statistic,  $|t|$ , is less than the limiting student  $t_\alpha$  value shown in Table 12. Therefore, it is concluded for Cases I and II that there is no significant difference in the mean  $N_i$  values for  $f = 1$  Hz and 6 Hz at  $\alpha = 0.05$  significance level.

The ratio of the number of cycles to crack initiation ( $a_c = 0.010''$ ) to the number of cycles to failure ( $N_i/N_f$ ) was determined for the dry air and 3.5% NaCl environment tests shown in Table 11. Bar plots and other statistical results are shown in Fig. 25. It is interesting to note that the average  $N_i/N_f$  ratio is approximately the same for both dry

Table 12 Small-Sample Test Evaluations for Differences in Mean  $N_1$  for Different Frequencies (7075-T7651; 3.5% NaCl)

Specimen No.	f (Hz)	$\Delta\sigma$ (ksi)	$N_1$ (Cycles)	$\bar{x}$	S(x)	S	Test Statistic t	$t_\alpha$	CASE
AI37	1	16.5	57000	71333	20648	15142	-0.782	2.78	I
AI38	↓	↓	62000	↓	↓	↓	↓	↓	↓
AI39	↓	↓	95000	↓	↓	↓	↓	↓	↓
AI31	6	↓	85000	81000	5679	↓	↓	↓	↓
AI32	↓	↓	83500	↓	↓	↓	↓	↓	↓
AI33	↓	↓	74500	↓	↓	↓	↓	↓	↓
AI34	1	20	21300	20767	1569	2987	0.282	2.57	II
AI35	↓	↓	22000	↓	↓	↓	↓	↓	↓
AI36	↓	↓	19000	↓	↓	↓	↓	↓	↓
AI11	6	↓	17500	20125	3637	↓	↓	↓	↓
AI12	↓	↓	23500	↓	↓	↓	↓	↓	↓
AI13	↓	↓	16500	↓	↓	↓	↓	↓	↓
AI24	↓	↓	23000	↓	↓	↓	↓	↓	↓

$$S = \sqrt{\frac{(n_1 - 1) S_1^2(x) + (n_2 - 1) S_2^2(x)}{n_1 + n_2 - 2}}$$

$$(\text{Test Statistics}) t = \frac{\bar{X}_1 - \bar{X}_2}{S \sqrt{\frac{1}{n_1} + \frac{1}{n_2}}}$$

$$S(x) = \sqrt{\frac{\sum (N_1 - \bar{x})^2}{n-1}}$$

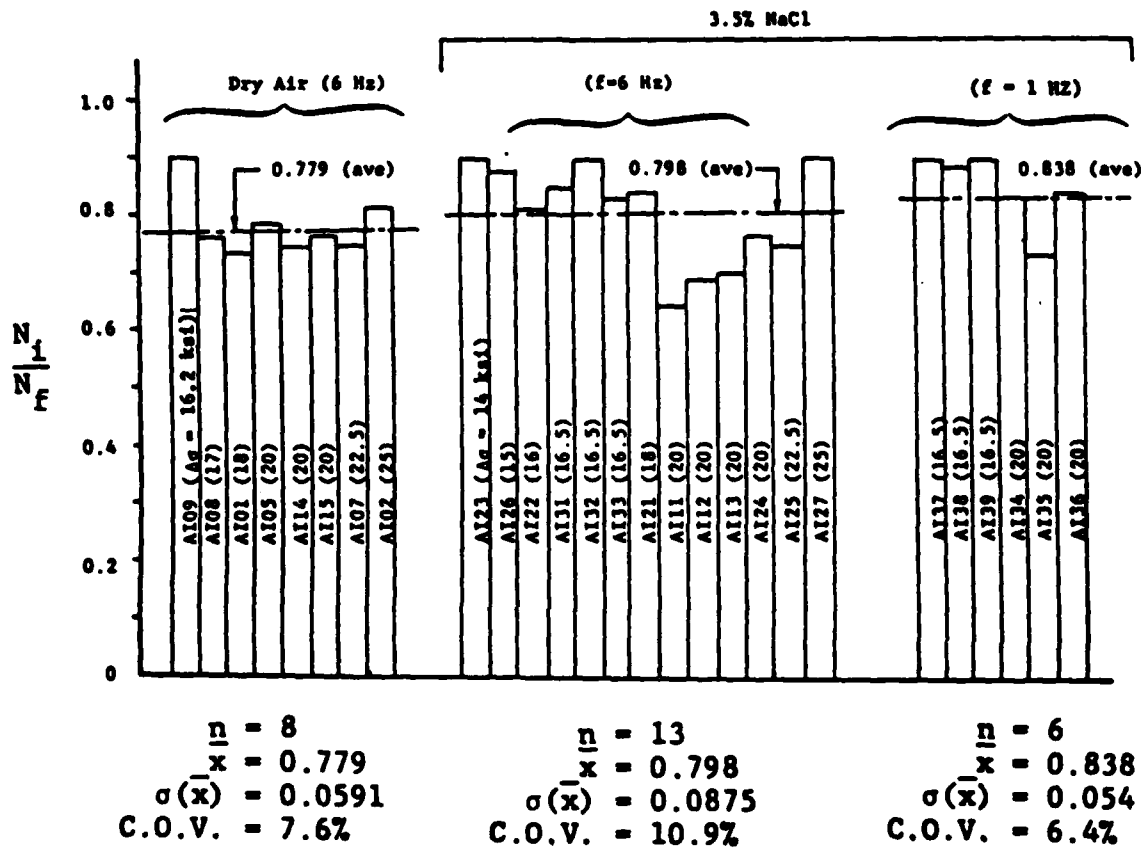


Fig. 25 Effect of Frequency on  $N_1/N_f$  Ratio for 7075-T7651 Aluminum Alloy ( $a_0 = 0.010''$ )

air and 3.5% NaCl environment. Also, based on the small sample test for difference in mean values [e.g., 29], it was determined that there is no significant difference in the mean  $N_i/N_f$  ratio for  $f = 1$  Hz and 6 Hz for  $\alpha = 0.05$  significance level.

#### 4.3.1.3 Discussion

The following conclusions are based on the test results and evaluations in subsection 4.3.1.

1. The crack initiation resistance of the 7075-T7651 aluminum alloy depends on the severity of the environment. For example, the resistance to crack initiation is higher in a dry air environment than in a 3.5% NaCl environment.

2. No significant differences in the mean  $N_i$  values were found in a 3.5% NaCl environment for  $f = 1$  Hz and 6 Hz at  $\alpha = 0.05$  significance level. This conclusion was reached for two different  $\Delta\sigma$  levels (i.e., 16.5 ksi and 20 ksi). A wider range of  $\Delta\sigma$  levels should be investigated to evaluate the effects of frequency on  $N_i$  results.

3. Based on constant amplitude test results, the number of cycles to crack initiation ( $a_c = 0.010$ ) is a significant

part of the total fatigue life. For example, the mean ( $N_i/N_f$ ) ratio varied from 0.779 to 0.838 (ref. Fig. 25). Interestingly, no significant differences were found in the mean ( $N_i/N_f$ ) ratio for either a dry air or a 3.5% NaCl environment. Also, the loading frequency did not have a significant effect on the mean ( $N_i/N_f$ ) ratio for  $\alpha = 0.05$  significance level.


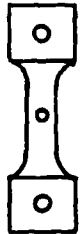


#### 4.3.2 $\beta$ -Annealed Ti-6Al-4V Alloy

Crack initiation test results for the titanium alloy are summarized in Table 13 for the dry air and 3.5% NaCl environments. The number of cycles to failure are also presented. Testing and data acquisition procedures used are described and discussed in subsection 3.3.3. Test results from Table 13 are evaluated and discussed in the following subsection and in Section V.

##### 4.3.2.1 Effect of Environment

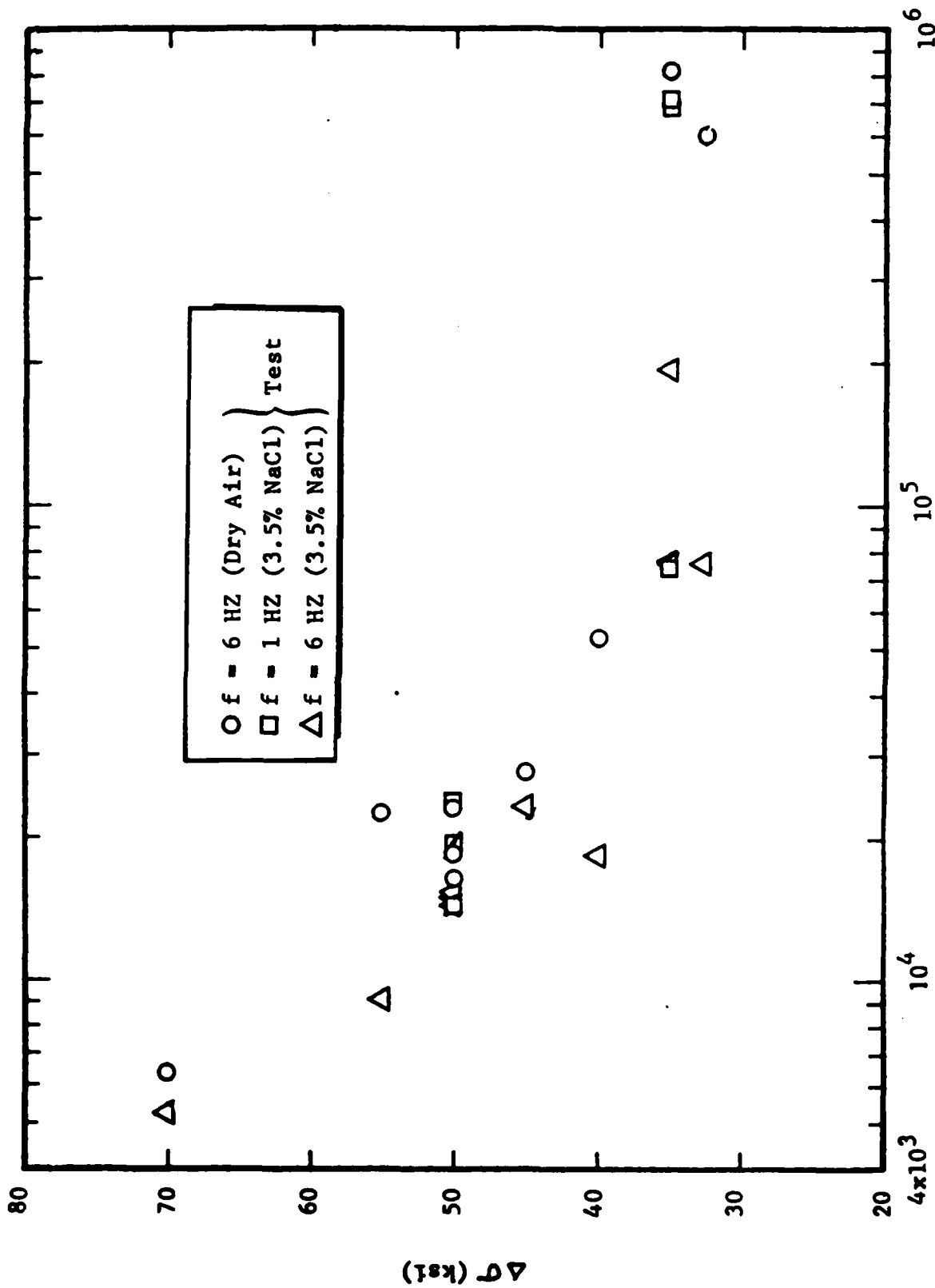
The crack initiation results from Table 11 are plotted in Fig. 26 as  $\Delta a$  versus  $N_i$  for dry air and 3.5% NaCl environments. These results indicate that the crack initiation resistance depends on the environment.

**Table 13 Normalized Number of Cycles to Crack Initiation  
( $a_0 = 0.010''$ ) and Failure for  $\beta$ -Annealed Ti-6Al-4V  
Alloy in Dry Air and in 3.5% NaCl Solution**

ENVIRONMENT	SPECIMEN		FREQUENCY (HZ)	$\Delta\sigma$ (KSI)	NO. OF CYCLES TO INITIATION ( $a_0 = 0.010''$ ) $N_i$	NO OF CYCLES TO FAILURE $N_f$
	TYPE	NO.				
DRY AIR 		TI08	6	32.5	600,000	660,027
		TI06	↓	35	820,000	872,434
		TI05	↓	40	52,400	72,841
		TI04	↓	45	27,500	43,797
		TI09	↓	50	16,505	29,610
		TI10	↓	↓	23,100	41,015
		TI11	↓	↓	18,500	25,519
		TI02	↓	55	22,600	25,308
		TI03	↓	60	---	13,995
		TI01	↓	70	6,400 ③	7,552
3.5% NaCl 		TI28	6	27.5	>1,000,000 ①	> 1,000,000 ②
		TI25	↓	30	>1,000,000 ①	> 1,000,000 ②
		TI26	↓	32.5	75,000	90,020
		TI22	↓	35	77,000	99,723
		TI24	↓	↓	76,000	105,982
		TI25	↓	↓	191,000	221,065
		TI26	↓	↓	> 1,000,000 ①	> 1,000,000 ②
		TI32	1	↓	710,000	765,252
		TI33	↓	↓	680,000	739,456
		TI34	↓	↓	73,000	81,574
		TI21	6	40	18,200	23,979
		TI23	↓	45	23,000	27,857
		TI21	↓	50	15,500	21,827
		TI22	↓	↓	14,300	19,418
		TI23	↓	↓	15,000	21,947
		TI29	1	50	24,000	27,887
		TI30	↓	↓	19,500	22,960
		TI31	↓	↓	14,200	16,988
		TI24	6	55	9,100	11,693
		TI27	↓	70	5,200	6,573

**NOTES:**

1. Test stopped before initiating an 0.010" crack.
2. Not tested to failure.
3. Crack size >0.010" before first eddy current reading.



$N_i$  (Number of Cycles to Initiation)

Fig. 26 Comparison of  $\Delta\sigma$  Versus  $N_i$  (Dry Air & 3.5% NaCl) for  $\beta$ -Annealed Ti-6Al-4V Alloy ( $a_0 = 0.010''$ )

#### 4.3.2.2 Effect of Frequency

The effect of loading frequency on the mean  $N_i$  and the mean  $(N_i/N_f)$  ratio is evaluated in this section. A standard small-sample test [e.g., 29] will be used to determine if there is a significant difference in the applicable mean values for  $\alpha = 0.05$  significance level.

$N_i$  results from Table 13 for  $\Delta\sigma = 35$  ksi and 50 ksi are listed in Table 14 for two different loading frequencies (i.e.,  $f = 1$  Hz and 6 Hz). The effects of loading frequency on  $N_i$  are evaluated using these results. Specimen TIM6 (3.5% NaCl,  $f = 6$  Hz,  $\Delta\sigma = 35$  ksi) from Table 13 was not included in the statistical analysis because the test was stopped before a crack size of 0.010" had been initiated.

Results of the small-sample tests for determining if there is a significant difference in the mean  $N_i$  values for different loading frequencies are given in Table 14. The results in both cases (III and IV) indicate that there is no significant difference in the mean  $N_i$  values for the same  $\Delta\sigma$  value and for two different loading frequencies at  $\alpha = 0.05$  significance level. This conclusion appears to be justified for Case IV ( $\Delta\sigma = 50$  ksi). However, due to the observed scatter for Case III and the fact that specimen TIM6 was not

Table 14 Small-Sample Test Evaluations for Differences in Mean N. for  
Different Frequencies ( $\beta$ -Annealed Ti-6Al-4V Alloy)

Specimen No.	f (Hz)	$\Delta\sigma$ (ksi)	$N_1$ (Cycles)	$\bar{X}$	S(x)	S	Test Statistic t	$t_\alpha$	CASE
TI32	1	35	71000	487667	359425	258415	1.77	2.78	III
TI33	↓	↓	680000	↓	↓	↓	↓	↓	↓
TI34	↓	↓	73000	↓	↓	↓	↓	↓	↓
TI22	6	↓	77000	114667	66108	3494	1.51	2.78	IV
TIM4	↓	↓	76000	↓	↓	↓	↓	↓	↓
TIM5	↓	↓	191000	↓	↓	↓	↓	↓	↓
TI29	1	50	24000	19233	4905	↓	↓	↓	↓
TI30	↓	↓	19500	↓	↓	↓	↓	↓	↓
TI31	↓	↓	14200	↓	↓	↓	↓	↓	↓
TIM1	6	↓	15500	14933	603	↓	↓	↓	↓
TIM2	↓	↓	14300	↓	↓	↓	↓	↓	↓
TIM3	↓	↓	15000	↓	↓	↓	↓	↓	↓

$$S = \sqrt{\frac{(n_1-1) S_1^2(x) + (n_2-1) S_2^2(x)}{n_1 + n_2 - 2}}$$

$$(\text{Test Statistics}) t = \frac{\bar{X}_1 - \bar{X}_2}{S \sqrt{\frac{1}{n_1} + \frac{1}{n_2}}}$$

$$S(x) = \sqrt{\frac{\sum (N_1 - \bar{x})^2}{n-1}}$$

included in the analysis, the effects of loading frequency at  $\Delta\sigma = 35$  ksi are not considered to be conclusive.

The ratio of  $N_i/N_f$ , determined from Table 13, is plotted in Fig. 27 for dry air and for 3.5% NaCl environments. Mean  $N_i/N_f$  values ranged from 0.753 to 0.881. In this case,  $N_i/N_f$  values for different  $\Delta\sigma$  values were used to determine the corresponding mean  $N_i/N_f$  ratio. Like the aluminum alloy, the initiation life ( $a_i = 0.010"$ ) represents a significant portion of the total fatigue life for the titanium alloy. Further testing and evaluation of the titanium alloy is recommended to better understand the corrosion fatigue mechanisms and the effects of loading frequency on crack initiation.

#### 4.4 FATIGUE CRACK PROPAGATION RESULTS AND EVALUATIONS

Several fatigue crack propagation tests were performed in Phase I (ref. Tables 3 and 4) to evaluate the effects of environment, R ratio, loading frequency, hold time, etc. on crack growth. Test results for the 7075-T7651 aluminum alloy and for the  $\beta$ -annealed Ti-6Al-4V alloy are presented in this section. Experimental results are compared and evaluated. These results are also used to evaluate the crack propagation models described in Section

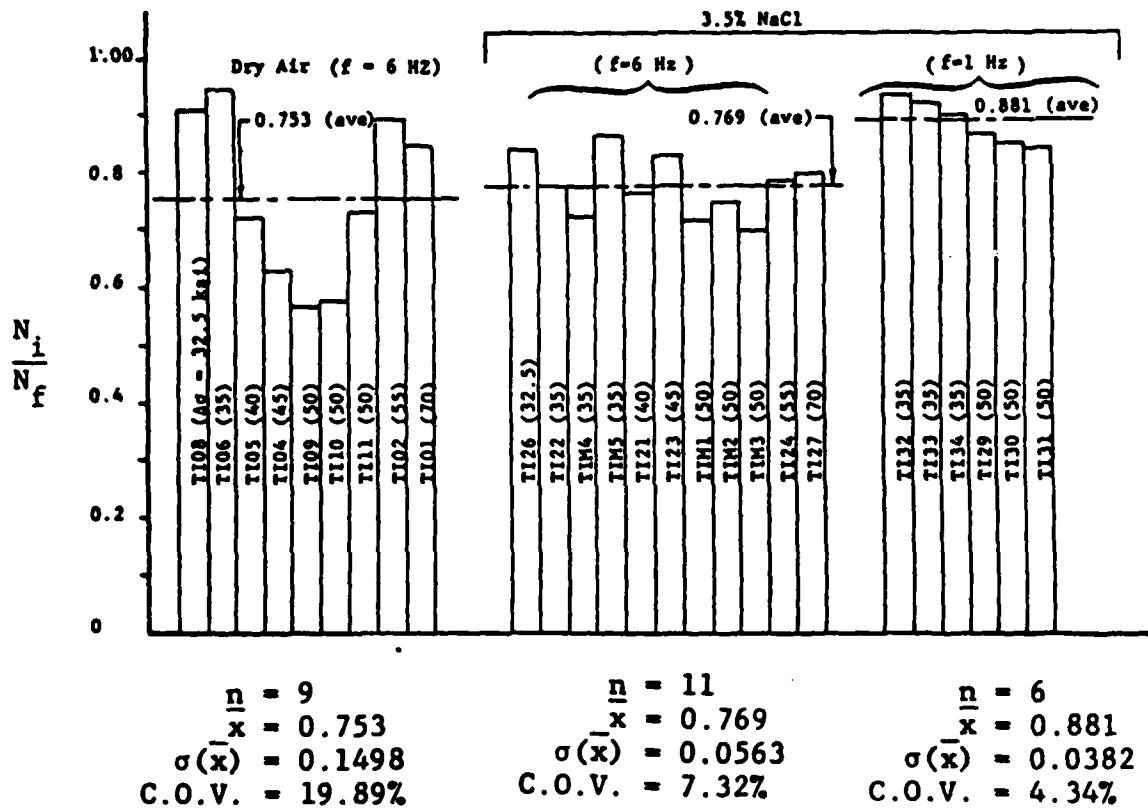


Fig. 27 Effect of Frequency on  $N_i/N_f$  Ratio for  $\beta$ -Annealed Ti-6Al-4V Alloy ( $a_0 = 0.010^h$ )

II. Details of the model evaluation are given in subsection 5.3.

#### 4.4.1 7075-T7651 Aluminum Alloy

Room temperature crack growth data for the 7075-T7651 aluminum alloy are presented in this section and in Appendix A. Results are evaluated and discussed.

##### 4.4.1.1 Effect of Environment

Results of the tests conducted in different environments (Table 4 of the test matrix) are shown in Fig. 28. These tests were conducted in 3.5% NaCl + H<sub>2</sub>SO<sub>4</sub> (pH = 3.5), ASTM artificial seawater, and distilled water. Results are also compared with data for 3.5% NaCl (R = 0.05, Freq. = 6 Hz). Little difference in propagation rate was observed in the 3.5% NaCl, 3.5% NaCl + H<sub>2</sub>SO<sub>4</sub> (pH = 3.5), and ASTM artificial seawater environments. Slower crack growth rates were observed in distilled water as expected.

A comparison of crack growth rates in dry air and 3.5% NaCl are shown in Figs. 29 and 30. Two different R values (R = 0.05 and R = 0.3) were compared. For R = 0.05, average crack rates were higher in the salt water environment for  $\Delta K$

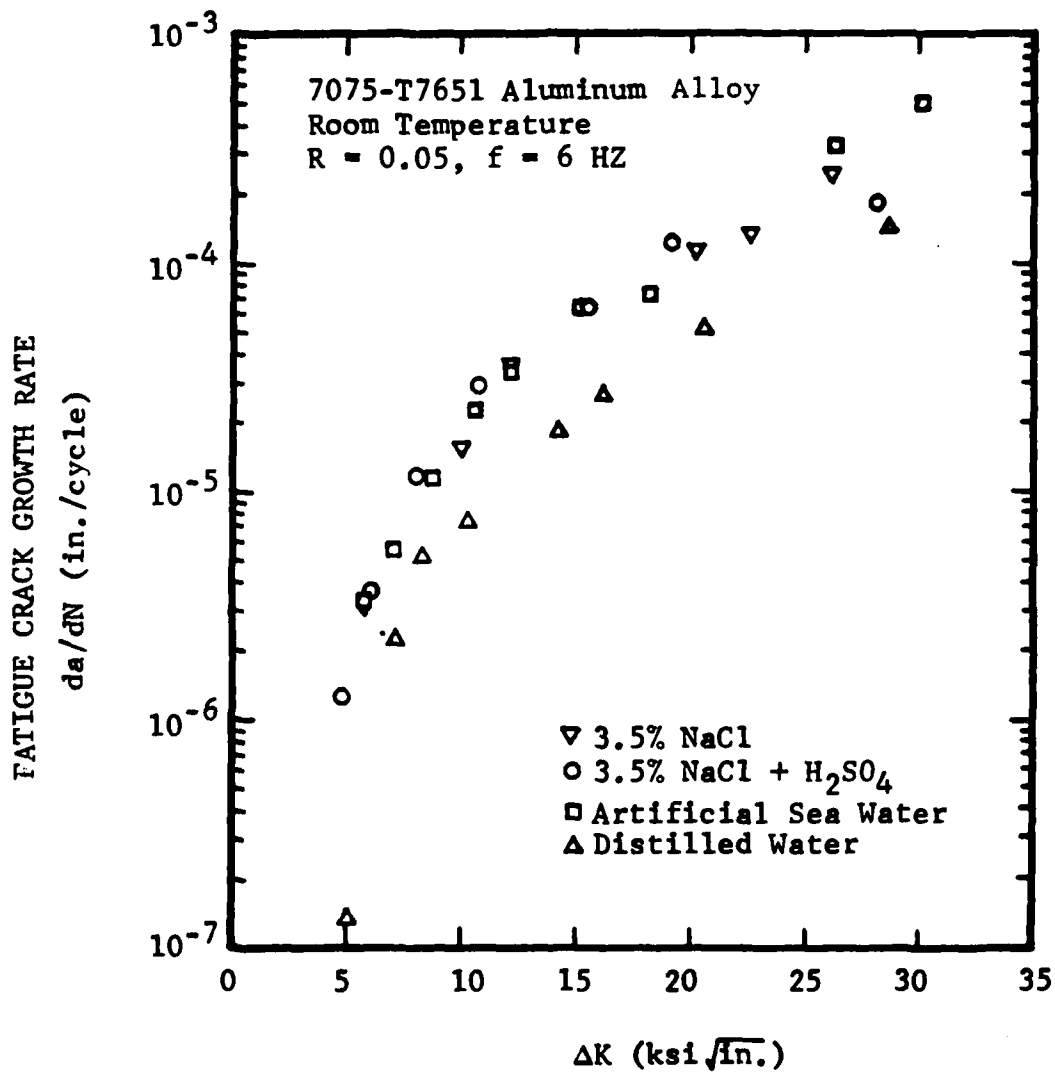


Fig. 28 Effect of Environment on Crack Growth Rates for 7075-T7651 Aluminum Alloy at Room Temperature ( $R=0.5, f = 6 \text{ Hz}$ )

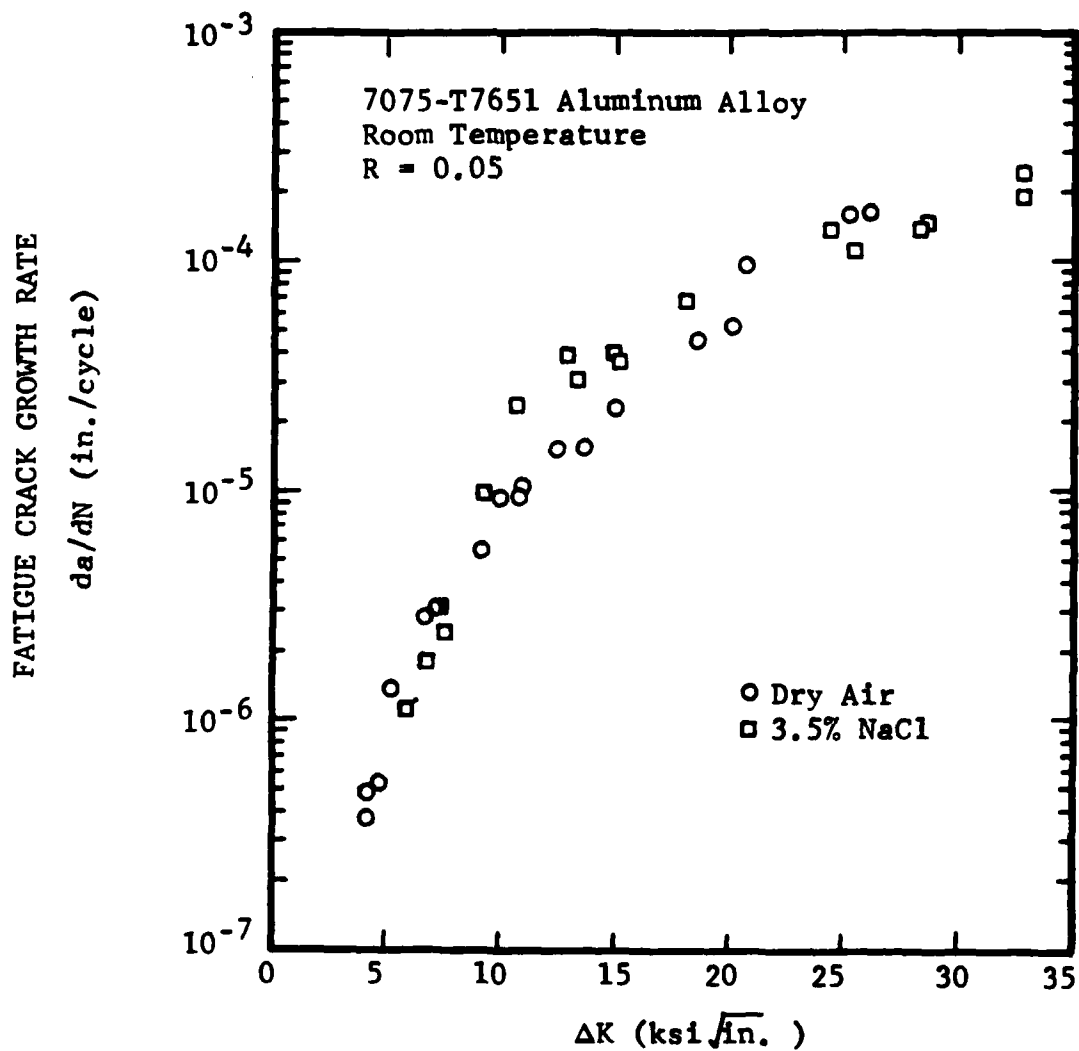


Fig. 29 Comparison of Crack Growth Rates for 7075-T7651 Aluminum Alloy in Both Dry Air and 3.5% NaCl Solution at Room Temperature ( $R = 0.05$ )

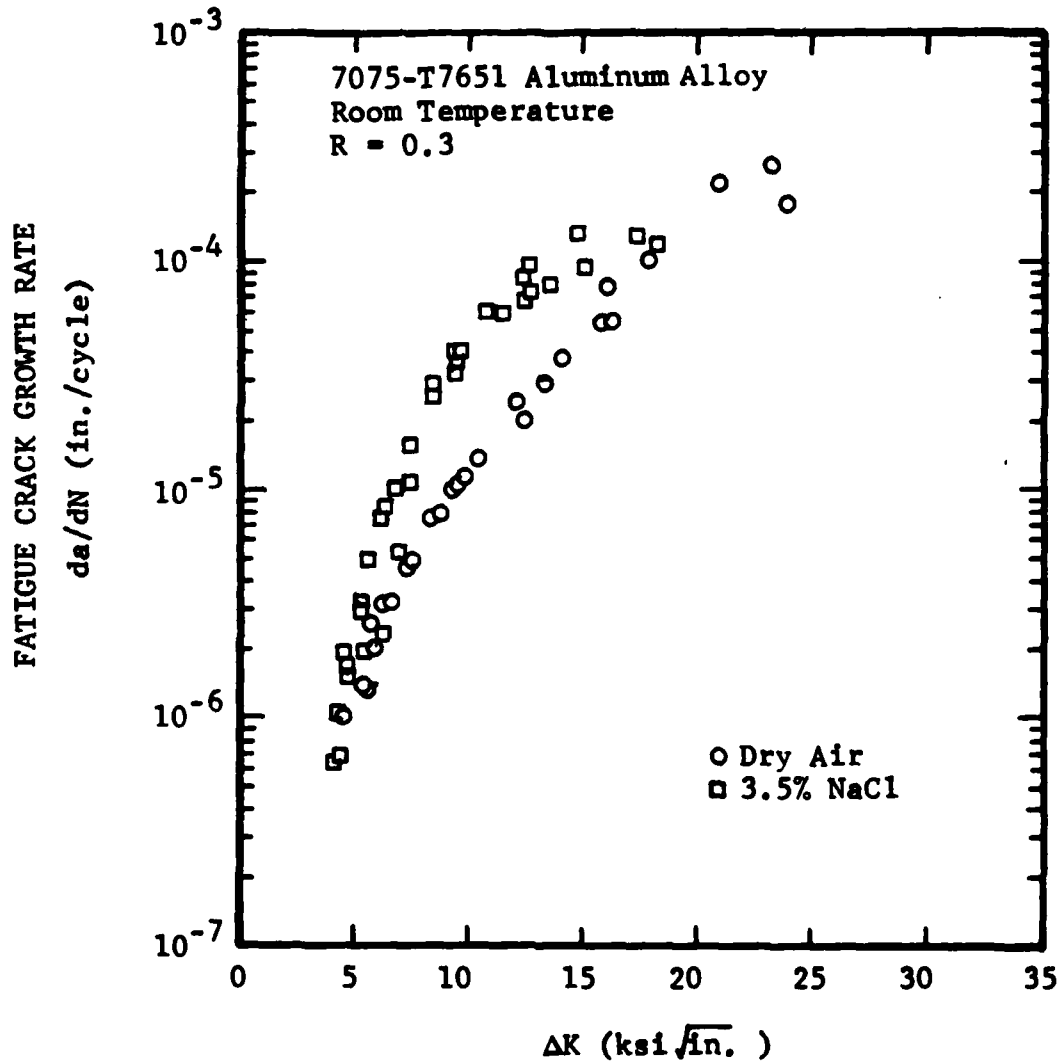


Fig. 30 Comparison of Crack Growth Rates for 7075-T7651 Aluminum Alloy in Both Dry Air and 3.5% NaCl Solution at Room Temperature (R = 0.3)

values between approximately 10 and 20 ksi  $\sqrt{\text{inch}}$ . For  $R = 0.3$ , crack rates were higher for  $\Delta K$  values ranging from approximately 5 ksi  $\sqrt{\text{inch}}$  to 18 ksi  $\sqrt{\text{inch}}$ . A larger difference in crack rate was observed at  $R = 0.3$ . Other investigators have also observed no difference in crack rate at very low and very high  $\Delta K$  values [30]. Our results are similar to those obtained for 7075-T73 and 7075-T6 sheet [31], where the largest difference in crack growth rates were observed in  $\Delta K = 7$  ksi  $\sqrt{\text{in.}}$  to  $\Delta K = 20$  ksi  $\sqrt{\text{in.}}$  range.

#### 4.4.1.2 Effect of R Ratio

The effect of  $R$  ratio on crack growth rate in dry air is shown in Fig. 31. Above a stress intensity range of approximately 10 ksi  $\sqrt{\text{inch}}$ , a considerable accelerated crack growth rate is observed at the higher mean stress ( $R = 0.3$ ). The sensitivity of aluminum alloys to mean loads given by the ratio  $R$  has been documented [32-34].

The effect of  $R$  ratio on crack growth rate in 3.5% NaCl is shown in Fig. 32. Practically identical growth rates are observed at the  $R$  ratios,  $R = 0.2, 0.3$ , and  $0.4$ . At the  $R$  ratio,  $R = 0.05$ , slower growth rate is observed in the stress intensity range,  $\Delta K = 7$  ksi  $\sqrt{\text{inch}}$  to  $\Delta K = 15$  ksi  $\sqrt{\text{inch}}$ . Similar results were obtained in a dry air environment where slower crack growth rates were obtained at low  $R$  values.

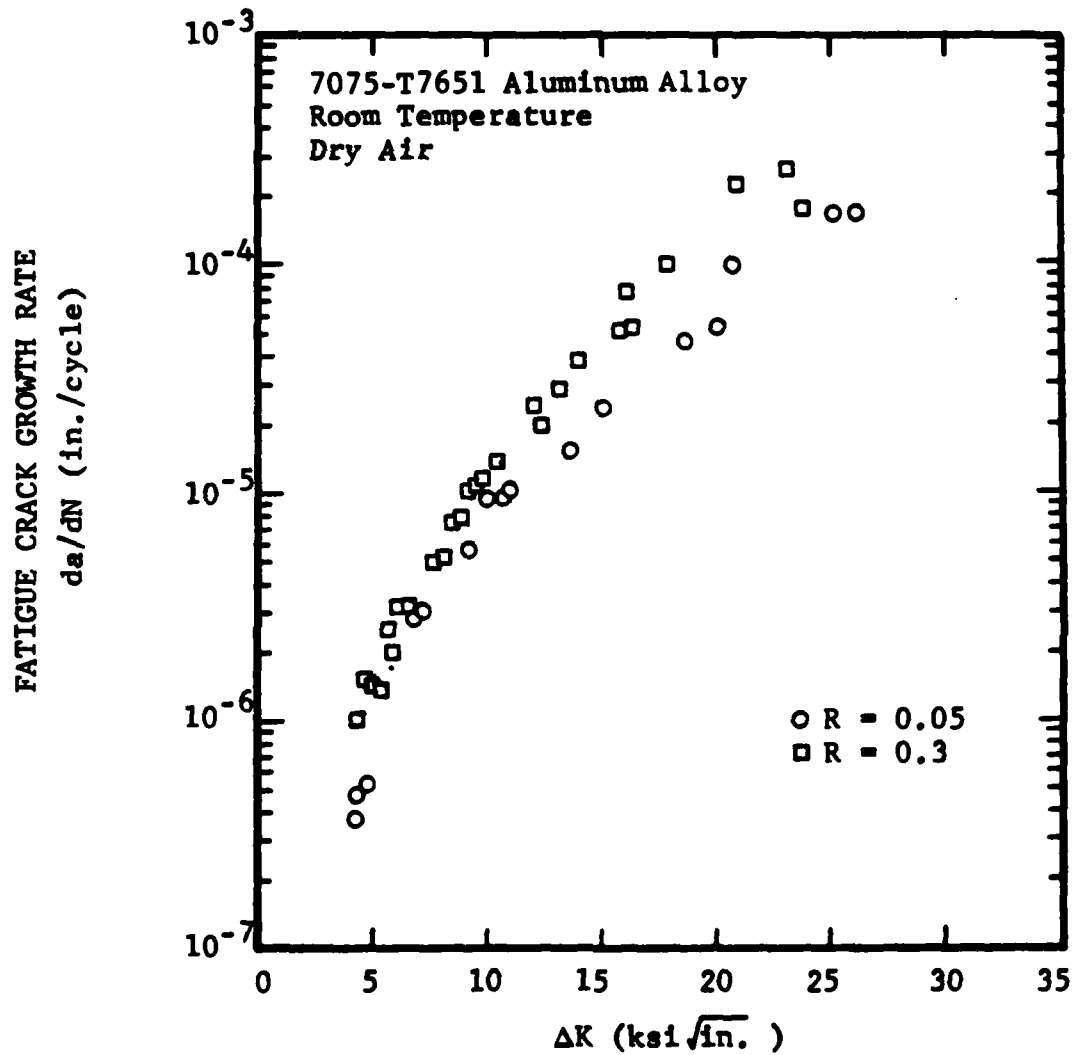


Fig. 31 Effect of R Ratio on Crack Growth Rates for 7075-T7651 Aluminum Alloy in Dry Air at Room Temperature (R = 0.05, 0.3)

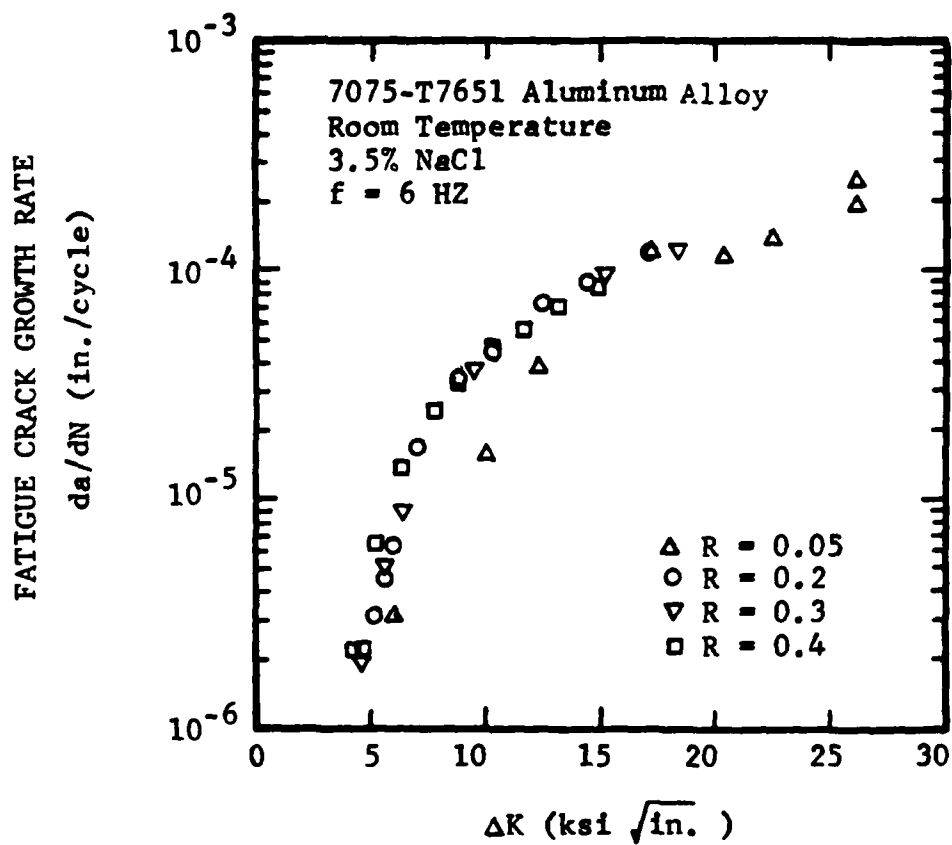


Fig. 32 Effect of R Ratio on Crack Growth Rates for 7075-T7651 Aluminum Alloy Exposed to 3.5% NaCl Solution at Room Temperature ( $f = 6$  HZ;  $R = 0.05, 0.2, 0.3, \text{ and } 0.4$ )

#### 4.4.1.3 Effect of Frequency

Dry air experiments were conducted at test frequencies of 0.1 Hz, 1.0 Hz, and 6.0 Hz. Two different R ratios of 0.05 and 0.3 were used. A comparison of crack growth rates for specimens tested at different frequencies is shown in Figs. 33 and 34. At an R ratio of  $R = 0.05$ , virtually no effect of frequency on crack growth rate was obtained (Fig. 33). For a higher mean stress ( $R = 0.3$ ), no effect is observed at a stress intensity range,  $\Delta K$ , below approximately 15 ksi  $\sqrt{\text{inch}}$  (Fig. 34). Results above 15 ksi  $\sqrt{\text{inch}}$  are inconclusive due to limited data at 1.0 and 6.0 Hz. In a vacuum and very dry gases, crack growth rates are usually found to be independent of cycle frequency [35].

Tests in 3.5% NaCl environment were conducted at frequencies ranging from 0.1 Hz to 6.0 Hz and mean loads ranging from  $R = 0.05$  to  $R = 0.4$ . The effect of cycle frequency on crack growth rate in a salt water environment is shown in Figs. 35 - 37. Little difference was observed in crack growth rates at the different cyclic frequencies, particularly at the lower stress intensity range. Previous results are inconclusive regarding the effects of cyclic frequency on crack growth in aluminum alloys. Frequency effects are usually small in aqueous environments,

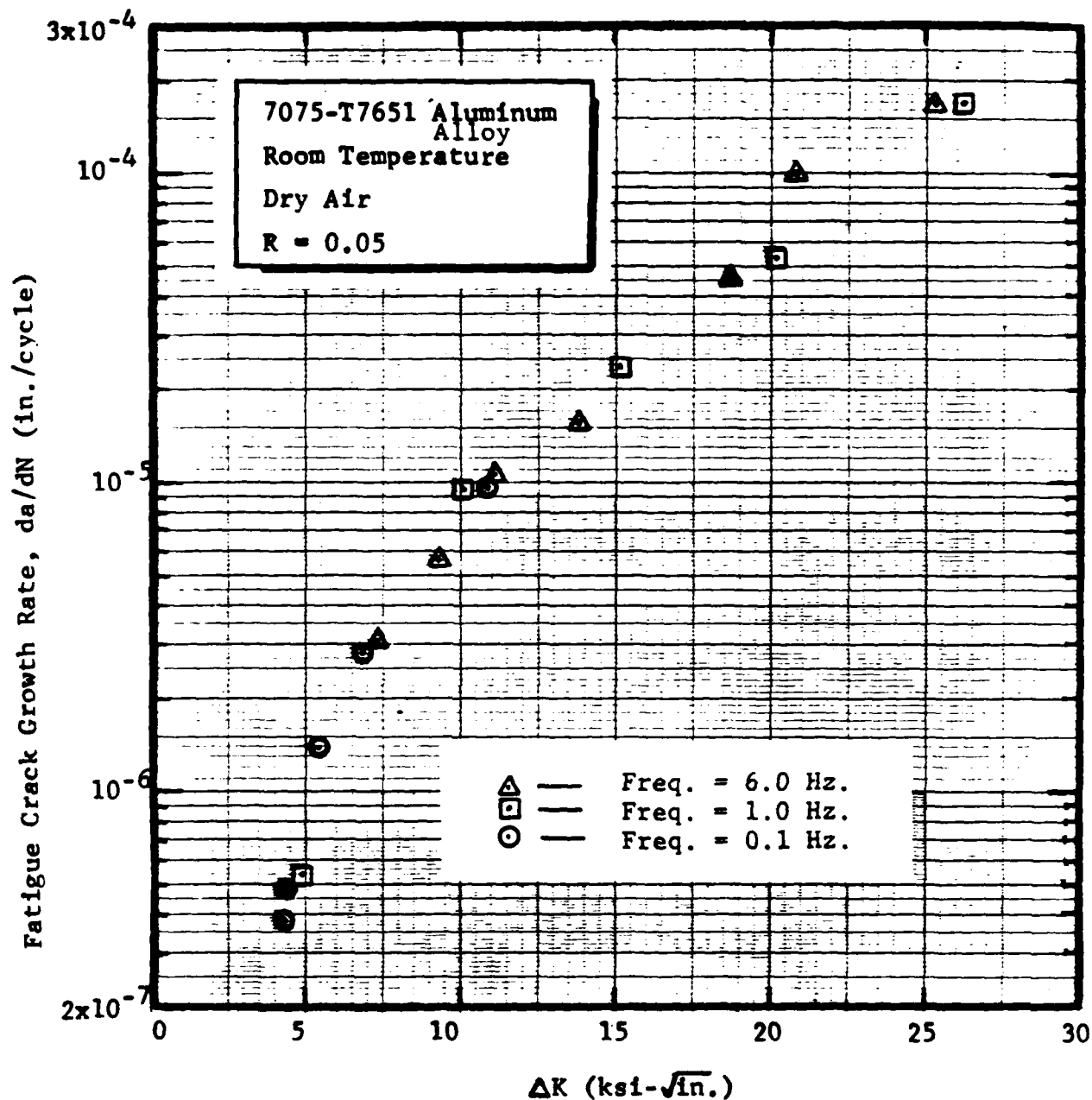


Fig. 33 Effect of Frequency on Crack Growth Rates for 7075-T7651 Aluminum Alloy in Dry Air at Room Temperature (R = 0.05; f = 0.1 Hz, 1 Hz and 6 Hz)

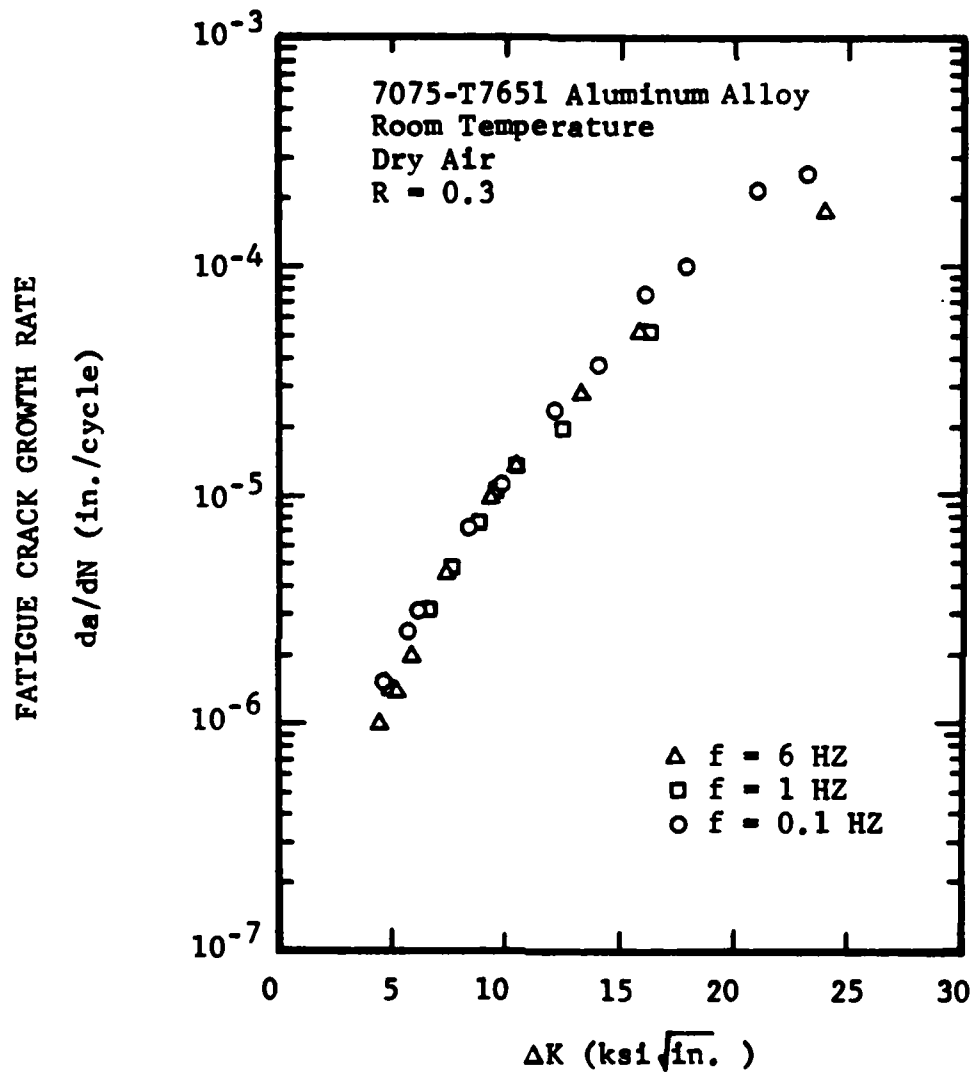


Fig. 34 Effect of Frequency on Crack Growth Rates for 7075-T7651 Aluminum Alloy in Dry Air at Room Temperature ( $R = 0.3$ ;  $f = 0.1$  HZ, 1 HZ, and 6 HZ)

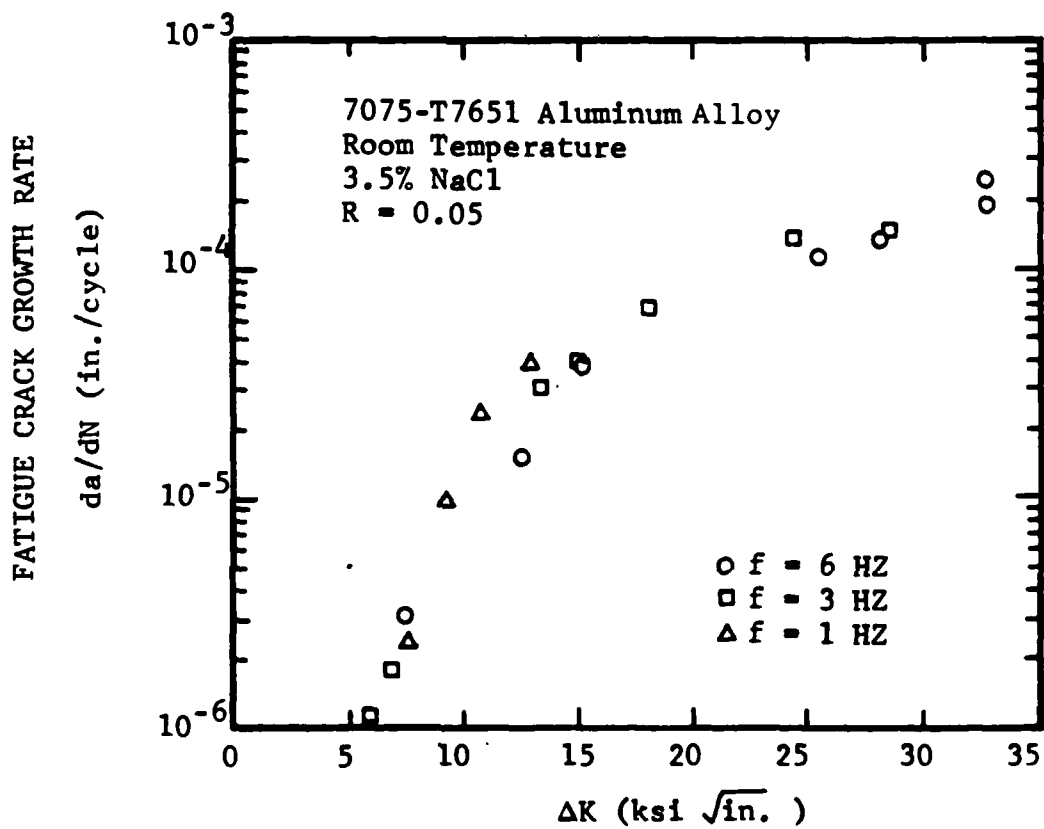


Fig. 35 Effect of Frequency on Crack Growth Rates for 7075-T7651 Aluminum Alloy Exposed to 3.5% NaCl Solution at Room Temperature ( $R = 0.05$ ;  $f = 1$  HZ, 3 HZ, and 6 HZ)

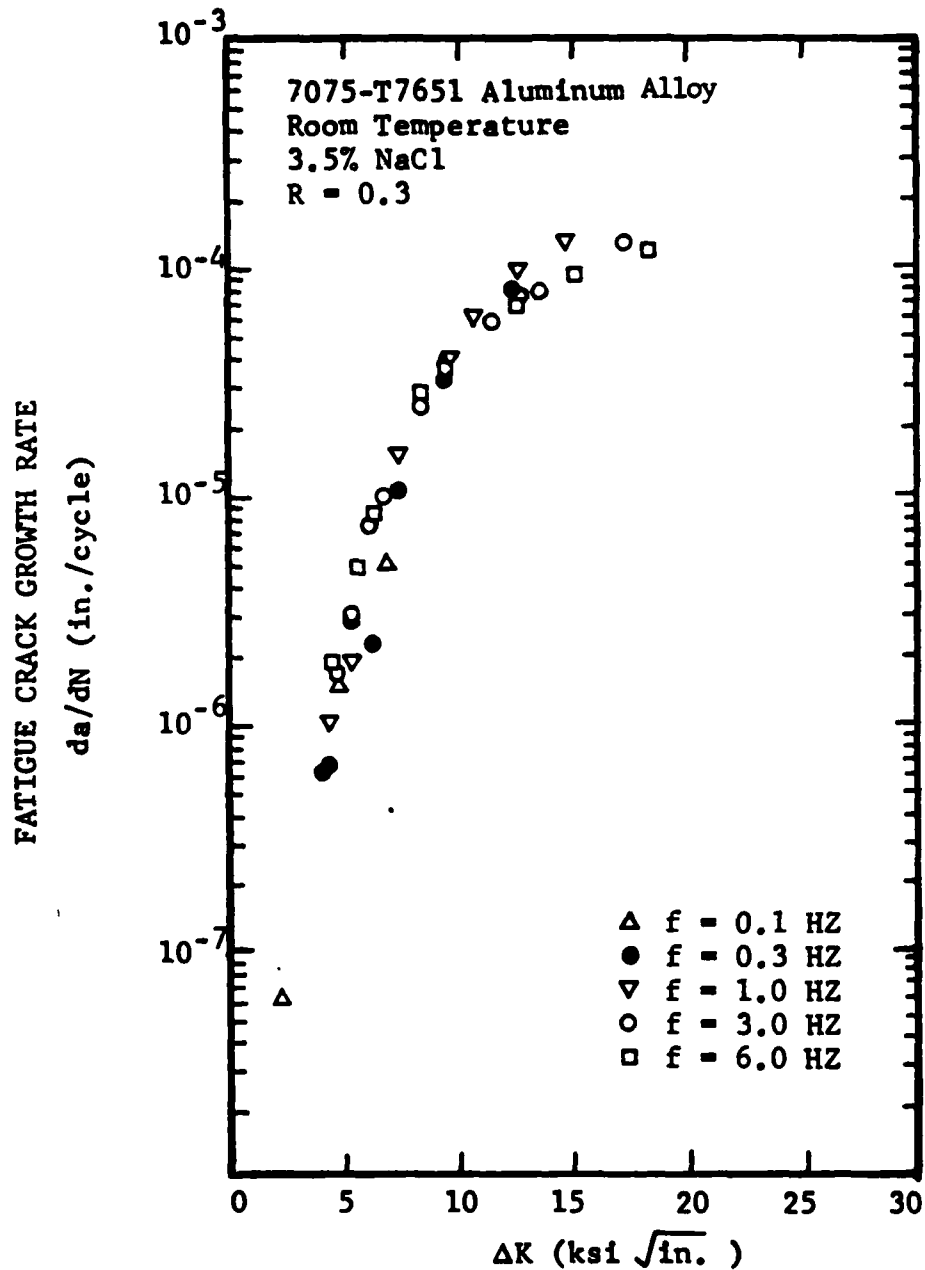


Fig. 36 Effect of Frequency on Crack Growth Rates for 7075-T7651 Aluminum Alloy Exposed to 3.5% NaCl Solution at Room Temperature (R = 0.3; f = 0.1HZ, 0.3HZ, 1 HZ, 3HZ, and 6HZ)

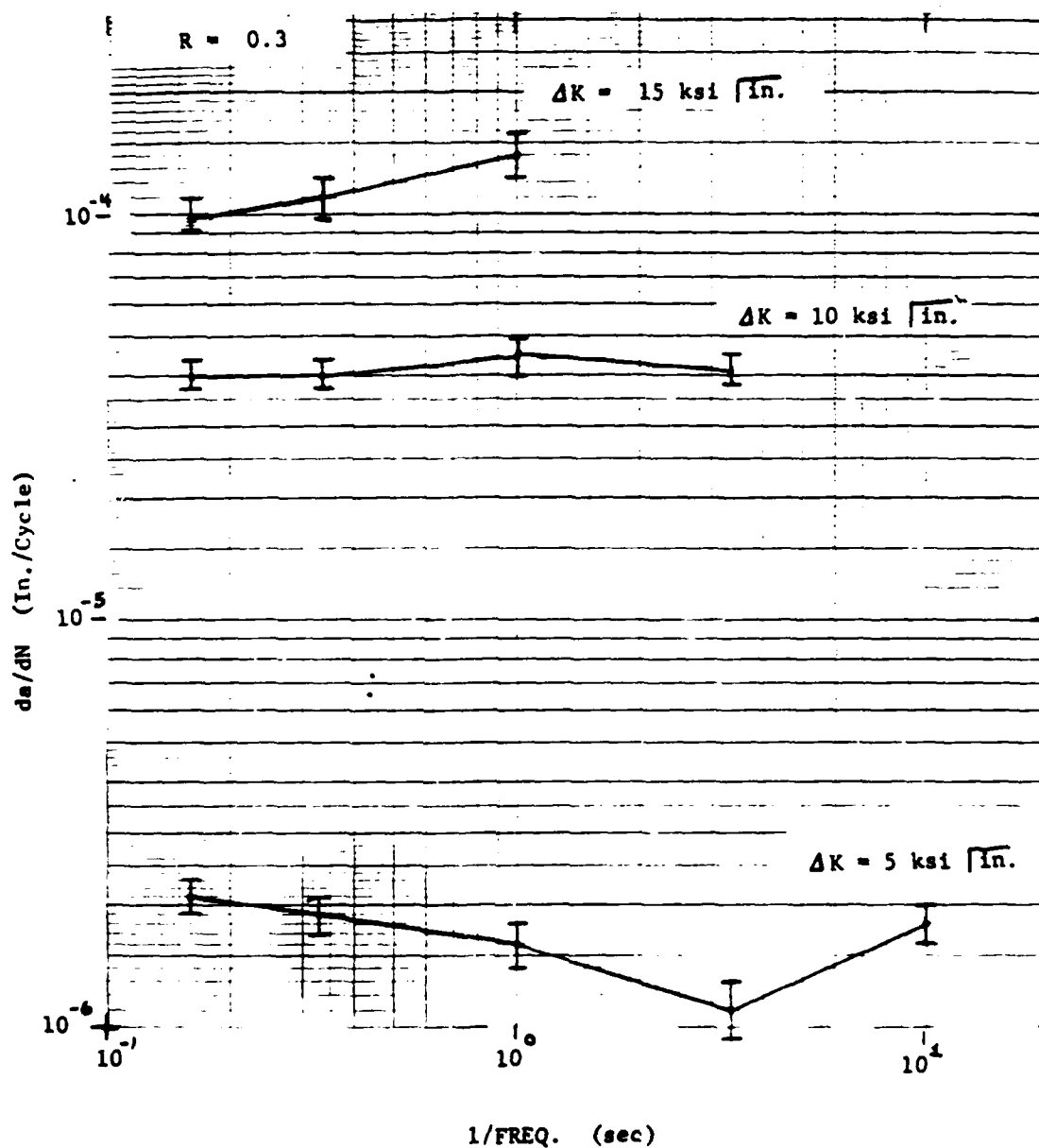


Fig. 3.7 Effect of Frequency on Fatigue Crack Growth in 7075-T7651 Aluminum Alloy Tested in 3.5% NaCl Solution at Room Temperature

especially if an alloy is immune to stress corrosion [30,36]. However, it has been shown that an alloy highly susceptible to stress corrosion and loaded in the short transverse direction exhibits an extreme frequency dependence at frequencies low enough to allow stress corrosion [30]. Tests on 7175-T7351 in salt water showed that at a frequency of 25 Hz, crack-propagation rates differ by a factor of no more than three [3].

#### 4.4.1.4 Effect of Holding Time

Tests were performed to evaluate the effect of holding time on crack growth rate in 3.5% NaCl solution. The tests were performed at room temperature with  $R = 0.05$ . Three different holding times,  $t_h$  (0s, 1s and 2.33s), and four different  $\Delta K$  values (8.8, 11, 17.5 and 22 MPa $\sqrt{m}$ ) were considered.

The effect of holding time on fatigue crack growth is shown in Fig. 38. These results indicate that there is no effect of holding time on the crack growth rate for the range of holding times considered ( $t_h = 0$  to 2.33s). The effects of longer holding times on  $da/dN$  should be investigated for this alloy.

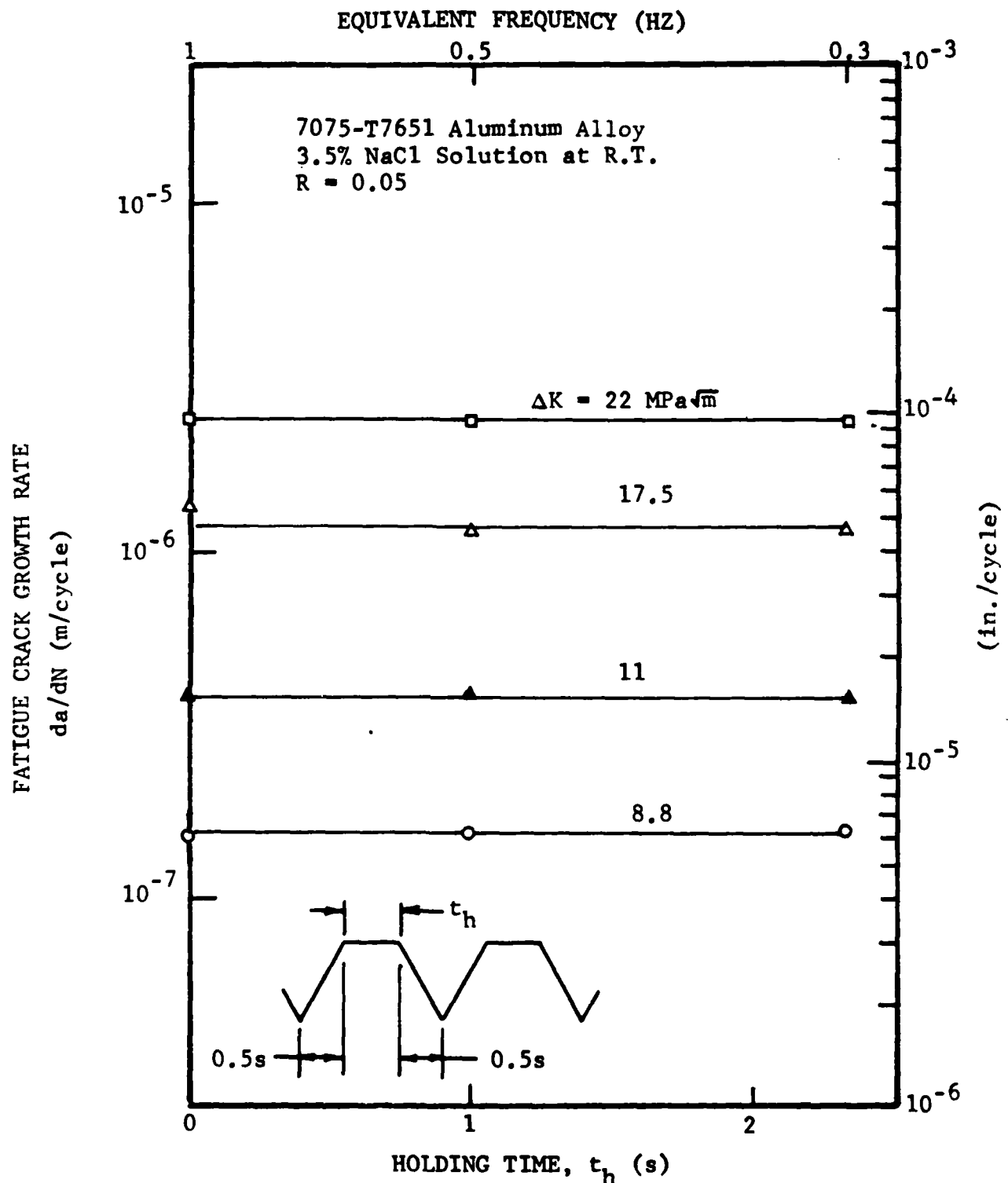


Fig. 38: Effect of Holding Time on the Kinetics of Fatigue Crack Growth in 7075-T7651 Aluminum Alloy Exposed to 3.5% NaCl Solution at Room Temperature (R = 0.05)

#### 4.4.2 $\beta$ -Annealed Ti-6Al-4V Alloy

Crack growth tests were performed according to the test matrix in Tables 3 and 4. Results are presented and evaluated in this section. Experimental testing procedures and data acquisition methods are described in Section III. The crack propagation models are evaluated in Section V.

##### 4.4.2.1 Effect of Environment

Crack growth tests were performed using three different aqueous environments: distilled water, ASTM artificial sea water and 3.5% NaCl + H<sub>2</sub>SO<sub>4</sub> (pH=3.5). The tests were performed at room temperature using  $f = 3$  Hz and  $R = 0.05$ . Test results for the three environments are superimposed in Fig. 39 for comparison. these results indicate no significant differences in the crack growth rates for the three environments considered.

Crack growth tests were also conducted in a vacuum environment at room temperature. A loading frequency of 5 Hz and an R ratio of 0.05 was used. Results are plotted in Fig. 40. These results provide a baseline for comparing other test results.

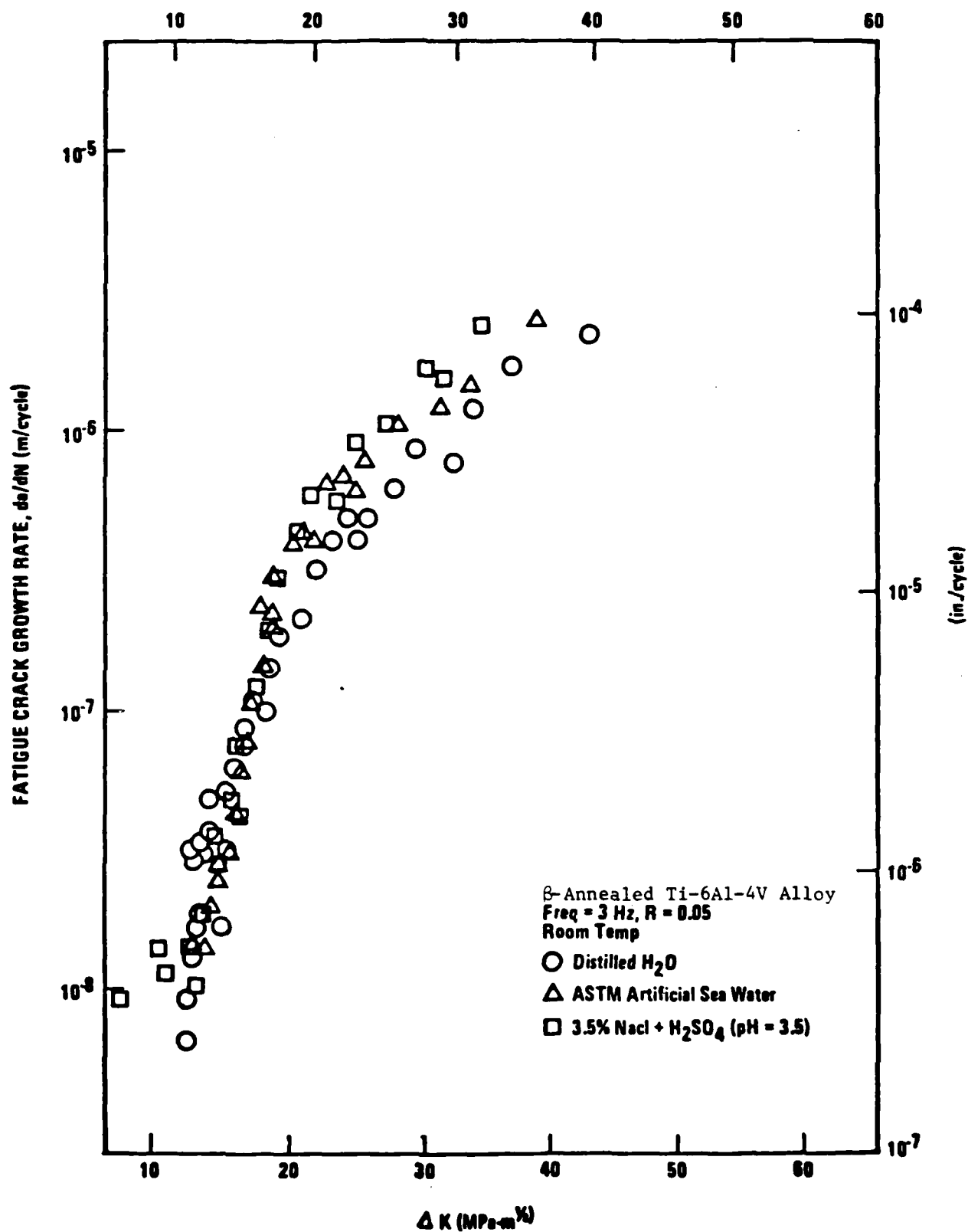
$\Delta K$  (KSI- $\sqrt{\text{in}}$ )

Fig. 39 Crack Propagation Rate vs.  $\Delta K$  for  $\beta$ - Annealed Ti-6Al-4V Alloy in Distilled Water, in ASTM Artificial Sea water, and in 3.5% NaCl + H<sub>2</sub>SO<sub>4</sub> (pH = 3.5)

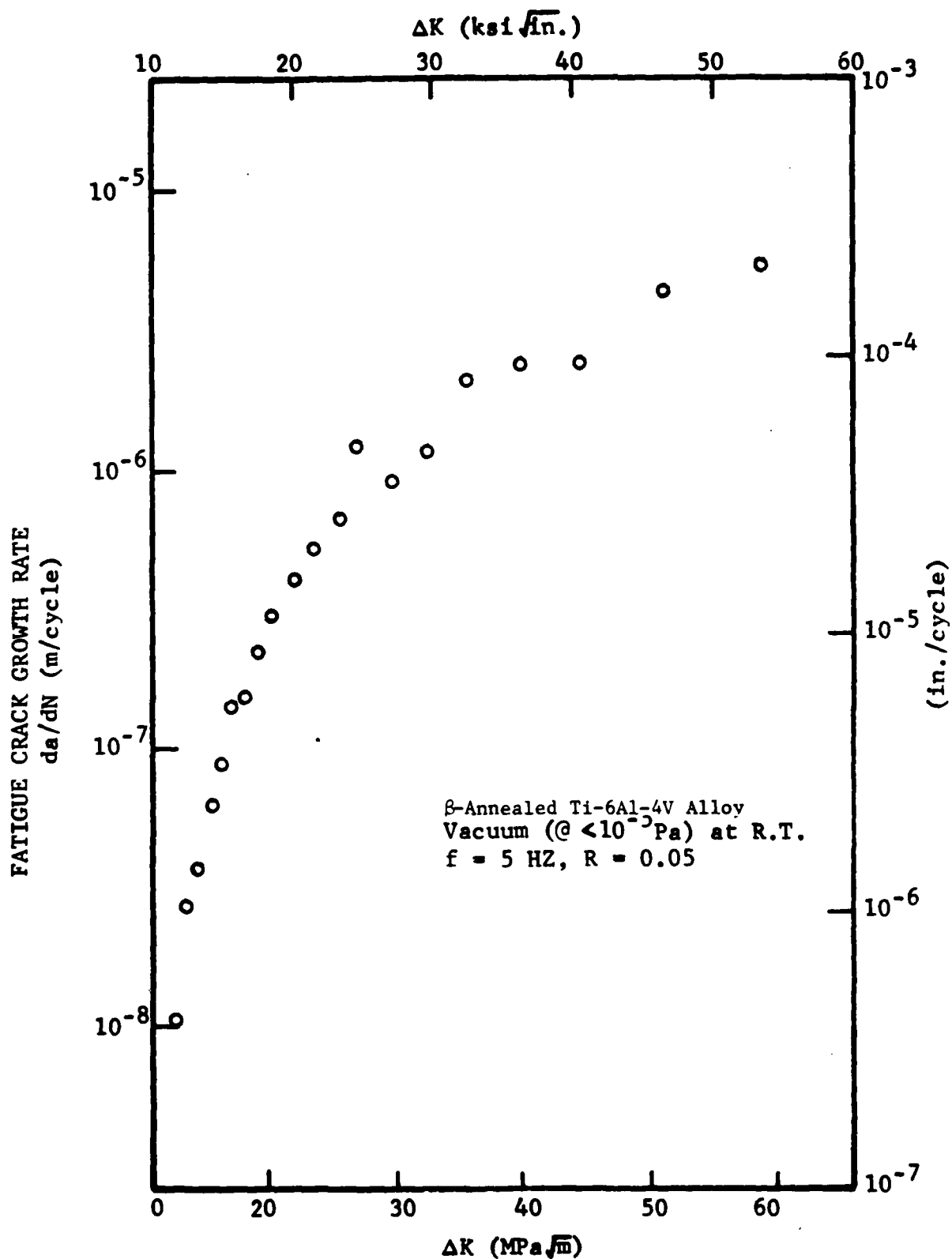


Fig. 40 Kinetics of Fatigue Crack Growth in  $\beta$ -Annealed Ti-6Al-4V Alloy in Vacuum (@  $<10^{-5}$  Pa) at Room Temperature ( $f = 5$  HZ,  $R = 0.05$ )

#### 4.4.2.2 Effect of R Ratio

The effect of the R ratio on  $da/dN$  in a 3.5% NaCl environment (room temperature) was investigated. Three R ratios were considered (0.05, 0.2 and 0.4) and a baseline frequency of 10 Hz was used. Experimental results for the three R ratios are superimposed in Fig.41 for comparison.

#### 4.4.2.3 Effect of Frequency

The effect of loading frequency on  $da/dN$  was investigated using a 3.5% NaCl solution at room temperature. The following R ratios and loading frequencies were considered:

- R = 0.05, f = 0.3 Hz and 3 Hz
- R = 0.3, f = 0.3 Hz, 3 Hz and 10 Hz.

Test results for R = 0.05 are plotted in Figs. 42 and 43 for f = 0.3 Hz and 3 Hz, respectively. Similarly, results for R = 0.3 are plotted in Figs. 44, 45 and 46 for f = 0.3 Hz, 3 Hz and 10 Hz, respectively. Figure 47 shows the effects of cyclic-load frequency on fatigue crack growth at

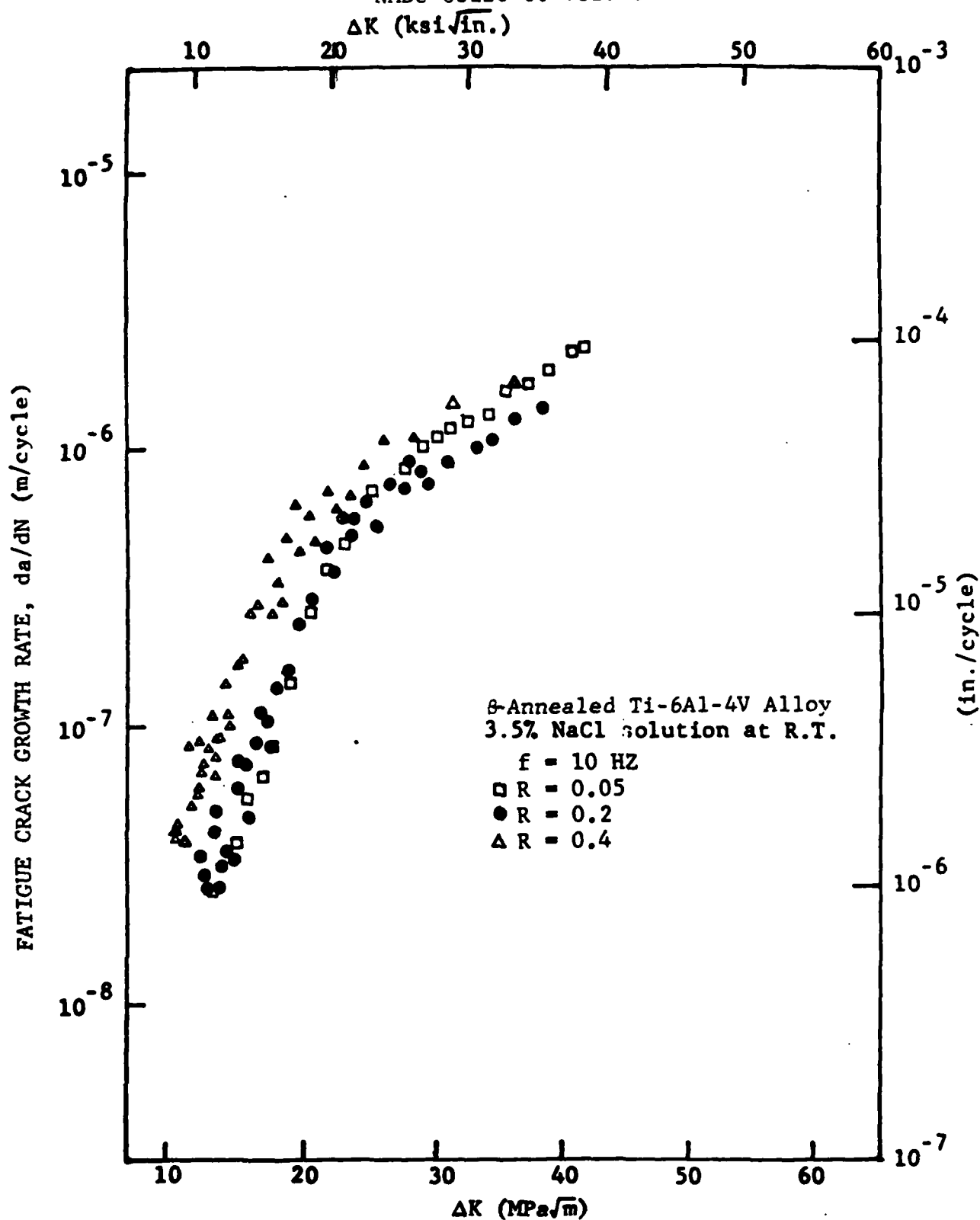


Fig. 41 Crack Propagation Rate vs.  $\Delta K$  for  $\beta$ -Annealed Ti-6Al-4V Alloy in a 3.5% NaCl Solution at Room Temperature ( $f = 10$  HZ;  $R = 0.05, 0.2$ , and  $0.4$ )

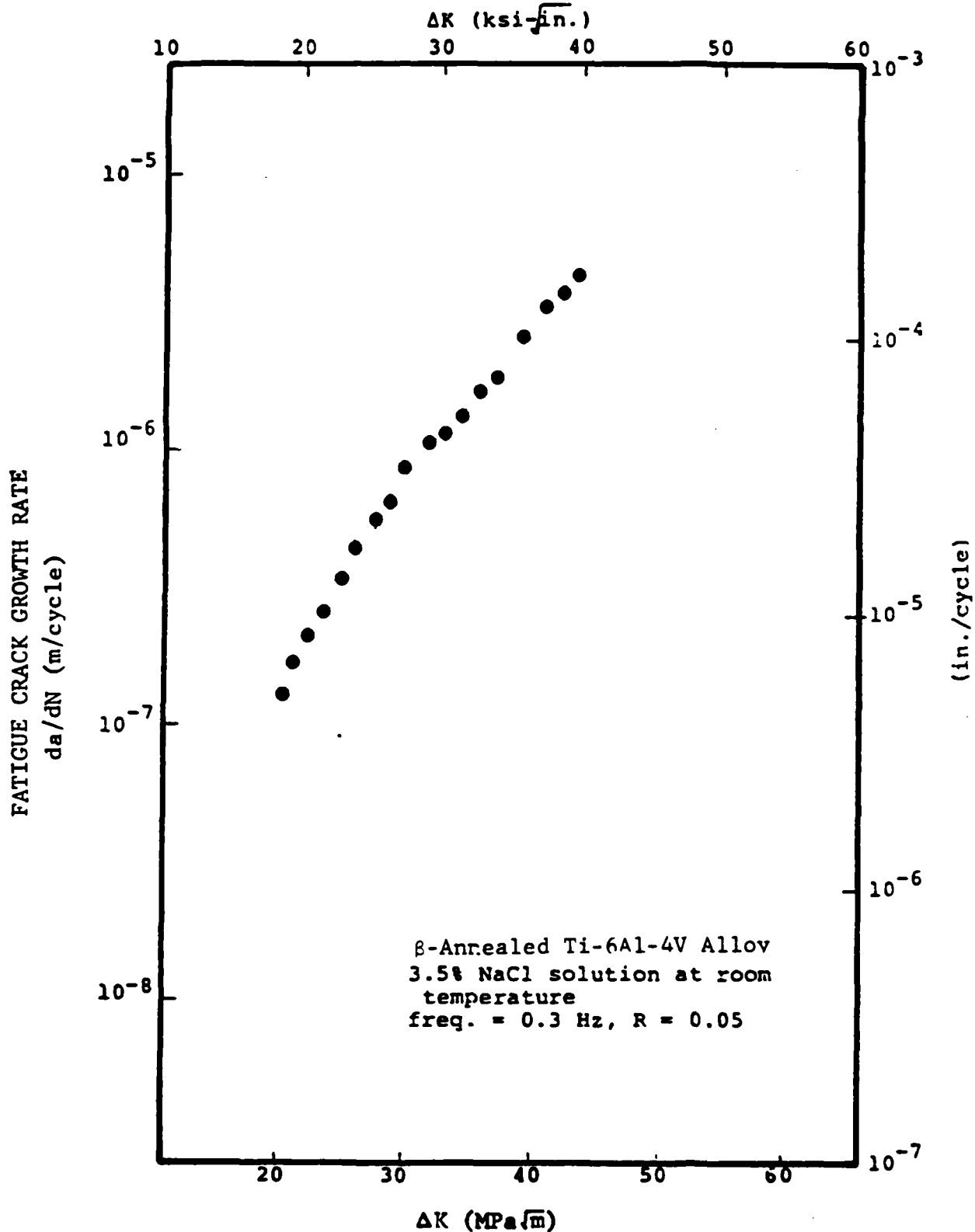


Fig. 42 Kinetics of Fatigue Crack Growth in  $\beta$ -Annealed Ti - 6Al - 4V Alloy Exposed to 3.5% NaCl Solution at Room Temperature ( $f = 0.3$  HZ,  $R = 0.05$ )

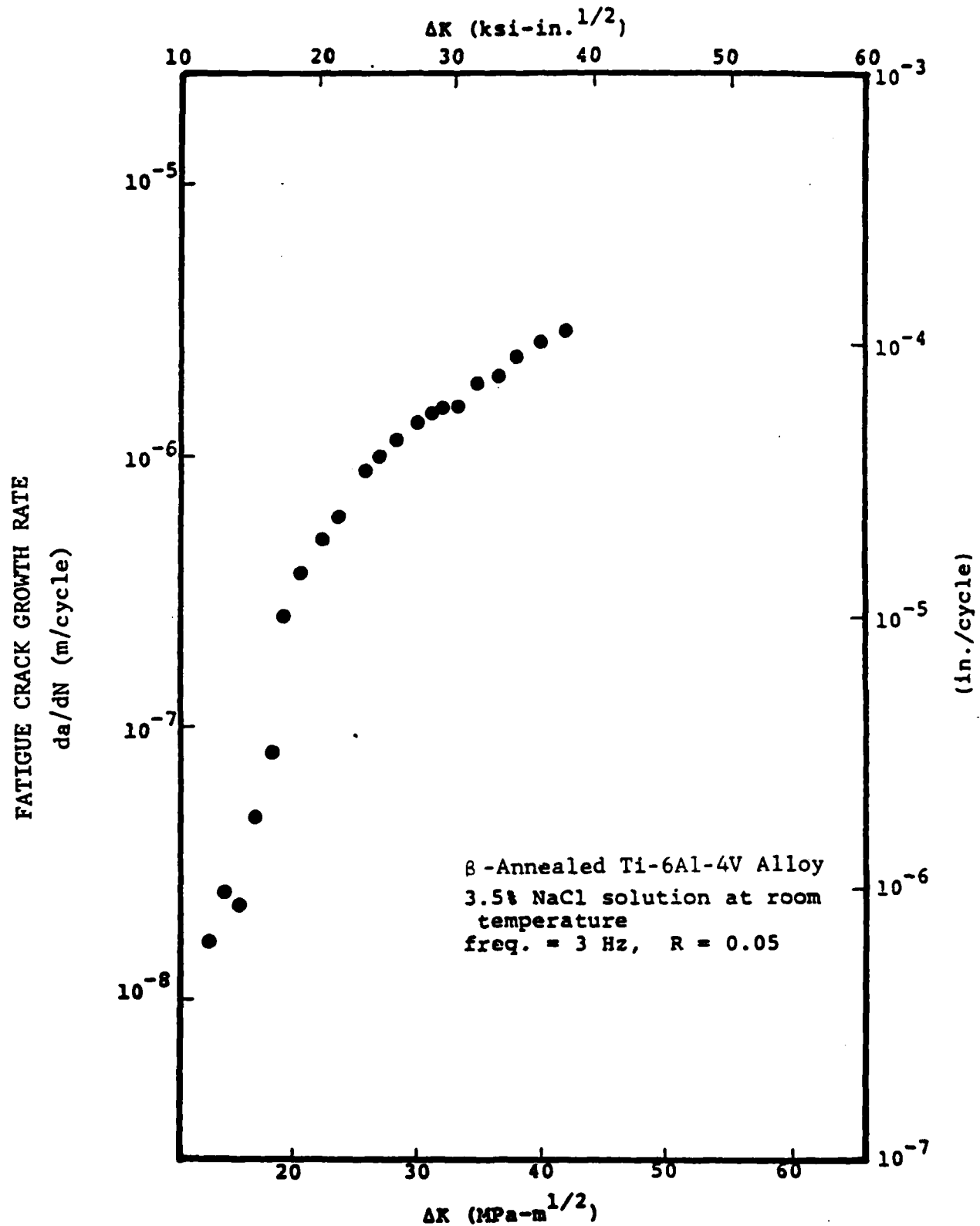


Fig. 43 Kinetics of Fatigue Crack Growth in  $\beta$ -Annealed Ti - 6Al - 4V Alloy Exposed to 3.5% NaCl Solution at Room Temperature ( $f = 3$  HZ,  $R = 0.05$ )

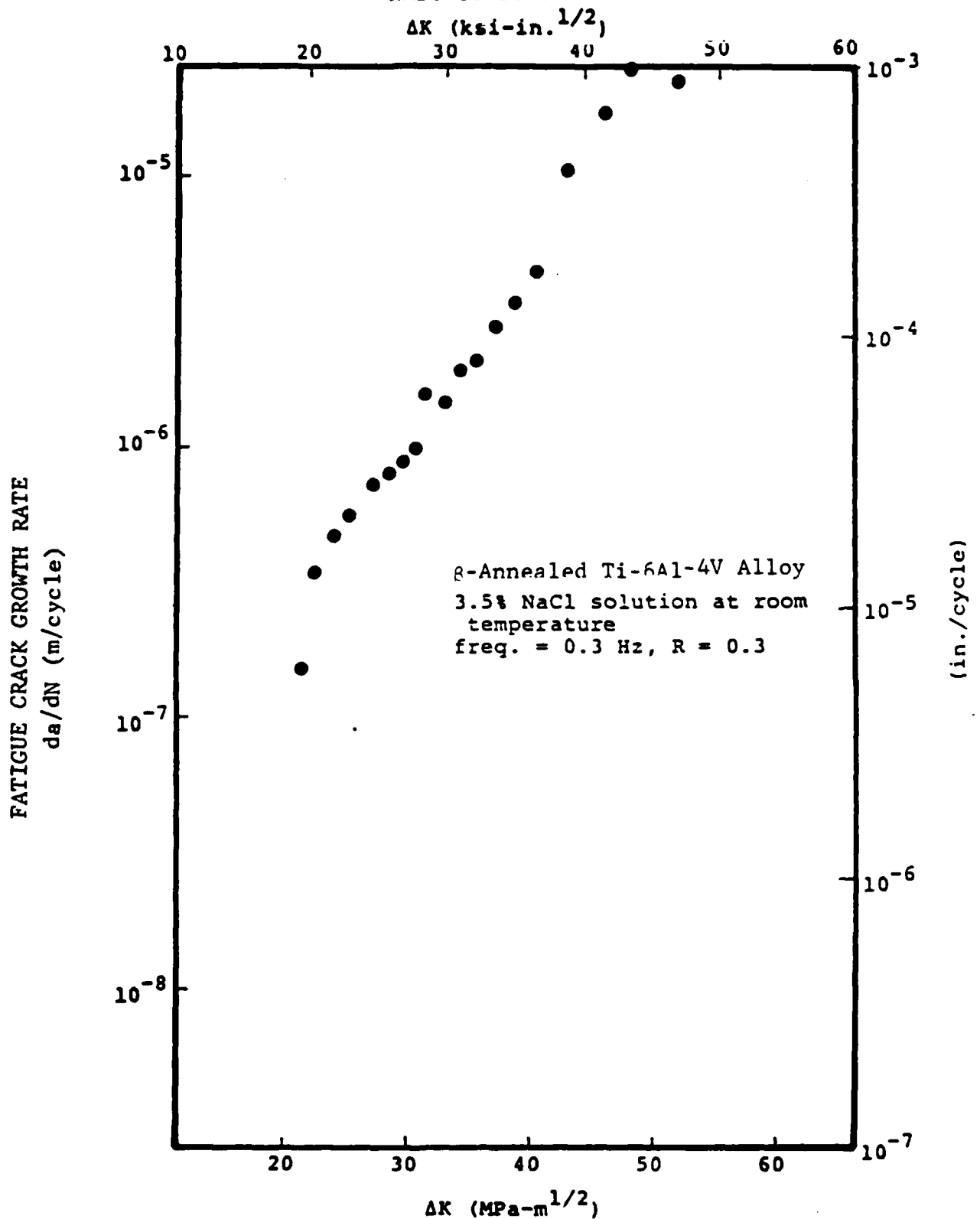


Fig. 44 Kinetics of Fatigue Crack Growth in 8-Annealed Ti - 6Al - 4V Alloy Exposed to 3.5% NaCl Solution at Room Temperature ( $f = 0.3$  HZ,  $R = 0.3$ )

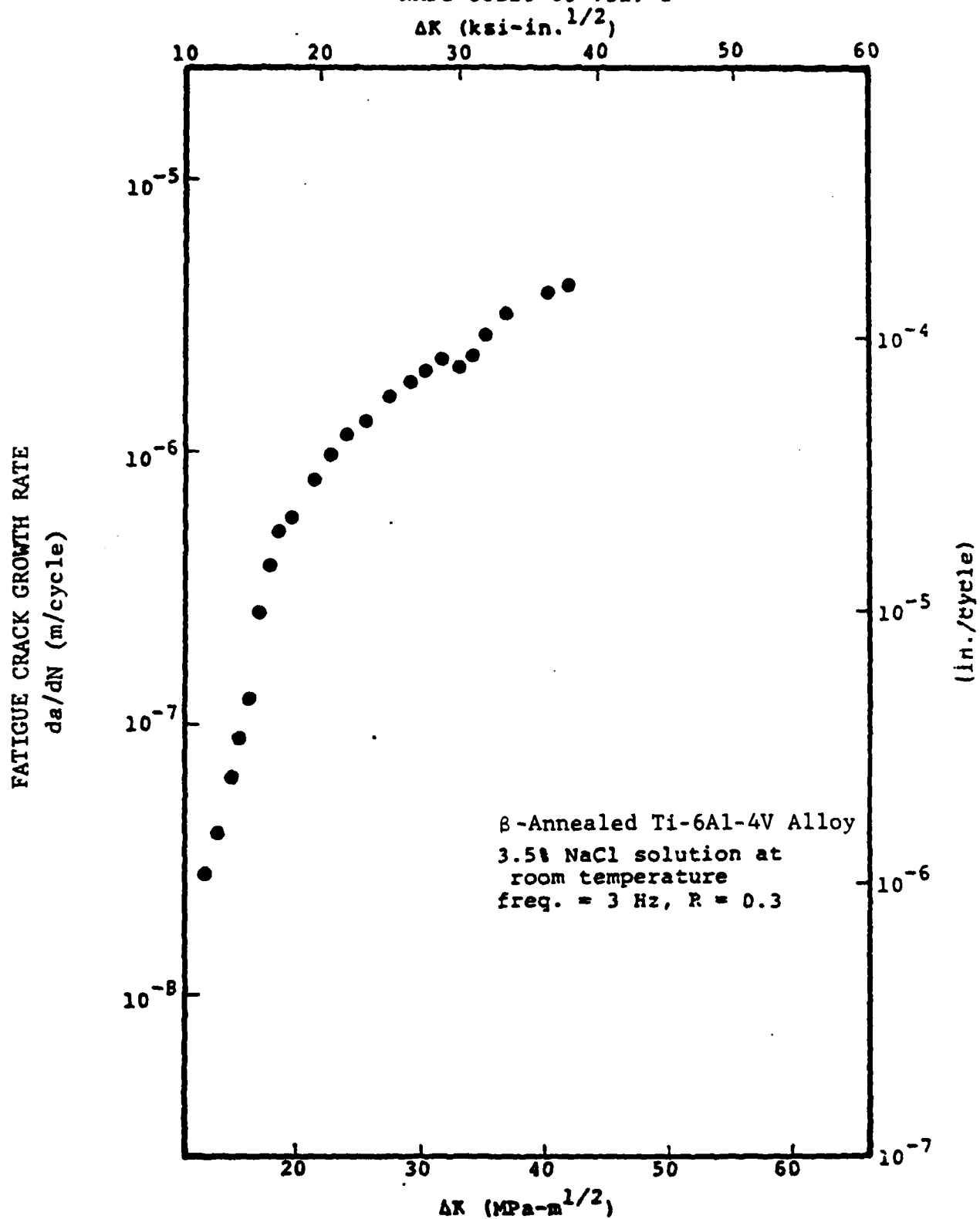


Fig. 45 Kinetics of Fatigue Crack Growth in  $\beta$ -Annealed Ti - 6Al - 4V Alloy Exposed to 3.5% NaCl Solution at Room Temperature ( $f = 3$  HZ,  $R = 0.3$ )

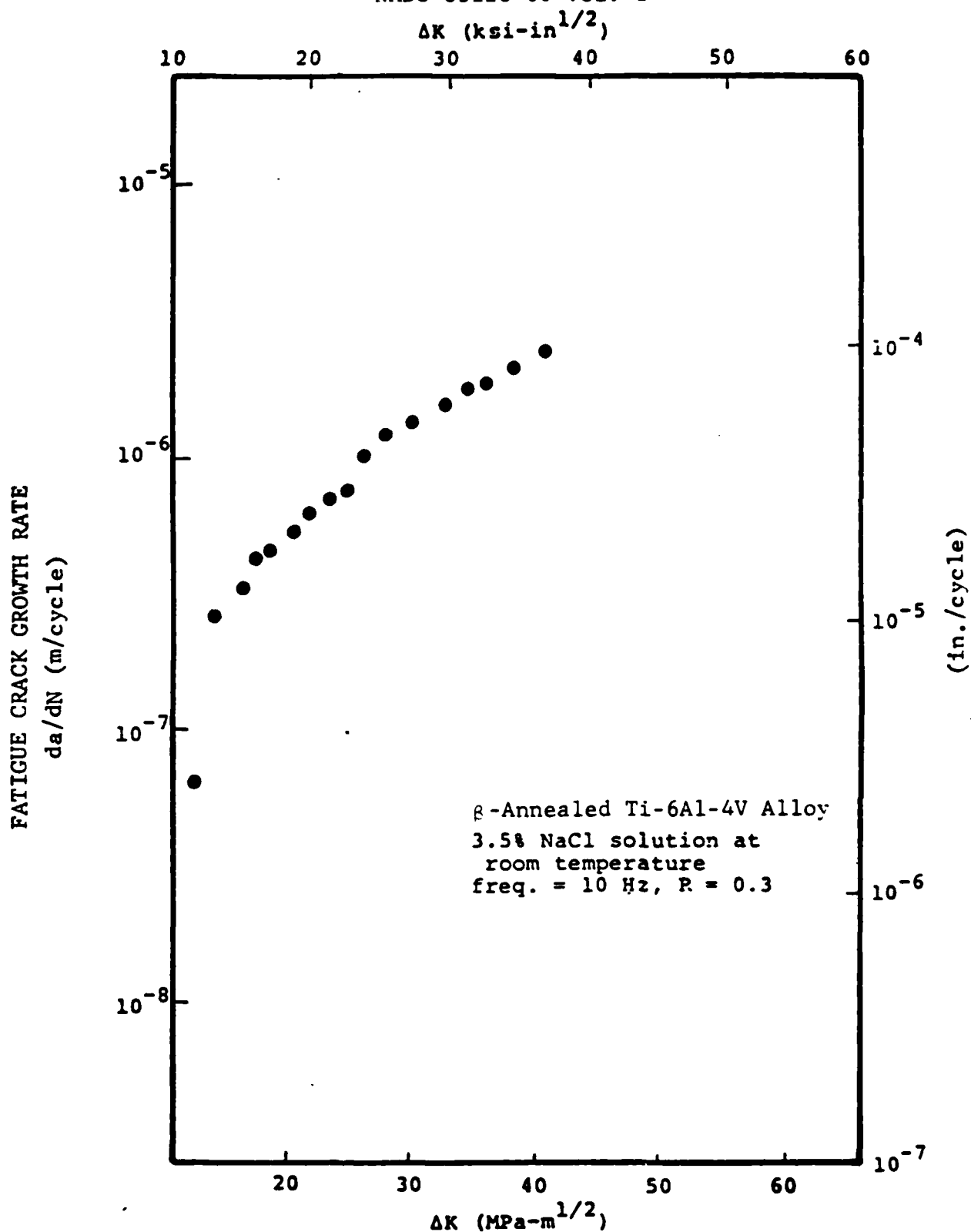


Fig. 46 Kinetics of Fatigue Crack Growth in  $\beta$ -Annealed Ti - 6Al - 4V Alloy Exposed to 3.5% NaCl Solution at Room Temperature ( $f = 10$  Hz,  $R = 0.3$ )

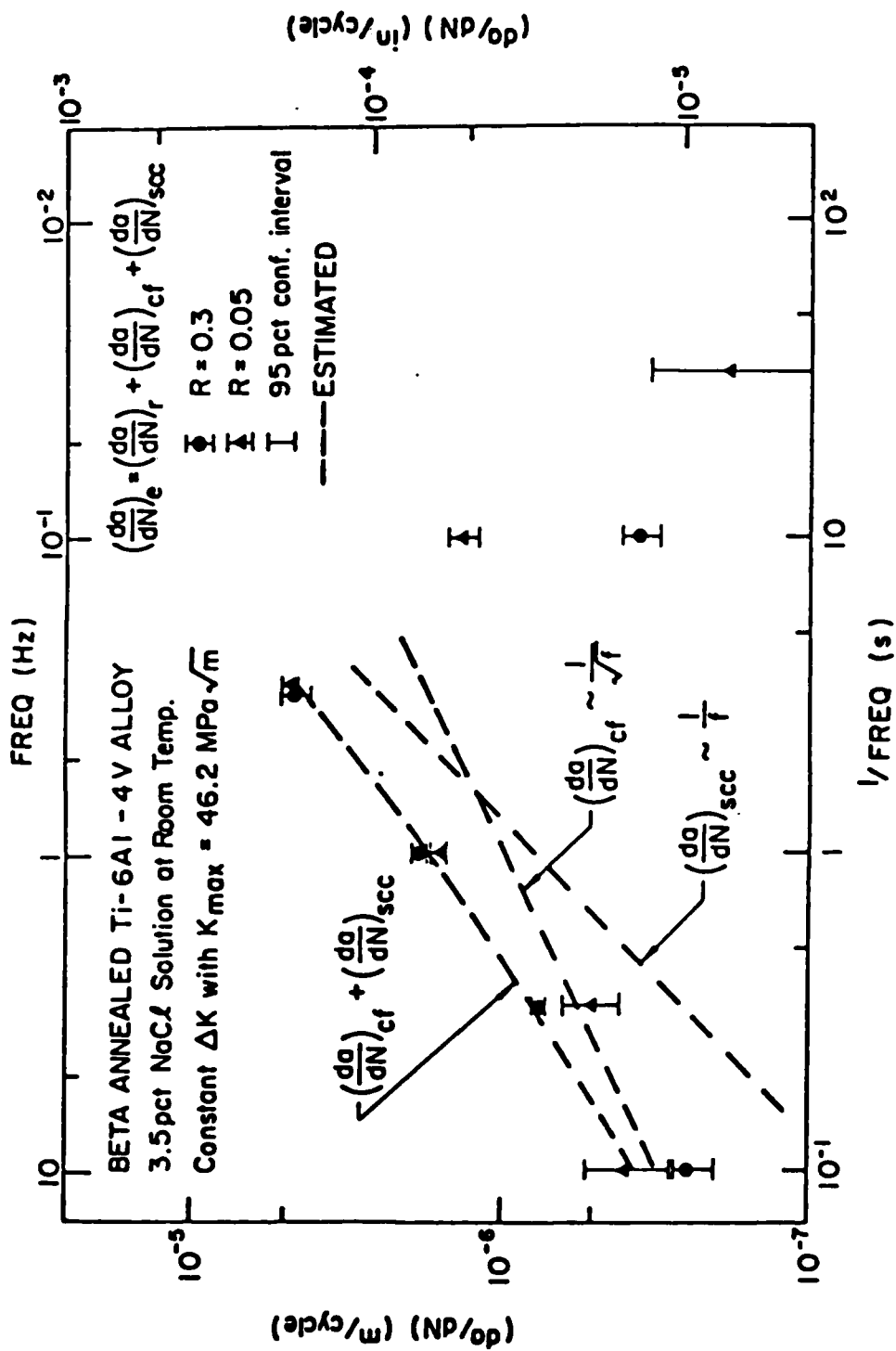


Fig. 47 Effect of Frequency on Fatigue Crack Growth in  $\beta$ -Annealed Ti-6Al-4V Alloy Tested in 3.5% NaCl Solution at Room Temperature

constant  $\Delta K$ . These results are for  $K_{\max}$  of  $46.2 \text{ MPa}\sqrt{\text{m}}$  at  $R = 0.05$  and  $0.3$ .

To assess the influence of environment on the micro-mechanism of crack growth, scanning electron microscopic (SEM) observations of fracture surfaces were carried out. Typical SEM microfractographs of a  $\beta$ -annealed Ti-6Al-4V alloy specimen tested in 3.5 pct NaCl solution at  $\Delta K = 42 \text{ MPa}\sqrt{\text{m}}$  and  $R = 0.05$  are shown in Fig. 48 for frequencies of 10, 0.3 and 0.03 Hz\*. Three different components may be identified.

The first component is composed of facets containing colonies of rod-like elements, and represents crack growth across colonies of similarly aligned and crystallographically oriented  $\alpha$ -platelets (see region B in Figure 48 b) [18]. The areal fraction of this component increased with decreasing frequency and reached a maximum at about 0.3 Hz, then decreased with further reduction in frequency. More detailed examinations indicate the existence of fatigue striations within each  $\alpha$ -platelet (Fig. 49). The striations are nearly parallel to the  $\alpha/\beta$  interface, i.e., the local growth direction is nearly

---

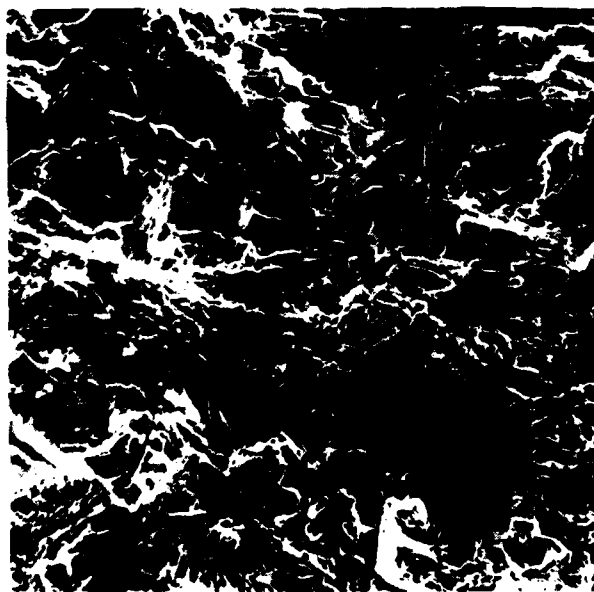
\*Crystallites, observed in the SEM microfractographs of Figs. 48-50, are predominant NaCl crystals deposited by drying the specimens after fracture.



(a)  $f = 10 \text{ HZ}$



(b)  $f = 0.3 \text{ HZ}$



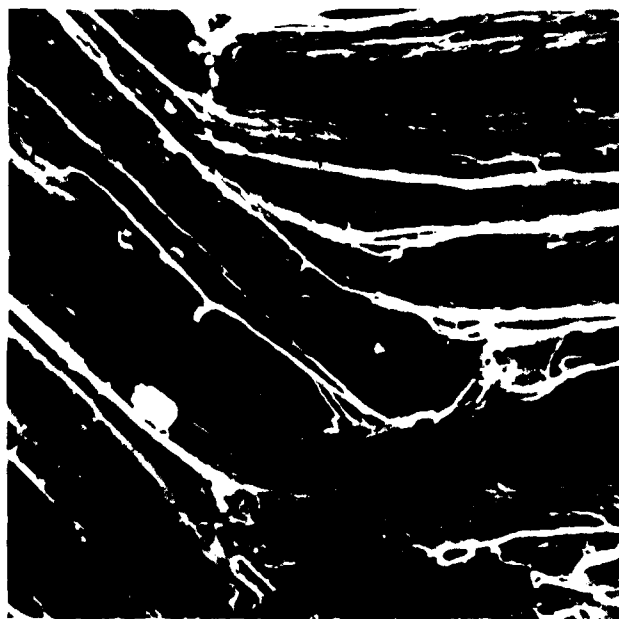
(c)  $f = 0.03 \text{ HZ}$

→  
Crack Growth  
Direction

Fig. 48 Representative SEM Microfractographs of  $\beta$ -Annealed Ti-6Al-4V Alloy Tested in Fatigue in 3.5% NaCl Solution at Room Temperature ( $R = 0.05$ ): (a)  $f = 10 \text{ HZ}$ , (b)  $f = 0.3 \text{ HZ}$ , and (c)  $f = 0.03 \text{ HZ}$ . Magnification: 80X. (Plate No. 13-001, 91-103, 13-069)



(a) 200X



(b) 800X

Fig. 49 SEM Microfractographs of Region B in Fig. 48b, Showing Crack Growth Across  $\alpha$ -Platelets and  $\alpha/\beta$  Interfaces: (a) 200X, and (b) 800X. (Plate No. 13-103, 13-104.)

perpendicular to these interfaces. The orientation suggests that the growth occurred along the (0001) basal plane and in the  $\langle 10\bar{1}0 \rangle$  directions [37], and is consistent with a mechanism of embrittlement involving the formation of fracture of titanium hydride [19]. Satisfactory explanation of the observed changes in rate and in fracture morphology with frequency in terms of this embrittlement mechanism, however, needs to be explored.

The second component appears as nearly flat facets (region A in Fig. 48a) or an intergranular fracture (region C in Fig. 48c) and was nearly absent at 0.3 Hz. Examination at higher magnification shows that the facets are covered with very fine striations (Fig. 50). SEM microfractographs of one of these facets, obtained from the mating fracture surfaces, are shown in Fig. 50. The spacing of the striations is several times smaller than the corresponding macroscopic crack growth rate. It is believed that these facets correspond to growth along the prior beta grain boundaries or through  $\alpha$ -phases that are formed along these boundaries. It is interesting to note that the striations appear to be ductile on one surface, and to have a very different and brittle appearance on the mating surface. The reason for this difference is now known, but the existence

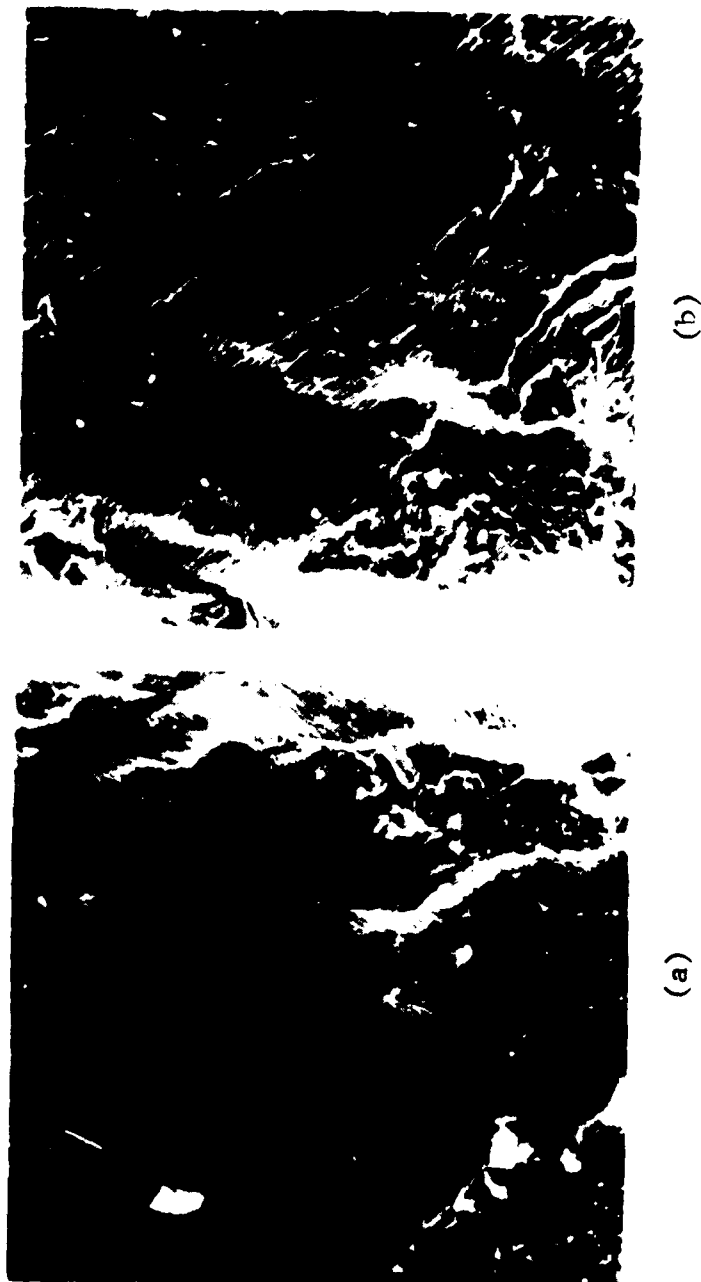


Fig. 50 SEM Microfractographs from Mating Surfaces of Region A in Fig. 48a Showing Fine Fatigue Striations: (a) Ductile Appearing Striations, and (b) Brittle Appearing Striations on Mating Surface. Magnification: 1000X. (Plate No. 13-024, 13-025.)

of this difference indicates the highly complex nature of corrosion fatigue in the  $\beta$ -annealed Ti-6Al-4V alloy.

The remaining component is ductile tearing. This component may be seen in the SEM microfractographics for 10 and 0.03 Hz and is nearly absent again at 0.3 Hz.

#### 4.4.2.4 Effect of Holding Time

The effects of holding time on  $da/dN$  were investigated for 3.5% NaCl solution at room temperature and  $R = 0.05$ . Thus different holding times were considered:  $t_h = 0s, 1s$  and  $2.3s$ . The resulting plots for  $da/dN$  versus  $K_{max}$  are shown in Fig. 51 for three holding times. Also, in Fig. 52,  $da/dN$  versus  $t_h$  plots are shown for various  $\Delta K$  values.

#### 4.4.2.5 Discussion

Unlike the case of 7075-T7651 aluminum alloy, fatigue crack growth response in the  $\beta$ -annealed Ti-6Al-4V alloy exposed to 3.5% NaCl solution is complicated. At the lower  $\Delta K$  levels reducing frequency tended to decrease the fatigue crack growth rate (see Figs. 40-46) to values below those observed in vacuum at 5 Hz. At the higher  $\Delta K$  levels, on the other hand, reducing frequency tended to increase the

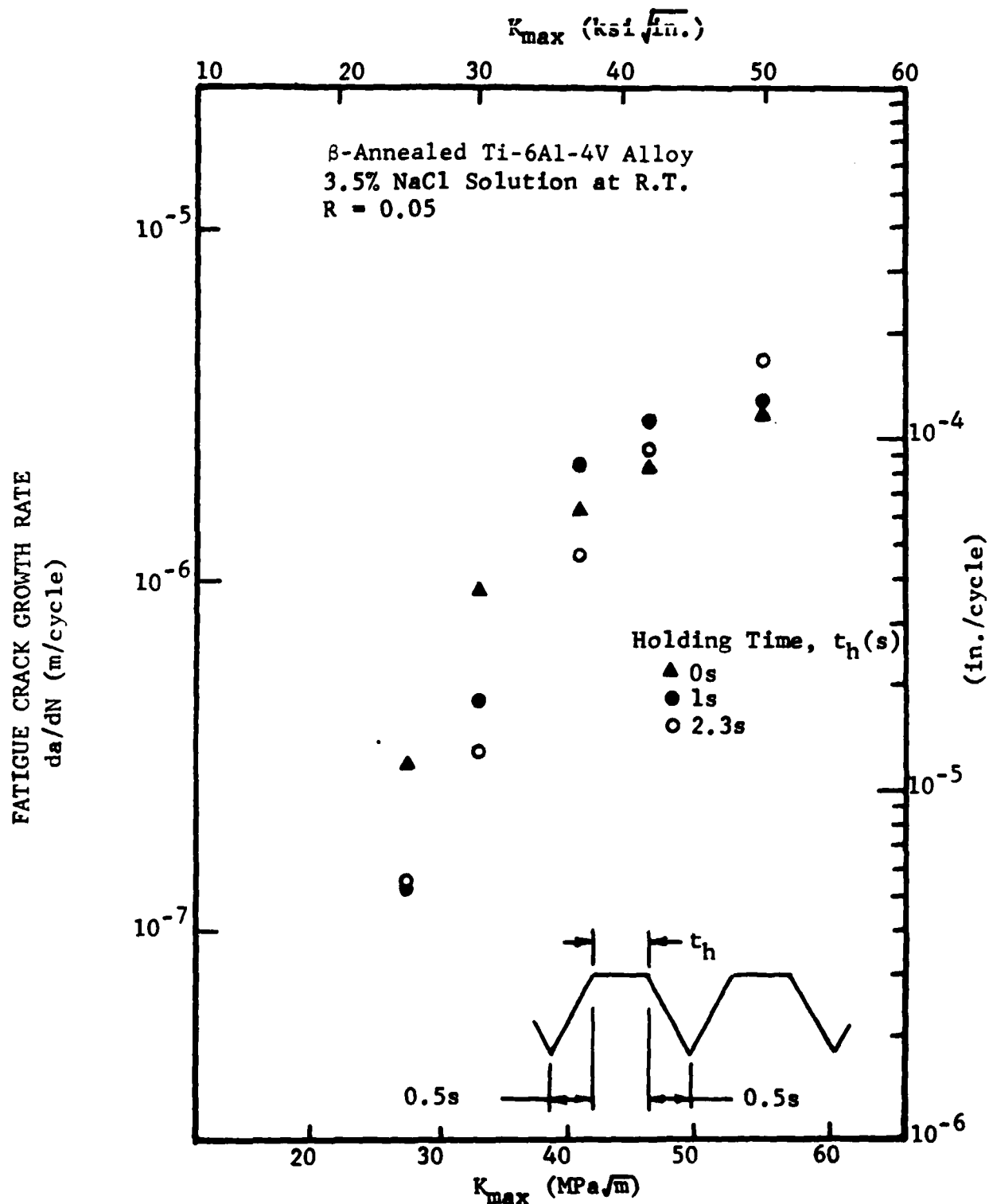


Fig. 51 Effect of Holding Time on the Kinetics of Fatigue Crack Growth in  $\beta$ -Annealed Ti - 6Al - 4V Alloy Exposed to 3.5% NaCl Solution at Room Temperature ( $R = 0.05$ )

EQUIV. FREQ. (Hz)

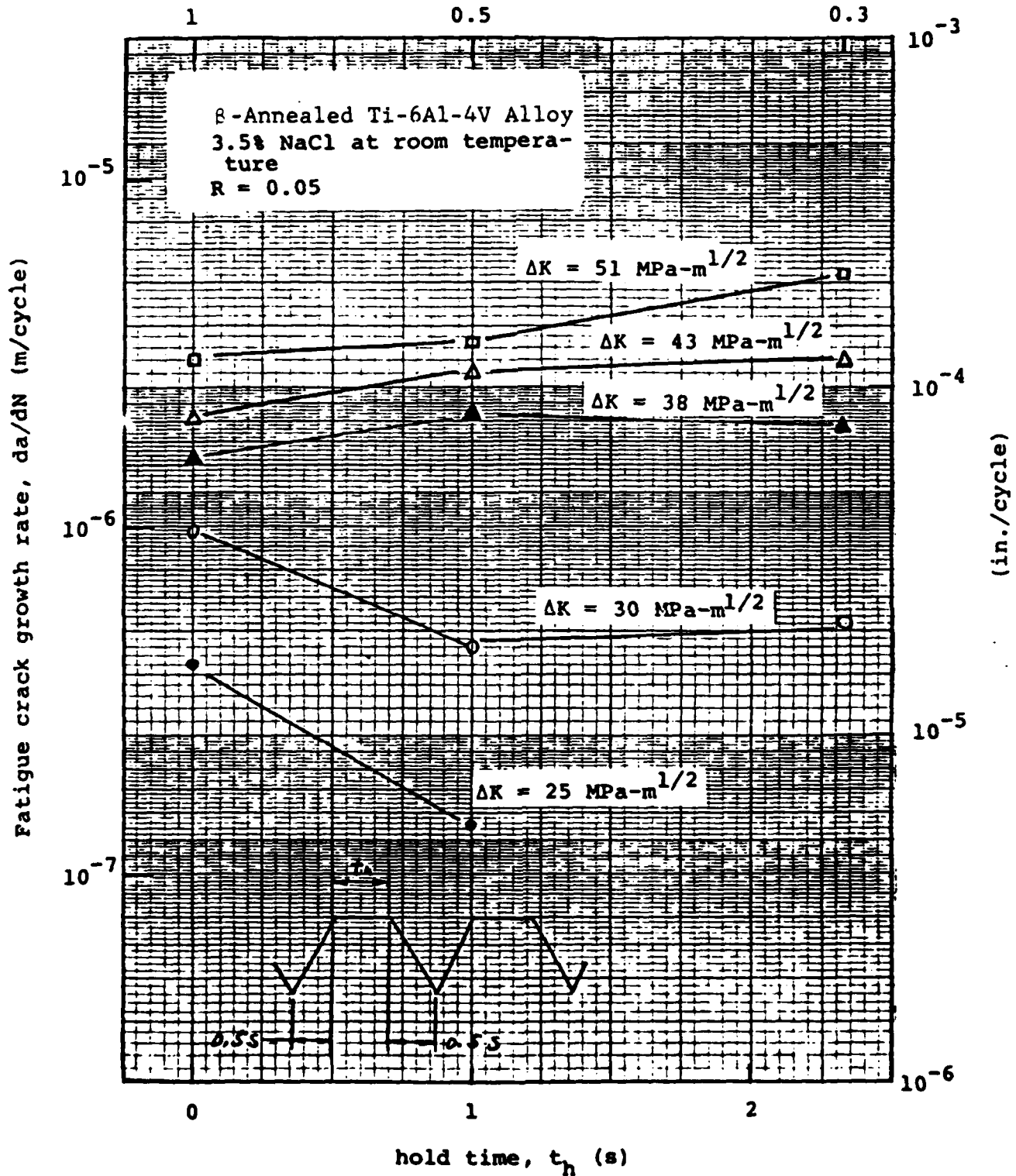


Fig. 52 Effect of Holding Time on the Kinetics of Fatigue Crack Growth in β-Annealed Ti - 6Al - 4V Alloy Exposed to 3.5% NaCl Solution at Room Temperature (R = 0.05)

crack growth rate. The change over from a decrease to an increase in rate depended on frequency, and resulted in a complex response at a prescribed K level. Figure 47 shows this change at  $K_{\max} = 46.2 \text{ MPa}\sqrt{\text{m}}$  for  $R = 0.05$  and  $0.3$ . Decreasing frequency from 10 Hz to 0.3 Hz resulted in an increase in growth rate. Further reductions in frequency led to a decrease in growth rate. A similar response was observed by increasing the holding time at maximum load, which is equivalent to a decrease in frequency (see Figs. 51 and 52). The observed changes in crack growth rate corresponded to changes in fracture surface morphology (or in micromechanism of crack growth). It is interesting to note that the data obtained under triangular wave loading are slower than those for sinusoidal loading at the same frequency.

There is no simple or suitable explanation for the observed behavior at this time. The essential absence of sustained-load crack growth eliminates the use of the  $(da/dN)_{\text{SCC}}$  term to account for the observed increases in growth rate with decreasing frequency. This explanation would not be suitable in any case because of the decreases in growth rate with reduction in frequency at the lower  $\Delta K$  levels and at the very low frequencies. Macroscopic crack-branching and strain-rate sensitivity for hydride formation

do not appear to offer satisfactory explanations either. A clear mechanistic understanding of the causes for the complex response is essential for the development of a quantitative methodology for corrosion fatigue of titanium alloys. The understanding must include studies of the changes in the crack tip environment, the kinetics of electrochemical reactions, and the interactions of the environment (hydrogen) with the microstructure.

## SECTION V

## EVALUATION OF CORROSION FATIGUE MODELS

## 5.1 Introduction

The stress-initiation life model and the crack propagation models, described in Section II, are evaluated and discussed in this section. Experimental results from Phase I are used to evaluate the models. The strain-initiation life approach will be evaluated in Phase II.

## 5.2 EVALUATION OF STRESS-INITIATION LIFE MODEL

The stress-initiation life model described in Section 2.2 is evaluated in this section. Crack initiation test results, summarized in Table 11 and 13, for 7075-T7651 aluminum alloy and  $\beta$ -annealed Ti-6Al-4V will be used to evaluate the model. The effects of different environments (i.e., dry air and 3.5% NaCl) and loading frequencies on the model parameters A and  $\Delta\sigma_{th}$  are investigated.

## 5.2.1 Evaluation of Model Parameters and Fit

The procedures for determining the parameters A and  $\Delta\sigma_{th}$  in Eq. 18 are described and discussed in this section.

$$N_i = A(\Delta\sigma^2 - \Delta\sigma_{th}^2)^{-1} \quad (18)$$

In Eq. 18,  $N_i$  = Number of cycles to crack initiation

$\Delta\sigma$  = Applied stress range

$A, \Delta\sigma_{th}$  = Empirical constants

Parameter results are presented for 7075-T7651 aluminum alloy and  $\beta$ -annealed Ti-6Al-4V and the following variables:

- o Environment (Dry Air, 3.5% NaCl)

- o Loading Frequency ( $f = 1 \text{ HZ}, 6 \text{ HZ}$ )

$A$  and  $\Delta\sigma_{th}$  are determined for the following cases:

- o Case I: Individual data sets

- o Case II: Normalized "A value" and compute the resulting  $\Delta\sigma_{th}$  value for each data set

- o Case III: Using the normalized "A value" compute  $\Delta\sigma_{th}$  for each specimen in the data set.

5.2.1.1 Model Calibration Procedures

Parameters A and  $\Delta\sigma_{th}$  can be defined using the classical least squares fit approach [e.g., 38]. Equation 8 can be rearranged in the least squares fit form,

$$Y = mx + b \quad (19)$$

where:  $Y = \Delta\sigma^2$

$$x = 1/N_i$$

$$m = A$$

$$b = \Delta\sigma_{th}^2$$

The sum error squared equation for determining m and b is as follows,

$$E_1^2 = \sum_{i=1}^n [Y_i - (mX_i + b)]^2 \quad (20)$$

Minimizing  $E_1^2$  with respect to m and b yields two equations with two unknowns.

$$\frac{\partial E_1^2}{\partial m} = 0 = nb + m \sum_{i=1}^n X_i - \sum_{i=1}^n Y_i \quad (21)$$

$$\frac{\partial E_1^2}{\partial b} = 0 = b \sum_{i=1}^n X_i + m \sum_{i=1}^n X_i^2 - \sum_{i=1}^n X_i Y_i \quad (22)$$

Eqs. 23 and 24 for  $b$  and  $m$ , respectively, can be determined from Eqs. 21 and 22.

$$b = \Delta\sigma_{th}^2 = \frac{(\sum Y)(\sum X^2) - (\sum X)(\sum XY)}{n\sum X^2 - (\sum X)^2} = \frac{\sum Y - m\sum X}{n} \quad (23)$$

$$m = A = \frac{n\sum XY - (\sum X)(\sum Y)}{n\sum X^2 - (\sum X)^2} = \frac{\sum Y - bn}{\sum X} \quad (24)$$

Two other variations of Eq. 18 were considered for determining the "best fit"  $A$  and  $\Delta\sigma_{th}$  values. For example, Eq. 18 can be arranged into Eq. 25 and 26 for a least squares fit.

$$E_2^2 = \sum_{i=1}^n \left[ N_i \Delta\sigma_i^2 - (A + \Delta\sigma_{th}^2) \right]^2 \quad (25)$$

$$E_3^2 = \sum_{i=1}^n \left[ N_i - \frac{A}{(\Delta\sigma_i^2 - \Delta\sigma_{th}^2)} \right]^2 \quad (26)$$

The reasons for using Eq. 20 instead of Eqs. 25 and 26 are as follows. In Eq. 25, the sum error squared is a function of the product  $N_i \Delta\sigma$ . Thus, the applicable variance for  $N_i$  and  $\Delta\sigma$  is not treated separately. Whereas in Eq. 20,  $N_i$  and  $\Delta\sigma$  are treated separately. When Eq. 26 is minimized with respect to  $A$  and  $\Delta\sigma_{th}$ , this results in two non-linear equations. Although the resulting equations can be solved by iteration to determine  $A$  and  $\Delta\sigma_{th}$ , this increases the complexity. Also, the resulting  $A$  and  $\Delta\sigma_{th}$  values will not necessarily provide a better fit than the approach used.

For direct comparison,  $A$  and  $\Delta\sigma_{th}$  should be determined on a common baseline for different test data sets. One way to make the  $A$  and  $\Delta\sigma_{th}$  values compatible is to normalize one of the parameters for all the data sets and determine the other parameter for each data set separately. Parameter " $A$ " can be normalized using the  $\Delta\sigma_i$  and  $N_i$  results for all data sets for a given material. For example, " $A$ " can be determined using Eq. 24. Then the  $\Delta\sigma_{th}$  value for each data set can be determined using the  $\Delta\sigma_i$  and  $N_i$  values for a given data set.

Using this procedure, a best fit " $A$ " value can be determined for multiple data sets. Since the resulting  $\Delta\sigma_{th}$  values for different data sets will be compatible, the  $\Delta\sigma_{th}$

values can be directly compared to assess the effects of environment and loading frequency on  $\Delta\sigma_{th}$ .

#### 5.2.1.2 Model Parameter Results and Plots

Stress-initiation life model parameters,  $A$  and  $\Delta\sigma_{th}$ , are summarized in Tables 15 through 17 for various cases. Results are based on the time-to-crack-initiation (TTCI) test results from Table 11 and 13 and the calibration procedures described in subsection 5.2.2.1. Only those tests with a known TTCI at  $a_0 = 0.010"$  were used.

Model parameter results for Cases I and II are summarized for each data set(s) in Table 15. TTCI data used and the resulting model parameters for cases I - III are summarized in Table 16 and 17 for 7075-T7651 aluminum alloy and  $\beta$ -annealed Ti-6Al-4V alloy, respectively.

$\Delta\sigma_{th}$  statistics for various data sets are also shown in Table 16 and 17. This includes the  $\Delta\sigma_{th}$  average and standard deviation. These results will be used later to estimate the 95% confidence interval for  $\Delta\sigma_{th}$ .

Plots of  $\Delta\sigma$  versus  $N_f$  (dry air and 3.5% NaCl) are shown in Figs. 53 and 54 for 7075-T7651 aluminum alloy and for

Table 15 Summary of Stress-Initiation Life Model Parameters for  
Aluminum and Titanium

Material	Environment	Frequency (Hz)	Data Set	No. Spec.	$A \times 10^{-6}$	$\Delta \sigma_{th}$	$A \times 10^{-6}$	$\Delta \sigma_{th}$
7075-T7651	Dry Air	6	1	10	10.026	14.658	4.087	17.657
Aluminum Alloy	3.5% NaCl	1	2	6	3.679	14.836		14.395
		6	3	13	4.619	14.237		14.820
		1 & 6	2 & 3	19	4.439	14.302		14.687
$\beta$ -Annealed Ti-6Al-4V Alloy	Dry Air	6	4	9	24.024	35.463	20.966	37.407
	3.5% NaCl	1	5	6	22.713	34.370		35.124
		6	6	11	20.266	31.157		30.493
		1 & 6	5 & 6	17	19.687	33.154		32.203
					Case I		Case II	

\*Normalized

Table 16 Summary of Crack Initiation Results ( $a_0 = 0.010''$ ) Stress-Initiation Life  
Model Parameters and Statistics (7075-T7651 Aluminum Alloy)

Environment	Data Set	Specimen	Frequency (Hz)	$\Delta\sigma$ (ksi)	$N_1$	$Ax10^{-6}$	$\Delta\sigma_{th}$	$Ax10^{-6}$	$\Delta\sigma_{th}$	$\Delta\sigma_{th}$	$\Delta\sigma_{th}$ Statistic
Dry Air	1	AI09	6	16.2	830000	10.026	14.658	4.087	17.657	16.047	$n=10$ $\bar{x} = 17.558$ $S(\bar{x}) = 1.965$
		AI08		17	105000					15.814	
		AI16		17	102000					15.777	
		AI17		17	103000					15.789	
		AI01		18	120000					17.028	
		AI05		20	57000					18.119	
		AI14		20	46000					17.639	
		AI15		20	46500					17.666	
		AI07		22.5	42000					20.222	
		AI02		25	25000					21.483	
3.5% NaCl	2	AI37	1	16.5	57000	3.679	14.836		14.395	14.161	$n=6$ $\bar{x} = 14.387$ $S(\bar{x}) = 0.511$ $n=19$ $\bar{x} = 14.639$ $S(\bar{x}) = 1.224$ $n=13$ $\bar{x} = 14.755$ $S(\bar{x}) = 1.447$
		AI38			62000					14.364	
		AI39			95000					15.140	
		AI34		20	21300					14.526	
		AI35			22000					14.636	
		AI36			19000					13.597	
		AI23	6	14	308000	4.619	14.237		14.820	13.518	
		AI26		15	260000					14.467	
		AI22		16	103000					14.708	
		AI31		16.5	85000					14.972	
	3	AI32			83500					14.943	$n=13$ $\bar{x} = 14.755$ $S(\bar{x}) = 1.447$
		AI33			74500					14.744	
		AI21		18	37000					14.613	
		AI11		20	17500					12.901	
		AI12			23500					15.036	
		AI13			16500					12.340	
		AI24			23000					14.909	
		AI25		22.5	18000					16.709	
		AI27		25	13500					17.951	

\* Normalized

Case I

Case II

Case III

Table 17 Summary of Crack Initiation Results ( $a_0 = 0.010''$ ) Stress-Initiation Life  
Model Parameters and Statistics (6-annealed Ti-6Al-4V Alloy)

Environment	Data Set	Specimen	Frequency (Hz)	$\Delta\sigma$ (ksi)	$N_i$	$A \times 10^{-6}$	$\Delta\sigma_{th}$	$A \times 10^{-6}$	$\Delta\sigma_{th}$	$\Delta\sigma_{th}$	$\Delta\sigma_{th}$ Statistics
Dry Air	4	T108	6	32.5	600000	24.024	35.463	20.966	37.407	31.958	$n=9$ $\bar{x} = 37.199$ $S(\bar{x}) = 4.166$
		T106		35	820000					34.613	
		T105		40	52400					34.639	
		T104		45	27500					35.533	
		T109		50	16505					35.067	
		T110		50*	23100					39.904	
		T111		50	18500					36.969	
		T102		55	22600					45.796	
		T101		70	6400					40.299	
		T132		35	710000	22.713	34.170		35.124	34.576	
3.5% NaCl	5	T133	1	35	680000					34.557	$n=6$ $\bar{x} = 34.971$ $S(\bar{x}) = 3.592$
		T134		35	73000					30.673	
		T129		50	24000					40.129	
		T130		50	19500					37.747	
		T131		50	14200					31.992	
		T126		32.5	75000	20.266	31.157		30.493	27.869	
		T122		35	77000					30.866	
		T1M4		35	76000					30.808	
		T1M5		35	191000					33.395	
		T121		40	18200					21.167	
	6	T123	6	45	23000					33.368	$n=11$ $\bar{x} = 30.274$ $S(\bar{x}) = 3.822$
		T1M1		50	15500					33.873	
		T1M2		50	14300					32.153	
		T1M3		50	15000					33.200	
		T124		55	9100					26.852	
		T127		70	5200					29.463	

\* Normalized

Case I

Case II

Case III

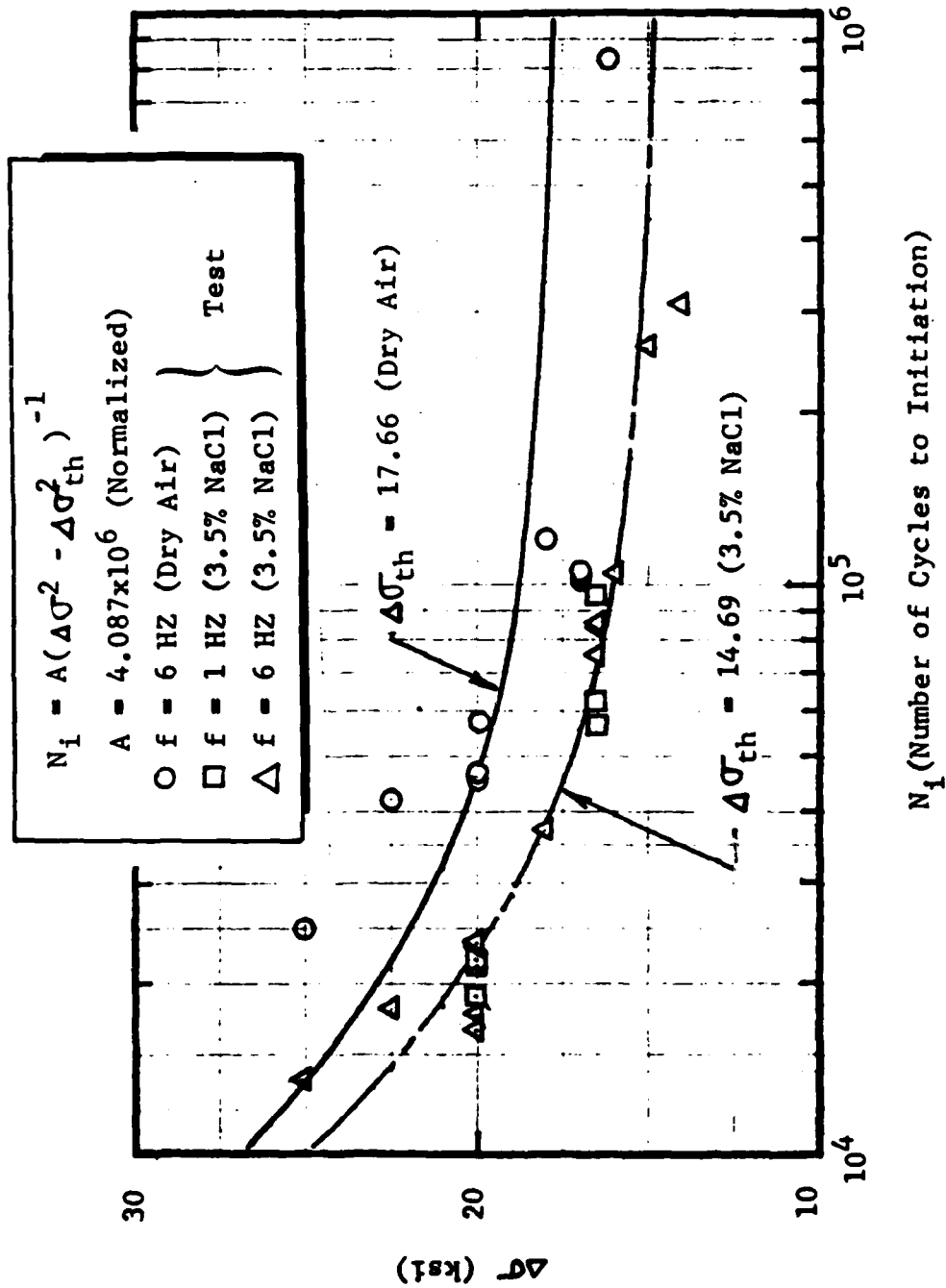
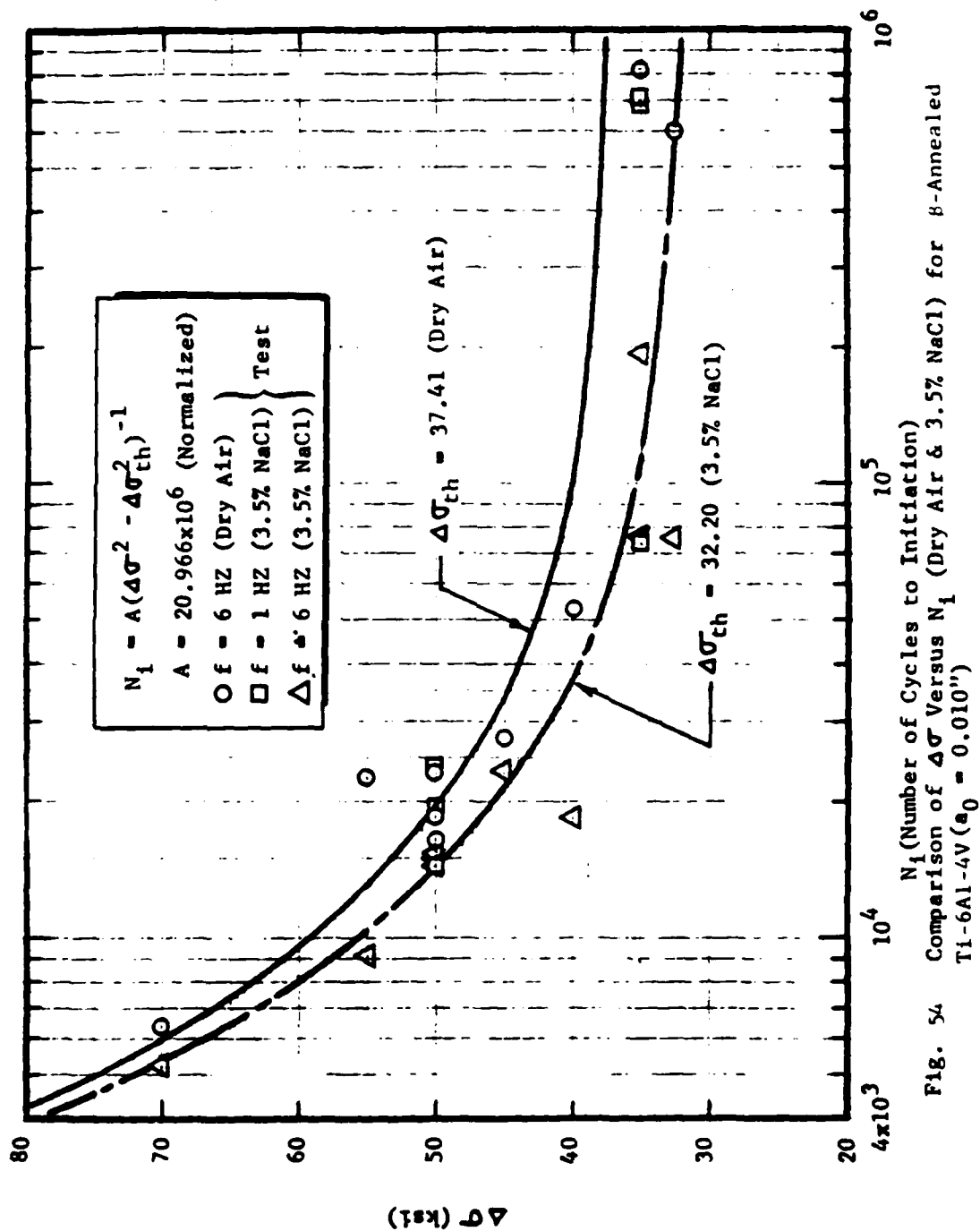


Fig. 53 Comparison of  $\Delta\sigma$  Versus  $N_i$  Curves (Dry Air & 3.5% NaCl) for 7075-T7651 Aluminum Alloy ( $a_0 = 0.010''$ )



$\beta$ -annealed Ti-6Al-4V alloy, respectively. In this case,  $\Delta\sigma_{th}$  values reflect 50% confidence.

#### 5.2.1.3 95% Confidence Interval for $\Delta\sigma$

A 95% confidence interval for  $\Delta\sigma$  versus  $N_i$  was estimated as follows:

1. Assume "A" is a constant for a given material and reflect the variance in the parameter  $\Delta\sigma_{th}$ . Compute the normalized "A" value for a given material by combining the results for different data sets (Ref. Subsection 5.2.1.1).

2. Rearrange Eq. 18 to obtain the following expression for  $\Delta\sigma_{th}$ :

$$\Delta\sigma_{th} = \sqrt{\Delta\sigma^2 - A/N_i} \quad (27)$$

3. Use the normalized "A" value from step 1 and Eq. 27 to compute the corresponding  $\Delta\sigma_{th}$  value for each  $\Delta\sigma$ ,  $N_i$  test result in the data set.

4. Assume the computed  $\Delta\sigma_{th}$  values are normally distributed and compute the corresponding average,  $(\bar{x})$ , and standard deviation,  $S(x)$ , for  $\Delta\sigma_{th}$ .

5. Use the standard t-test [e.g., 38] to estimate the 95% confidence interval for  $\Delta\sigma_{th}$ . In Eq. 28,  $\mu$  = expected  $\Delta\sigma_{th}$  value for given probability,

$$\mu = \bar{x} \pm t \frac{s(x)}{\sqrt{n}} \quad (28)$$

$\bar{x}$  = average  $\Delta\sigma_{th}$ ,  $t$  = student's t distribution statistic for  $n-1$  degrees of freedom,  $S(x)$  = standard deviation for  $\Delta\sigma_{th}$  and  $n$  = number of tests in data set.

6. Once  $\Delta\sigma_{th}$  values have been determined for different probabilities (i.e.,  $P = 0.025, 0.50$  and  $0.975$ ) using Eq. 28,  $\Delta\sigma$  values can be determined using Eq. 29.

$$\Delta\sigma = \sqrt{\Delta\sigma_{th}^2 + A/N_i} \quad (29)$$

Using the procedure above, the 95% confidence interval was estimated for 7075-T7651 aluminum alloy and  $\beta$ -annealed Ti-6Al-4V. Results are plotted in Figs. 55 - 58.

#### 5.2.1.4 Effect of Loading Frequency

For a given material and environment is there a significant difference in the mean  $\Delta\sigma_{th}$  values for two different loading frequencies (i.e.,  $f = 1$  Hz and 6 Hz)? The small sample test [e.g., 29] will be used to determine if the loading frequency has a significant effect on  $\Delta\sigma_{th}$  values for  $\alpha = 0.05$  significance level.

The standard deviation can be estimated using the individual sample variances to generate a pooled sample,  $S$  (Eq. 30).

$$S = \sqrt{\frac{(n_1-1)S_1^2 + (n_2-1)S_2^2}{n_1 + n_2 - 2}} \quad (30)$$

In Eq. 30:  $n_1, n_2$  = sample size for data set

1 and 2, respectively

$S_1, S_2$  = standard deviation for data

set 1 and 2, respectively.

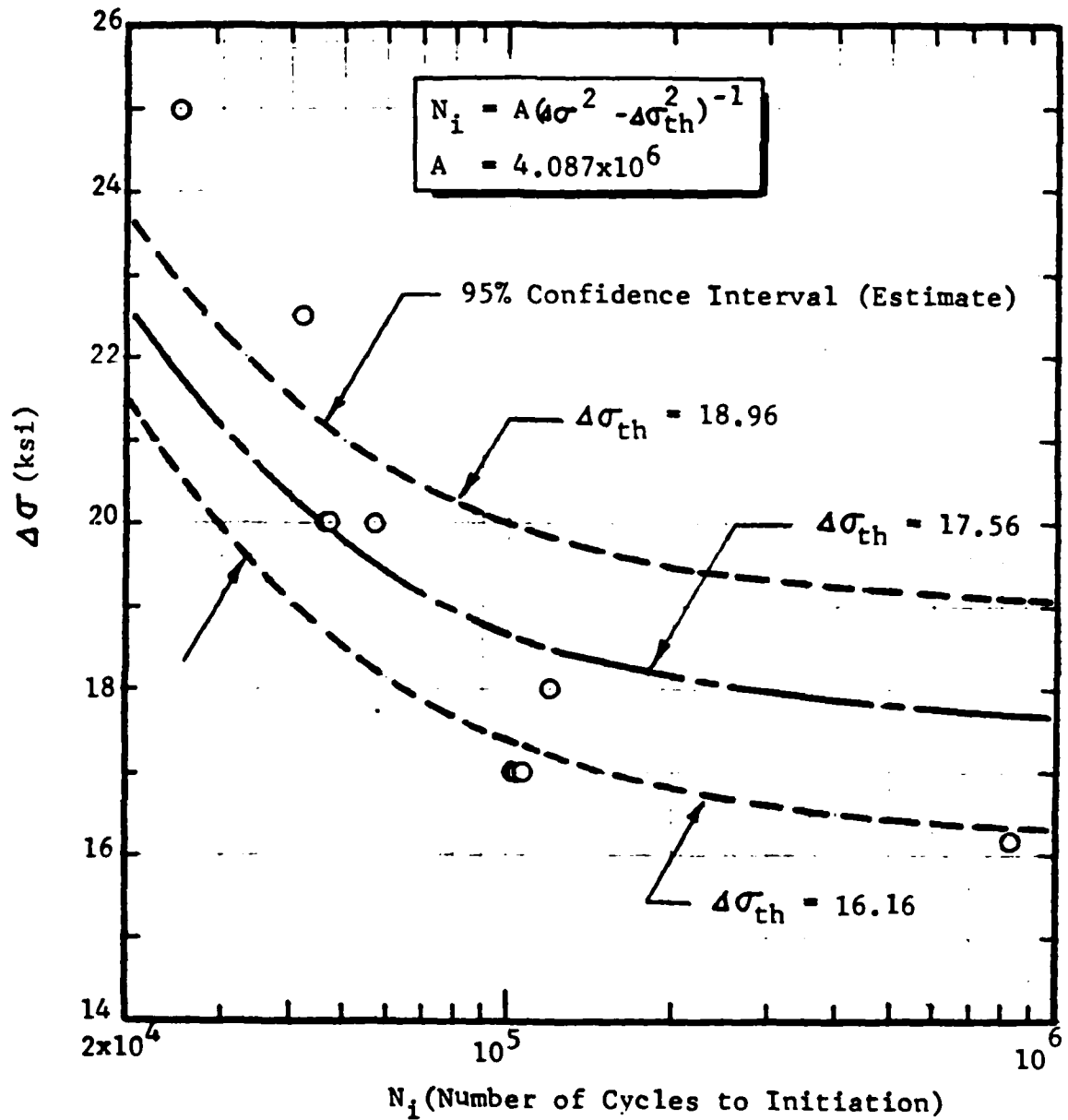


Fig. 55 95% Confidence Interval for  $\Delta\sigma$  Versus  $N_i$  for 7075-T7651 Aluminum Alloy in Dry Air ( $f = 6$  HZ;  $a_0 = 0.010''$ )

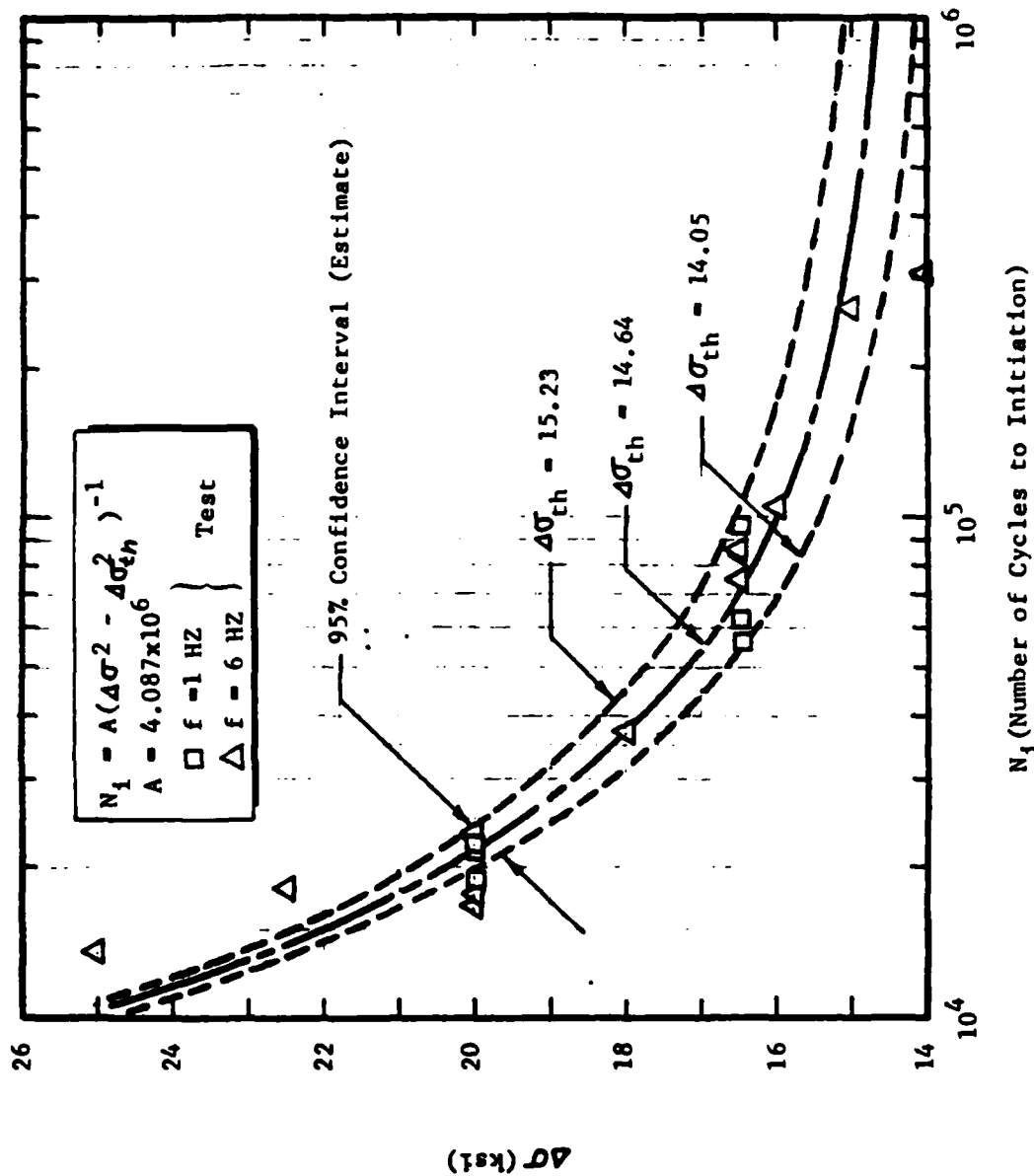


Fig. 56 95% Confidence Interval for  $\Delta\sigma$  Versus  $N_1$  for 7075-T7651 Aluminum Alloy in 3.5% NaCl Solution ( $a_n = 0.010''$ )

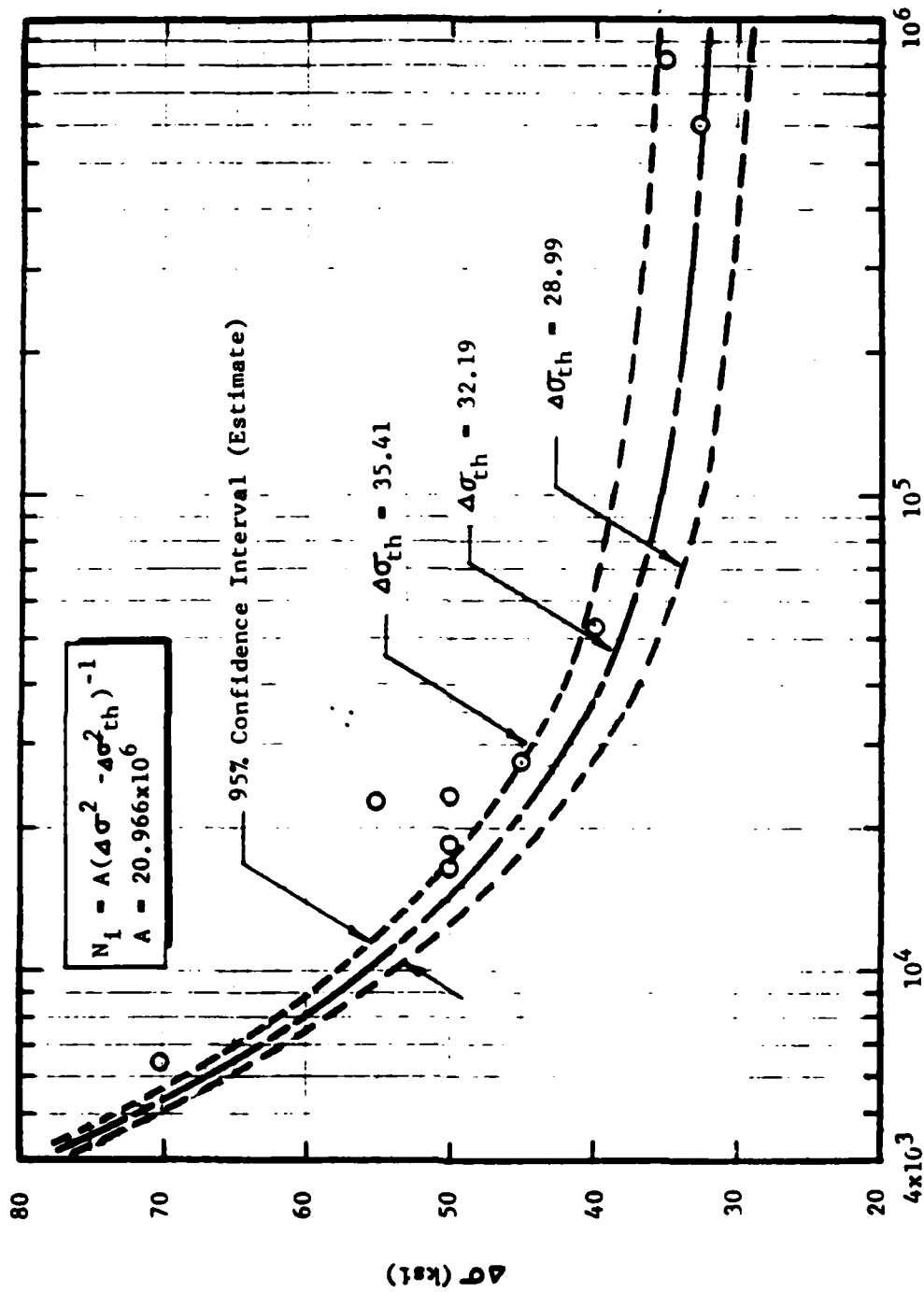


Fig. 57 95% Confidence Interval for  $\Delta\sigma$  Versus  $N_i$  for  $\beta$ -Annealed Ti-6Al-4V in Dry Air ( $f = 6\text{Hz}$ ;  $a_0 = 0.010''$ )

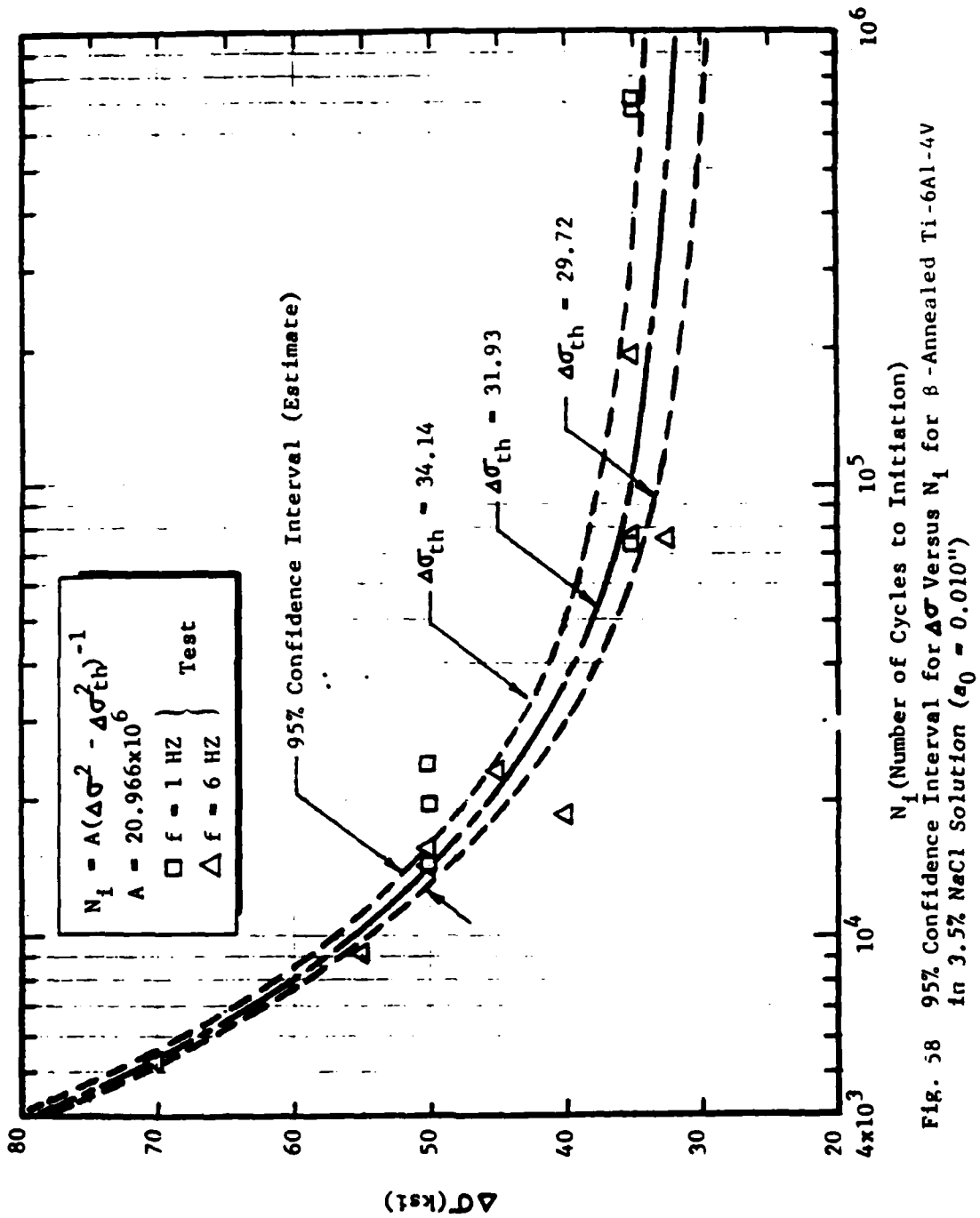


Fig. 58 95% Confidence Interval for  $\Delta\sigma$  Versus  $N_i$  for  $\beta$ -Annealed Ti-6Al-4V in 3.5% NaCl Solution ( $a_0 = 0.010''$ )

The Student's t-statistic is given by Eq. 31 [e.g., 29].

$$t = \frac{(\bar{x}_1 - \bar{x}_2)}{S \sqrt{\frac{1}{n_1} + \frac{1}{n_2}}} \quad (31)$$

7075-T7651 Aluminum Alloy (3.5% NaCl)

Using Eqs. 30 and 31 and the  $\Delta\sigma_{th}$  statistics from Table 17 determine if loading frequency has a significant effect on the mean  $\Delta\sigma_{th}$  at a significance level of  $\alpha = 0.05$ . The following results are from Table 16. Substituting the values below:

$$\bullet f_1 = 1 \text{ HZ}, n_1 = 6, \bar{x}_1 = 14.387, S_1(x) = 0.511$$

$$\bullet f_2 = 6 \text{ Hz}, n_2 = 13, \bar{x}_2 = 14.755, S_2(x) = 1.447$$

into Eq. 30,  $S = 1.246$  is obtained. Then using Eq. 31, the value for  $t$  is  $-0.591$ .

In this case the critical  $t$  value for  $n_1 + n_2 - 2$  degrees of freedom is 2.11 [29]. Since the critical  $t$  is greater than

$|-0.591|$  it is concluded that the effect of loading frequency on the mean  $\Delta\sigma_{th}$  is not significant at a significance level of  $\alpha = 0.05$ .

$\beta$ -Annealed Ti-6Al-4V (3.5% NaCL)

The procedure described above and the following results from Table 17 will be used to decide if loading frequency has a significant effect on the mean  $\Delta\sigma_{th}$  at the significance level of  $\alpha = 0.05$ . Using the following data from Table 17 and Eqs. 30 and 31,

- $f = 1 \text{ Hz}$ ,  $n_1 = 6$ ,  $\bar{X}_1 = 34.971$ ,  $S_1(x) = 3.592$
- $f = 6 \text{ HZ}$ ,  $n_2 = 11$ ,  $\bar{X}_2 = 30.274$ ,  $S_2(x) = 3.822$

the following values for  $S$  and  $t$  are obtained:  $S = 3.747$  and  $t = 2.469$ .

In this case, the critical  $t$  value for  $n_1+n_2-2$  degrees of freedom is 2.13. Since  $2.469 > 2.13$ , it is concluded that the effect of loading frequency on the mean  $\Delta\sigma_{th}$  is significant at a significance level of  $\alpha = 0.05$ .

### 5.2.2 Conclusions

The following conclusions are based on the results presented in Section 5.2.1.

1. In general, the stress-initiation life model fits the observed test results reasonably well for both 7075-T7651 aluminum alloy and  $\beta$ -annealed Ti-6Al-4V (Ref. Figs. 53-58).

2. The stress-initiation life model parameters  $A$  and  $\Delta\sigma_{th}$  appear to be sensitive to the effect of environment (dry air versus 3.5% NaCl). For example, compare  $\Delta\sigma_{th}$  values in Figs. 53 and 54.

3. A broader 95% confidence band was observed for the dry air environment than for the 3.5% NaCl environment for 7075-T7651 aluminum alloy. For example, compare Figs. 55 and 56. In this case, the wider confidence band for the dry air environment is due, in part, to the smaller sample size. Additional crack initiation tests should be performed in a dry air environment to assess the effects of scatter on the  $\Delta\sigma$  versus  $N_i$  response.

4. The 95% confidence band ( $\Delta\sigma$  versus  $N_i$ ) for the  $\beta$ -annealed Ti-6Al-4V in dry air (Fig. 57) was slightly broader than the corresponding band for 3.5% NaCl (Fig. 58).

5. The effects of loading frequency on the mean  $\Delta\sigma_{th}$  were not significant at the significance level of  $\alpha = 0.05$  for the 7075-T7651 aluminum alloy. However, such effects were found to be significant for  $\beta$ -annealed Ti-6Al-4V for  $\alpha = 0.05$ . Additional crack initiation tests are needed to better understand the effects of loading frequency on crack initiation for  $\beta$ -annealed Ti-6Al-4V.

6. The stress-initiation life model is promising for analytically predicting the time to crack initiation for both dry air and 3.5% NaCl environments. Given the data base, the model parameters  $A$  and  $\Delta\sigma_{th}$  can be easily determined. The stress initiation life model is semi-empirical, but so are some of the other models currently available (e.g., strain-initiation life approach). Further work is required to demonstrate the model for spectrum loading and different environments and to assess the effects of scatter. To make the stress-initiation life model work for spectrum loading, a suitable cycle counting scheme is required.

7. In Phase I, the stress-initiation life model was evaluated using test results for simple dog-bone specimens with an open hole in the center of the specimen. The stress-initiation life model also needs to be evaluated using suitable crack initiation data obtained under a bolt load transfer condition.

8. Since the stress-initiation life model must account for R ratio effects, a larger data base is needed to implement this approach than for the strain-initiation life approach [5,6]. Further work is required to evaluate the effects of the R ratio on the  $\Delta\sigma$  versus  $N_i$  relationship. The strain-initiation life approach will be evaluated in Phase II.

### 5.3 EVALUATION OF CRACK PROPAGATION MODELS

The crack propagation models described in Section 2.3 are evaluated in this section for two materials: 7075-T7651 aluminum alloy and  $\beta$ -annealed Ti-6Al-4V alloy. Test results for the model evaluations are presented and also discussed in section 4.4.

Two models were considered for the corrosion fatigue of aluminum and titanium alloys in aqueous environments - the

transport controlled model (at saturation) and the diffusion controlled model. These models are evaluated considering the dependence of  $(da/dN)_{cf}$  on frequency and holding time. The transport controlled model predicts an independence of frequency and holding time, and the diffusion controlled model yields an inverse square-root dependence on frequency or on holding time. Both models were derived based on considerations of rate controlling processes, and do not allow for other restrictions. The diffusion controlled model was derived with the implicit assumption that the supply of hydrogen would be ample.

Although the effect of  $\Delta K$  is included explicitly only for the diffusion controlled model, the dependence of  $(da/dN)_{cf}$  on  $(\Delta K)^2$  is implied for the transport-controlled model. If the amount of hydrogen produced per cycle is proportional to the available fresh surface area, it will likely be concentrated in a zone near the crack tip. This suggests that the "saturation" growth rate,  $(da/dN)_{cf,s}$ , for the transport and surface reaction controlled case is a function of  $(\Delta K)^2$  and is independent of the load ratio (R).

Data for the 7075-T7651 aluminum alloy tested in 3.5% NaCl clearly show that the fatigue crack growth rates (based on constant amplitude loading) are independent of frequency

and holding time at maximum load (Ref., Figs. 35-39). These results are consistent with the concept of limited reactions of this alloy with the environment, and corresponds to "saturation" in enhancement. Since the crack growth rate,  $da/dN$ , is independent of frequency and holding time for the 7075-T7651 aluminum alloy, the two mechanistic crack propagation models considered in this report are not essential for design. Further evaluations are required to determine if the cycle dependent component of corrosion fatigue,  $(da/dN)_{cf}$ , is indeed proportional to  $(\Delta K)^2$  and independent of the load ratio (R) for the 7075-T7651 aluminum alloy.

The crack growth response of  $\beta$ -annealed Ti-6Al-4V alloy in 3.5% NaCl solution is complex and very different from that of the aluminum alloys. At the higher frequencies, fatigue crack growth rates increased with decreasing frequency (Fig. 48). With further decreases in frequency, the rates reached a maximum and then decreased with frequency. Holding time showed a similar effect on the rate of crack growth (Figs. 52 and 53), and saw-tooth waveform appeared to result in slower crack growth than sinusoidal loading at the same frequency. The data suggest that crack growth conforms to the model for diffusion controlled crack growth at the higher frequencies. The decrease in rate with

further reductions in frequency and the apparent waveform effect, however, are not understood at this time. These effects may be related to the formation and rupture of titanium hydrides, and should be carefully examined in Phase II of this program.

Based on the results and conclusions from the Phase I effort, it is clear that further research is needed to develop a mechanistic understanding of the corrosion fatigue behavior of the  $\beta$ -annealed Ti-6Al-4V alloy. Unlike the titanium alloy, the crack propagation behavior of the 7075-T7651 aluminum alloy is fairly well understood. For this reason, the corrosion fatigue methodology will be developed and verified in Phase II for only the 7075-T7651 aluminum alloy. Further mechanistic studies will be performed in Phase II to develop a better understanding of the crack growth behavior of the  $\beta$ -annealed Ti-6Al-4V alloy in a corrosive environment.

SECTION VI  
CONCLUSIONS AND RECOMMENDATIONS

6.1 CONCLUSIONS

The following conclusions are based on the results of the Phase I effort:

1. The fatigue crack growth rate for 7075-T7651 aluminum alloy appears to be independent of the test frequency and holding time in the aqueous environments. No significant differences in the crack growth rates were found for distilled water, 3.5% NaCl solution, 3.5% NaCl + H<sub>2</sub>SO<sub>4</sub>, and synthetic seawater environments. This independence is attributed to the fact that the reaction between the aqueous environments and 7075-T7651 appear to be limited, and suggests that the corrosion fatigue crack growth behavior should be considered a limiting case of the transport-controlled or surface-reaction controlled crack growth model.

2. Since the crack growth rate is independent of the test frequency for the 7075-T7651 aluminum alloy, a special corrosion fatigue model for crack propagation, such as the superposition model [18,19], is not needed for this alloy.

3. The fatigue crack growth response for the  $\beta$ -annealed Ti-6Al-4V alloy, exposed to 3.5% NaCl solution, is a complex function of frequency, load-ratio, stress-intensity range, holding-time, etc. Therefore, a better understanding of the corrosive fatigue mechanisms is needed for this titanium alloy before a reliable predictive methodology can be developed.

4. The stress-initiation life model looks promising for predicting the number of cycles to crack initiation for both the 7075-T7651 aluminum alloy and the  $\beta$ -annealed Ti-6Al-4V alloy. The model parameters "A" and " $\Delta\sigma_{th}$ " appear to be sensitive to the effect of environment (dry air and 3.5% NaCl) on crack initiation. Further research is needed to demonstrate the model for spectrum loading and different environments, and to assess the effects of scatter.

5. Further work is required to evaluate the effects of R ratio on the cycle-dependent component of corrosion fatigue  $(da/dN)_{cf}$  for the 7075-T7651 aluminum alloy. It is believed that  $(da/dN)_{cf}$  is proportional to  $(\Delta K)^2$  but this remains to be proven.

6. Based on constant amplitude test results for dog-bone specimens with a center hole, it was found that the

number of cycles to crack initiation ( $a_0 = 0.010''$ ) was a significant part of the total fatigue life for both 7075-T7651 aluminum alloy and  $\beta$ -annealed Ti-6Al-4V alloy. There was no significant difference in the average ratio of  $N_i/N_f$  (no. of cycles to crack initiation/no. of cycles to failure) in either dry air or a 3.5% NaCl environment for either 7075-T7651 aluminum alloy or  $\beta$ -annealed Ti-6Al-4V alloy. No significant difference in the mean  $N_i/N_f$  values for  $f = 1$  Hz and 6 Hz were found at  $\alpha = 0.05$  significance level for either the aluminum alloy or titanium alloy.

## 6.2 RECOMMENDATIONS

1. The corrosion fatigue predictive methodology proposed in Phase I for mechanically-fastened joints should be further developed, evaluated and verified in Phase II for the 7075-T7651 aluminum alloy.

2. Since the fatigue crack growth behavior of the  $\beta$ -annealed Ti-6Al-4V alloy is very complex, further understanding of the causes for this behavior is needed before predictive methods for corrosion fatigue can be developed for mechanically-fastened joints for this alloy. Further work in Phase II with this alloy should be limited to developing a better understanding of the effect of

frequency on fatigue crack growth. Particular emphasis should be placed on the characterization of fatigue crack growth and on examining the influence of microstructure.

3. The corrosion fatigue behavior of mechanically-fastened joints is complex. Therefore, the Phase II tests should minimize the number of test variables so that the effects of selected variables on corrosion fatigue crack initiation and crack propagation can be more readily determined. The effects of specimen preconditioning (i.e., pretest and presoak in 3.5% NaCl) on fatigue crack initiation and crack propagation should be investigated for the 7075-T7651 aluminum alloy to determine if "preconditioning" has a significant effect on the predictive methodology for corrosion fatigue.

4. The corrosion fatigue predictive methodology for mechanically-fastened joints should be further developed in Phase II to account for spectrum loading and the effects of scatter in the baseline data.

5. The strain-controlled initiation model [5,6] for predicting the TTCI should be evaluated in Phase II.

## SECTION VII

### PHASE II TEST PLAN

#### 7.1 INTRODUCTION

A Phase II test plan was developed under Task 3 of the Phase I effort. The plan is described and discussed in this section.

#### 7.2 TEST OBJECTIVES AND PHILOSOPHY

Basic objectives of the Phase II tests are to: (1) develop and verify corrosion fatigue testing methodology and data acquisition methods, (2) develop statistically-valid test data for making analytical corrosion fatigue predictions for crack initiation and total life, and (3) acquire experimental test results for verifying the analytical corrosion fatigue methodology for mechanically-fastened joints.

The corrosion fatigue behavior of mechanically-fastened joints is complex. Therefore, the following philosophy was reflected in the Phase II test plan:

- Minimize the number of test variables to isolate the effects of corrosion fatigue.
- Use test replications to acquire statistically-valid data.
- Test specimens will include the fundamental elements of a mechanically-fastened joint.
- Develop a better understanding of the corrosion fatigue behavior of straight-bore holes - with and without: fasteners and load transfer through the fasteners.
- Due to the complexity of corrosion fatigue, state-of-the-art analytical corrosion fatigue methodology should be developed and verified in progressive steps with increasing structural complexities.
- Build on the test data and understandings from the Phase I effort.
- Develop and verify the corrosion fatigue analytical methodology for 7075-T7651 aluminum alloy.

- Develop a better understanding of the corrosion fatigue mechanisms for  $\beta$ -annealed Ti-6Al-4V alloy.

### 7.3 TEST VARIABLES

The corrosion fatigue variables reflected in the Phase II test plan are summarized in Table 18.

### 7.4 TEST PLAN

Test specimens required for the Phase II test plan are summarized in Table 19. The test matrix for Tasks 5 and 6 is presented in Tables 20 and 21, respectively. Further details for the titanium tests are given in Table 22.

Test specimen details are shown in Figs. 6, 59-61. The test setup for the bolt load transfer tests is shown in Fig. 62.

### 7.5 SPECIMEN PRECONDITIONING

Specimens for selected tests will be preconditioned as follows:





1. Specimens will be fatigue tested in lab air using a selected stress level and load spectrum. The test will be stopped after applying the maximum load in the spectrum.

Table 18 Test Variables

Material	<ul style="list-style-type: none"> <li>o 7075-T7651 Aluminum Alloy</li> <li>o 8-Annealed Ti-6Al-4V Alloy</li> </ul>
Environment	<ul style="list-style-type: none"> <li>o Dry Air</li> <li>o Constant Immersion</li> <li>o Modified Constant Immersion</li> </ul> } (3.5% NaCl)
Type Loading	<ul style="list-style-type: none"> <li>o Strain-Controlled</li> <li>o Constant Amplitude</li> <li>o Spectrum</li> </ul>
Load Spectra	<ul style="list-style-type: none"> <li>o F-16 400 hour block</li> <li>o Spectrum B (to be determined)</li> </ul>
Test Duration	<ul style="list-style-type: none"> <li>o 1 week</li> <li>o 4 weeks</li> </ul>
Test Specimens	<ul style="list-style-type: none"> <li>o Un-notched axial (strain-control)</li> <li>o Compact tension</li> <li>o Dog-bone with center hole</li> </ul>
Bolt Load Transfer	<ul style="list-style-type: none"> <li>o 0% LT</li> <li>o 20% LT</li> <li>o X LT *</li> </ul>
Bolt Type	<ul style="list-style-type: none"> <li>o Steel Protruding Head (cad-plated) (e.g., NAS 6204)</li> </ul>
Stress Level	1-2 levels
Hole Finish	Polished
*Preconditioning	<ul style="list-style-type: none"> <li>o None</li> <li>o Pretest and presoaking 3.5% NaCl</li> </ul>

\* to be determined

Table 19 Summary of Test Specimens for Phase II

Specimen		Material	No. of Specimens			
Config.	Type		Task 4	Task 5	Task 6	$\Sigma$
	S-C	7075-T7651	5	45	0	50
		Ti-6Al-4V	5	25	0	30
	CT	7075-T7651	0	4	0	4
		Ti-6Al-4V	0	12	0	12
	NLT	7075-T7651	5	100	0	105
	LT		5	0	40	45
$\Sigma$			20	186	40	246

Notes

- Task 4 - Experimental Methodology Development and Evaluation  
 Task 5 - Acquisition of Data for Prediction of Environmentally-Assisted Crack Growth in Aircraft Joints  
 Task 6 - Prediction Methodology Evaluation and Verification  
 S-C = Strain-controlled  
 CT = Compact Tension  
 NLT = No Load Transfer (through the fastener)  
 LT = Load transfer (through the fastener)

AD-A136 414

DEVELOPMENT OF FATIGUE AND CRACK PROPAGATION DESIGN AND  
ANALYSIS METHODOLOGY (U) GENERAL DYNAMICS FORT WORTH TX  
FORT WORTH DIV Y H KIM ET AL. MAR 83

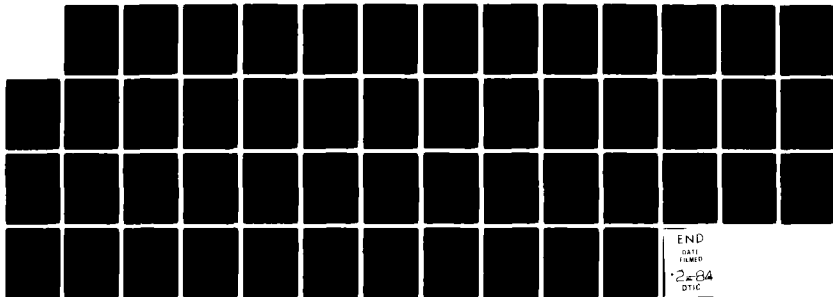
3/3

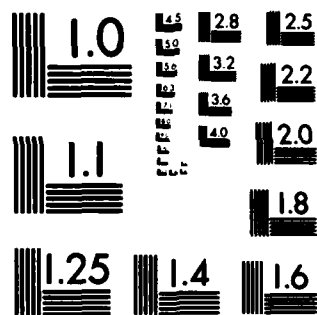
UNCLASSIFIED

NADC-83126-60-VOL-1 N62269-81-C-0268

F/G 20/11




NL





MICROCOPY RESOLUTION TEST CHART  
NATIONAL BUREAU OF STANDARDS-1963-A

Table 20 Phase II Tests for Task 5

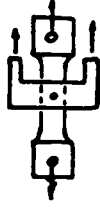
Specimen	Material	Specimen Details				Type Loading	Loading Freq.	Environ.			Data			No. Specimens	Test No.	
		Surf or Hole	% LT	Bolt	PC?			Dry Air	CI	CI	Crack Growth	TTCI	TTF			
	7075-T7651	P	--	--	No	S-C	1CPS (max)	x	-	-	-	x	-	20 20 5	I(a) I(b) I(c)	
	6Al-4V T1	P	--	--		S-C	1CPS (max)	x	-	-	-	x	-	10 10 5	I(d) I(e) I(f)	
	7075-T7651	UP	--	--		CA	oo	x	-	-	x	-	-	2 2	II(a) II(b)	
	6Al-4V T1	UP	--	--		CA	(Ref. Table 22)	x	-	-	x	-	-	6 6	II(c) II(d)	
	7075-T7651	P	0	No	No	SPA	Fast	x	-	-	x	x	x	6(2)*	III(a) (b) (c) (d)	
							Slow	x	-	-	x	x	x	6		
							Fast	-	-	x	x	x	x	6		
							Slow	-	-	x	x	x	x	10(3)*		
				Yes			Fast	x	-	-	x	x	x	3	(e)	
							Slow	x	-	-	x	x	x	3	(f)	
							Fast	-	-	x	x	x	x	4	(g)	
							Slow	-	-	x	x	x	x	4	(h)	
			Yes	No			Fast	x	-	-	x	x	x	3	(i)	
							Slow	x	-	-	x	x	x	3	(j)	
							Fast	-	-	x	x	x	x	4	(k)	
							Slow	-	-	x	x	x	x	4	(l)	
				Yes		Fast	x	-	-	x	x	x	3	(m)		
						Slow	x	-	-	x	x	x	3	(n)		
						Fast	-	-	x	x	x	x	4	(o)		
						Slow	-	-	x	x	x	x	4	(p)		
				No	No		SP3	Fast	x	-	-	x	x	x	3	(q)
								Slow	x	-	-	x	x	x	3	(r)
								Fast	-	-	x	x	x	x	4	(s)
								Slow	-	-	x	x	x	x	4	(t)
						Yes		Fast	x	-	-	x	x	x	3	(u)
								Slow	x	-	-	x	x	x	3	(v)
								Fast	-	-	x	x	x	x	4	(w)
								Slow	-	-	x	x	x	x	4	(x)
							CA	6HZ	x	-	-	x	x	x	3 4	(y) (z)

191

**Notes**

- P - Polished  
 UP - Unpolished  
 PC - Specimen preconditioned (pre-tested and then soaked in 3.5% NaCl solution at room temperature for 72 hrs.)  
 S-C - Strain-Controlled  
 CA - Constant Amplitude  
 SPA - F-16 400 hour block spectrum  
 SP3 - Spectrum to be determined  
 CI - Constant Immersion in 3.5% NaCl solution  
 CI\* - Constant Immersion in 3.5% NaCl solution with periodic lab air exposure during TTCI measurements  
 TTCI - Time-To-Crack-Initiation  
 TTF - Time-To-Failure  
 — - To be determined  
 FAST - 1 service life in 2 days  
 SLOW - 1 service life in 16 days  
 ( )\* - No. of specimens out of total dedicated to Task 4

Table 21 Phase II Verification Tests for Task 6

Specimen	Material	Specimen Details				Type Loading	Loading Freq.	Environment			Data			No. Spec.	Test No.
		Surf. or Hole	2 LT	Bolt	PC?			Dry Air	CI*	CI	Crack Growth	TTCI	TTF		
	7075-T7651	P	20	Cad-Plated Steel	No	CA	6 Hz	x	-	-	-	x	x	4	1V(a)
							0.1 Hz	-	x	-	-	x	x	4	1V(b)
						SPA	Fast	x	-	-	x	x	x	4	1V(c)
							Fast	-	x	-	x	x	x	4	1V(d)
							Slow	-	x	-	x	x	x	4	1V(e)
							Slow	-	-	x	-	-	x	4	1V(f)
						SPB	Fast	x	-	-	x	x	x	4	1V(g)
							Fast	-	x	-	x	x	x	4	1V(h)
							Slow	-	x	-	x	x	x	4	1V(i)
							Slow	-	-	-	-	-	x	4	1V(j)

40

**Notes**

P - Polished

PC - Specimen preconditioned (pre-tested and then soaked in 3.5% NaCl solution at room temperature for 72 hrs.)

CA - Constant Amplitude

SPA - F-16 400 hour block spectrum

SPB - Spectrum to be determined

CI - Constant Immersion in 3.5% NaCl solution

CI\* - Constant Immersion in 3.5% NaCl solution with periodic lab air exposure during TTCI measurements

TTCI - Time-To-Crack-Initiation

TTF - Time-To-Failure

\*\* - To be determined

FAST - 1 service life in 2 days

SLOW - 1 service life in 16 days

Table 22 Titanium Crack Growth Tests for Phase II

Environment	K Level		
	Low	Med	High
Reference (oxygen)	o o	o o	o o
Vacuum	x	x	x
3.5 pct NaCl	o x	o x	o x

NOTE: o New tests for Phase II (3 extra specimens to be available for testing as required)

x Constant-load or constant-K test from Phase I.

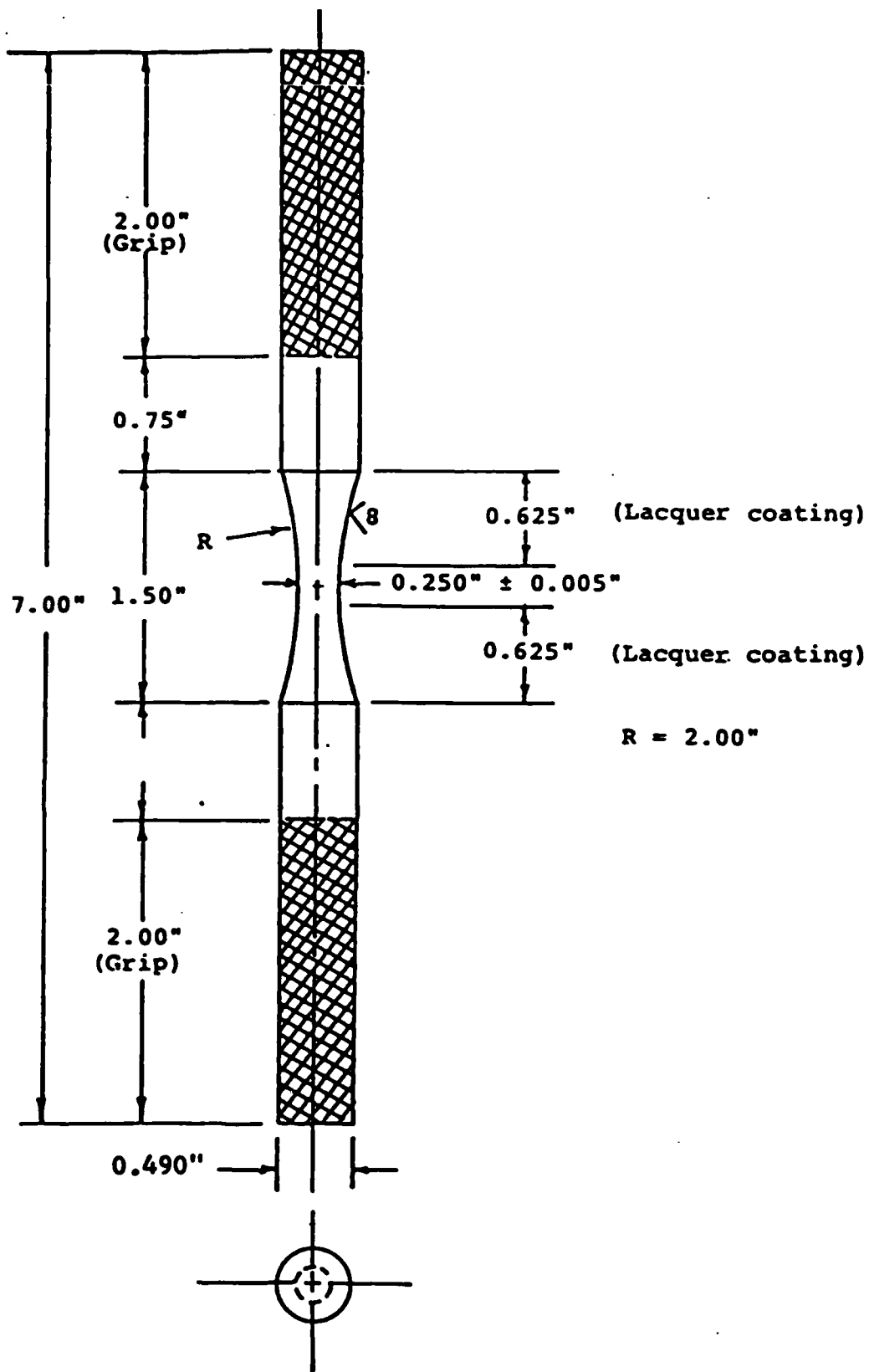


Fig. 59 Strain-Controlled Specimen

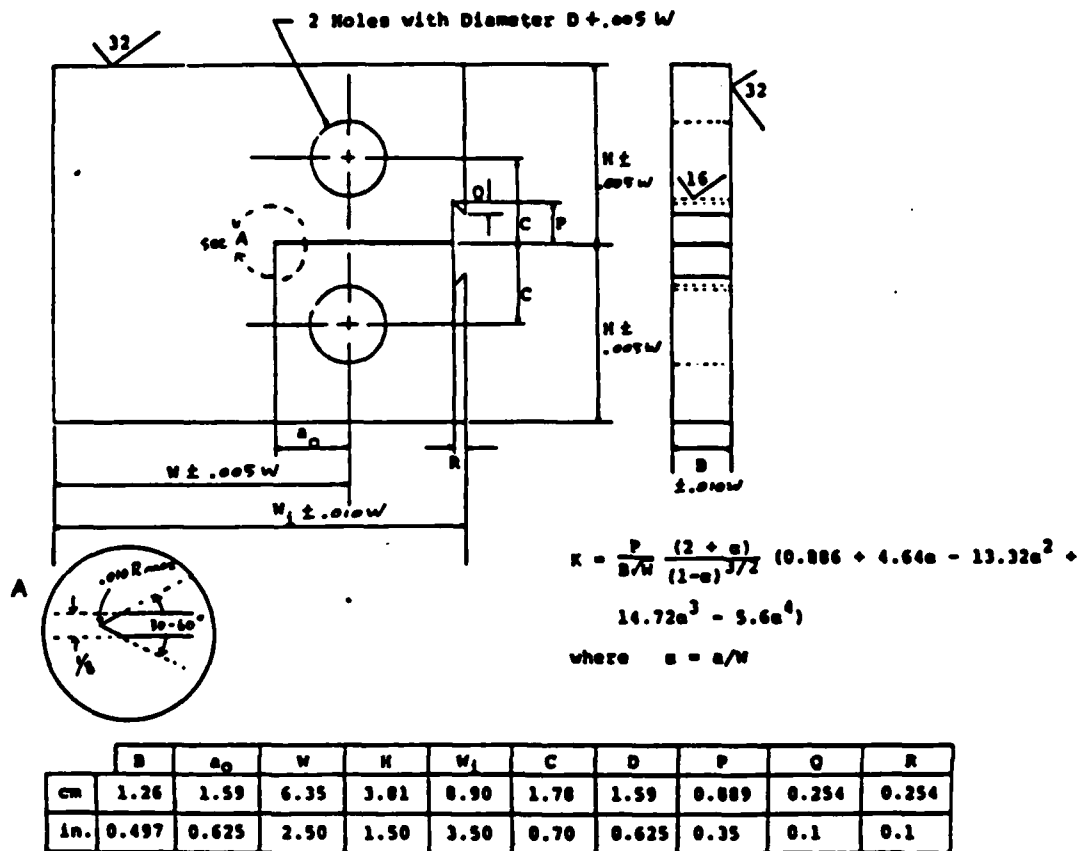
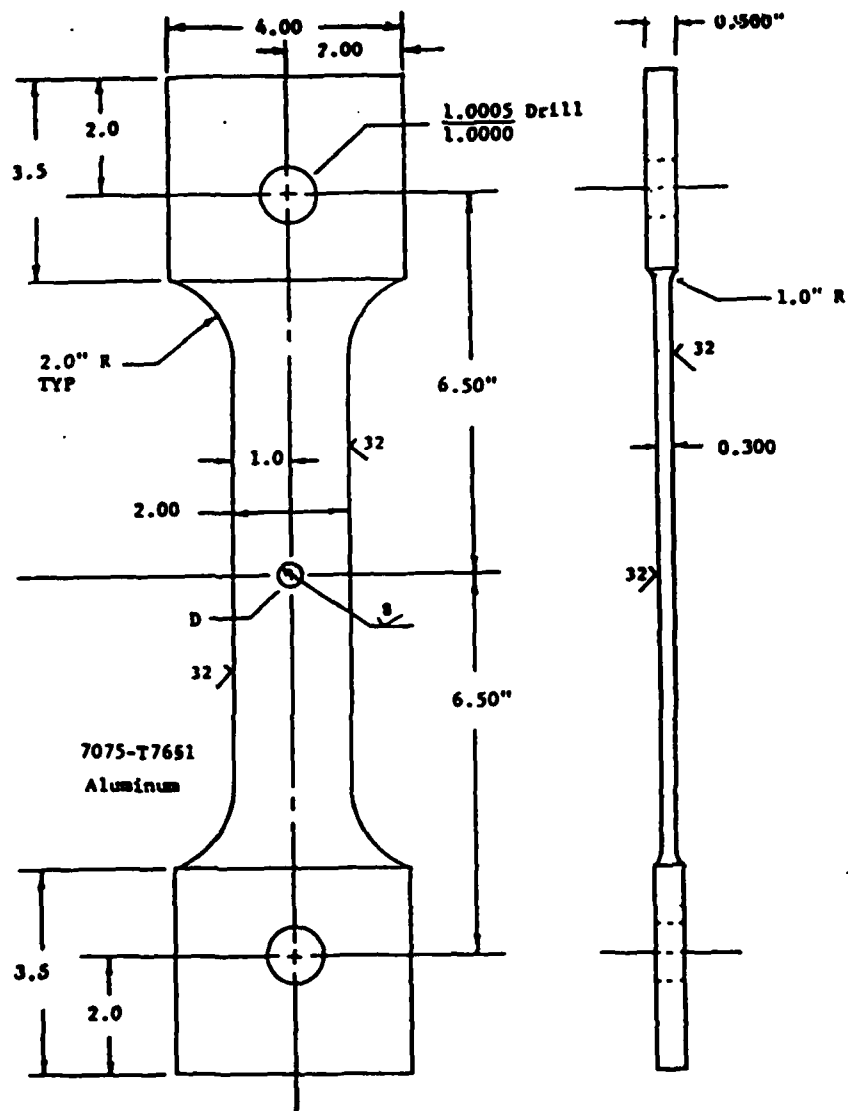


Fig. 60 Compact Tension Specimen for  $\beta$ -Annealed Ti-6Al-4V Alloy



**Fig. 61 Dog-Bone Specimen**

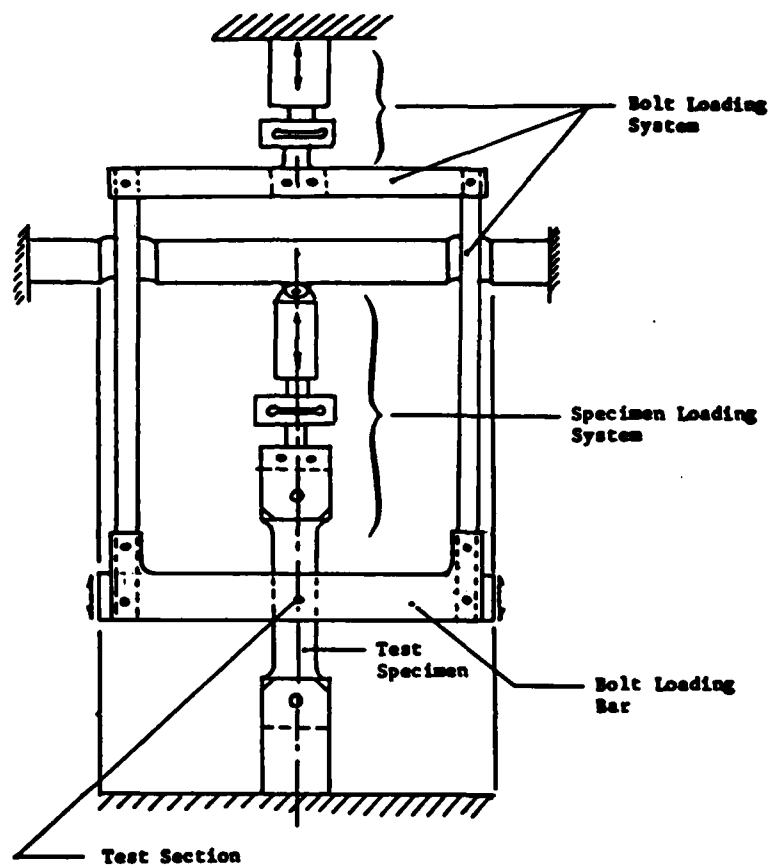


Fig. 62 Setup for Bolt Load Transfer Tests

2. Pre-tested specimens will be soaked in a 3.5% NaCl solution at room temperature for 72 hours.

3. Specimens will then be cleaned and dried using the procedures described in AGARD report 695 [22].

4. If the preconditioned specimen cannot be fatigue tested immediately, it will be stored at room temperature in a plastic bag with dessicant until it can be tested.

NADC-83126-60 Vol. I

THIS PAGE INTENTIONALLY LEFT BLANK

APPENDIX A

FATIGUE CRACK PROPAGATION  
RESULTS FOR 7075-T7651 ALUMINUM ALLOY

COMPACT TENSION AT H/W=0.486  
 AP-01  
 7075-T7651 L-T ORIENTATION  
 RT: DRY

GENERAL DYNAMICS  
 FORT WORTH DIVISION  
 JULY 16, 1982

6 CPM  
 R= 0.05 B= 0.4505 W= 2.561

NO. OF PTS.	TOTAL CYCLES	AVG. CRACK LENGTH (IN)	DELTA CRACK LENGTH (IN)	LSQ FIT DA/DN (IN/CYC)	CORR. COEFF.	STD. ERR. OF EST.	AVG. DEL-K (KSI-SQRT)
4	70000	0.8506	0.0357	4.81E-07	0.990	0.000	4.44
3	75000	0.8942	0.0281	3.78E-07	0.999	0.011	4.42
4	15295	0.9625	0.0265	1.39E-06	0.754	0.032	5.49
9	68745	1.1082	0.1916	2.81E-06	0.997	0.027	6.00
3	12417	1.4269	0.1142	9.64E-06	0.973	0.319	10.4

COMPACT TENSION AT H/W=0.486  
 AP-02  
 7075-T7651 L-T ORIENTATION  
 RT: SALT WAT.

GENERAL DYNAMICS  
 FORT WORTH DIVISION  
 AUG 4, 1982

180 CPM  
 R= 0.3 B= 0.451 W= 2.5518

NO. OF PTS.	TOTAL CYCLES	AVG. CRACK LENGTH (IN)	DELTA CRACK LENGTH (IN)	LSQ FIT DA/DN (IN/CYC)	CORR. COEFF.	STD. ERR. OF EST.	AVG. DEL-K (KSI-SQRT)
4	43478	0.8439	0.0721	1.71E-06	0.996	0.000	4.72
3	24000	0.9275	0.0723	3.12E-06	0.984	0.034	5.44
5	6400	0.9925	0.0457	7.59E-06	0.987	0.126	6.14
3	3000	1.0244	0.0286	1.00E-05	0.970	0.328	6.75
3	2319	1.0724	0.0566	2.50E-05	0.993	1.156	8.36
5	3523	1.2069	0.1143	3.26E-05	0.996	1.675	9.45
4	1400	1.3055	0.0830	5.89E-05	1.000	7.317	11.50
3	808	1.3996	0.0577	7.14E-05	1.000	7.849	12.74
3	683	1.4545	0.0537	7.86E-05	1.000	8.989	13.62
3	750	1.5605	0.0964	1.27E-04	0.997	24.107	17.33

COMPACT TENSION AT H/W=0.486  
 AP-03  
 7075-T7651 L-T ORIENTATION  
 RT, WET  
 SALT WATER  
 6 CPM  
 R= 0.3 B= 0.451 W= 2.5487

GENERAL DYNAMICS  
 FORT WORTH DIVISION  
 JUL 21, 1982

NO. OF PTS.	TOTAL CYCLES	AVG. CRACK LENGTH (IN)	DELTA CRACK LENGTH (IN)	LSQ FIT DA/DN (IN/CYC)	CORR. COEFF.	STD. ERR. OF EST.	AVG. DEL-K (KSI-SQRT)
3	40000	0.7851	0.0024	6.06E-08	0.999	0.004	2.39
4	54966	0.8565	0.0826	1.48E-06	0.990	0.000	4.63
5	25625	1.0882	0.1408	5.18E-06	0.988	0.074	6.82

COMPACT TENSION AT H/W=0.486  
 AP-04  
 7075-T7651 L-T ORIENTATION  
 RT, DRY

GENERAL DYNAMICS  
 FORT WORTH DIVISION  
 AUG 31, 1982

360 CPM  
 R= 0.3 B= 0.451 W= 2.5487

NO. OF PTS.	TOTAL CYCLES	AVG. CRACK LENGTH (IN)	DELTA CRACK LENGTH (IN)	LSQ FIT DA/DN (IN/CYC)	CORR. COEFF.	STD. ERR. OF EST.	AVG. DEL-K (KSI-SQRT)
5	68474	0.8499	0.0728	1.05E-06	0.997	0.000	4.63
6	78531	0.9565	0.1140	1.41E-06	0.985	0.016	5.46
4	38858	1.0687	0.0823	2.08E-06	0.998	0.007	6.00
4	22964	1.1588	0.1076	4.67E-06	0.998	0.202	7.41
3	12000	1.3481	0.1227	1.02E-05	0.999	0.799	9.39
3	4250	1.4326	0.0565	1.33E-05	1.000	0.752	10.34
5	2920	1.5230	0.0917	3.00E-05	0.993	2.764	13.29
3	1043	1.6357	0.0574	5.50E-05	1.000	2.720	15.85
3	345	1.8470	0.0637	1.84E-04	0.998	5.186	23.97

COMPACT TENSION AT H/W=0.486  
 AP-05  
 7075-T7651 L-T ORIENTATION  
 RT, SALT  
 SALT WATER  
 60 CPM  
 R= 0.3 B= 0.451 W= 2.545

GENERAL DYNAMICS  
 FORT WORTH DIVISION  
 AUG 12, 1982

NO. OF PTS.	TOTAL CYCLES	AVG. CRACK LENGTH (IN)	DELTA CRACK LENGTH (IN)	LSQ FIT DA/DN (IN/CYC)	CORR. COEFF.	STD. ERR. OF EST.	AVG. DEL-K (KSI-SQRI)
4	42000	0.8382	0.0458	1.05E-06	0.993	0.009	4.49
3	18000	0.9211	0.0325	1.93E-06	0.951	0.072	5.35
3	12000	1.1436	0.1899	1.54E-05	0.990	0.837	7.42
4	2244	1.2736	0.0879	4.06E-05	0.993	4.625	9.65
3	1065	1.3779	0.0643	6.03E-05	1.000	6.685	10.81
3	627	1.4463	0.0617	9.83E-05	1.000	17.253	12.64
	416	1.5575	0.0540	1.30E-04	1.000	26.474	14.77

COMPACT TENSION AT H/W=0.486  
 AP-06  
 7075-T7651 L-T ORIENTATION  
 RT, DRY

GENERAL DYNAMICS  
 FORT WORTH DIVISION  
 JUL 23, 1982

60 CPM  
 R= 0.3 B= 0.451 W= 2.549

NO. OF PTS.	TOTAL CYCLES	AVG. CRACK LENGTH (IN)	DELTA CRACK LENGTH (IN)	LSQ FIT DA/DN (IN/CYC)	CORR. COEFF.	STD. ERR. OF EST.	AVG. DEL-K (KSI-SQRI)
3	29201	0.9122	0.0419	1.43E-06	0.993	0.001	5.09
3	18855	1.0839	0.0588	3.20E-06	0.999	0.066	6.69
3	4500	1.1002	0.0225	4.90E-06	0.995	0.222	7.69
4	12267	1.1908	0.0975	7.79E-06	0.994	0.191	8.35
4	5554	1.2698	0.0584	1.05E-05	1.000	0.349	9.55
3	3966	1.3594	0.0544	1.38E-05	0.999	0.679	10.49
3	2807	1.4995	0.0563	2.00E-05	0.999	0.557	12.50
3	1102	1.6076	0.0601	5.44E-05	0.999	3.224	16.31

COMPACT TENSION AT H/W=0.486  
 AP-08  
 7075-T7651 L-T ORIENTATION  
 RT, SALT

GENERAL DYNAMICS  
 FORT WORTH DIVISION  
 AUG 9, 1982

180 CPM  
 R= 0.05 B= 0.4505 W= 2.549

NO. OF PTS.	TOTAL CYCLES	AVG. CRACK LENGTH (IN)	DELTA CRACK LENGTH (IN)	LSQ FIT DA/DN (IN/CYC)	CORR. COEFF.	STD. ERR. OF EST.	AVG. DEL-K (KSI-SQRI)
5	44434	0.8552	0.0491	1.11E-06	1.000	0.657	4.82
5	25209	0.9120	0.0455	1.80E-06	0.999	0.575	5.48
3	1814	1.3938	0.0562	3.10E-05	1.000	0.462	10.77
3	1474	1.4773	0.0591	4.00E-05	0.999	0.385	11.57
3	831	1.5520	0.0565	6.80E-05	1.000	0.912	14.50
3	411	1.7240	0.0543	1.32E-04	1.000	1.162	19.48
3	359	1.8039	0.0535	1.49E-04	1.000	1.250	22.90

COMPACT TENSION AT H/W=0.486  
 AP-09  
 7075-T7651 L-T ORIENTATION  
 RT, SALT

GENERAL DYNAMICS  
 FORT WORTH DIVISION  
 AUG 24, 1982

18 CPM  
 R= 0.3 B= 0.4505 W= 2.5495

NO. OF PTS.	TOTAL CYCLES	AVG. CRACK LENGTH (IN)	DELTA CRACK LENGTH (IN)	LSQ FIT DA/DN (IN/CYC)	CORR. COEFF.	STD. ERR. OF EST.	AVG. DEL-K (KSI-SQRI)
5	0	0.8425	0.0662	6.64E-07	0.512	0.001	4.39
3	30000	0.8174	0.0186	6.39E-07	0.989	0.000	4.17
4	50423	0.9319	0.1391	2.72E-06	0.975	0.025	5.45
2	12000	1.0132	0.0269	2.24E-06	1.000	0.000	6.28
3	15000	1.1242	0.1655	1.05E-05	0.967	0.433	7.34
2	6000	1.3162	0.2324	3.87E-05	1.000	0.000	9.37
2	2000	1.5114	0.1580	7.90E-05	1.000	0.000	12.44

COMPACT TENSION AT H/W=0.486  
AP-13  
7075-T7051 L-T ORIENTATION  
R.T., DRY

GENERAL DYNAMICS  
FORT WORTH DIVISION  
APR. 1, 1982

60 CPM  
R= 0.05 B= 0.4495 W= 2.5419

NO. OF PTS.	TOTAL CYCLES	AVG. CRACK LENGTH (IN)	DELTA CRACK LENGTH (IN)	LSQ FIT DA/DN (IN/CYC)	CORR. COEFF.	STD. ERR. OF EST.	AVG. DEL-K (KSI-SQRT)
4	140026	0.8685	0.0760	5.33E-07	0.987	0.000	4.17
4	9485	0.9572	0.0920	9.43E-06	0.992	1.04	10.44
4	3750	1.0495	0.0870	2.35E-05	0.999	7.768	15.1
5	2400	1.1506	0.1300	5.33E-05	1.000	29.739	27.7
4	1000	1.3025	0.1660	1.69E-04	0.998	485.666	26.45

#### COEFFICIENTS

C= 3.9860E-09 UIN/CYC

N= 3.328830

R SQUARE = 0.988823232

COMPACT TENSION AT H/W=0.486  
AP-14  
7075-T7051 L-T ORIENTATION  
RT, DRY

GENERAL DYNAMICS  
FORT WORTH DIVISION  
MAR 24, 1982

SILICA GEL

360 ~~120~~ CPM

R= 0.05 B= 0.4525 W= 2.5466

NO. OF PTS.	TOTAL CYCLES	AVG. CRACK LENGTH (IN)	DELTA CRACK LENGTH (IN)	LSQ FIT DA/DN (IN/CYC)	CORR. COEFF.	STD. ERR. OF EST.	AVG. DEL-K (KSI-SQRT)
18	34000	0.8690	0.0272	7.44E-07	0.964	0.004	5.54
11	15000	0.9143	0.0494	3.02E-06	0.989	0.009	7.44
9	3000	0.9583	0.0477	5.75E-06	0.992	0.020	9.31
8	4550	1.0017	0.0453	1.02E-05	0.996	0.046	11.18
13	3600	1.0259	0.0223	1.55E-05	0.852	0.132	13.91
14	2600	1.1948	0.1145	4.55E-05	0.999	1.007	18.76
9	1000	1.3006	0.1258	9.71E-05	0.917	2.019	20.87
19	1440	1.4549	0.2271	1.63E-04	1.000	16.367	25.34
10	180	1.6089	0.1232	7.10E-04	0.970	82.750	27.59

COMPACT TENSION AT H/W=0.486  
 AP15  
 7075-T7651 L-T ORIENTATION  
 RT, DRY

GENERAL DYNAMICS  
 FORT WORTH DIVISION  
 AUG 24, 1982

6 CPM  
 R= 0.3 B= 0.449 W= 2.5502

NO. OF PTS.	TOTAL CYCLES	AVG. CRACK LENGTH (IN)	DELTA CRACK LENGTH (IN)	LSQ FIT DA/DN (IN/CYC)	CORR. COEFF.	STD. ERR. OF EST.	AVG. DEL-K (KSI-SQRI)
5	41463	0.8542	0.0635	1.52E-06	0.995	0.000	4.75
4	39422	0.9558	0.0997	2.51E-06	0.991	0.012	5.74
5	31859	1.0555	0.0994	3.11E-06	1.000	0.008	6.25
4	18872	1.1526	0.1327	7.14E-06	0.997	0.231	5.61
3	8225	1.2837	0.0600	7.28E-06	1.000	0.219	8.49
3	5970	1.3232	0.0670	1.12E-05	0.991	0.710	9.91
3	4500	1.4171	0.1093	2.38E-05	0.995	1.060	12.20
2	1500	1.5002	0.0559	3.72E-05	1.000	0.000	14.21
2	428	1.5891	0.0326	7.61E-05	1.000	0.000	16.19
2	291	1.6494	0.0291	1.00E-04	1.000	0.000	17.92
3	328	1.7342	0.0716	2.17E-04	0.991	2.489	20.99
2	93	1.7880	0.0331	3.55E-04	1.000	0.000	23.34

COMPACT TENSION AT H/W=0.486  
 AP-16  
 7075-T7651 L-T ORIENTATION  
 RT, SALT

GENERAL DYNAMICS  
 FORT WORTH DIVISION  
 AUG 25, 1982

360 CPM  
 R= 0.3 B= 0.4491 W= 2.546

NO. OF PTS.	TOTAL CYCLES	AVG. CRACK LENGTH (IN)	DELTA CRACK LENGTH (IN)	LSQ FIT DA/DN (IN/CYC)	CORR. COEFF.	STD. ERR. OF EST.	AVG. DEL-K (KSI-SQRI)
4	38121	0.8822	0.0714	1.87E-06	0.998	0.000	4.65
2	8000	0.9458	0.0388	4.86E-06	1.000	0.000	5.64
2	2500	0.9748	0.0217	8.69E-06	1.000	0.000	6.37
5	6072	1.0560	0.1164	1.91E-05	1.000	0.329	7.26
4	3449	1.1591	0.0942	2.72E-05	0.998	1.257	8.40
3	1514	1.2833	0.0544	3.59E-05	1.000	1.358	9.16
4	1240	1.4675	0.0847	6.80E-05	0.999	6.739	12.64
3	614	1.5898	0.0573	9.32E-05	1.000	7.003	15.12
3	432	1.7004	0.0520	1.20E-04	1.000	9.720	18.30

COMPACT TENSION AT H/W=0.486  
AP-19  
7075-T7651 L-T ORIENTATION  
RT, SALT

GENERAL DYNAMICS  
FORT WORTH DIVISION  
AUG 27, 1982

360 CPM  
R= 0.2 B= 0.45 W= 2.549

NO. OF PTS.	TOTAL CYCLES	AVG. CRACK LENGTH (IN)	DELTA CRACK LENGTH (IN)	LSQ FIT DA/DN (IN/CYC)	CORR. COEFF.	STD. ERR. OF EST.	AVG. DEL-K (KSI-SQRI)
2	12000	0.8625	0.0369	3.08E-06	1.000	0.000	5.20
2	4000	0.8877	0.0179	4.48E-06	1.000	0.000	5.52
3	10075	0.9817	0.0627	6.22E-06	0.995	0.002	5.98
6	8406	1.0491	0.1398	1.67E-05	0.997	0.056	7.03
6	3823	1.1509	0.1258	3.28E-05	0.998	0.252	8.73
2	620	1.3107	0.0280	4.51E-05	1.000	0.000	10.18
3	1200	1.3621	0.0859	7.12E-05	1.000	2.080	12.34
3	636	1.4801	0.0558	8.77E-05	1.000	2.495	14.26
4	663	1.5475	0.0798	1.20E-04	0.998	2.940	17.07

COMPACT TENSION AT H/W=0.486  
AP-20  
7075-T7651 L-T ORIENTATION  
RT, WET  
60 CPM  
R= 0.05 B= 0.4495 W= 2.5575

GENERAL DYNAMICS  
FORT WORTH DIVISION  
MAR 12, 1982

NO. OF PTS.	TOTAL CYCLES	AVG. CRACK LENGTH (IN)	DELTA CRACK LENGTH (IN)	LSQ FIT DA/DN (IN/CYC)	CORR. COEFF.	STD. ERR. OF EST.	AVG. DEL-K (KSI-SQRI)
10	45000	0.8923	0.1110	2.40E-06	0.941	0.000	6.13
4	15000	1.0581	0.1472	9.94E-06	0.984	0.062	7.43
3	6000	1.2173	0.1416	2.36E-05	0.998	0.382	8.59
5	2000	1.3182	0.0796	3.98E-05	0.999	0.618	10.39

COMPACT TENSION AT H/W=0.486  
 AP21  
 7075-T7651 L-T ORIENTATION  
 RT, SALT  
 3.5% SOLUTION  
 360 CPM  
 R= 0.4 B= 0.451 W= 2.5505

GENERAL DYNAMICS  
 FORT WORTH DIVISION  
 AUG 25, 1982

NO. OF PTS.	TOTAL CYCLES	AVG. CRACK LENGTH (IN)	DELTA CRACK LENGTH (IN)	LSQ FIT DA/DN (IN/CYC)	CORR. COEFF.	STD. ERR. OF EST.	AVG. DEL-K (KSI-SQRI)
2	10800	0.8501	0.0233	2.15E-06	1.000	0.000	4.25
3	22810	0.9120	0.0491	2.18E-06	0.997	0.008	4.67
3	9914	0.9665	0.0624	6.39E-06	0.990	0.070	5.39
5	8343	1.0546	0.1133	1.36E-05	0.998	0.109	6.36
6	5433	1.1627	0.1304	2.35E-05	0.999	0.387	7.57
5	3643	1.3087	0.1100	3.01E-05	0.999	0.416	8.71
4	1356	1.3962	0.0667	4.83E-05	0.997	2.023	10.34
3	998	1.4862	0.0523	5.25E-05	0.999	4.179	11.56
3	803	1.5689	0.0561	6.98E-05	1.000	5.656	13.03
3	662	1.6512	0.0578	8.72E-05	1.000	7.233	14.94

COMPACT TENSION AT H/W=0.486  
 AP-22  
 7075-T7651 L-T ORIENTATION  
 RT, WET  
~~360 CPM~~  
 R= 0.65 B= 0.45 W= 2.543

GENERAL DYNAMICS  
 FORT WORTH DIVISION  
 MAR 22, 1982

NO. OF PTS.	TOTAL CYCLES	AVG. CRACK LENGTH (IN)	DELTA CRACK LENGTH (IN)	LSQ FIT DA/DN (IN/CYC)	CORR. COEFF.	STD. ERR. OF EST.	AVG. DEL-K (KSI-SQRI)
10	9000	0.8386	0.0217	3.12E-06	0.946	0.638	5.99
7	3000	0.9017	0.0397	1.55E-05	0.826	0.557	10.03
9	2880	1.0049	0.1046	3.79E-05	0.993	0.416	12.18
14	1625	1.2180	0.1743	1.12E-04	0.999	0.203	20.38
8	875	1.3706	0.1222	1.36E-04	0.989	0.040	22.61
9	640	1.5298	0.1631	2.45E-04	0.995	0.000	26.17
10	1120	1.7146	0.2091	1.91E-04	1.000	0.013	26.20

COMPACT TENSION AT H/W=0.486  
 AP-23  
 7075-T7651 L-T ORIENTATION  
 RT, WET  
 3.5%NaCl, 3.5%PH-H2SO4  
 360 CPM  
 R= 0.05 B= 0.45 W= 2.5529

GENERAL DYNAMICS  
 FORT WORTH DIVISION  
 SEP 9, 1982

NO. OF PTS.	TOTAL CYCLES	AVG. CRACK LENGTH (IN)	DELTA CRACK LENGTH (IN)	LSQ FIT DA/DN (IN/CYC)	CORR. COEFF.	STD. ERR. OF EST.	AVG. DEL-K (KSI-SQRT)
3	23988	0.8458	0.0311	1.27E-06	0.981	0.000	4.95
4	14000	0.9259	0.0521	3.70E-06	0.999	0.015	6.28
5	10698	1.0480	0.1263	1.19E-05	0.994	0.096	8.04
4	2980	1.2110	0.0838	2.94E-05	0.995	0.640	10.78
4	1291	1.4478	0.0820	6.31E-05	1.000	2.715	15.63
3	519	1.5214	0.0627	1.21E-04	1.000	16.264	19.07
3	237	1.7513	0.0430	1.82E-04	1.000	30.912	28.34

COMPACT TENSION AT H/W=0.486  
 AP-24  
 7075-T7651 L-T ORIENTATION  
 RT, WET  
 ARTIFICIAL SEAWATER  
 360 CPM  
 R= 0.05 B= 0.45 W= 2.5495

GENERAL DYNAMICS  
 FORT WORTH DIVIS  
 SEP 8, 1982

NO. OF PTS.	TOTAL CYCLES	AVG. CRACK LENGTH (IN)	DELTA CRACK LENGTH (IN)	LSQ FIT DA/DN (IN/CYC)	CORR. COEFF.	STD. ERR. OF EST.	AVG. DEL-K (KSI-SQRT)
2	6000	0.8315	0.0201	3.36E-06	1.000	0.000	5.91
2	6000	0.9147	0.0335	5.58E-06	1.000	0.000	7.09
4	3500	1.0047	0.0414	1.16E-05	0.998	0.146	8.76
5	4459	1.1601	0.0965	2.24E-05	0.996	0.357	10.64
4	2351	1.3105	0.0777	3.35E-05	0.999	0.615	12.32
4	1301	1.4399	0.0837	6.45E-05	0.998	2.897	15.07
3	1053	1.5310	0.0772	7.24E-05	0.988	3.963	18.46
2	111	1.7417	0.0361	3.25E-04	1.000	0.000	26.46
2	75	1.8054	0.0380	5.08E-04	1.000	0.000	30.08

COMPACT TENSION AT H/W=0.486  
 AP-25  
 7075-T765/ L-T ORIENTATION  
 RT, WET  
 DISTILLED WATER  
 360 CPM  
 R= 0.05 B= 0.4495 W= 2.5407

GENERAL DYNAMICS  
 FORT WORTH DIVISION  
 SEP 8, 1982

NO. OF PTS.	TOTAL CYCLES	AVG. CRACK LENGTH (IN)	DELTA CRACK LENGTH (IN)	LSO FIT DA/DN (IN/CYC)	CORR. COEFF.	STD. ERR. OF EST.	AVG. DEL-T (MSI-SOP)
5	48142	0.7953	0.0036	1.39E-07	0.544	0.001	5.07
3	9000	0.9602	0.0202	2.24E-06	1.000	0.085	7.27
3	6424	0.9623	0.0342	5.26E-06	0.995	0.101	8.43
6	15417	1.1051	0.1176	7.57E-06	0.999	0.244	10.43
5	4517	1.3482	0.0857	1.89E-05	1.000	1.163	14.30
3	2198	1.4528	0.0576	2.62E-05	0.999	1.499	16.20
3	1324	1.5673	0.0690	5.24E-05	0.987	4.375	20.55
8	414	1.7525	0.0596	1.44E-04	0.999	11.464	28.59

FATIGUE TEST-CONSTANT K-SAMPLE TYPE:WOL-MATERIAL:AL7075-T7651

SPEC. NO.:AL-28 DATA PTS=41 WAVE FORM:TRIANGLE WAVE WITH HOLD TIME

B=.45 IN W=2.55 IN E=10.3E6 TEMP=70 DEG F

K RANGE=5 TO 20 (KSI SQR(IN)) LOAD RATIO=.05

SLOPE =0.5 SEC HOLD TIME=0 SEC

ENVIRONMENT=3.5% SALT WATER PH(6.2 TO 8)

OBS NO.	KMAX (KSI SQR(IN))	LOAD (LBS)	CRACK LENGTH (INCH)	CYCLES	DA/DN (IN/CYCLE)
1	3.80131	486.335	.877	40	.0224715
2	5.03952	489.288	.909	10127.5	1.00679E-06
3	5.01262	482.391	.92	31534.5	4.95913E-07
4	4.99957	476.86	.93	62335.5	3.34307E-07
5	5.02265	474.919	.94	76356	7.13670E-07
6	5.00108	468.579	.951	106041	3.80934E-07
7	5.00608	464.435	.963	128974	5.10137E-07
8	7.97992	733.067	.974	133083	2.73083E-06
9	8.00356	728.446	.984	134439	7.61063E-06
10	7.97941	719.858	.995	136035	6.36403E-06
11	7.9856	713.824	1.006	137661	6.83272E-06
12	7.98338	706.833	1.017	139091	7.68533E-06
13	8.00189	702.034	1.027	140828	5.80310E-06
14	8.00942	696.524	1.037	142196	7.47803E-06
15	7.96705	686.627	1.048	144029	5.72289E-06
16	8.00294	682.884	1.06	145527	8.26436E-06
17	8.00746	676.513	1.07	147068	6.73591E-06
18	9.98262	835.297	1.082	148392	8.79151E-06
19	9.99054	826.409	1.096	149309	1.58560E-05
20	10.009	818.356	1.108	150090	1.51985E-05
21	9.99865	809.607	1.118	150906	1.23775E-05
22	9.97275	800.185	1.129	151451	1.91376E-05
23	9.98609	793.575	1.14	151932	2.32225E-05
24	9.99439	786.559	1.151	152684	1.39760E-05
25	14.9453	1164.65	1.162	153269	1.94872E-05
26	14.9628	1154.52	1.172	153543	3.82118E-05
27	14.942	1141.78	1.183	153750	5.23191E-05
28	14.9348	1130.36	1.193	153957	4.84537E-05
29	14.9499	1119.81	1.206	154232	4.52731E-05
30	14.9591	1108.46	1.216	154507	3.90179E-05
31	14.9409	1095.96	1.227	154714	5.22707E-05
32	14.9803	1088.01	1.237	154923	4.81817E-05
33	14.957	1075.7	1.248	155097	6.01151E-05
34	14.9633	1064.81	1.259	155322	4.17094E-05
35	19.9394	1403.85	1.27	155546	5.95402E-05
36	19.9831	1391.82	1.281	155652	1.08396E-04
37	19.9788	1374.38	1.294	155792	9.48565E-05
38	19.9565	1354.49	1.308	155931	9.50364E-05
39	19.9781	1337.81	1.321	156071	9.20713E-05
40	19.9326	1317.66	1.332	156210	8.42449E-05
41	19.9504	1301.14	1.346	156350	9.74996E-05

NADC-83126-60 Vol. I

FATIGUE TEST-CONSTANT K-SAMPLE TYPE:WOL-MATERIAL:AL7075-T7651

SPEC. NO.:AL-29 DATA PTS=26 WAVE FORM:TRIANGLE WAVE WITH HOLD TIME

B=.45 IN W=2.55 IN E=10.3E6 TEMP=70 DEG F

K RANGE=8 TO 20 (KSI SQR(IN)) LOAD RATIO=.05

SLOPE =1.67 SEC HOLD TIME=0 SEC

ENVIRONMENT=3.5% SALT WATER PH(6.2 TO 8)

OBS NO. #	KMAX (KSI SQR(IN))	LOAD (LBS)	CRACK LENGTH (INCH)	CYCLES	DA/DN (IN/CYCLE)
1	20.0133	1033.45	1.522	36	1.04226E-04
2	20.0311	1033.45	1.533	134.5	1.13807E-04
3	19.9539	1012.76	1.544	233.5	1.13738E-04
4	19.9273	995.124	1.555	332.5	1.07273E-04
5	19.9818	981.588	1.566	431.5	1.12626E-04
6	20.0217	964.514	1.58	562	1.09272E-04
7	19.9121	938.761	1.593	694	1.00075E-04
8	19.9226	921.36	1.604	793	1.09091E-04
9	15.1234	687.646	1.614	826	3.03333E-04
10	14.9256	666.987	1.625	1454.5	1.74065E-05
11	14.9243	654.829	1.636	1717	4.12573E-05
12	14.9257	643.054	1.647	1948	4.54977E-05
13	14.9086	629.783	1.659	2209	4.66670E-05
14	14.9176	616.994	1.67	2471.5	4.47618E-05
15	14.9337	603.88	1.684	2735.5	5.07574E-05
16	9.92898	392.772	1.695	6233.5	3.05602E-06
17	9.91914	384.897	1.705	7522	7.84635E-06
18	9.95039	378.874	1.715	8842.5	7.61838E-06
19	10.0092	373.629	1.726	9735	1.21232E-05
20	9.92393	363.078	1.736	10594	1.16997E-05
21	9.93573	356.157	1.746	11882.5	8.47492E-06
22	9.95563	349.5	1.757	13072	8.60872E-06
23	9.91943	341.239	1.767	14162.5	9.25263E-06
24	7.95227	268.014	1.777	26175	8.52442E-07
25	7.97848	263.384	1.787	32842.5	1.51181E-06
26	7.97043	257.665	1.797	39741	1.48728E-06

NADC-83126-60 Vol. I

FATIGUE TEST-CONSTANT K-SAMPLE TYPE:WOL-MATERIAL:AL7075-T7651

SPEC. NO.:AL-29 DATA PTS=55 WAVE FORM:TRIANGLE WAVE WITH HOLD TIME

B=.45 IN W=2.55 IN E=10.3E6 TEMP=70 DEG F

K RANGE=8 TO 20 (KSI SQR(IN)) LOAD RATIO=.05

SLOPE =.5 SEC HOLD TIME RANGE=1 TO 2.33 SEC

ENVIRONMENT=3.5% SALT WATER PH(6.2 TO 8)

ORF NO. #	KMAX (KSI SQR(IN))	LOAD (LBS)	HOLD TIME (SEC)	CRACK LENGTH (INCHS)	CYCLES	DA/DN (IN/CYCLE)
1	7.93205	784.152	1	.991	37.5	1.02374E-06
2	7.98522	780.817	1	.901	2845.5	3.60222E-06
3	8.00403	775.817	1	.911	4366.5	6.93557E-06
4	8.00017	768.037	1	.923	6514.5	5.57728E-06
5	8.00365	760.338	1	.936	8332.5	6.94332E-06
6	7.97239	749.943	1	.946	10249.5	5.38447E-06
7	8.02825	748.579	1	.956	11902.5	6.20386E-06
8	7.97784	736.902	2.33	.968	13654.5	6.66211E-06
9	7.98208	729.687	2.33	.98	14877	1.01530E-05
10	8.02785	726.008	2.33	.993	17386.5	5.00536E-06
11	8.02449	718.466	2.33	1.004	19104	6.19621E-06
12	7.96878	707.045	2.33	1.014	21085.5	5.19305E-06
13	7.99609	703.136	2.33	1.024	22209	9.25673E-06
14	7.98863	695.909	2.33	1.036	23860.5	6.81806E-06
15	9.97547	860.925	2.33	1.046	25314	7.01067E-06
16	9.99178	854.2	2.33	1.057	26041.5	1.59037E-05
17	9.97773	844.498	2.33	1.069	26901	1.32402E-05
18	9.98092	835.87	2.33	1.082	27529.5	2.04137E-05
19	9.96609	825.633	2.33	1.093	28323	1.49465E-05
20	9.96415	817.158	2.33	1.105	29182.5	1.29610E-05
21	9.99478	811.444	2.33	1.116	30009	1.41440E-05
22	10.0058	804.019	1	1.128	30505.5	2.31823E-05
23	9.98435	793.732	1	1.14	31531.5	1.22515E-05
24	9.96304	783.802	1	1.151	32062.5	2.02824E-05
25	9.97574	777.339	1	1.162	32857.5	1.31447E-05
26	10.0249	773.787	1	1.172	33454.5	1.76214E-05
27	9.99574	763.525	1	1.184	34315.5	1.43786E-05
28	9.9764	754.231	1	1.195	35110.5	1.26792E-05
29	9.96651	746.348	1	1.205	35674.5	1.86172E-05
30	14.9672	1109.11	1	1.217	36205.5	2.27117E-05
31	14.994	1099.19	1	1.228	36472.5	4.06370E-05
32	14.9494	1084.3	1	1.24	36739.5	4.34828E-05
33	14.9731	1073.98	1	1.251	36940.5	5.79108E-05
34	14.9598	1061.23	1	1.262	37207.5	4.17978E-05
35	14.9793	1051.55	1	1.273	37408.5	5.06966E-05
36	14.9721	1039.88	1	1.284	37642.5	4.85039E-05
37	15.0014	1029.63	2.33	1.296	37876.5	5.24363E-05
38	14.9577	1014.81	2.33	1.307	38109	4.52042E-05
39	14.9445	1003.22	2.33	1.317	38341.5	4.32686E-05
40	14.9361	991.681	2.33	1.328	38574	4.73981E-05
41	14.9522	980.392	2.33	1.34	38806.5	5.43225E-05
42	14.9439	966.567	2.33	1.353	39105	4.25795E-05
43	14.9596	954.849	2.33	1.365	39370.5	4.32014E-05

NADC-83126-60 Vol. I

44			2.33	1.376	39537	6.7501E-01
45	19.9176	1238.52	2.33	1.388	39670.5	9.4007E-05
46	20.0006	1226.2	2.33	1.4	39771	1.19105E-04
47	19.9296	1203.58	2.33	1.414	39937.5	8.19823E-05
48	19.9249	1183.72	2.33	1.428	40071	1.02397E-04
49	19.9208	1164.96	2.33	1.44	40204.5	9.03365E-05
50	19.9724	1151.42	1	1.45	40305	1.07265E-04
51	19.9362	1130.7	1	1.465	40440	1.10148E-04
52	19.974	1112.57	1	1.478	40575	9.51855E-05
53	19.9287	1092.57	1	1.489	40710	8.14809E-05
54	19.9515	1076.35	1	1.502	40812	1.24804E-04
55	19.9221	1056.64	1	1.514	40947	8.77045E-05

NADC-83126-60 Vol. I

THIS PAGE INTENTIONALLY LEFT BLANK

APPENDIX B

FATIGUE CRACK PROPAGATION RESULTS  
FOR  $\beta$ -ANNEALED Ti-6Al-4V ALLOY

## FATIGUE TEST-CONSTANT LOAD-SAMPLE TYPE:CT-MATERIAL:TI-6AL-4V

SPEC. NO.:TI-4 DATA PTS.=101

B=.5 IN W=2.5 IN E=1.6E7

CONST LOAD =2165.25 (LBS)

LOAD RATIO=.05

FREQ=5 HZ

TEMP=70 DEG F

ENVIRONMENT=VACUUM

OBS NO. #	KMAX (KSI SQR(IN))	FREQ (HZ)	CRACK LENGTH (INCHS)	CYCLES	DA/DN (IN/CYCLE)
1	12.0641	5	.735	753578	9.75056E-07
2	12.1825	5	.744	794103	2.33066E-07
3	12.3024	5	.754	825711	2.98721E-07
4	12.4225	5	.763	844506	4.96249E-07
5	12.5428	5	.772	862050	5.31522E-07
6	12.664	5	.782	880313	5.10430E-07
7	12.7862	5	.791	894884	6.39628E-07
8	12.9093	5	.8	904577	9.61312E-07
9	13.0343	5	.81	916443	7.94536E-07
10	13.161	5	.819	923369	1.36096E-06
11	13.2897	5	.829	929085	1.66813E-06
12	13.4204	5	.838	934863	1.64988E-06
13	13.5522	5	.848	944594	9.79040E-07
14	13.6853	5	.857	953674	1.04924E-06
15	13.8189	5	.867	959411	1.64006E-06
16	13.9563	5	.877	966295	1.43187E-06
17	14.095	5	.886	972647	1.48001E-06
18	14.2319	5	.895	976128	2.69923E-06
19	14.372	5	.905	980327	2.29054E-06
20	14.5126	5	.914	983973	2.54389E-06
21	14.6531	5	.924	987188	2.91818E-06
22	14.7952	5	.933	991633	2.08459E-06
23	14.9423	5	.943	995361	2.63519E-06
24	15.0912	5	.952	997960	3.56137E-06
25	15.2373	5	.961	1.00029E+06	3.4998E-06
26	15.387	5	.971	1.00222E+06	4.99673E-06
27	15.5422	5	.98	1.00373E+06	5.41721E-06
28	15.7002	5	.99	1.00617E+06	3.92294E-06
29	15.8565	5	.999	1.00789E+06	5.36452E-06
30	16.0119	5	1.008	1.01038E+06	3.70320E-06
31	16.1693	5	1.018	1.01216E+06	5.17978E-06
32	16.3356	5	1.028	1.01452E+06	4.23304E-06
33	16.5081	5	1.037	1.01640E+06	5.13830E-06
34	16.676	5	1.046	1.01779E+06	6.61148E-06
35	16.8554	5	1.057	1.01939E+06	6.65627E-06
36	17.0396	5	1.066	1.02149E+06	4.47620E-06
37	17.2161	5	1.076	1.02305E+06	6.10260E-06
38	17.3929	5	1.085	1.02432E+06	7.21254E-06
39	17.5702	5	1.094	1.02546E+06	8.14043E-06
40	17.7555	5	1.104	1.02663E+06	8.29911E-06
41	17.9437	5	1.113	1.02742E+06	1.17089E-05
42	18.1302	5	1.123	1.02828E+06	1.07557E-05
43	18.3276	5	1.133	1.02895E+06	1.49553E-05

44	18.5294	5	1.142	1.02945E+06	1.33572E-05
45	18.7249	5	1.151	1.03052E+06	1.04712E-05
46	18.9211	5	1.16	1.03200E+06	6.14862E-06
47	19.1265	5	1.17	1.03300E+06	9.66001E-06
48	19.3403	5	1.179	1.03373E+06	1.30547E-05
49	19.5514	5	1.188	1.03434E+06	1.48853E-05
50	19.7673	5	1.198	1.03506E+06	1.33610E-05
51	19.9882	5	1.207	1.03555E+06	1.87144E-05
52	20.2088	5	1.217	1.03603E+06	1.93124E-05
53	20.4319	5	1.226	1.03646E+06	2.10233E-05
54	20.6589	5	1.235	1.03693E+06	1.96809E-05
55	20.8911	5	1.244	1.03746E+06	1.72453E-05
56	21.1246	5	1.253	1.03807E+06	1.47704E-05
57	21.3637	5	1.262	1.03844E+06	2.49189E-05
58	21.6174	5	1.272	1.03896E+06	1.87693E-05
59	21.8758	5	1.281	1.03939E+06	2.13953E-05
60	22.1284	5	1.29	1.03978E+06	2.30001E-05
61	22.4013	5	1.3	1.04014E+06	2.85278E-05
62	22.6796	5	1.309	1.04037E+06	3.89130E-05
63	22.9471	5	1.319	1.04053E+06	5.72503E-05
64	23.2329	5	1.328	1.04079E+06	3.76921E-05
65	23.5396	5	1.338	1.04105E+06	3.88847E-05
66	23.8425	5	1.348	1.04127E+06	4.14545E-05
67	24.1445	5	1.357	1.04176E+06	1.96734E-05
68	24.4546	5	1.366	1.04201E+06	3.68400E-05
69	24.7802	5	1.377	1.04239E+06	2.67371E-05
70	25.1579	5	1.388	1.04272E+06	3.56364E-05
71	25.5295	5	1.398	1.04292E+06	4.63498E-05
72	25.8842	5	1.408	1.04302E+06	1.03300E-04
73	26.2389	5	1.417	1.04332E+06	2.93668E-05
74	26.5829	5	1.426	1.04358E+06	3.58847E-05
75	26.9341	5	1.435	1.04383E+06	3.51601E-05
76	27.2864	5	1.444	1.04409E+06	3.45381E-05
77	27.6811	5	1.454	1.04427E+06	5.81668E-05
78	28.085	5	1.463	1.04439E+06	7.45833E-05
79	28.4823	5	1.473	1.04451E+06	8.07504E-05
80	28.8934	5	1.482	1.04457E+06	1.52332E-04
81	29.3211	5	1.492	1.04477E+06	4.98503E-05
82	29.7492	5	1.501	1.04489E+06	7.23332E-05
83	30.2074	5	1.512	1.04499E+06	1.07800E-04
84	30.7804	5	1.524	1.04515E+06	8.04380E-05
85	31.371	5	1.535	1.04529E+06	7.67137E-05
86	31.8915	5	1.545	1.04543E+06	6.75006E-05
87	32.3892	5	1.554	1.04559E+06	5.83120E-05
88	32.928	5	1.564	1.04569E+06	1.04600E-04
89	33.5256	5	1.575	1.04583E+06	7.75712E-05
90	34.0976	5	1.584	1.04595E+06	7.46667E-05
91	34.6163	5	1.593	1.04605E+06	8.53002E-05
92	35.1889	5	1.603	1.04612E+06	1.46714E-04
93	35.7963	5	1.612	1.04618E+06	1.52000E-04
94	36.4641	5	1.624	1.04626E+06	1.44625E-04
95	37.2179	5	1.635	1.04634E+06	1.37876E-04
96	37.9529	5	1.645	1.04642E+06	1.28625E-04
97	38.7588	5	1.657	1.04650E+06	1.53874E-04
98	39.5725	5	1.667	1.04655E+06	1.94402E-04
99	40.3215	5	1.677	1.04661E+06	1.65000E-04
100	41.056	5	1.686	1.04667E+06	1.45833E-04
101	41.7693	5	1.695	1.04671E+06	2.21249E-04

FATIGUE TEST-CONSTANT LOAD-SAMPLE TYPE:CT-MATERIAL:TI-6AL-4V

SPEC. NO.:TI-5 DATA PTS.=85

B=.5 IN W=2.5 IN E=1.6E7

CONST LOAD =1500 (LBS) LOAD RATIO=.05

FREQ RANG =10 HZ TEMP=70 DEG F

ENVIRONMENT=3.5% SALT WATER PH(6.2 TO 8)

OBS NO. #	KMAX (KSI SQR(IN))	FREQ (HZ)	CRACK LENGTH (INCHS)	CYCLES	DA/DN (IN/CYCLE)
1	11.867	10	.854	1102.5	7.74448E-04
2	11.9948	10	.864	12437.5	9.20599E-07
3	12.122	10	.875	25293.5	7.98696E-07
4	12.2535	10	.885	34671	1.12012E-06
5	12.385	10	.895	43061.5	1.23617E-06
6	12.5282	10	.907	53103.5	1.11093E-06
7	12.666	10	.917	61073.5	1.32911E-06
8	12.8132	10	.928	70596.5	1.17306E-06
9	12.9625	10	.94	82093.5	9.71731E-07
10	13.1109	10	.95	91319.5	1.18654E-06
11	13.2562	10	.961	98758.5	1.42062E-06
12	13.4078	10	.972	104952	1.75539E-06
13	13.5799	10	.984	113042	1.50247E-06
14	13.7376	10	.995	120174	1.53645E-06
15	13.8104	10	1	126965	7.36277E-07
16	14.0469	10	1.016	133598	2.41217E-06
17	14.2126	10	1.027	138633	2.18471E-06
18	14.3657	10	1.037	143157	2.21043E-06
19	14.5212	10	1.047	148438	1.89358E-06
20	14.6791	10	1.057	153711	1.89645E-06
21	14.8556	10	1.068	158673	2.21686E-06
22	15.0189	10	1.078	163069	2.27479E-06
23	15.2015	10	1.089	167256	2.62719E-06
24	15.3704	10	1.099	171327	2.45640E-06
25	15.5596	10	1.11	175512	2.62842E-06
26	15.7346	10	1.12	179848	2.30627E-06
27	15.9127	10	1.13	183804	2.52783E-06
28	16.1122	10	1.141	187306	3.14104E-06
29	16.3157	10	1.152	191416	2.67641E-06
30	16.5042	10	1.162	194732	3.01568E-06
31	16.7156	10	1.173	198230	3.14466E-06
32	16.9116	10	1.183	201203	3.36360E-06
33	17.1113	10	1.193	203682	4.03388E-06
34	17.3148	10	1.203	205738	4.86381E-06
35	17.5433	10	1.214	207989	4.88673E-06
36	17.7768	10	1.225	210086	5.24555E-06
37	17.9935	10	1.235	212033	5.13610E-06
38	18.2146	10	1.245	213487	6.87757E-06
39	18.4402	10	1.255	214754	7.89275E-06
40	18.6938	10	1.266	216097	8.19056E-06
41	18.9295	10	1.276	217210	8.98472E-06
42	19.1702	10	1.286	218133	1.08342E-05
43	19.4161	10	1.296	219055	1.08460E-05
44	19.6673	10	1.306	219863	1.23764E-05
45	19.9501	10	1.317	220676	1.35300E-05
46	20.2398	10	1.328	221369	1.58731E-05
47	20.5367	10	1.339	222175	1.36477E-05

NADC-83126-60 Vol. I

48	20.8131	10	1.349	222872	1.43472E-05
49	21.1532	10	1.361	223562	1.73913E-05
50	21.444	10	1.371	224183	1.61030E-05
51	21.802	10	1.383	224727	2.20588E-05
52	22.1393	10	1.394	225349	1.76849E-05
53	22.4536	10	1.404	225817	2.13675E-05
54	22.7757	10	1.414	226284	2.14133E-05
55	23.1393	10	1.425	226674	2.82052E-05
56	23.4785	10	1.435	227138	2.15517E-05
57	23.8262	10	1.445	227492	2.82486E-05
58	24.2191	10	1.456	227847	3.09860E-05
59	24.5859	10	1.466	228198	2.84900E-05
60	25.0005	10	1.477	228553	3.09860E-05
61	25.4665	10	1.489	228946	3.05343E-05
62	25.8664	10	1.499	229263	3.15457E-05
63	26.3187	10	1.51	229614	3.13391E-05
64	26.7846	10	1.521	229929	3.49204E-05
65	27.2647	10	1.532	230209	3.92858E-05
66	27.8054	10	1.544	230488	4.30106E-05
67	28.3172	10	1.555	230767	3.94267E-05
68	28.8939	10	1.567	231009	4.95866E-05
69	29.3899	10	1.577	231249	4.16666E-05
70	29.9523	10	1.588	231491	4.54547E-05
71	30.5331	10	1.599	231695	5.39218E-05
72	31.1886	10	1.611	231937	4.95866E-05
73	31.7531	10	1.621	232140	4.92610E-05
74	32.3941	10	1.632	232345	5.36587E-05
75	33.0571	10	1.643	232547	5.44550E-05
76	33.6797	10	1.653	232714	5.98802E-05
77	34.6511	10	1.668	232918	7.35299E-05
78	35.5312	10	1.681	233085	7.78444E-05
79	36.2339	10	1.691	233211	7.93650E-05
80	37.1079	10	1.703	233378	7.18561E-05
81	37.8633	10	1.713	233505	7.87401E-05
82	38.8039	10	1.725	233632	9.44879E-05
83	39.7835	10	1.737	233759	9.44889E-05
84	40.8916	10	1.75	233887	1.01563E-04
85	41.9602	10	1.762	234013	9.52378E-05

## FATIGUE TEST-CONSTANT LOAD-SAMPLE TYPE:CT-MATERIAL:TI-6AL-4V

SPEC. NO.:TI-6 DATA PTS.=80

B=.5 IN W=2.5 IN E=1.6E7

CONST LOAD =1500 (LBS) LOAD RATIO=.05

FREQ RANG =3 HZ TEMP=70 DEG F

ENVIRONMENT=3.5% SALT WATER PH(6.2 TO 8)

OBS NO. #	KMAX (KSI SQR(IN))	FREQ (HZ)	CRACK LENGTH (INCHS)	CYCLES	DA/DN (IN/CYCLE)
1	12.61	3	.913	150011	6.08535E-06
2	12.7422	3	.923	163315	7.58042E-07
3	12.8771	3	.933	181566	5.57173E-07
4	13.0228	3	.944	197681	6.72602E-07
5	13.1743	3	.955	216178	6.00909E-07
6	13.3158	3	.965	231165	6.82926E-07
7	13.4671	3	.976	242910	9.18434E-07
8	13.6262	3	.987	257333	7.74596E-07
9	13.7734	3	.997	267379	1.01413E-06
10	13.9219	3	1.008	276544	1.10529E-06
11	14.0903	3	1.019	289075	9.02560E-07
12	14.2441	3	1.029	299403	9.84700E-07
13	14.3991	3	1.039	309104	1.04010E-06
14	14.5582	3	1.049	318164	1.12583E-06
15	14.7205	3	1.06	328635	9.77935E-07
16	14.8957	3	1.07	339349	1.01457E-06
17	15.0607	3	1.081	352493	7.66126E-07
18	15.2346	3	1.091	363895	9.14750E-07
19	15.4188	3	1.102	374790	9.96784E-07
20	15.5962	3	1.112	383146	1.23026E-06
21	15.7831	3	1.123	391238	1.31364E-06
22	15.9781	3	1.134	398646	1.47003E-06
23	16.1719	3	1.144	405367	1.58012E-06
24	16.3651	3	1.155	410807	1.90993E-06
25	16.5624	3	1.165	415465	2.23485E-06
26	16.7649	3	1.176	421833	1.64574E-06
27	16.9649	3	1.186	428076	1.62742E-06
28	17.1699	3	1.196	435446	1.38535E-06
29	17.3951	3	1.207	440722	2.08302E-06
30	17.6109	3	1.217	443375	3.88992E-06
31	17.8245	3	1.227	445199	5.48794E-06
32	18.0734	3	1.239	447028	6.24386E-06
33	18.2966	3	1.249	448984	5.12271E-06
34	18.5308	3	1.259	450139	8.91768E-06
35	18.7835	3	1.27	451080	1.15516E-05
36	19.0225	3	1.28	452052	1.03497E-05
37	19.2701	3	1.29	453183	9.01859E-06
38	19.5314	3	1.301	454153	1.08557E-05
39	19.8024	3	1.311	455015	1.23781E-05
40	20.0996	3	1.323	455693	1.68437E-05
41	20.4298	3	1.335	456450	1.63276E-05
42	20.7134	3	1.345	457018	1.82218E-05
43	20.9976	3	1.356	457450	2.34492E-05
44	21.2882	3	1.366	458044	1.70371E-05

NADC-83126-60 Vol. I

45	21.589	3	1.376	458615	1.79158E-05
46	21.8962	3	1.386	459077	2.20780E-05
47	22.2534	3	1.398	459534	2.52953E-05
48	22.6214	3	1.409	460049	2.24854E-05
49	22.9679	3	1.42	460484	2.43910E-05
50	23.3503	3	1.431	460920	2.61468E-05
51	23.708	3	1.442	461248	3.16461E-05
52	24.0843	3	1.452	461572	3.28087E-05
53	24.4487	3	1.462	461873	3.33224E-05
54	24.8832	3	1.474	462174	3.86377E-05
55	25.2846	3	1.484	462474	3.48004E-05
56	25.6843	3	1.494	462747	3.70693E-05
57	26.1052	3	1.505	463018	3.82657E-05
58	26.555	3	1.516	463266	4.34278E-05
59	27.0128	3	1.526	463511	4.34691E-05
60	27.4591	3	1.536	463730	4.60730E-05
61	27.924	3	1.547	463947	4.70970E-05
62	28.3982	3	1.557	464140	5.24867E-05
63	28.8861	3	1.567	464333	5.24873E-05
64	29.3924	3	1.577	464525	5.31773E-05
65	29.9248	3	1.587	464718	5.39895E-05
66	30.5621	3	1.6	464910	6.28643E-05
67	31.1397	3	1.61	465102	5.51045E-05
68	31.7941	3	1.622	465294	6.05726E-05
69	32.435	3	1.633	465488	5.63921E-05
70	33.0791	3	1.643	465652	6.50607E-05
71	33.7843	3	1.655	465791	8.12236E-05
72	34.4675	3	1.665	465930	7.60427E-05
73	35.1496	3	1.675	466069	7.34535E-05
74	35.9607	3	1.687	466207	8.49271E-05
75	36.7067	3	1.698	466319	9.28576E-05
76	37.5377	3	1.709	466431	9.98207E-05
77	38.4514	3	1.721	466543	1.05626E-04
78	39.3606	3	1.732	466665	9.27868E-05
79	40.421	3	1.745	466768	1.23009E-04
80	41.634	3	1.758	466880	1.23572E-04

FATIGUE TEST-CONSTANT LOAD-SAMPLE TYPE:CT-MATERIAL:TI-6AL-4V

SPEC. NO.:TI-9 DATA PTS.=51

B=.5 IN W=2.5 IN E=1.6E7

CONST LOAD =1544.12 (LBS) LOAD RATIO=.05

FREQ RANG =.3 HZ TEMP=70 DEG F

ENVIRONMENT=3.5% SALT WATER PH(6.2 TO 8)

OBS NO.	KMAX (KSI SQR(IN))	FREQ (HZ)	CRACK LENGTH (INCHS)	CYCLES	DA/DN (IN/CYCLE)
1	18.6527	.3	1.23	1024	1.20133E-03
2	18.8905	.3	1.241	3072	5.08304E-06
3	19.126	.3	1.251	5007.5	5.21829E-06
4	19.3443	.3	1.261	7100.5	4.78261E-06
5	19.6088	.3	1.271	9036	5.19740E-06
6	19.8783	.3	1.282	10814	6.10240E-06
7	20.1418	.3	1.292	12479.5	6.22630E-06
8	20.4172	.3	1.303	14145	6.36451E-06
9	20.6959	.3	1.313	15495.5	7.76004E-06
10	20.9681	.3	1.323	16801	7.66756E-06
11	21.2667	.3	1.334	18106.5	8.21909E-06
12	21.5697	.3	1.344	19367	8.43317E-06
13	21.8768	.3	1.355	20560	8.81809E-06
14	22.2033	.3	1.366	21595.5	1.05360E-05
15	22.514	.3	1.376	22631	9.78265E-06
16	22.8309	.3	1.386	23644	9.96051E-06
17	23.1603	.3	1.396	24612	1.05786E-05
18	23.5137	.3	1.407	25512.5	1.18934E-05
19	23.8541	.3	1.417	26435.5	1.08992E-05
20	24.2072	.3	1.427	27133.5	1.45845E-05
21	24.565	.3	1.437	27764	1.59557E-05
22	24.9305	.3	1.447	28372	1.64801E-05
23	25.3065	.3	1.457	28980	1.65297E-05
24	25.7196	.3	1.468	29498	2.07528E-05
25	26.1243	.3	1.478	29993.5	2.06864E-05
26	26.5436	.3	1.489	30444	2.29522E-05
27	27.0033	.3	1.5	30917	2.32980E-05
28	27.4568	.3	1.51	31345	2.46730E-05
29	27.9045	.3	1.52	31705.5	2.81278E-05
30	28.3781	.3	1.531	32133.5	2.43691E-05
31	28.8759	.3	1.542	32494	2.95421E-05
32	29.3639	.3	1.552	32809.5	3.21397E-05
33	29.8986	.3	1.562	33057.5	4.35080E-05
34	30.4578	.3	1.573	33283	4.85142E-05
35	31.0044	.3	1.584	33553.5	3.83365E-05
36	31.5765	.3	1.594	33801.5	4.24597E-05
37	32.1519	.3	1.605	34027	4.55432E-05
38	32.7569	.3	1.615	34230	5.15765E-05
39	33.3915	.3	1.626	34455.5	4.71841E-05
40	34.0732	.3	1.637	34636	6.12742E-05
41	34.8312	.3	1.649	34816.5	6.57619E-05
42	35.5356	.3	1.659	34974.5	6.74046E-05
43	36.2341	.3	1.669	35087.5	9.04429E-05
44	36.9961	.3	1.68	35200.5	9.53980E-05
45	37.8768	.3	1.692	35313.5	1.06283E-04
46	38.8356	.3	1.705	35426.5	1.11151E-04
47	39.6369	.3	1.715	35494.5	1.48677E-04
48	40.4584	.3	1.725	35562.5	1.47353E-04
49	41.4711	.3	1.737	35653	1.31491E-04
50	42.5398	.3	1.749	35721	1.77206E-04
51	43.5573	.3	1.76	35766.5	2.42197E-04

## FATIGUE TEST-CONSTANT K-SAMPLE TYPE:CT-MATERIAL:TI-6AL-4V

SPEC. NO.:TI-11 DATA PTS.=75

B=.5 IN W=2.5 IN E=1.4E7

CONST K LEVEL =42 KSI SQR(IN) LOAD RATIO=.05

FREQ RANG =10 TO 0.03 HZ TEMP=70 DEG F

ENVIRONMENT=3.5% SALT WATER PH(6.2 TO 8)

OBS NO.	LOAD (LBS)	FREQ (HZ)	CRACK LENGTH (INCHS)	CYCLES	DA/DN (IN/CYCLE)
1	4500.19	3	1.013	163.5	6.19462E-03
2	4449.23	3	1.024	285.5	8.76237E-05
3	4398.02	3	1.034	418	8.16597E-05
4	4349.82	3	1.045	532	8.99131E-05
5	4301.6	3	1.055	639	9.64481E-05
6	4253.95	3	1.065	757	8.69490E-05
7	4207.33	3	1.075	856.5	1.01508E-04
8	4157.95	3	1.086	979	8.78363E-05
9	4108.05	3	1.097	1105	8.68260E-05
10	4061.66	3	1.107	1226.5	8.41971E-05
11	4013.22	3	1.118	1337	9.71949E-05
12	3964.12	3	1.129	1439.5	1.06829E-04
13	3918.39	3	1.139	1539	1.03015E-04
14	3870.25	3	1.15	1661	8.89350E-05
FREQ. CHANGE FROM F= 3 TO F= 1					
15	3822.4	1	1.161	1745.5	1.28283E-04
16	3777.64	1	1.171	1808	1.63040E-04
17	3731.27	1	1.182	1872	1.65781E-04
18	3687.46	1	1.192	1948	1.32501E-04
19	3644.11	1	1.202	2014.5	1.50526E-04
20	3598.72	1	1.212	2089	1.41342E-04
21	3554.99	1	1.222	2155.5	1.53233E-04
22	3511.67	1	1.233	2241	1.18596E-04
23	3468.87	1	1.243	2329.5	1.13673E-04
24	3424.64	1	1.253	2400	1.48085E-04
25	3379.01	1	1.264	2479.5	1.36100E-04
26	3336.31	1	1.274	2560.5	1.25555E-04
27	3293.19	1	1.284	2631.5	1.45212E-04
28	3250.76	1	1.295	2704	1.40552E-04
FREQ. CHANGE FROM F= 1 TO F= .3					
29	3209.12	.3	1.305	2763	1.70170E-04
30	3167.53	.3	1.315	2791	3.59642E-04
31	3122.9	.3	1.326	2834	2.52324E-04
32	3080.14	.3	1.336	2863.5	3.53898E-04
33	3038.78	.3	1.346	2893	3.43731E-04
34	2992.97	.3	1.357	2930	3.04863E-04
35	2949.22	.3	1.368	2969.5	2.73925E-04
36	2908.19	.3	1.378	3005	2.87043E-04
37	2868.05	.3	1.388	3049	2.27500E-04
38	2827.63	.3	1.399	3101	1.94616E-04
39	2787.47	.3	1.409	3145.5	2.26966E-04
40	2744.7	.3	1.419	3184	2.80520E-04
41	2703.94	.3	1.43	3224	2.58499E-04
42	2664.33	.3	1.44	3260.5	2.76438E-04
43	2624.86	.3	1.45	3300	2.55696E-04

## FREQ. CHANGE FROM F= .3 TO F= .1

44	2585.44	.1	1.46	3330	3.37664E-04
45	2542.68	.1	1.471	3379.5	2.23032E-04
46	2502.17	.1	1.482	3456.5	1.36493E-04
47	2463.72	.1	1.492	3532	1.32715E-04
48	2425.3	.1	1.502	3610.5	1.28152E-04
49	2387.1	.1	1.512	3685.5	1.34001E-04
50	2344.55	.1	1.523	3755	1.61869E-04
51	2303.17	.1	1.534	3825	1.57143E-04
52	2261.16	.1	1.545	3940	9.76521E-05
53	2222.31	.1	1.556	4046	9.84905E-05
54	2184.63	.1	1.566	4147	1.00792E-04
55	2147.04	.1	1.576	4207.5	1.68761E-04
56	2110.06	.1	1.586	4287	1.27044E-04
57	2073.64	.1	1.596	4353.5	1.50376E-04

## FREQ. CHANGE FROM F=.1 TO F= 10

58	2027.43	10	1.609	4428	1.71409E-04
59	1982.74	10	1.621	4596	7.40481E-05
60	1942.63	10	1.633	4734	8.14493E-05
61	1904.03	10	1.644	4851.5	9.26809E-05
62	1863.54	10	1.655	4950	1.16751E-04
63	1822.2	10	1.667	5089.5	8.48027E-05
64	1786.11	10	1.677	5198.5	9.54123E-05
65	1751.57	10	1.687	5308	9.15070E-05
66	1711.67	10	1.699	5447	8.38847E-05
67	1670.91	10	1.711	5577	9.23854E-05
68	1634.88	10	1.722	5713	7.86764E-05
69	1596.92	10	1.733	5822	1.04220E-04
70	1562.66	10	1.743	5952	7.95392E-05
71	1528	10	1.754	6076	8.49991E-05
72	1494.46	10	1.764	6158.5	1.24606E-04

## FREQ. CHANGE FROM F=10 TO F=.03

73	1460.81	.03	1.775	6297.5	7.48205E-05
74	1427.82	.03	1.785	6412.5	8.93914E-05
75	1394.07	.03	1.795	6559.5	7.21768E-05

FATIGUE TEST-CONSTANT K-SAMPLE TYPE:CT-MATERIAL:TI-6AL-4V

SPEC. NO.:TI-13 DATA PTS.=86

B=.5 IN W=2.5 IN E=1.6E7

CONST K LEVEL =42 KSI SQR(IN) LOAD RATIO=.3

FREQ RANG =10 TO 0.03 HZ TEMP=70 DEG F

ENVIRONMENT=3.5% SALT WATER PH(6.2 TO 8)

OBS NO. #	LOAD (LBS)	FREQ (HZ)	CRACK LENGTH (INCHS)	CYCLES	DA/DN (IN/CYCLE)
1	4782.34	10	.955	1211	7.88617E-04
2	4729.44	10	.966	1382	6.23102E-05
3	4678.93	10	.976	1553.5	5.97840E-05
4	4628.95	10	.986	1724	5.99532E-05
5	4579.73	10	.996	1896	5.89417E-05
6	4526.26	10	1.007	2067	6.48945E-05
7	4477.64	10	1.018	2272	4.95614E-05
8	4425.19	10	1.029	2466	5.69071E-05
9	4374.75	10	1.039	2673	5.16424E-05
10	4327.07	10	1.049	2856	5.55737E-05
11	4278.44	10	1.06	3061	5.09268E-05
12	4227.61	10	1.071	3244	6.00001E-05
13	4180.58	10	1.081	3438	5.26807E-05
14	4132.1	10	1.092	3600	6.54319E-05
FREQ. CHANGE FROM F= 10 TO F= 3					
15	4077.27	3	1.104	3800	6.03002E-05
16	4027.49	3	1.115	3942	7.76052E-05
17	3981.62	3	1.125	4086	7.09030E-05
18	3934.91	3	1.135	4220	7.79851E-05
19	3888.72	3	1.146	4346	8.24597E-05
20	3838.79	3	1.157	4503	7.19113E-05
21	3793.3	3	1.167	4645	7.28167E-05
22	3747.46	3	1.178	4775	8.05387E-05
23	3700.23	3	1.189	4925	7.22663E-05
24	3655.96	3	1.199	5078	6.67323E-05
25	3612.19	3	1.209	5207	7.86042E-05
26	3565.27	3	1.22	5330.5	8.84214E-05
27	3519.34	3	1.231	5463	8.10569E-05
28	3476.39	3	1.241	5587.5	8.10441E-05
FREQ. CHANGE FROM F= 3 TO F= 1					
29	3431.92	1	1.251	5729.5	7.38728E-05
30	3384.02	1	1.263	5822.5	1.22043E-04
31	3341.92	1	1.273	5910.5	1.13864E-04
32	3298.71	1	1.283	5989	1.31592E-04
33	3256.62	1	1.293	6064	1.34667E-04
34	3214.21	1	1.303	6132	1.50295E-04
35	3170	1	1.314	6233.5	1.05419E-04
36	3127.91	1	1.324	6323.5	1.13666E-04
37	3086.19	1	1.334	6406	1.23394E-04
38	3042.93	1	1.345	6501	1.11579E-04
39	3000.75	1	1.355	6599	1.05919E-04
40	2959.75	1	1.366	6684.5	1.18480E-04
41	2917.35	1	1.376	6770	1.23041E-04
42	2875.97	1	1.386	6843.5	1.40271E-04
43	2835.13	1	1.397	6934	1.12929E-04

FREQ. CHANGE FROM F= 1 TO F= .3					
44	2791.68	.3	1.408	6998	1.70626E-04
45	2751.66	.3	1.418	7090	1.09783E-04
46	2709.88	.3	1.428	7168.5	1.34904E-04
47	2669.47	.3	1.439	7236	1.52445E-04
48	2628.45	.3	1.449	7296	1.74832E-04
49	2587.69	.3	1.459	7363	1.56269E-04
50	2548.09	.3	1.47	7435	1.41944E-04
51	2509.02	.3	1.48	7498	1.60794E-04
52	2467.75	.3	1.491	7562	1.67970E-04
53	2428.43	.3	1.501	7606.5	2.31234E-04
54	2390.02	.3	1.511	7653.5	2.14894E-04
55	2351.87	.3	1.521	7700.5	2.14470E-04
56	2312.78	.3	1.531	7738	2.76798E-04
57	2272.21	.3	1.542	7769	3.49356E-04
FREQ. CHANGE FROM F=.3 TO F=.1					
58	2233.71	.1	1.553	7810.5	2.48915E-04
59	2196.05	.1	1.563	7885.5	1.35466E-04
60	2158.88	.1	1.573	8057.5	5.86052E-05
61	2122.16	.1	1.583	8264.5	4.83575E-05
62	2085.13	.1	1.593	8442.5	5.70222E-05
63	2048.16	.1	1.603	8666	4.55929E-05
64	2007.27	.1	1.615	8883	5.22582E-05
65	1970.29	.1	1.625	9066.5	5.62395E-05
66	1932.96	.1	1.635	9255.5	5.54500E-05
67	1897.04	.1	1.645	9434.5	5.67037E-05
68	1860.35	.1	1.656	9619	5.65310E-05
69	1823.38	.1	1.666	9794.5	6.02853E-05
70	1787.49	.1	1.677	9936.5	7.28167E-05
71	1751.02	.1	1.687	10104	6.31638E-05
72	1716.68	.1	1.697	10288.5	5.43633E-05
73	1676.11	.1	1.709	10536	4.82424E-05
74	1641.79	.1	1.72	11062.5	1.93352E-05
75	1607.25	.1	1.73	11430	2.80818E-05
76	1573.73	.1	1.74	11709	3.61649E-05
77	1539.48	.1	1.75	11872.5	6.35469E-05
FREQ. CHANGE FROM F=.1 TO F=.03					
78	1506.73	.03	1.76	12187	3.18283E-05
79	1473.5	.03	1.771	12343	6.56415E-05
80	1438.38	.03	1.782	12661.5	3.42541E-05
81	1405.08	.03	1.792	13008.5	3.00864E-05
82	1373.16	.03	1.802	13219.5	4.78199E-05
83	1341.45	.03	1.812	13434	4.71330E-05
84	1303.06	.03	1.825	13697	4.69961E-05
85	1272.18	.03	1.835	14060.5	2.76205E-05
86	1240.44	.03	1.845	14271	4.95010E-05

## FATIGUE TEST-CONSTANT LOAD-SAMPLE TYPE:CT-MATERIAL:TI-6AL-4V

SPEC. NO.:TI-17 DATA PTS.=36

B=.5 IN W=2.5 IN E=1.6E7

CONST LOAD =2000 (LBS) LOAD RATIO=.3

FREQ RANG =10 HZ TEMP=70 DEG F

ENVIRONMENT=3.5% SALT WATER PH(6.2 TO 8)

OBS NO. #	KMAX (KSI SQR(IN))	FREQ (HZ)	CRACK LENGTH (INCHS)	CYCLES	DA/DN (IN/CYCLE)
1	15.9378	10	.976	42936	2.27421E-05
2	16.3198	10	.999	43817.5	2.55530E-05
3	18.2143	10	1.003	45069	3.37915E-06
4	18.6151	10	1.024	47035	1.04272E-05
5	19.0516	10	1.045	49116	1.03989E-05
6	19.4886	10	1.066	50910	1.16890E-05
7	19.9751	10	1.089	53423	8.97333E-06
8	20.4461	10	1.11	56044	8.03128E-06
9	20.9214	10	1.13	57696	1.24213E-05
10	21.4718	10	1.153	59849	1.06224E-05
11	21.9919	10	1.174	61031	1.75719E-05
12	22.5669	10	1.196	63364.5	9.45363E-06
13	23.1103	10	1.216	65055.5	1.18510E-05
14	23.7549	10	1.239	66164	2.05502E-05
15	24.4427	10	1.262	67489	1.75170E-05
16	25.0693	10	1.282	68707	1.65928E-05
17	25.7561	10	1.304	69781	1.97392E-05
18	26.4566	10	1.324	70821.5	1.98655E-05
19	27.2332	10	1.346	71752	2.34712E-05
20	28.0226	10	1.367	72574	2.57299E-05
21	28.8724	10	1.389	73504	2.32795E-05
22	29.7759	10	1.411	74400	2.43973E-05
23	30.6865	10	1.432	75007	3.44481E-05
24	31.6065	10	1.452	75721	2.81232E-05
25	32.6547	10	1.473	76399.5	3.19676E-05
26	33.7388	10	1.495	76862	4.58594E-05
27	34.8788	10	1.516	77434	3.68707E-05
28	36.0529	10	1.536	77896	4.44158E-05
29	37.3049	10	1.557	78286	5.29998E-05
30	38.697	10	1.579	78748.5	4.68107E-05
31	40.2534	10	1.601	79104	6.38258E-05
32	41.7641	10	1.622	79494.5	5.29063E-05
33	43.497	10	1.644	79813.5	6.96238E-05
34	45.2004	10	1.665	80096	7.23189E-05
35	47.1247	10	1.686	80379	7.62897E-05
36	49.0963	10	1.707	80627.5	8.30987E-05

## FATIGUE TEST-CONSTANT LOAD-SAMPLE TYPE:CT-MATERIAL:TI-6AL-4V

SPEC. NO.:TI-18 DATA PTS.=46

B=.5 IN W=2.5 IN E=1.6E7

CONST LOAD =2000 (LBS) LOAD RATIO=.3

FREQ RANG =3 HZ TEMP=70 DEG F

ENVIRONMENT=3.5% SALT WATER PH(6.2 TO 8)

OBS NO. #	KMAX (KSI SQ(R(IN)))	FREQ (HZ)	CRACK LENGTH (INCHS)	CYCLES	DA/DN (IN/CYCLE)
1	15.4276	3	.843	30.5	.027637
2	15.7478	3	.863	31937.5	6.27920E-07
3	16.0839	3	.884	51640.5	1.04441E-06
4	16.4358	3	.905	69940.5	1.14962E-06
5	16.7843	3	.925	88886.5	1.07331E-06
6	17.1443	3	.945	102307	1.52625E-06
7	17.5067	3	.965	114554	1.64057E-06
8	17.8946	3	.986	127968	1.55986E-06
9	18.0862	3	.997	135187	1.40061E-06
10	18.4815	3	1.017	142430	2.81995E-06
11	18.8808	3	1.037	150376	2.51951E-06
12	19.2807	3	1.056	155890	3.52921E-06
13	19.7087	3	1.077	162994	2.84206E-06
14	20.1523	3	1.097	168618	3.60063E-06
15	20.609	3	1.117	173852	3.85364E-06
16	21.0964	3	1.138	178097	4.89283E-06
17	21.5927	3	1.158	181616	5.79424E-06
18	22.1063	3	1.179	183627	1.01144E-05
19	22.6367	3	1.199	185637	1.00597E-05
20	23.1848	3	1.219	186946	1.53552E-05
21	23.7616	3	1.239	188124	1.72581E-05
22	24.4304	3	1.262	189251	2.00354E-05
23	25.0634	3	1.282	190092	2.42926E-05
24	25.7645	3	1.304	191037	2.28994E-05
25	26.446	3	1.324	191774	2.72727E-05
26	27.1838	3	1.345	192433	3.15478E-05
27	27.9351	3	1.365	193092	3.06677E-05
28	28.7635	3	1.386	193725	3.35545E-05
29	29.6049	3	1.407	194254	3.87901E-05
30	30.4693	3	1.427	194757	3.99007E-05
31	31.4123	3	1.448	195208	4.61419E-05
32	32.4194	3	1.469	195607	5.28318E-05
33	33.4639	3	1.489	196006	5.19050E-05
34	34.5587	3	1.51	196353	5.92216E-05
35	35.7971	3	1.532	196700	6.32854E-05
36	37.0042	3	1.552	197021	6.28972E-05
37	38.3253	3	1.573	197316	7.06782E-05
38	39.7441	3	1.594	197585	7.83644E-05
39	41.3094	3	1.616	197880	7.40338E-05
40	42.8793	3	1.636	198176	6.93919E-05
41	44.5736	3	1.657	198419	8.56379E-05
42	46.3191	3	1.677	198610	1.05236E-04
43	48.2134	3	1.698	198775	1.23818E-04
44	50.2232	3	1.718	198940	1.22909E-04
45	52.4626	3	1.739	199080	1.50429E-04
46	54.8793	3	1.76	199219	1.52086E-04

## FATIGUE TEST-CONSTANT LOAD-SAMPLE TYPE:CT-MATERIAL:TI-6AL-4V

SPEC. NO.:TI-19 DATA PTS.=25

B=.5 IN W=2.5 IN E=1.6E7

CONST LOAD =2000 (LBS) LOAD RATIO=.3

FREQ RANG =.3 HZ TEMP=70 DEG F

ENVIRONMENT=3.5% SALT WATER PH(6.2 TO 8)

ORF NO. #	KMAX (KSI SQR(IN))	FREQ (HZ)	CRACK LENGTH (INCHS)	CYCLES	DA/DN (IN/CYCLE)
1	27.0579	.3	1.267	22.5	.0563227
2	27.8082	.3	1.289	3609.5	6.06076E-06
3	28.5603	.3	1.31	5590.5	1.05048E-05
4	29.3229	.3	1.33	7065.5	1.36813E-05
5	30.1155	.3	1.35	8452.5	1.44557E-05
6	30.978	.3	1.371	9553.5	1.89101E-05
7	31.8795	.3	1.392	10786.5	1.68126E-05
8	32.8472	.3	1.413	11733.5	2.23548E-05
9	33.8351	.3	1.433	12592.5	2.38999E-05
10	34.9375	.3	1.455	13341.5	2.90121E-05
11	36.0949	.3	1.477	14068.5	2.96974E-05
12	37.3173	.3	1.498	14751.5	3.15519E-05
13	38.5375	.3	1.519	15324.5	3.55150E-05
14	39.8915	.3	1.54	15875.5	3.87114E-05
15	41.3144	.3	1.561	16206.5	6.38368E-05
16	42.7691	.3	1.581	16559.5	5.76770E-05
17	44.2991	.3	1.602	16824	7.63327E-05
18	46.0381	.3	1.623	17089	8.14339E-05
19	47.951	.3	1.645	17288	1.11558E-04
20	50.1274	.3	1.669	17465	1.32881E-04
21	52.9052	.3	1.696	17620	1.78516E-04
22	56.1644	.3	1.726	17687	4.40895E-04
23	59.931	.3	1.757	17732	6.84667E-04
24	63.1908	.3	1.781	17755	1.05218E-03
25	69.1634	.3	1.82	17800	8.76223E-04

FATIGUE TEST-CONSTANT LOAD-SAMPLE TYPE:CT-MATERIAL:TI-6AL-4V

SPEC. NO.:TI-23 DATA PTS.=31 WAVE FORM:TRIANGLE WAVE WITH HOLD TIME

B=.5 IN W=2.5 IN E=1.6E7 TEMP=70 DEG F

CONST LOAD =2000 (LBS) LOAD RATIO=.05

SLOPE =.5 SEC HOLD TIME=0 SEC

ENVIRONMENT=3.5% SALT WATER PH(6.2 TO 8)

OBS NO. #	KMAX (KSI SQR(IN))	SLOPE (SEC)	CRACK LENGTH (INCHS)	CYCLES	DA/DN (IN/CYCLE)
1	22.9503	.5	1.116	36	.7309939
2	23.3926	.5	1.137	4534.5	4.22156E-06
3	23.8346	.5	1.157	7546.5	6.69654E-06
4	24.3206	.5	1.178	10899	6.40117E-06
5	24.8072	.5	1.199	13743	7.28904E-06
6	25.3733	.5	1.222	15303	1.48461E-05
7	25.9038	.5	1.243	16491	1.75084E-05
8	26.4531	.5	1.264	17646	1.78529E-05
9	27.0103	.5	1.284	18529.5	2.26486E-05
10	27.6195	.5	1.304	19278	2.78690E-05
11	28.2604	.5	1.325	19992	2.92156E-05
12	28.9683	.5	1.347	20673	3.20412E-05
13	29.7559	.5	1.37	21319.5	3.53905E-05
14	30.4888	.5	1.39	21833.5	3.90274E-05
15	31.3088	.5	1.411	22311	4.43558E-05
16	32.1706	.5	1.432	22789	4.37867E-05
17	33.1209	.5	1.454	23232	4.88938E-05
18	34.1339	.5	1.475	23710.5	4.51620E-05
19	35.1592	.5	1.496	24087	5.44487E-05
20	36.3497	.5	1.518	24463.5	5.91237E-05
21	37.501	.5	1.538	24773.5	6.49352E-05
22	38.7657	.5	1.559	25048.5	7.53095E-05
23	40.1334	.5	1.58	25323	7.63569E-05
24	41.529	.5	1.6	25566	8.23869E-05
25	43.0741	.5	1.621	25840.5	7.55917E-05
26	44.8791	.5	1.643	26082	9.36235E-05
27	46.7805	.5	1.665	26290	1.06586E-04
28	48.8195	.5	1.688	26464	1.27242E-04
29	50.9235	.5	1.709	26638	1.22529E-04
30	53.2473	.5	1.731	26777.5	1.57563E-04
31	55.5397	.5	1.751	26883	1.92416E-04

## FATIGUE TEST-CONSTANT K-SAMPLE TYPE:CT-MATERIAL:TI-6AL-4V

SPEC. NO.:TI-24 DATA PTS.=40 WAVE FORM:TRIANGLE WAVE WITH HOLD TIME

B=.5 IN W=2.5 IN E=1.6E7 TEMP=70 DEG F

K RANGE=25 TO 50 (KSI SQR(IN)) LOAD RATIO=.05

SLOPE =.5 SEC HOLD TIME=1 SEC

ENVIRONMENT=3.5% SALT WATER PH(6.2 TO 8)

OBS NO. #	KMAX (KSI SQR(IN))	LOAD (LBS)	CRACK LENGTH (INCHS)	CYCLES	DA/DN (IN/CYCLE)
1	24.924	1889.27	1.261	37.5	1.0336267
2	25.0426	1877.94	1.271	3010.5	3.50487E-06
3	25.0419	1855.65	1.283	5191.5	5.21783E-06
4	25.0763	1833.61	1.295	7504.5	5.42152E-06
5	25.0617	1811.33	1.306	10147.5	4.08627E-06
6	25.0424	1789.05	1.317	12559.5	4.39468E-06
7	25.0321	1767.78	1.327	14410.5	5.61321E-06
8	25.0358	1747.18	1.338	16162.5	6.01027E-06
9	25.0488	1727.27	1.348	17815.5	6.33396E-06
10	25.0268	1705.75	1.358	19798.5	5.05290E-06
11	25.0307	1685.48	1.368	21451.5	6.20090E-06
12	25.0479	1665.62	1.379	23302.5	5.64560E-06
13	25.04	1644.02	1.389	24856.5	6.71814E-06
14	30.0639	1948.33	1.4	25420.5	1.85992E-05
15	30.1	1920.4	1.412	25951.5	2.32957E-05
16	30.035	1891.51	1.422	26449.5	2.02610E-05
17	30.0684	1868.07	1.433	27112.5	1.56411E-05
18	30.0569	1841.64	1.443	27742.5	1.65237E-05
19	30.0045	1813.48	1.453	28306.5	1.78548E-05
20	30.0615	1791.62	1.463	28936.5	1.61587E-05
21	30.0386	1763.45	1.474	29401.5	2.31181E-05
22	30.0828	1739.02	1.485	29899.5	2.16666E-05
23	37.1531	2115.76	1.495	30100.5	5.13436E-05
24	37.2545	2084.43	1.507	30235.5	8.82219E-05
25	37.1567	2045.66	1.518	30370.5	7.92592E-05
26	37.1616	2010.72	1.529	30505.5	8.36302E-05
27	37.2059	1978.57	1.54	30640.5	8.19259E-05
28	37.2206	1943.43	1.552	30775.5	8.51110E-05
29	37.2924	1912.4	1.563	30910.5	8.22217E-05
30	37.3294	1872.55	1.576	31045.5	9.87415E-05
31	37.2137	1832.9	1.587	31180.5	8.04442E-05
32	42.3538	2035.28	1.601	31348.5	8.53567E-05
33	42.1713	1987.1	1.612	31450.5	1.10001E-04
34	42.1671	1946.35	1.624	31552.5	1.13529E-04
35	42.3338	1904.74	1.638	31687.5	1.04444E-04
36	42.3393	1867.1	1.649	31789.5	1.06765E-04
37	42.3126	1825.57	1.661	31891.5	1.14412E-04
38	42.5111	1782.96	1.676	32026.5	1.09926E-04
39	42.3193	1735.07	1.687	32128.5	1.14901E-04
40	51.2446	2057.54	1.698	32197.5	1.54058E-04

FATIGUE TEST-CONSTANT K-SAMPLE TYPE:CT-MATERIAL:TI-6AL-4V

SPEC. NO.:TI-25 DATA PTS.=39 WAVE FORM:TRIANGLE WAVE WITH HOLD TIM

B=.5 IN W=2.5IN E=1.6E7 TEMP=70 DEG F

K RANGE=25 TO 50 (KSI SQR(IN)) LOAD RATIO=.05

SLOPE =.5 SEC HOLD TIME=2.33 SEC

ENVIRONMENT=3.5% SALT WATER PH(6.2 TO 8)

OBS NO.	KMAX (KSI SQR(IN))	LOAD (LBS)	CRACK LENGTH (INCHS)	CYCLES	DA/DN (IN/CYCLE)
1	24.9917	2635.77	.892	37	1.0241122
2	25.1343	2635	.903	1755	6.39175E-0
3	25.0383	2610.53	.914	3175.5	7.66065E-0
4	25.0537	2587.65	.925	5355	4.94334E-0
5	25.0529	2564.03	.935	6973.5	6.44857E-0
6	25.0603	2541.7	.946	8856	5.47780E-0
7	25.0174	2514.35	.956	10540.5	6.14963E-0
8	25.0563	2494.5	.967	12489	5.53040E-0
9	25.0484	2470.65	.977	14602.5	4.98651E-0
10	25.046	2446.42	.988	16782	5.07593E-0
11	25.0553	2424.29	.999	18433.5	6.48240E-0
12	25.0983	2404.68	1.01	20415	5.40587E-0
13	30.0358	2849.69	1.021	21736.5	8.36170E-0
14	30.0377	2823	1.032	22464	1.46528E-0
15	30.0046	2794.76	1.042	23422.5	1.04956E-0
16	30.0445	2772.31	1.052	24084	1.59032E-0
17	30.0493	2746.54	1.063	24943.5	1.23560E-0
18	30.0598	2718.57	1.075	25770	1.42770E-0
19	30.0934	2693.68	1.086	26794.5	1.11762E-0
20	30.0232	2662.36	1.097	27588	1.30561E-0
21	30.0802	2641.02	1.108	28282.5	1.57811E-0
22	37.0605	3223.1	1.118	28680	2.62137E-0
23	37.0496	3189.88	1.129	28879.5	5.50376E-0
24	37.0831	3158.52	1.141	29211	3.52942E-0
25	37.1126	3130.19	1.151	29476.5	3.98114E-0
26	37.0436	3092.26	1.162	29742	4.16577E-0
27	37.0744	3063.21	1.173	29974.5	4.69674E-0
28	37.0663	3033.22	1.183	30108	7.60296E-0
29	37.0866	3001.33	1.195	30307.5	5.82458E-0
30	37.0818	2967.69	1.207	30540	4.96346E-0
31	42.1404	3329.52	1.22	30673.5	9.85017E-0
32	42.1588	3292.51	1.231	30807	8.80899E-0
33	42.1942	3248.18	1.246	30940.5	1.07640E-0
34	42.1146	3207.1	1.256	31074	7.99997E-0
35	42.0947	3170.44	1.267	31207.5	8.03747E-0
36	42.1907	3130.89	1.281	31341	1.06517E-0
37	42.1391	3085.53	1.294	31474.5	9.44575E-0
38	42.2367	3050.47	1.307	31608	9.54299E-0
39	50.308	3577.71	1.321	31708.5	1.40000E-0

## FATIGUE TEST-CONSTANT K-SAMPLE TYPE:CT-MATERIAL:TI-6AL-4V

SPEC. NO.:TI-25 DATA PTS.=4 WAVE FORM:TRIANGLE WAVE WITH HOLD TIME  
 B=.5 IN W=2.5 IN E=1.6E7 TEMP=70 DEG F  
 K RANGE=25 TO 50 (KSI SQR(IN)) LOAD RATIO=.05  
 SLOPE =.5 SEC HOLD TIME=1 SEC  
 ENVIRONMENT=3.5% SALT WATER PH(6.2 TO 8)

OBS NO.	KMAX (KSI SQR(IN))	LOAD (LBS)	CRACK LENGTH (INCHS)	CYCLES	DA/DN (IN/CYCLE)
1	50.2635	3136.92	1.429	37.5	.0381112
2	50.4575	3100.99	1.441	106.5	1.67971E-04
3	50.2215	3040.24	1.452	208.5	1.09510E-04
4	50.3779	2991.57	1.466	310.5	1.36666E-04

## FATIGUE TEST-CONSTANT K-SAMPLE TYPE:CT-MATERIAL:TI-6AL-4V

SPEC. NO.:TI-25 DATA PTS.=5 WAVE FORM:TRIANGLE WAVE WITH HOLD TIME  
 B=.5 IN W=2.5 IN E=1.6E7 TEMP=70 DEG F  
 K RANGE=25 TO 50 (KSI SQR(IN)) LOAD RATIO=.05  
 SLOPE =.5 SEC HOLD TIME=2.33 SEC  
 ENVIRONMENT=3.5% SALT WATER PH(6.2 TO 8)

OBS NO.	KMAX (KSI SQR(IN))	LOAD (LBS)	CRACK LENGTH (INCHS)	CYCLES	DA/DN (IN/CYCLE)
1	50.5343	3435.05	1.36	37	.0367684
2	50.1816	3362.19	1.373	105	1.78824E-04
3	50.328	3319.27	1.386	172.5	1.92889E-04
4	50.3422	3268.94	1.398	240	1.86518E-04
5	50.4046	3209.7	1.414	340.5	1.53731E-04

NADC-83126-60 Vol. I

THIS PAGE INTENTIONALLY LEFT BLANK

# REFERENCES

1. Y. H. Kim, M. E. Fine and T. Mura: "Fatigue Crack Initiation: Theory," presented at AIME 109th Annual Meeting, Las Vegas, NV., Feb. 1980.
2. Y.H. Kim and M.E. Fine: "Theoretical Prediction of the Number of Cycles to Fatigue Crack Initiation due to the Irreversible Slip Step Formation," to be published in Met. Trans., 1980.
3. Y. H. Kim, "Initiation and Growth of Fatigue Microcracks and Strain-Controlled Fatigue Properties in Steel Alloys: Microstructure and Mechanics," Ph.D Thesis, Northwestern Univ., Evanston, Illinois, 1979.
4. Y.H. Kim, M. E. Fine and T. Mura, "Plastic Yielding at the Tip of a Blunt Notch During Static and Fatigue Loading," Eng. Fract. Mech. Vol. II, 1979, pp. 653.
5. L. F. Coffin, Jr. and J. F. Tavernelli, "The Cyclic Straining and Fatigue Metals," Trans. Met. Soc., AIME, Vol. 215, Oct. 1959, pp. 794.
6. S.S. Manson, "Fatigue: A Complex Subject - Some Simple Approximations," Experimental Mechanics, July 1975, pp. 1.
7. R.W. Landgraf, M.R. Mitchell and N.R. Pointe, "Monotonic and Cyclic Properties of Engineering Materials," Ford Motor Co. Tech Report, Dearborn, Michigan, 1972.
8. J. Morrow and G.M. Sinclair, ASTM STP 237, Symposium on Basic Mechanisms of Fatigue, ASTM, 1958, pp.83.
9. J. Morrow, "Cyclic Plastic Strain Energy and Fatigue of Metals," ASTM STP 378, Int. Friction Damping, and Cyclic Plasticity," ASTM, 1965, pp. 45.
10. W. Brose, N.E. Dowling and J. Morrow, "Effect of Periodic Large Strain Cycles on the Fatigue Behavior of Steels," SAE Paper No. 740221, SAE, Detroit, Michigan, Feb. 1974.
11. M.E. Fine and R.O. Ritchie, "Fatigue Crack Initiation and Near-Threshold Crack Growth," Fatigue and Microstructure, 1978 ASM Materials Science Seminar, American Society for Metals, Oct. 1978, pp.245.

12. E.A. Starke, Jr. and G. Lütjering, "Cyclic Plastic Deformation and Microstructure," Fatigue and Microstructure, 1978 ASM Materials Science Seminar, American Society for Metals, Oct. 1978, pp. 205.
13. P.N. Thielen and M.E. Fine: "Fatigue Studies on 4140 Steel," Met. Trans. A, Vol. 6A, 1975, pp. 2133.
14. S.I. Kwun, "Fatigue Behavior of Quenched and Tempered N6-Bearing HSLA Steel," Ph.D. Thesis, Marquette Univ., Milwaukee, Wisconsin, 1978.
15. T.W. Weir, G.W. Simmons, R.G. Hart, and R.P. Wei, "A Model for Surface Reaction and Transport Controlled Fatigue Crack Growth", Scripta Met., 14, 1980, pp. 357-364.
16. R.P. Wei, and G.W. Simmons, "Surface Reactions and Fatigue Crack Growth", proceedings 27th Sagamore Army Materials Research Conference, New York, July, 1980 (to be published).
17. Y.H. Kim and S.D. Manning, "A Superposition Model For Corrosion Fatigue Crack Propagation In Aluminum Alloys," Paper presented at the 14th National Symposium on Fracture Mechanics, UCLA, Los Angeles, CA, 30 June-2 July 1981; Fracture Mechanics, ASTM STP 791, 1983,
18. R.P. Wei, "Some Aspects of Environment-Enhanced Fatigue Crack Growth", Eng. Fract. Mech., Vol. 1, 1970, p. 633.
19. R.P. Wei, "On Understanding Environment-Enhanced Fatigue Crack Growth -- A Fundamental Approach", Fatigue Mechanisms, ASTM STP 675, American Society for Testing and Materials, 1979, pp. 816-840.
20. R.P. Wei, "Rate Controlling Processes and Crack Growth Response", in Hydrogen Effects in Metals, I.M. Bernstein and Anthony W. Thompson, eds., The Metallurgical Society of AIME, Warrendale, PA, 1981, pp. 677-690.
21. R.P. Wei, unpublished research, Lehigh University, 1982.
22. R.J.H. Wanhill and J.J. De Luccia, "An AGARD-Coordinated Corrosion Fatigue Cooperative Testing Programme", AGARD Report No. 695, February 1982.

23. W. G. Clark, Jr., and S. J. Hudak, Jr., "Variability in Fatigue Crack Growth Rate Testing," Journal of Testing and Evaluation, JTEVA, Vol. 3, No. 6, 1975, pp. 454-476.
24. T. V. Duggan and M. W. Proctor, "Measurement of Crack Length from Changes in Specimen Compliance," in The Measurement of Crack Length and Shape During Fracture and Fatigue, Engineering Materials Advisory Service, LTD., United Kingdom, 1980, pp. 1-27.
25. R. P. Wei and R. L. Brazill, "An a.c. Potential System for Crack Length Measurement," in The Measurement of Crack Length and Shape During Fracture and Fatigue, Engineering Materials Advisory Services, LTD., United Kingdom, 1980, pp. 190-201.
26. "Standard Test Method for Constant-Load-Amplitude Fatigue Crack Growth Rates Above  $10^{-8}$  M/Cycle," ASTM Designation: E647-81, in 1981 Annual Book of ASTM Standards, Part 10, Metals-Mechanical, Fracture, and Corrosion Testing; Fatigue: Erosion and Wear; Effect of Temperature, 1981, pp. 765-783.
27. R. I. Jaffee, Met. Trans., Vol. 10A, 154 (1979).
28. H. N. Hahn, D. J. Duquette, ACTA Met., 26, 279 (1978).
29. W. Mendenhall and L. Ott, Understanding Statistics, Durbury Press, Belmont, CA, 1972.
30. M. O. Speidel, Paper 2.2, Proceedings of the Eighth ICAF Symposium, ed. J. Branger and F. Berger, Lausanne, June 1975.
31. G. R. Chanani, AFML-TR-76-156, September 1976.
32. C. M. Bianco, J. C. Radon, and L. E. Culver, J. Test. Eval., 3, 407 (1975).
33. H. P. Chu, J. Eng. Mat. and Tech., 96, 261 (1974).
34. Fatigue of Aircraft Materials, April (1977) p. 4-7.
35. F. J. Bradshaw and C. Wheeler, International J. Fract. Mech., 5, 255 (1969).
36. R. J. Wanhill, AGARD Report No. 659, Corrosion Fatigue of Aircraft Materials, April (1977) p. 2-3.

37. B. D. Cullity, Elements of X-Ray Diffraction, Addison-Wesly Publishing Company, Inc., 1959, p. 40.
38. M. R. Spiegel, Theory and Problems of Statistics, Schaum Publishing Co., New York, 1961.

FAA

	<u>No. of Copies</u>
FAA, Washington, DC 20591 (Attn: J. R. Soderquist). . . .	1
FAA, Technology Center, Atlantic City, NJ 08405 (Attn: Mr. D. Nesterok, ACT-330). . . . .	1

NASA

NASA, Langley Research Center, Hampton, VA 23365 (Attn: Mr. H. Hardrath). . . . .	1
NASA, Washington, DC 20546 (Attn: Airframes Branch, FS-120)	1
NASA, Lewis Research Center, Cleveland, OH 44135 (Attn: Technical Library). . . . .	1
NASA, George C. Marshall Space Flight Center, Huntsville, AL 35812 (Attn: Technical Library). . . . .	1

USAF

AFWAL, WPAFB, OH 45433 (Attn: AFWAL/FIBE). . . . .	1
(Attn: FIBEC). . . . .	1
(Attn: FIBAA). . . . .	1
(Attn: AFWAL/FIB). . . . .	1
Ogden ALC, Hill AFB, UT 84055 (Attn: MANCC). . . . .	1
Oklahoma City ALC, Tinker AFB, OK 73145 (Attn: MAQCP). . .	1
Sacramento ALC, McClellan AFB, CA 95652 (Attn: MANE). . .	1
San Antonio ALC, Kelly AFB, TX 78241 (Attn: MMETM). . . .	1
Warner Robbins ALC, Robins AFB, GA 30198 (Attn: MMSRD/Dr. T. Christian). . . . .	1

U. S. Army

Applied Technology Laboratory, USARTL (AVRADCOM), Fort Eustis, VA 23604 (Attn: H. Reddick). . . . .	1
U. S. Army Materials and Mechanics Research Center (DRXMR-PL), Watertown, MA 02172. . . . .	1
U. S. Army Research Office, Durham, NC 27701 . . . . .	1

INFO. SERVICES

DTIC, Cameron Station, Alexandria, VA 22314 . . . . .	12
MCIC, Battelle Columbus Laboratories, 505 King Avenue, Columbus, OH 43201 . . . . .	1
NTIS, U. S. Dept. of Commerce, Springfield, VA 22151 . . .	2

NON-GOVERNMENT ACTIVITIES

	<u>No. of Copies</u>
ALCOA, ALCOA Labs, ALCOA Center, PA 15069	
(Attn: Mr. J. G. Kaufman) . . . . .	1
Battelle Columbus Labs, 505 King Avenue, Columbus, OH 43201	
(Attn: Dr. B. Leis) . . . . .	1
Boeing Commercial Airplane Co., P. O. Box 3707, Seattle, WA	
98124 (Attn: Mr. T. Porter) . . . . .	1
Douglas Aircraft Co., 3855 Lakewood Blvd., Long Beach, CA 90846	
(Attn: Mr. Luce, Mail Code 7-21) . . . . .	1
Drexel University, Phila., PA 19104 (Attn: Dr. Averbuch) . . .	1
Fairchild Industries, Hagerstown, MD 21740 (Attn: Tech. Library)	1
General Dynamics, Convair Division, San Diego, CA 92138	
(Attn: Mr. G. Kruse) . . . . .	1
General Dynamics Corporation, P. O. Box 748, Ft. Worth, TX 76101	
(Attn: Dr. S. Manning) . . . . .	1
Grumman Aerospace Corporation, South Oyster Bay Road, Bethpage, L.I., NY 11714 (Attn: Dr. H. Armen)	
(Attn: Dr. B. Leftheris) . . . . .	1
(Attn: Dr. H. Eidenoff) . . . . .	1
Lehigh University, Bethlehem, PA 18015	
(Attn: Prof. G. C. Sih) . . . . .	1
(Attn: Prof. R. P. Wei) . . . . .	1
Lockheed-California Co., 2555 N. Hollywood Way, Burbank, CA 91520	
(Attn: Mr. E. K. Walker) . . . . .	1
Lockheed Georgia Co., Marietta, GA 30063 (Attn: Mr. T. Adams)	1
McDonnell Douglas Corporation, St. Louis, MO 63166	
(Attn: Mr. L. Impellizeri) . . . . .	1
(Attn: Dr. R. Pinckert) . . . . .	1
Northrop Corporation, One Northrop Ave., Hawthorne, CA 90250	
(Attn: Mr. Alan Liu) . . . . .	1
(Attn: Dr. M. Ratwani) . . . . .	1
Rockwell International, Columbus, OH 43216	
(Attn: Mr. F. Kaufman) . . . . .	1
Rockwell International, Los Angeles, CA 90009	
(Attn: Mr. J. Chang) . . . . .	1
Rockwell International Science Center, 1049 Camino Dos Rios, Thousand Oaks, CA 91360 (Attn: Dr. F. Morris) . . . . .	1
Rohr Corporation, Riverside, CA 92503 (Attn: Dr. F. Riel) . .	1
Sikorsky Aircraft, Stratford, CT 06622 . . . . .	1
University of Dayton Research Institute, 300 College Park Ave., Dayton, OH 45469 (Attn: Dr. J. Gallagher) . . . . .	1
University of Illinois, College of Engineering, Urbana, IL 61801	
(Attn: Dept. of Mechanics and Industrial Eng., Profs. J. D. Morrow, D. F. Socie) . . . . .	2
Vought Corporation, Dallas, TX 75265	
(Attn: Dr. C. Dumisnil) . . . . .	1
(Attn: Mr. T. Gray) . . . . .	1
University of Pennsylvania, Dept. of Mechanical Engineering and Applied Mechanics, 111 Towne Bldg. D3, Phila., PA 19104	
(Attn: Dr. Burgers) . . . . .	1